SONOCHEMICAL SYNTHESIS AND CHARACTERIZATION OF HYDROXYAPATITE/METAL-BASED COMPOSITE MATERIALS FOR BIOMEDICAL APPLICATIONS

Marija Vukomanović

Doctoral Dissertation
Jožef Stefan International Postgraduate School
Ljubljana, Slovenia, June 2012

Evaluation Board:

Prof. Dr. Danilo Suvorov, Jožef Stefan Institute, Advanced Materials Department, Jamova 39, Ljubljana, Slovenia

Prof. Dr. Maja Remškar, Jožef Stefan Institute, Condensed Matter Physics Department, Jamova 39, Ljubljana, Slovenia

Prof. Dr. Rok Kostanjšek, Biotechnical Faculty, Biology Department, Jamnikarjeva 101, Ljubljana, Slovenia

MEDNARODNA PODIPLOMSKA ŠOLA JOŽEFA STEFANA
JOŽEF STEFAN INTERNATIONAL POSTGRADUATE SCHOOL

Marija Vukomanović

SONOCHEMICAL SYNTHESIS AND CHARACTERIZATION OF HYDROXYAPATITE/METAL-BASED COMPOSITE MATERIALS FOR BIOMEDICAL APPLICATIONS

Doctoral Dissertation

SONOKEMIJSKA SINTEZA IN KARAKTERIZACIJA MATERIALOV NA OSNOVI HIDROKSIAPATIT/KOVINE ZA BIOMEDICINSKO UPORABO

Doktorska disertacija

Supervisor: Assist. Prof. Dr. Srečo Davor Škapin

Co-Supervisor: Prof. Dr. Dragan Uskoković

Ljubljana, Slovenia, June 2012

Index

Abstract

A new approach for the synthesis of silver (Ag), platinum (Pt) and gold (Au) nanoparticles and their composites with hydroxyapatite (HAp) is developed via a sonochemical process. The major goal was to design physicochemical properties of material in order to achieve: (i) intensive antibacterial activity and (ii) maximal reduction of toxicity for humans and their environment.

Silver, with natural ability for antibacterial activity, was investigated for study of the mechanism of antibacterial activity and sources of toxicity. Sonochemically formed HAp/Ag composites have three sources of antibacterial activity: Ag-ions, incorporated within apatite structure, smaller Ag nanoparticles, embedded within apatite plate-like particles, and larger Ag nanoparticles, attached onto the surface of the apatite particles. These metal particles have a cubic and hexagonal structure and they are spherical and hexahedral in shape. Beside the presence of different factors able to affect antibacterial activity of HAp/Ag composite, such as silver state, structure, particles shape and size, antibacterial activity of the composite was amplified only by irradiation by light. It confirmed that reactive oxidative stress driven by reactive radicals is the major mechanism of its action. A non-selectivity of this mechanism is a major source of very high toxicity of this metal which is able to induce necrosis of almost 100% of human cells for 1 h. These results confirm an urgent need for finding a more suitable replacement of this metal, widely present in practice. These findings encouraged us to develop more human-friendly materials with enhanced antibacterial activity.

The first strategy used for development of suitable Ag-replacement concerned activation of platinum, as a bioinert and non-toxic metal. Bio-inspired approach to photocatalysis with a selection of biologically acceptable building blocks that can be activated by non-toxic visible light is used for its activation. Combination of HAp with platinum (Pt^0 and Pt^{n+}) provided formation of a novel photocatalitically active material. Thus formed hybrid semiconductor/metallic nanocomposites made of apatite plate-like particles with Pt metallic nanoparticles attached on their surface and two different types of surface adsorbed Pt-complexes belong to innovative solutions for design of functional bioactive materials. This material can be activated by exposure to both, ultraviolet (UV) as well as visible (VIS) light. UV activation is allowed by semiconductive HAp phase, while activity induced by VIS is related to complexes adsorbed on HAp surface. Pt metallic nanoparticles have the ability of electron trapping which provides extension of material's activity during the period when it is kept in the dark. Thus developed material has an intensive ability for degradation of non-degradable dyes which confirmed its ability to form high concentration of reactive radicals. However, in contrast to Ag, Pt nanoparticles have dual nature able to release and to accept electrons. It regulates radical formation, decreases toxicity but in the same time limits intensity of developed antibacterial activity. Developed material succeeds only in overcoming the toxicity issue of silver.

The second strategy used for development of suitable replacement of Ag-based antibacterial materials was activation of gold. Similar to the platinum, gold is also bioinert and non-toxic metal. The strategy used for its activation concerned surface

functionalization. Naturally-sourced amino acids are the most effective in this process. Finally-formed materials contain HAp plate-like particles with functionalized Au nanoparticles attached onto their surface. In this case amino acids are involved into attachment of Au nanoparticles onto HAp surface. Thus designed material has an amphiphilic structure with hydrophobic gold and hydrophilic amino acid. In comparison with Ag and Pt, this material is unable for photocatalytic activity and production of reactive radicals which is partially the source of its non-toxicity. The major mechanism of its action against bacteria is charge. Accordingly, it classifies developed HAp/Au/functionalized material into analogous of the group of the special type of antibacterial agents known as antibacterial peptides. It is able for electrostatic interactions with bacterial cells that destroy the structure and change a permeability of their walls. Positively charged groups of amino acids attached onto Au are prone to interact with negatively charged surface of bacteria. This mechanism is selective since human cells have a completely different surface charge than bacteria which decreased affinity of material to interact with them and ensured its non-toxicity for human cells. Developed material succeeds in overcoming the problem of toxicity of silver and in the same time it has a very strong antibacterial activity which even exceeds intensity of silver activity against bacteria.

Newly developed HAp/Pt and HAp/Au composites are good alternatives to composite with silver. HAp/Pt possesses ability for self-cleaning while HAp/Au has intensive antibacterial activity. Capabilities of developed materials together with green method for their production and high decrease of their toxicity for human cells are significant improvements compared to highly toxic Ag. These properties introduce newly developed composites as novel nanomaterials with a potential to improve health care using smart mechanisms able to “recognize” mammalian cells.

Povzetek

Za sintezo nanodelcev srebra (Ag), platine (Pt) in zlata (Au) ter njihovih kompozitov s hidroksiapatitom (HAp) sem razvila nov pristop z uporabo sonokemijske sintezne metode. Glavni cilj mojega doktorskega raziskovalnega dela je bila sinteza nano-kompozitnih materialov, ki se naj odlikujejo z naslednjimi lastnostmi: (i) visoka antibakterijska učinkovitost in (ii) čim manjša strupenost za človeka in njegovo okolje.

Materiale na osnovi srebra, ki se odlikuje z naravnim antibakterijskim delovanjem, sem raziskovala z namenom študija mehanizma antibakterijske aktivnosti in strupenosti. HAp/Ag kompoziti, ki sem jih sintetizirala s sonokemijsko metodo, imajo tri vire protimikrobnega delovanja: i) Ag-ione, ki so vgrajeni v strukturo apatita, ii) manjše nanodelce Ag, vključene v ploščicam-podobne delce apatita, in iii) večje nanodelce Ag, ki so pritrjeni na površino delcev apatita. V teh kompozitih delci Ag kristalizirajo v kubični in heksagonalni strukturi in nastopajo v okrogli oziroma v obliki heksaedrov. Na protimikrobno delovanje HAp/Ag kompozita lahko vplivajo različni dejavniki, kot so oksidacijsko stanje srebra, kristalna struktura, oblika in velikost delcev. V okviru doktorskega dela sem tem materialom povečala antibakterijsko aktivnost z obsevanjem s svetlobo.

Potrdila sem, da je glavni mehanizem protimikrobnega delovanja HAp/Ag kompozita oksidacijski stres. Neselektivnost tega mehanizma je glavni vir zelo visoke strupenosti kovine v tem kompozitu, ki lahko povzroči nekrozo skoraj 100 % človeških celic v eni uri. S temi rezultati sem dejansko potrdila nujno potrebo po iskanju bolj ustreznih antibakterijskih materialov, ki bi lahko nadomestili Ag, ki je na tržišču zelo razširjeno kot antibakterijsko sredstvo. Te ugotovitve so bile osnova za nadaljnje raziskave novih materialov.

Prva strategija, ki sem jo uporabila za razvoj ustrezne zamenjave za srebro, je bila aktiviranje platine, ki je biološko inertna in nestrupena kovina. Za aktivacijo platine sem uporabila biomimetični pristop, pri čemer sem uporabila biološko sprejemljive sestavne komponente in pripravljene materiale obsevala z vidno svetlobo, s čimer sem omogočila proces fotokatalize. Z ustrezno kombinacijo HAp s platino (Pt^0 in Pt^{n+}) sem sintetizirala nov fotokatalitsko aktivni material. Tako pripravljen hibridni nanokompozit na osnovi polprevodnik/kovina je bil sestavljen iz ploščic apatita s Pt kovinskimi nanodelci, ki so bili pritrjeni na njihovi površini, pri čemer sem uporabila dve vrsti površinsko adsorbiranih Pt-kompleksov. Ta postopek sinteze predstavlja inovativno rešitev za tvorbo funkcionalnih bioaktivnih materialov. Pridobljeni material se lahko aktivira z obsevanjem z ultravijolično (UV) in/ali vidno svetlobo (VIS). Z UV svetlobo aktiviramo polprevodniško HAp fazo, medtem ko VIS aktivira kovinske komplekse, ki so adsorbirani na površini HAp-a. Pt kovinski nanodelci imajo lastnost, da lahko »skladiščijo« elektrone, kar omogoča, da je takšen material aktiven tudi v temi. Material, ki sem ga razvila, je omogočal intenzivno razgradnjo organskega barvila, kar potrjuje, da tvori v vodnem mediju visoko koncentracijo reaktivnih radikalov. V nasprotju z Ag imajo Pt nanodelci dvojno naravo, ki omogoča, da lahko sprostijo ali sprejmejo elektrone, kar vpliva na nastanek radikalov. Z regulacijo tvorbe radikalov vplivamo na zmanjšanje strupenosti, hkrati pa se zmanjša tudi antibakterijska aktivnost. Tako pripravljen material ima

pomembno prednost pred Ag, ker je nestrupen.

V drugem pristopu, ki sem ga uporabila za razvoj novih antibakterijskih materialov, primernih za zamenjavo Ag, sem uporabila zlato (Au) z ustrezno aktivacijo. Podobno kot Pt je tudi Au bioinertna in nestrupena kovina. Bistvo te aktivacije je bila funkcionalizacija površine nanodelcev Au. Raziskave so pokazale, da naravne aminokisline omogočajo najbolj učinkovito aktivacijo. Tako pripravljeni materiali so bili sestavljeni iz delcev HAp v obliki tankih ploščic, na katerih so pritrjeni funkcionalizirani nanodelci Au. Pri teh materialih omogočajo prisotne aminokisline trdno vez kovinskih nanodelcev na površino delcev HAp. Tako formiran material ima amfifilno strukturo, ki je sestavljena iz hidrofobnega zlata in hidrofilnih aminokislin. Za razliko od Ag in Pt kompozitov ta material ne kaže fotokatalitskih lastnosti, ker ne tvori reaktivnih radikalov, ki delno tudi povzročajo strupenost. Vir antibakterijske aktivnosti tega materiala je naboj na površini kovinskih nanodelcev, kar razvršča ta material v skupino analogov antibakterijskih peptidov. Zaradi tega naboja pride v stiku z bakterijami do elektrostatične interakcije z njihovimi celicami, ki uniči njihovo strukturo in spremeni prepustnost njihovih sten. Pozitivno nabite skupine aminokislin, ki so pritrjene na Au nanodelce, imajo visoko nagnjenost k interakciji z negativno nabitimi stenami bakterij. Ta mehanizem je selektiven, saj imajo na primer človeške celice povsem drugačen površinski naboj kot bakterije in zato je reaktivnost materiala s človeškimi celicami povsem zanemarljiva. Zato je ta material za človeka nestrupen za razliko od antibakterijskih materialov na osnovi Ag, hkrati pa material izkazuje večjo antibakterijsko učinkovitost kot Ag.

Novo razviti kompozitni materiali HAp/Pt in HAp/Au so glede na svoje izjemne lastnosti dobra zamenjava za kompozite s srebrom. HAp/Pt izkazuje samočistilno delovanje zaradi svojih fotokatalitskih lastnosti, medtem ko izkazuje HAp/Au intenzivno protibakterijsko delovanje. Lastnosti novih materialov, kot tudi sintezna metoda in uporabljene surovine, ki so del t. i. »zelene kemije«, s čimer se zmanjša strupenost na najnižjo raven, so pomembne izboljšave v primerjavi s strupenimi materiali na osnovi Ag. Te lastnosti novo razvitih kompozitov se lahko uporabijo za izboljšano zdravstveno oskrbo, saj »uporabljajo« pametne mehanizme prepoznavanja celic sesalcev od drugih celic.

1 Introduction

1.1 Antibacterial materials

1.1.1 Historical overview

Practical application of antibacterial agents started in a very distant past- – in the ancient Greek and Indian cultures. They used mould and plants as natural sources able to prevent or stop infections. Further on in history, mould has been used by many different cultures and nations within traditional medication. As part of old types of medications, medical usage of gold is associated with very old civilizations. Over 5000 years ago Egyptians ingested gold for "mental, bodily and spiritual purification" (Mahdihassan, 1988) while the Chinese (2500 BC) used it as a "drug of longevity" (Higby, 1982; Fricker, 1996). Indian culture used gold for revitalization and the same medicine is also used today under the name Swarna Bashma (Mahdihassan, 1984; Mahdihassan, 1985). In the 19th century, colloidal Au has been used against alcoholism and even today it is applied as an alternative medicine against addiction diseases (alcohol, nicotine, caffeine and carbohydrate dependence) (Patra et al., 2010).

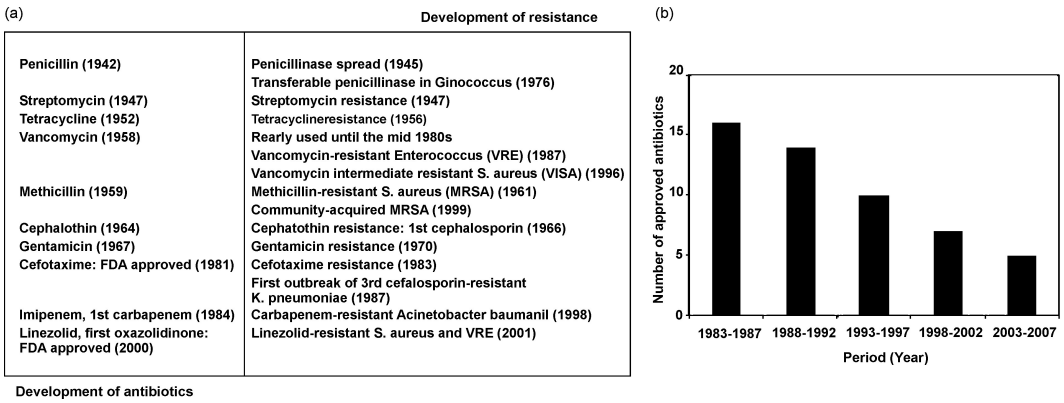

Figure 1: *History of the development of antibiotics and subsequent appearance of the microbial resistance (a) (Huh and Kwon, 2011); number of new antibiotics approved by the Federal Agency for Food and Drugs in US* (*Taubes, 2008).*

Beside moulds and plants as organic sources able to provide antibacterial activity, inorganic antibacterial agents were also used. One of the oldest documented examples of medical application of silver as an inorganic source of antibacterial agent originates from 1884. This document concerns usage of silver-nitrate for eye infections in order to prevent development of *Neisseria gonorrhoeae* (Silvestry-Rodriguez et al., 2007).

Sir Alexander Fleming (during 1920s), Howard Florey and Ernst Chan (during 1940s) were the first who discovered that moulds release substance which is able to prevent bacterial growth and isolated it from the mould named *Penicillium notatum*. This substance has been named penicillin. Officially this event is concerned as a beginning of

"era of antibiotics". Discovery of natural-sourced antibiotics, extracted from the fungi, was followed by development of a large number of synthetic analogous able to have the same or improved effect. This invention had a crucial impact on the human health since it resolved very serious infections such as tuberculosis, gangrene, syphilis and similar.

Development of antibiotics was followed by development of their major side effect-bacterial resistivity. Bacteria were able to mutate as a consequence of the frequent stress induced by exposure to antibacterial agents. These mutations resulted in formation of new strains with a high ability for resistance and appearance of the multi-resistivity. The last caused a need for a continuous development of new classes of antibiotics or for a constant need for increasing the range of antibacterial activity of currently available antibiotics (Huh and Kwon, 2011). However decreased number of newly developed antibiotics was acceptable to be used as a safety and low-toxic medications (Figure 1).

At beginning of the last century infectious diseases were one of the leading causes of worldwide death (Cohen, 2000). Even today, besides living in the modern era of advances technologies, we are faced with infectious diseases as still unresolved issue. Infecting by dangerous pathogens during routine procedures such as blood sampling is not impossible today. Recent infectious caused by mutated breed of *E. coli* in Germany when more than 1500 people were infected and pandemic worldwide flu, both induced by completely novel strains which were highly toxic and infectious ended by high number of fatal cases. These are just ones in a sequence of many indications why there is a need for further much intensive research in the field of improvement of the way for fighting against pathogens (Simmons et al., 2010; Huh and Kwon, 2011).

1.1.2 Challenges for the use of nanotechnology against infections

The latest effort in exploring a novel, more effective ways for development of antimicrobial agents is associated with investigation of nanotechnology as a high-potential tool applicable for their design. As illustrated in Figure 2, nanotechnology is concerned to be used for formation of so-called "nanoantibiotics". "Nanoantibiotics" are defined as nanomaterials which are capable to show antibacterial activity by themselves (Li et al., 2008) or to elevate the efficacy and safety of other antibacterials by improvement of the way for their administration (Abeylath and Turos, 2008). They are developed in two directions: (i) for formation of nanosized carriers of the already existing antibiotics as a novel platform for improvement of their delivery and (ii) for design of novel antimicrobial nanoparticles. Usage of nanoparticles is expected to have significant benefit against resistivity, but safety after long-term exposure to them is also unknown issue. Detailed testing before final usage is certainly the best way to find out the answers.

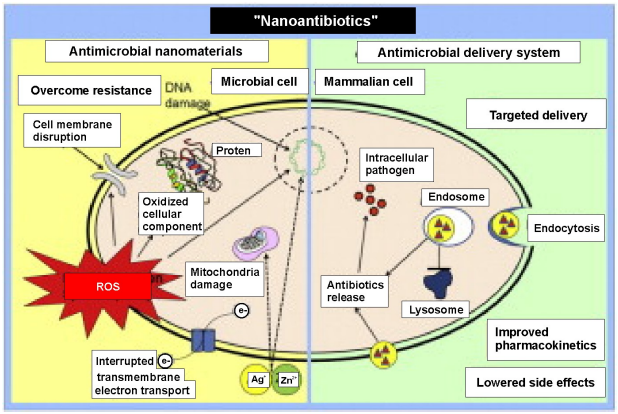

Figure 2: *Strategies for the application of nanotechnology in discovery of antimicrobials: (i) novel antimicrobial nanomaterials and (ii) novel antibiotic delivery systems* (*Huh and Kwon, 2011).*

1.1.2.1 Antibiotic drug delivery

First strategy for development of "nanoantibiotics" is controlled drug delivery. It is an innovative way for administration of the drugs. The idea is in the use of nanoparticles as carriers of a drug. These nanoparticles are prone to capture a drug and to deliver it directly to the place of its activity and/or to release it in a controlled manner (Huh and Kwon, 2011). Major advantages of such approach are: (i) more efficient medication, (ii) increase of the required doses and (iii) reduction of the side effects of the drug.

Recently, this approach has been used for development of core/shell nanoparticles formed of polymeric shell and bioceramic core. These particles were simultaneously loaded by two forms of commercially-available antibiotic and investigations showed their ability to provide controlled release of the drug during the period of at least 30 days. System has been developed as a novel strategy for local, controlled delivery of antibiotics which are already used is dental practice and for prevention of bone infections such as clindamycin-base and clindamycin-phosphate (Vukomanović et al., 2011a; Vukomanović et al., 2011b; Vukomanović et al., 2011c; Vukomanović et al., 2012a).

1.1.2.2 Novel antimicrobial nanoparticles

Second strategy for development of "nanoantibiotics" is synthesis of novel antibacterial nanomaterials. Usage of inorganic nanoparticles as active agents has been recently suggested as highly perspective direction for development of these novel types of drugs (Dastjerdi and Montazer, 2010; Huh and Kwon, 2011). Materials with natural antimicrobial activity are investigating together with materials with potential for synthetic activation. Major approaches to their design are: (i) formation of composites and hybrids, (ii) photoactivation and (iii) surface functionalization.

Some of the examples of the implementation of listed strategies for discovery of novel antibacterial nanomaterials are formation of HAp/Ag composite with specific three-sourced antibacterial centres (Vukomanović et al., 2011d), photoactivation of a novel HAp/Pt composite (Vukomanović et al., 2012b) and functionalization used for activation of HAp/Au composite (Vukomanović et al., 2012c).

1.1.2.2.1 Hybrids and composites formation

Numerous investigations performed on development of antibacterial materials showed that most of them need to be coupled with additional components in order to achieve satisfied antibacterial activity and good bioactivity (Huh and Kwon, 2011; Dastjerdi and Montazer, 2010). Formation of composites and hybrids are shown to be a useful approach for that purpose. During development of material with an additional antibacterial component it should be take into account that this property depends on different factors, such as the type of material, (Sondi and Salopek-Sondi, 2004; Estaban-Cubillo et al., 2006; Ren et al., 2009; Aydin-Sevinc and Hanley, 2010) its morphological and structural properties (particle size, shape and the surface crystallographic planes), (Nair et al. 2007; Morones et al., 2005; Pal et al., 2007; Sau et al., 2010) as well as its stability (Marambio-Jones et al., 2010; Sharma et al., 2009). A control over these parameters provides control over the antibacterial response, maintains its safety and minimizes any side effects. These properties may be effectively controlled within composite.

1.1.2.2.2 Photoactivation

Combination of photons and engineered nanostructures has been introduced as advanced cleaning method with ability to use solar energy (Shannon et al., 2008). Idea originates from the highly sophisticated process of photosynthesis and it has been already used as an option for renewable energy production (Nam et al., 2010). Systems thus obtained have

enormous field of application starting from basic ones regarding hygiene and health care as well as air, water and earth purification. During development of these sort of systems major investigations have been performed on titanium-dioxide (TiO_2) as a well-known and highly effective photocatalyst which can be activated by UV light (Hashimoto et al., 2005; Žunič et al., 2011) and on its more efficient modifications (Diebold, 2011) in the form of metal-semiconductor and semiconductor-semiconductor composites, metal- or non-metal- doped structures and surface-sensitized structures containing dyes- all able to be activated by visible light (Stroyuk et al., 2009; Kamat, 2002). Alternatively, numerous inorganic semiconductors (zinc-oxide, (Paracchino et al., 2011) silver-orthophosphate (Yi et al., 2010) and organic semiconductors (polymeric) (Wang et al., 2009a) have been investigated for this purpose.

Similar approach could be used for directing of photocatalytic process to the field of design of biomaterials. In such a manner naturally-sourced materials are activated by harmless visible light for application in biomedicine. There are many examples for significant achievements reached by the application of models taken from the Nature (Hou et al., 2011; Dragnea, 2008; Huh and Kwon, 2011; Yoon et al., 2010). The main advantage of this approach is that selection of the natural building blocks increases compatibility of these systems to human and its environment.

1.1.2.2.3 Functionalization

Functionalization is approach used for modification of the surface chemistry of material. Due to the high affinity for formation of chemical bonds with thiolates, dithiolates, amines, carboxylates, cyanides, isothiocyanates, phosphines etc., functionalization of the surface of metallic nanoparticles is easy and fast process. Functionalization provides ability for attachment of variety of molecular species on the surface of metallic nanoparticles. There is a possibility for attachment of one or simultaneous attachment of many different functionalizing molecules. Accordingly it may be designed as a carrier of drug. In that case, the special benefit is in development of the route of administration of medicament when it can be led exactly to the predefined place of its action (target drug delivery). Alternatively, this approach may be used for design of the solubility, surface charge, wettability and other properties which are able to provide completely new behaviour of material. It has special benefits during development of novel pharmaceuticals or in design of the material for other specific biomedical applications. This approach is also interesting from the standpoint of development or increase of biocompatibility of material. Attachment of the specially-selected molecular species enables favourable interactions with cells and improvements of transport processes. Consequently, the possibility for reduction of their aggregation and for surface adsorptions of proteins and other products of metabolism is decreased. It decreases the probability for these particles to be recognized by immune system. Accordingly, their bioavailability is significantly increased (Dreaden et al., 2011; Dreaden et al., 2012).

1.1.3 Inorganic antibacterial materials

As it was already mentioned, inorganic sources with antibacterial activity had been taken into consideration as option for replacement of organic, synthetic antimicrobials (Dastjerdi and Montazer, 2010). Different metals with natural ability to have antibacterial activity (like zinc, copper, silver, titanium, etc.), their compounds or composites with other materials (ceramics, polymers and/or glasses) have potential to be applied for this purpose (Saito and Nakanaga, 2003). So far these materials have been investigated in the form of bulk, micro-/nanoparticles or ions.

Incorporation of Ti-ions within apatite structure provides possibility for formation of

material applicable for formation of antibacterial paints (Wakamura, 2008) while deposition of HAp/ZnO nanoparticles onto the surface of Ti-implants allows formation of material able to promote osseointegration and to provide antibacterial properties (Malshe and Jiang, 2011).

Carbon nanotubes (CNT) are strong antibacterial agent. Their activity increases with increased number of layers, meaning that multi-wall CNT are much stronger in antibacterial activity in comparison to single-wall CNT. It was a direct consequence of electronic structure and ability for production of reactive oxygen species (ROS). Consequently, toxicity had the same dependency (Jia et al. 2005).

So far silver has been considered as the most effective inorganic antibacterial agent. This metal is a natural antibiotic with a wide range of antibacterial activity including Gram positive and Gram negative bacteria. Moreover, except bacteria this metal is effective against many other pathogens including viruses and fungi. Because of these benefits this metal has been widely used in practice and there are an enormous number of products available in the market containing silver, including cosmetics, medical devices, medicines, clothing, paintings, filters, air conditions, appliances, etc. As antibacterial agent it has been formulated in the following forms: hydrosol (Willoughby, 2010); metallic layer (Martelli et al., 2010), metallic nanoparticles (Dingeldein et al., 2010) or metallic ions (Di Nunzio and Verne, 2007) made onto/in different titanium-based, ceramic or glass/ceramic implants; metal oxide within bioactive glass (Bellantone et al., 2000); metallic nanoparticles within polymeric support (Bokorny et al., 2008) etc.

Some of the major groups of nanomaterials with possibility for antibacterial action are summarized in Table 1. According to the investigated mechanisms majority of them (including Ag and Cu metals, ZnO_2 and TiO_2 oxides, doped HAp, CNT and NO-releasing nanoparticles) are using productions of ROS for activity against bacteria. As it is explained in more details in next chapters, ROS is non-selective and have the same effect for all cells. It means that for all these materials high level of toxicity can be expected.

Materials with other-than-ROS activity are Au metal, fullerenes, clay mineral and Ga_2O_3 oxide. For Ga_2O_3 it has been determined that Ga^{3+} ions are the centre of antibacterial activity since these ions have the same radius as Fe^{3+}ions. Accordingly, Ga^{3+} ions are able to replace Fe^{3+} ion and to interfere with their metabolic pathway (Valappil et al., 2008). However since they are unable to perform their function, cell death takes place. Fe-ions have important role in both, mammalian and bacterial cells which makes this mechanism non-selective and toxic for both type of cells. After testing of the fullerenes C60, mechanism of action of these materials was assigned to ROS production (Marković et al., 2007). However, some other investigations were claiming non-ROS mechanism (Lyon et al., 2008). *In vivo* investigations performed by inhalation of these materials confirmed their non-toxicity (Baker et al., 2008). In the case of clay, mechanism of action is still unexplored. Activity of this material probably depends on its mineral composition and may be assigned to present metals (Wilson, 2003). Beneficial effects of clays are known since antic times; however their changes due to the formation of nanosized particles require additional testing.

Among described materials, only Au nanoparticles have mechanism which provides selectivity. Interaction of these particles with cells is based on charge and includes strong electrostatic forces (Huh and Kwon, 2011). They are able to reinforce activity of standard antibiotics and to provide significant reduction of bacteria with developed resistivity (Huang et al., 2009). After attachment to Au nanoparticles lower concentration of antibiotic was required for sufficient antibacterial activity which contributed to decreasing of their side effects (Chamundeeswari et al., 2010). Without any modifications these particles do not show antibacterial activity and they are completely non-toxic for human cells (AshaRani et al., 2010). Therefore they have a good basis for further investigations.

Table 1: *Antibacterial nanomaterials, proposed mechanism of antibacterial activity and practical applications (Huh and Kwon, 2011; Dastjerdi and Montazer, 2010).*

Material	Mechanism	Applications	References
Ag NPs	**ROS mechanism**	Antibacterial and	(Rai et al., 2009)
Ag/HAp/TiO_2	cell membrane, electron	antifungal agent	(Mo et al., 2008)
Ag-zeolite	transport and DNA	dressings, coatings	(Matsuura et al., 1997)
Ag/HAp	damages, ion-release	of medical devices	(Liu et al., 2008)
Ag/borosilicate		filters	(Mertens and Polman, 2006)
Ag/polymer			(Kim et al., 2009)
Cu NPs	**ROS mechanism**	Cosmetics, roll-ons	
Cu/sepiolite	membrane and wall	Potential antibacterial	(Esteban-Cubillo et al., 2006)
Cu/polypropylene	damage	agent, UV protector	(Wel et al., 2008)
CuO			(Ren et al., 2009)
Au NPs	Interaction with cell	Photothermal	
Au/antibiotic	membrane, strong	treatment, diagnostic	(Gu at al., 2003)
Au/C	electrostatic interactions	agent	(Gao et al., 2010)
Au/pyrimidines		Potential antibacterial	(Zhao et al., 2010)
		agent and drug carrier	
ZnO NPs	**ROS mechanism**	Cosmetics, creams	(Aydin-Sevinç and Hanley, 2010)
ZnO/Ag	Intracellular	lotions, ointments, roll-ons	(Lu et al., 2008)
ZnO/HAp	Accumulation	mouthwash, and sprays	(Malshe and Jiang, 2011)
ZnO/Pt	membrane damage,	UV protectors,	(Zhang et al., 2010a)
	ion-release H_2O_2	hydrophobic coatings,	
	production	medical devices dressings	
Ga_2O_3 NPs	Release of Ga^{3+}-ions,	Possible antibacterial agent	(Valappil et al., 2008)
	interference with Fe		
	Metabolite pathways		
TiO_2 NPs	**ROS mechanism**	Antibacterial agent	
TiO_2/Pt	cell membrane and	creams and foot-care	(Sivakumar et al., 2010)
TiO_2/Ag	wall damage	cosmetics, water and air	(Sun et al., 2009)
TiO_2/HAp		purifiers, UV protectors	(Nishikawa et al., 2005)
Doped HAp NPs	**ROS mechanism**	Potential antibacterial	
HAp/Ti		agent for coatings of	(Wakamura, 2008)
HAp/Ag		dental and bone implants	(Rameshbabu et al., 2007)
HAp/F			(Ge et al., 2010)
Carbon nanotubes	**ROS mechanism**	Antibacterial agent	(Jia et al. 2005)
SWCNT	oxidation of cell	surface- coatings	(Brady-Estevez et al., 2008)
MWCNT	membrane	water filters	(Srivastava et al., 2004)
CNT/PLGA	proteins and lipids	biofouling-resistant	(Aslan et al., 2010)
CNT/ZnO_2		membranes, UV protector	
Fullerenes	Destruction of cell	Potential disinfection	(Lyon et al., 2005)
	Membrane integrity	applications	(Marković et al., 2007)
	enhanced activity of		(Lyon et al., 2008)
	infiltrating neutrophil		
Clay nanoparticles	Unknown	Cosmetics,	(Wilson, 2003)
Clay/PVP	possibly related to	spa-treatments,	(Seckin, et al., 1997)
Clay/polypropylene	presence of metals	UV protector	(Pavlikova et al., 2003)
NO-releasing NPs	**ROS mechanism**	Infected wound and	(Weller, 2009)
		diabetic foot treatment	

1.2 Noble metals in biomedicine

1.2.1 Physicochemical properties of noble metals

For the last forty years significant effort has been given to the synthesis of noble metal nanoparticles with a special insight into ability for control of their morphological properties and precise design of their surface characteristics. Among other benefits, control over the morphology and surface provide extraordinary optical properties which have a key role in the practical applications of these materials.

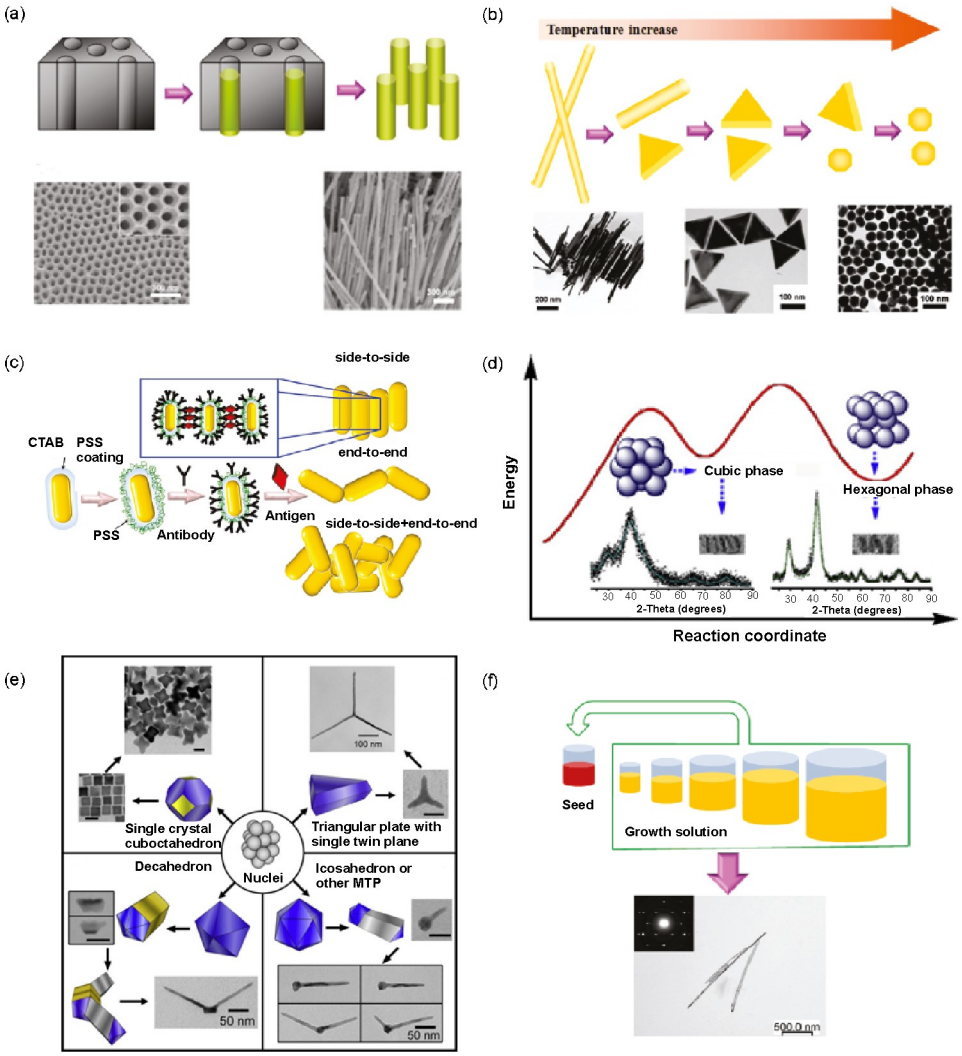

Figure 3: *Strategies for growth-control of metallic nanoparticles: template-mediated growth (a), temperature-influenced growth (b), functionalization-mediated growth (c); seed-mediated growth (d-f) (influence of the interface tension (d), influence of the defects (e) and influence of the volume (f)) (Chen and Liu, 2011; Peng and Yang, 2009).*

Different strategies used for development of the architecture of metallic nanoparticles in order to achieve precise tuning of their applicability are the best picture of versatility of their properties. Some of these strategies are illustrated in Figure 3. Application of the templates (soft and hard) provides strict control over their growth and aggregation. Along with the applied templates, growth-control may be affected by parameters such as temperature, concentration or precursor type when slow growth-rate induces formation of larger and more regular structures. Special type of control over morphological properties

is provided by modification of the surface chemistry. In that case surface-adsorbed species direct growth process usually using electrostatic interactions and have a role of soft templates. Seed-mediated growth provides a lot of possibilities for manipulation over the morphology and structure of formed crystals. Parameters of the seeds are leading the structure parameters of the growing phase while presence of defects and tension at the interface may lead to versatile morphological and structure modifications driven by the tendency for energetically more favourable state (Chen and Liu, 2011; Peng and Yang, 2009).

Finding the best way for stabilization of the surface of metallic nanoparticles in order to prevent their agglomeration and ingrowths into larger structures led to the application of variety of organic substances. Their major property is ability to compensate surface charge and provide nanoparticle stability. These molecules are used during the process of particle formation or in the post-synthesis step. The level at which stabilization has been achieved strongly depends on the strength of interaction of these molecules and nanoparticles surface (chemical bonding or physical interactions) as well as on the size, charges and type of the functional groups in the molecules used for modification of the surface. The highest level of nanoparticle stability has been achieved by changing the surface of nanoparticles using chemical bonding of the organic molecules in the process of surface functionalization. For Au nanoparticles modification of the surface using this approach is based on their high affinity for formation of Au-S and Au-N bonds. There is a possibility for attachment of one or many different molecules with S- or N- containing groups onto the surface of these particles. According to the schematic illustration presented in Figure 4a, these molecules can be added along with the reduction agent and during particle formation they are automatically attached onto surface. In the next steps the side of the molecule opposite to the attachment to Au surface is used for attachment of other functionalizing molecules. Alternatively, the molecules which are meant to be chemically attached onto Au surface are used as their reduction agents. Accordingly, strong bonding is achieved and there is no risk for modification of the functionalizing molecules by strong, aggressive nature of reducing agents. This approach is highly applicable for design of Au nanoparticles as drug delivery carriers (Ghosh et al. 2008).

Stabilization of the surface provides control over morphological properties of metallic nanoparticles and has potential to influence their size and shape. As illustrate in Figure 4b, these changes are accompanied by the change of optical properties. For Au nanoparticles increasing the aspect ratio- starting form sphere to elongated rod-like morphology induces red shift of the surface plasmon resonance band of so-formed nanoparticles (Figure 4b(a)). Au nanoparticles may be formed in the form of core-shells as it was illustrated in Figure 4b(b) in the case of $Au@SiO_2$. Increasing the thickness of the Au layer as a shell moves the maximum of the surface plasmon resonance band to the lower wavelengths. Nanocages are formed as a result of galvanic displacement method, when more noble metals are reduced by less noble once. In that case increased content of Au shifts the maximum to higher wavelengths (Figure 4b(c)) (Dreaden et al., 2011; Dreaden et al., 2012).

Attachment of the molecular species onto the surface of metallic nanoparticles changes dielectric properties of their environment. Moreover, this type of surface modification may have opposite effect on their stability resulting in induction of their aggregation. In both cases, change of the dielectric properties of nanoparticle surroundings and agglomeration induces changes in optical properties. Surface plasmon resonance band is red shifted with increase of the dielectric permittivity and refractive index, while aggregation induces decrease of its intensity (Figure 4c) (Dykman and Khlebtsov, 2012).

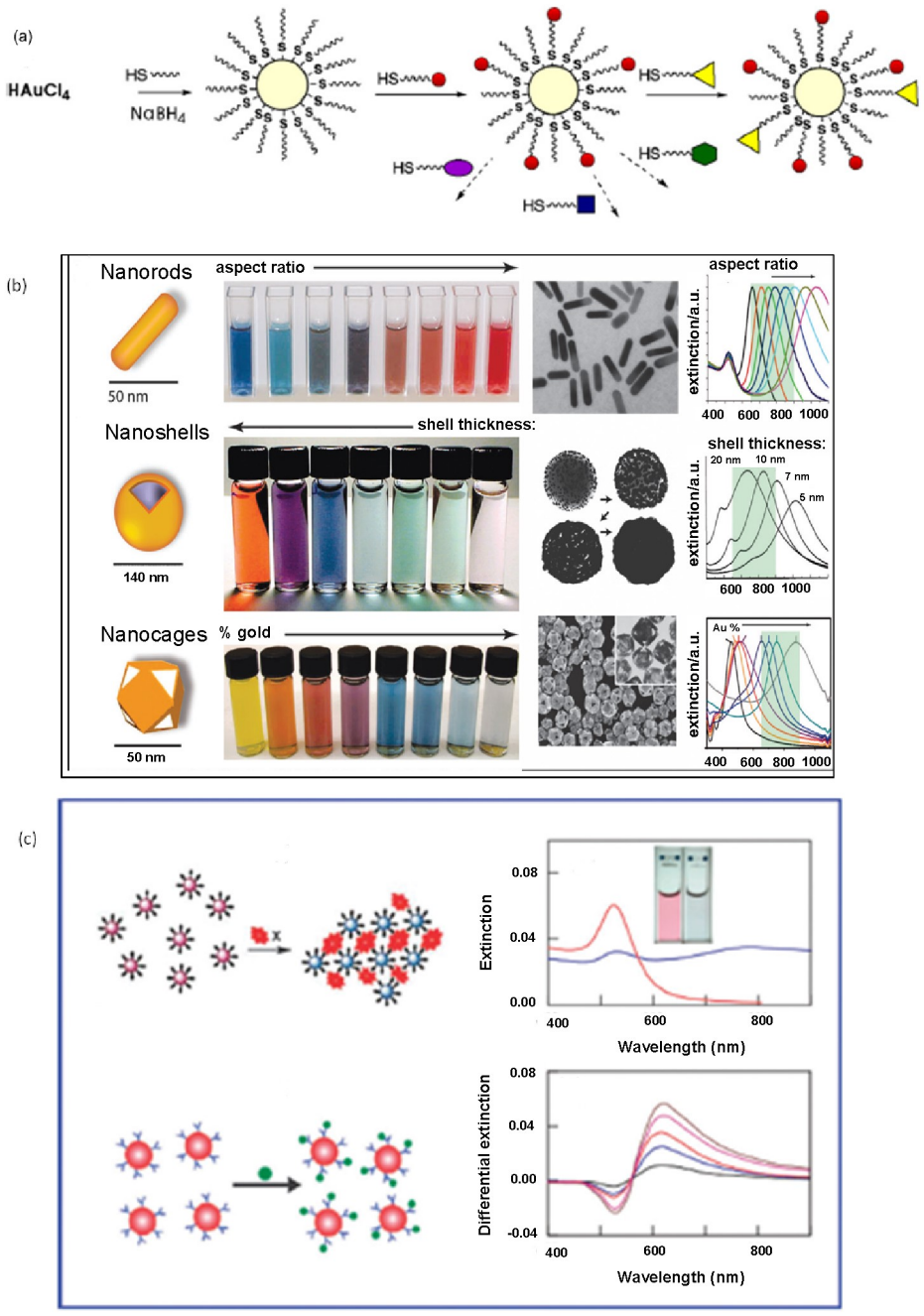

Figure 4: *Affinity of Au to form Au-S bonding (Ghosh et al., 2008) (a); optical properties of Au nanoparticles depend on their shape and size (Dreaden et al., 2011; Dreaden et al., 2012) (b), optical properties of Au nanoparticles depend on the surface functionalization (Dykman and Khlebtsov, 2012) (c).*

Described changes of optical properties of noble metals are consequence of their delocalized electrons whose density may be affected by external electromagnetic field. Free electrons of noble metals have collective plasmon oscillations. Coupling of the incident electromagnetic field (i.e. photons) with surface plasmons with similar frequency and angular momentum induces adsorption or scattering. Consequently, these matching induce surface plasmon resonance which is accompanied by increase of the magnitude of the resonating electromagnetic fields for several orders and enhance of the number of radiative and non-radiative processes. As already mentioned, wavelength of the surface plasmon resonance band maximum depends on the particle size and shape as well as on dielectric environment. Plasmonic metals are Li, Na, K, Mg, Al, Fe, Cu, Ag, Au and Pt.

Among them only Au and Pt are chemically inert and non-corrosive, while Au additionally has resonance in visible region. These properties are highly important for its biomedical application (Dreaden et al., 2011; Daniel and Astruc, 2004).

1.2.2 Medical applicability of noble metals

In the past noble metals are used for different medical purposes. Silver, as the only natural antimicrobial agent in the group of noble metals, has been used for different clinical conditions including epilepsy, wound healing, acnes, venereal infections and leg ulcer treatments. Silver foil was used to improve healing of the operative wounds and to prevent development of post-operative infections (Klasen, 2000).

Nowadays application of noble metals in medicine can be classified into two broad fields: (i) diagnosis and imaging and (ii) therapeutics (Wong and Liu, 2010).

1.2.2.1 Noble metals in diagnosis and imaging

Early diagnostic is the best way for easy and successful treatment of diseases. It is a rule which is true even for some very hard medical conditions such as cancer or detection of pathogens. Unique electrical, magnetic, luminescent and catalytic properties of metal nanoparticles enable fast, sensitive and low-cost detection of pathogens as well as their susceptibility or resistivity to some drug. Noble metals have some important properties such as surface plasmon resonance and ability for multivalent binding that were used for development of variety of analytic tools for fast and easy biomedical detection. It made them highly applicable for formation of biomarkers, biosensors and contrast agents (Wong and Liu, 2010).

Analytical tools developed by usage of the properties of metallic nanoparticles are: (i) spectroscopic analysis (surface Plasmon resonance spectroscopy (SPRS), local surface Plasmon resonance spectroscopy (LSPRS), fluorescence spectroscopy (FS), surface enhanced Raman spectroscopy (SERS) and mass spectrometry (MS) and (ii) electronic detection (electrochemical detection and chemiresistive sensing) (Zamborini et al., 2012).

Due to the specific catalytic abilities, Pt nanoparticles are particularly investigated for development of biosensors and biomarkers. They can be bind to the specific support and with addition of bioactive enzyme it can be designed as highly sensitive biosensor. Accordingly, it is able to provide precise electrochemical detection of low concentrations of some agents such as peroxides which is important for bioelectrochemical applications (Yang et al., 2006).

1.2.2.2 Noble metals in therapeutics

As therapeutics, noble metals are used for development of new drugs, medical procedures and medical devices.

Silver has been extensively used as antimicrobial agent for formation of (i) wound dressings and (ii) antibacterial coatings (Rai et al., 2009; Wong and Liu, 2010). An example of wound dressings is Anticoat® made of two polyamide ester membranes covered with Ag-ion containing nanocrystalline layers (Wright et al. 1998). In formation of antibacterial coating silver has been used for formation of: (i) silver-impregnated catheters, (ii) orthopaedic devices and (iii) surgical mesh (Wong and Liu, 2010). Among surface-impregnated catheters central venous catheters, ventricular drainage catheters and vascular prostheses are formed. Incorporation of central venous catheter is a common procedure in U.S. with implantation of about 5 million implants per year (Raad, 1998). This procedure is frequently followed by post-implantation infections and clinical practice showed that addition of the antimicrobial layer on the surface of implant helps in

overcoming this issue. Since development of the resistive species became an issue, silver coatings are used as more efficient solutions (Khare et al., 2007). In orthopaedics and dentistry, silver has been used in formation of different biomaterials for antibacterial coverage onto the surface of bone and dental implants. Composites of silver with bioceramics (as hydroxyapatite), made by supporting the metallic nanoparticles on the surface of ceramics (Kiyotomi et al., 2010) or by simultaneous incorporation of metallic particles inside and their deposition on the surface of ceramics (Lester, 2010) are materials highly applicable for this purpose. Surgical meshes are commonly used for bridging the large wounds and for reinforcement of the tissue repair. Infections related to their incorporation in the organism are usually associated with *Staphylococcus* development. Incorporation of silver inside these meshes has been found as useful procedure to overcome this issue (Wong and Liu, 2010). Besides listed examples related to the currently used Ag therapeutics in practice, its applications as anti-infective, antiviral (against HIV infection) and anti-platelets (against thrombotic disorders) drug is suggested for the future (Wong and Liu, 2010). However, inability of silver to make a difference between cells of pathogens and other live cells is a serious lack of this metal. This property makes silver toxic for human and its environment which is the main reason for the need to replace it with a "green" substitution.

Other members of noble metals (gold and platinum) are good candidates for silver replacement. These materials are inert which makes them "green" and non-toxic for human and its environment.

Gold has extraordinary surface properties which have been intensively investigated for carrying of various drugs while its surface plasmon resonance is considered for photothermal therapy. Au nanoparticles have possibility to adsorb light from 530 nm (SPR) and Au-antibody conjugated nanoparticles (with tuned SPR) absorb light form near infrared region (650-950 nm). Both are able to convert absorbed light to a heat. This great property has been developed as photothermal therapy and employed for targeted destroying of cancer cells, bacteria and viruses. In this case, Au nanoparticles are irradiated by lasers and they are acting as drugs themselves without addition of any other therapeutics. For this type of medical treatment it is very important that NIR light exposure has high-deep penetration into tissue, Au nanoparticles absorb light from this region with high efficacy and biological tissue have the lowest attenuation for these wavelengths (Ghosh et al., 2008; Dreaden et al., 2012). This approach is highly perspective and promising especially for cancer therapy.

Because of the strong affinity of gold to bind different molecules with amino and thiol groups, Au nanoparticles has been intensively studied as carriers of various types of drugs. It has been confirmed that, after appropriate labelling, these particles have potential to carry drug molecules attached onto their surface to the specific cells or even inside cell to the specific cellular compartments. Therefore, Au nanoparticles are used as carriers of both small molecules and macromolecules. Among small molecules transport of anticancer agents has been the most intensively studied. Some of the example are delivery of tamoxifen (anticancer agent) (Dreaden et al., 2009) for selective, target delivery to cancer cells (Figure 5a). Similar to the small molecules, Au nanoparticles are highly successful in delivery of biomolecules – peptides, proteins, DNK and RNK to the specific cells. These approaches are of great interest for development of the strategy for design of anticancer drugs (Patra et al., 2010; Ghosh et al., 2008). Au nanoparticles are unable to provide antibacterial effect which is available for Ag nanoparticles, but they can be design for it. An example is addition of magnetic component to Au nanoparticles combined with antibiotic which formed drug delivery system used for targeting of antibiotics to the bacteria in order to increase their activity (Rademacher et al., 2007). In all these cases there is a need to develop a strategy to release of the drug molecule from

the surface of Au nanoparticles. There is an example of composite made of thermoresponsible polymer with Au nanoparticles and loaded drug. After exposure to the light Au nanoparticles absorbed light transform into heat, polymer is transferred from rigid to viscoelastic form and drug is released (Figure 5b) (Hribar et al., 2011).

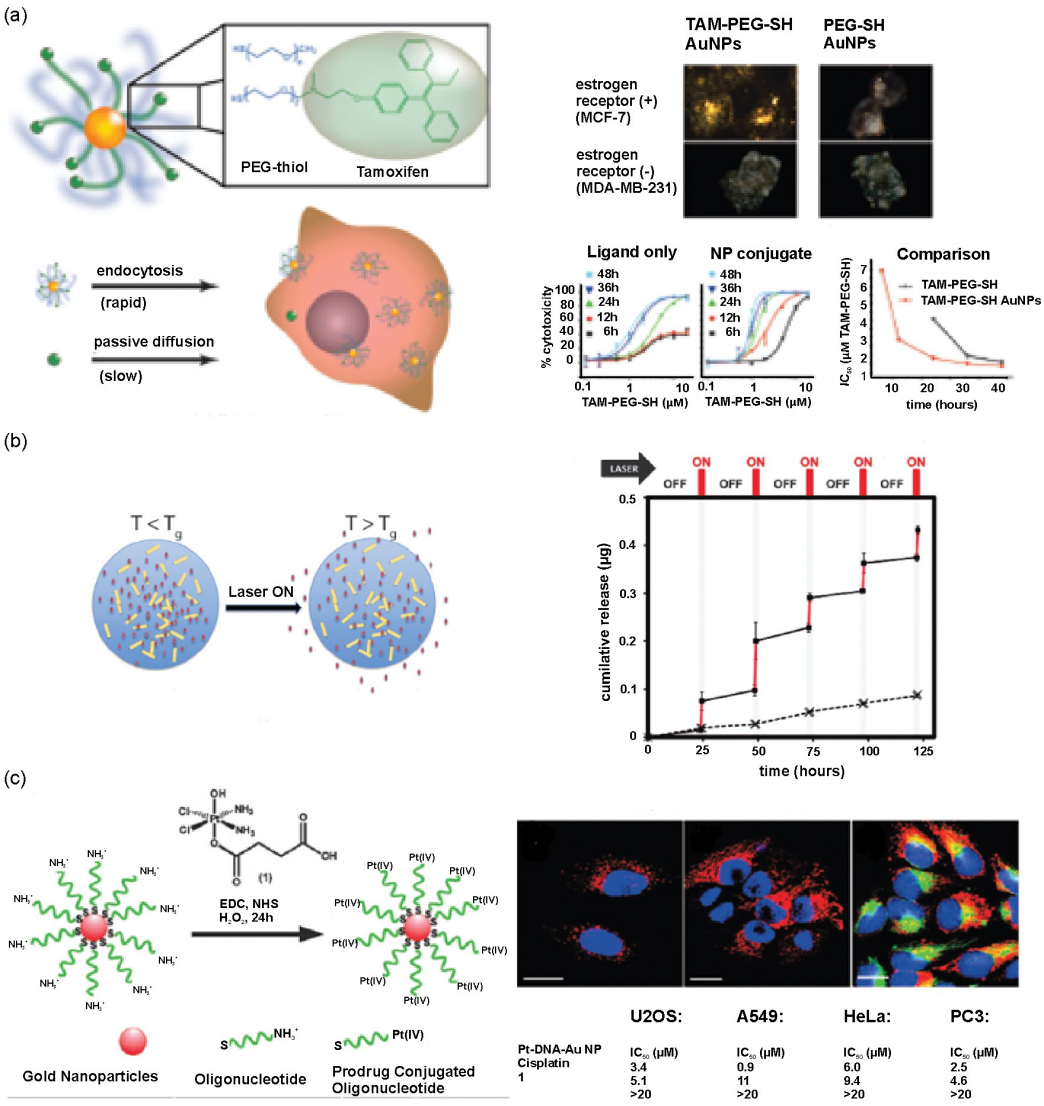

Figure 5: *Au nanoparticles as drug carriers: (a) PEG-thiol mediated capping the drug onto Au nanoparticles surface (Dreaden et al., 2009), (b) light-mediated release of the drug from thermoresponsible polymer matrix with loaded Au nanoparticles and molecules of the drug (Hribar et al., 2011) and (c) oligonucleotide mediated capping of Pt-complex onto Au-nanoparticles (Dhar et al., 2009).*

Unlike Au nanoparticles, medical applicability of platinum as therapeutics is not so intensively studied. It has been confirmed that some of its complexes as (cisplatin) have anticancer activity (Barefoot, 2001). There is a strategy developed for attachment of the Pt-complex onto the surface of Au nanoparticles in order to deliver it directly to cancer cells (Dhar et al., 2009). Complex is attached indirectly to the surface of Au nanoparticles using fluorescently-labelled oligonucleotide. After incubation with cervical cancer cells, significant intracellular accumulation has been demonstrated. Accordingly, target delivery increased the concentration of anticancer agents required to induce cancer cell death (Figure 5c). Same as for the gold, Pt nanoparticles does not have any antibacterial effect however its catalytic ability provides possibility to design this property.

1.2.2.3 Human health-related usage of noble metals

Because of its intensive antibacterial activity silver has been used for various other non-medical, human health related purposes (Sharma et al., 2009). Some of the examples are production of antibacterial textile and filters. Bioaerosols are air-born, biological sourced particles able to induce acute or chronic respiratory diseases. They are usually accumulated in heating, air-conditioning or ventilating systems and have potential for fast multiplying under increased humidity. Filters containing activated carbon fibers are usually used against bioaerosols, however since bacteria preferentially binds these fibers, addition of silver is used as more effective solution (Yoon et al., 2008). Similar was achieved in formation of ceramic-contained silver as filter for water purification. The usage of this filter has been suggested as a healthy, improved technology, although level of the silver in purified water was around 0.1 mg/mL (Oyanedel-Craver and Smith, 2008).

1.3 Hydroxyapatite in biomedicine

1.3.1 Hydroxyapatite bioceramics

As a member of orthophosphates, HAp belongs to the group of materials highly important in biomedicine. It has high level of similarity to the mineral part of the mammalian bone. This material possesses very high bioactivity and possibility to stimulate formation of cells and reparation of bone tissue. Therefore it has high potential to contribute to the better biocompatibility and bioactivity of composites it is forming as a component (Kiyotomi and Noritsugu, 2010; Lester, 2010).

Table 2: *Calcium orthophosphates and their major properties (Dorozhkin, 2010).*

Ca/P ratio	Compound	Formula	Solubility at 25°C -log(Ks) and g/L	pH stability range at 25°C
0.5	Monocalcium phosphate monohydrate (MCPM)	$Ca(H_2PO_4)_2 \cdot H_2O$	1.14/~18	0.0-2.0
0.5	Monocalcium phosphate anhydrous (MCPA)	$Ca(H_2PO_4)_2$	1.14/~17	
1.0	Dicalcium phosphate dihydrate (DCPD), mineral brushite	$CaHPO_4 \cdot 2H_2O$	6.59/~0.088	2.0-6.0
1.0	Dicalcium phosphate anhydrous (DCPA), mineral monetite	$CaHPO_4$	6.90/~0.048	
1.33	Octacalcium phosphate (OCP)	$Ca_8(HPO_4)_2(PO_4)_4\ 5H_2O$	96.6/~0.0081	5.5-7.0
1.5	α-tricalcium phosphate (α -TCP)	$\alpha\text{-}Ca_3(PO_4)_2$	25.5/~0.0025	
1.5	β-tricalcium phosphate (α -TCP)	$\beta\text{-}Ca_3(PO_4)_2$	28.9/~0.0005	
1.2-2.2	Amorphous calcium phosphate (ACP)	$Ca_xH_y(PO_4)_z\ nH_2O$ n=3-4.5; 15-20% H_2O		5.0-12.0
1.5-1.67	Calcium-deficient hydroxyapatite (CDHA)	$Ca_{10-x}(HPO_4)_x(PO_4)_{6-x}$ 0<x<1	85.1/~0.0094	6.5-9.5
1.67	Hydroxyapatite (HA or OHAp)	$Ca_{10}(PO_4)_6(OH)_2$	116.8/~0.0003	9.5-12
1.67	Fluoroapatite (FA or FAp)	$Ca_{10}(PO_4)_6F_2$	120.0/~0.0002	7-12
2.0	Tetracalcium phosphate (TTCP or TetCP) mineral hilgenstockite	$Ca_4(PO_4)_2O$	38-44/~0.0007	

Physico-chemical properties of HAp such as particles size, shape, size distribution, degree of agglomeration, crystallinity, surface charge, wettability etc. are highly important for its biological response and they can be influenced by the route used for its formation (Juhasz and Best, 2012). It has been shown that calcium-to-phosphate ratio of this material has important influence on its solubility and degradability which affect interactions *in vivo*. As for the natural-sourced apatite which is Ca-deficient and carbonated HAp, better bioactivity is reached for HAp with decreased Ca/P ratio. Stoichiometric HAp is stable in the range between 9.5 and 12, while stability ranges of Ca-deficient HAp and octacalcium-phosphate (as the major HAp precursor phase) are between 6.5 and 9.5 and 5.5-7.0, respectively. These ranges may be effectively used for the synthesis of HAp with improved biological reply and for the doping of different ions within apatite structure in order to reach parallel tune of two properties of this material-electrical properties and bioactivity (Doroszhkin, 2010). Some of the physico-chemical properties of orthophosphates are summarized in Table 2.

HAp has long been used for the reparation and reconstruction of bone tissues which is the main field of the practical application of this material. Because of the brittle nature and low mechanical properties its usage in mainly related to formation of bone cements and bioactive coatings made onto the surface of bioinert materials (Dorozhkin, 2009). In the form of composites, its mechanical properties can be improved which provides possibility to extend its applicability (Ignjatović et al., 1999; Ignjatović et al., 2007). Some of the relatively new field of application of this material is its usage in formation of carriers for controlled delivery of drugs. An example is formation of core-shell structure made of HAp core and polymeric shell. Material contains a drug which can be released in a controlled manner depend on the degradation of polymeric layer. In so-formed material, HAp influences degradation of the polymer, controls microenvironmental acidity and contribute to bioactivity (Vukomanović et al., 2011a; Vukomanović et al., 2011b; Vukomanović et al. 2011c; Vukomanović et al. 2012a).

1.3.2 Hydroxyapatite (bio) semiconductor

Concerning the electronic structure, HAp is a natural-sourced, wide-band gap semiconductor (Figure 6a) (Aronov et al., 2007a; Aronov et al., 2007b). It possesses very interesting surface properties including a hydrophilic nature, very good affinity for adsorption of various macromolecules (including proteins and nucleic acids) and a high density of surface polar groups which provide good bioactivity. As already mentioned, as a major constituent of inorganic part of the bone, this material is intensively studied as a bioceramic with high applicability in the field of biomedicine for regeneration and replacement of bone tissue (Yamagishi et al., 2005). Unlike its applicability in regenerative medicine, its potential biomedical usage in the form of photocatalyst is not extensively studied.

Under the irradiation by UV light there is a modification of PO_4^{3-} groups on the surface of HAp and formation of trapped electrons and highly reactive $OH^{\cdot}$ and $O^{2-\cdot}$ species (Nishikawa, 2003a; Nishikawa, 2003b; Nishikawa, 2007). Consequently, the material possesses photo-induced activity and ability to decompose non-degradable azo dyes (as calmagite) (Reddy et al., 2007). Besides in solutions, exposure of HAp to UV light provide its ability to decompose gaseous, organic substances with very bad small like methyl mercaptane (Nishikawa and Omamiuda, 2002) as well as highly toxic organic substances like dimethyl sulphide (Nishikawa, 2004). Since its high adsorptive nature and ability to storage electrons, HAp has been also used for formation of composite with TiO_2 in order to improve its ability to induce degradation of organics under UV irradiation (Nishikawa et al., 2005; Ye et al., 2007; Funakoshi and Nonami, 2006). Domination of a

PO_4^{3-}- sublattice together with Ca-channels which are present in these systems makes them highly acceptable for a variety of ion-exchanges. These structural changes are suitable to induce significant variations in the electronic structure (Figure 6b) (de Araujo et al. 2010) which provide useful possibility for modulation of the band gap of apatites affecting their optical properties (Rulis et al., 2004). It has been shown that doping of HAp with different ions (Cr^{3+}, Zn^{2+}, Fe^{3+}) provides broadening of the adsorption band of HAp from UV to visible region (Figure 7). The last was considered as an interesting tool for the application in sunscreen production. Doping of HAp with Ti-ions resulted in decreasing of the band gap energy of this material due to the formation of hybridized band within forbidden layer which allowed decomposition of acetaldehyde by near UV light with lower photon energy (Tsukada et al., 2011). The same Ti-doped material had ability to decompose albumin and to induce antibacterial effect against *E. coli* after exposure to UV light (Wakamura et al., 2003).

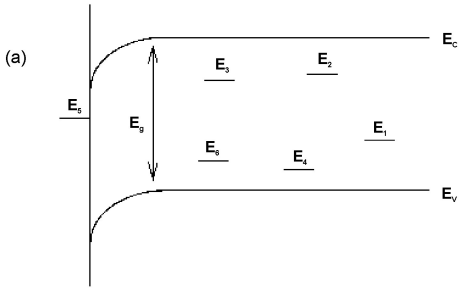

Table 3 Energy structure of electron (hole) states in Hydroxyapatite measured by surface photovoltage spectroscopy method

Sample type	E_1 (eV)	E_2 (eV)	E_3 (eV)	E_4 (eV)	E_5 (eV)	E_6 (eV)	E_g (eV)
A	2.6	2.8	3.0	3.2	3.3	3.4	3.9
P	2.6	2.9	3.0	3.2	3.3	3.4	3.9

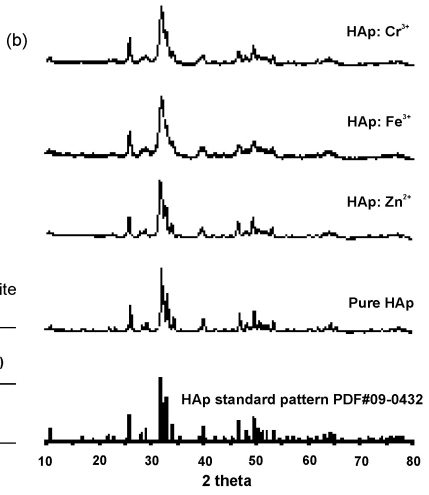

Figure 6: *Band diagram of hydroxyapatite:E_1-E_4 and E_6 are bulk states, E_5 is a surface state and E_g is a band gap (Aronov et al., 2007a) (a); X-ray diffraction patterns and UV/VIS spectra of HAp and HAp doped materials (de Araujo et al. 2010) (b).*

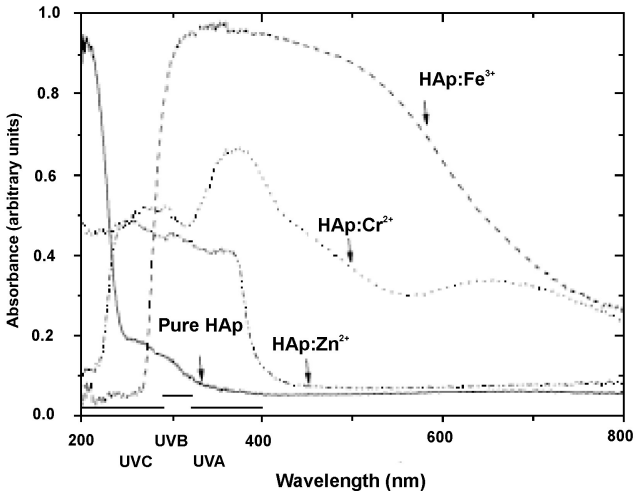

Figure 7: *UV/VIS spectra of HAp and HAp doped materials (de Araujo et al. 2010).*

1.4 Hydroxyapatite/noble metal composites

1.4.1 Hydroxyapatite/silver

So far, four different concepts for the formation of hybrids and composites formed of HAp and Ag have been reported: (a) HAp particles with Ag ions incorporated into the structure, (Shirkhanzadeh et al., 1995; Rameshbabu et al., 2007; Hwang et al., 2008; Ewald et al., 2011; Ciobanu et al., 2011) (b) HAp particles with Ag nanoparticles attached to the surface (Chen et al., 2006; Arumugam et al., 2007; Liu et al., 2008; Diaz et al. 2009; Sygnatowicz et al., 2010), (c) functionally graded HAp/Ag materials composed of Ag nanoparticles that were gradient-style distributed inside the HAp matrix (Bai et al., 2010) and (d) HAp/Ag composites with combination of incorporated Ag-ions and embedded/attached Ag nanoparticles (Vukomanović et al., 2011d) (Figure 8).

The incorporation of Ag ions into apatite is based on the ion-exchange ability of the apatite structure, and for that purpose methods based on ion adsorption from the solution during aging, (Shirkhanzadeh et al., 1995) electrostatic spraying (Rameshbabu et al., 2007), microwave processing (Hwang et al., 2008), solid state processing (Ewald et al., 2011) and co-precipitation (Ciobanu et al., 2011) were applied. In this case, a slow-rate release of Ag ions from the apatite structure, provide antibacterial effect of the material.

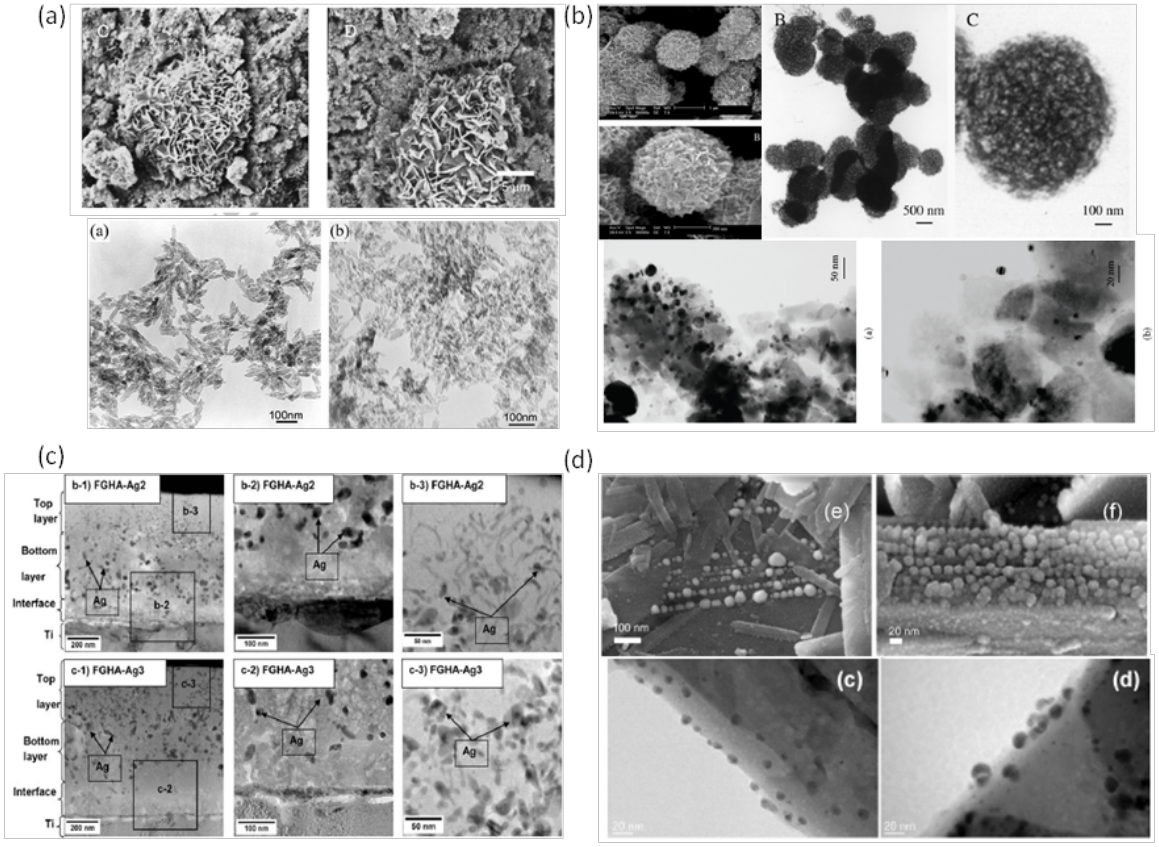

Figure 8: *HAp/Ag materials: (a) Ag-doped HAp (Ewald et al., 2011; Rameshbabu et al., 2007) , (b) Ag nanoparticles onto HAp (Liu et al., 2008; Diaz et al. 2009), (c) Ag nanoparticles with a gradient-style distribution within HAp matrix (Bai et al., 2010) and (d) Ag-ions doped and Ag nanoparticle attached/embedded HAp (Vukomanović et al., 2011d).*

The HAp/Ag material with Ag particles attached to the HAp surface was obtained using the sol-gel method (Sygnatowicz et al., 2010), chemical reduction by the OH-

groups from the surface of the HAp (Arumugam et al., 2007), magnetron co-sputtering (Chen et al., 2006), electrostatic adsorption of ultrasonically-dispersed previously synthesized Ag particles (Liu et al., 2008) and the colloidal chemical route followed by a thermal treatment (Diaz et al. 2009). For these materials, the metallic Ag nanoparticles deposited on the surface were responsible for the antibacterial activity.

A similar effect was achieved in the case of a functionally graded HAp/Ag composite. The material was obtained by the processes of simultaneous, ion-beam-assisted deposition and thermal reduction. The Ag particles incorporated within the HAp were responsible for the antibacterial activity and for the improvement of the mechanical properties of these bioceramics (Bai et al., 2010).

Sonochemistry offers huge possibilities for the development of nano-sized and nano-structured materials, basically because it enables a control of their structure and morphology. In the case of noble metals obtained by this method, both physical and chemical effects related to intensive mixing and the formation of reactive radicals are included (Bang and Suslick, 2010). There are several examples of the application of sonochemistry for the formation of Ag nanoparticles. This method allowed the formation of various morphologies and structures of Ag, starting from rod-like (Zhu et al., 2010) and sphere-like nanoparticles (Perkas et al., 2008), to dendrite nanostructures (Wang et al., 2009b) and amorphous Ag (Salkar et al., 1999). It is interesting to note that, like with many other methods, in all of these concepts of sonochemical synthesis involving Ag nanoparticles the same silver precursor ($AgNO_3$) is used.

Although the sonochemical approach has made a significant contribution to the synthesis of Ag nanoparticles, less attention has been given to the possibility of forming their composites with HAp. Therefore, we developed a homogeneous sonochemical precipitation method for the synthesis of Ag nanoparticles and their composites with HAp. During this procedure different sources of silver were used in order to study morphological and structural properties of the resulting materials and to investigate the mechanism of their formation after the application of this new approach to synthesis. Consequently, among already existing concepts for formation of HAp/Ag composites, we developed the forth, the new one. Formed material had three sources with potential antibacterial activity: (i) Ag-ions incorporated within HAp structure, (ii) smaller Ag nanoparticles embedded within apatite plates and (iii) larger Ag nanoparticles mechanically attached onto the surface of these plates. Formed Ag nanoparticles had two different structures, hexagonal and cubic, and two different particle shape, spherical and hexahedral (Vukomanović et al., 2011d).

1.4.2 Hydroxyapatite/platinum

One of the rare examples when visible light- induced activity of HAp has been achieved is formation of HAp/Ag/TiO_2 composite (Liu et al., 2010). It has been explained that formation of composite with silver nanoparticles visible-light induced activity can be assisted by near-field amplitudes of localized surface plasmon resonance (Bračko et al., 2011). Searching for the biomimetic approach in order to form human and environmental friendly materials leads to other members of noble metals- platinum (Pt) and gold (Au) (AshaRani et al., 2010). In the case of platinum nanoparticles mention effect is missing, however doping of semiconductor by Pt-ions and/or functionalization of its surface by PtX_n complex results in activity of finally-formed material under visible light, as it has been shown for TiO_2/Pt-ion and TiO_2/$PtCl_x$ (Burgeth and Kisch, 2002; Kim et al., 2005a).

According to our opinion, application of this approach to HAp in order to form HAp/Pt composite with adsorbed complexes has potential to provide significant improvement of photocatalytic performances of this material. It is expected that activation of this material

could be extended to visible region in order to form a novel, bio-sourced, high-performance photocatalyst applicable in biomedicine. This hypothesis was proven and HAp/Pt material, which was synthesized for the first time by Vukomanović and co-workers (Vukomanović et al., 2012b), had strong photocatalytic activity that could be initiated by visible or ultraviolet light and it had ability for extended activity in dark due to the action of Pt nanoparticles. Developed material had stronger activity in comparison with commercial P25 titanium dioxide. HAp/Pt composite was formed by modified homogeneous precipitation method previously used for formation of HAp/Ag composite (Vukomanović et al., 2011d). During formation of the composite, sonochemical synthesis resulted in formation of HAp with Pt-complex attached onto its surface. After thermal reduction under Ar/H_2 atmosphere, complex was partially reduced inducing formation of Pt nanoparticles attached onto HAp plates. It was formed as a hybrid semiconductor/metallic composites made of apatite plates with Pt metallic nanoparticles attached on their surface and two different types of surface adsorbed complexes. So-formed material had interesting photocatalytic activity.

1.4.3 Hydroxyapatite/gold

There are a few examples of composites formed of Au nanoparticles and HAp bioceramics. Basically, their difference depends on the type of the potential application. HAp/Au composites have been considered for different biomedical and non-biomedical applications such as: (1) catalytic activity in oxidation of CO (Dominguez et al., 2009); (2) electrocatalytic detection of hydrogen-peroxide as biosensor (Monkawa et al., 2006; You et al., 2009; Aryal et al., 2006; Sastry et al., 2008; Gupta et al., 2006); (3) detection of protein adsorption as biosensor (Monkawa et al., 2006); (4) regulation of the cell function by promoting of the cellular growth and as carriers of the drugs (including known anti-infective agents) in the form of bioactive coatings (Biris et al., 2010; Jin and Oh, 2008) and (5) inactivation of Gram positive and Gram negative bacteria as antibacterial agent (Vukomanović et al., 2012c).

For the case of preparation of catalyst, Au nanoparticles were supported onto the surface of previously synthesized HAp by the procedure of deposition-precipitation. So obtained material was able to induce CO oxidation (Dominquez et al., 2009).

Formation of biosensor concerns different formulations of this material. One of them is thin film of HAp nanocrystals deposited onto the surface of Au substrate. The material is suitable for protein adsorption analysis (Monkawa et al., 2006). Another example is composite formed of HAp nanotubes with surface-deposited Au nanoparticles. After immobilization of haemoglobin onto HAp/Au, formed material was useful for electrocatalytic detection of hydrogen peroxide (You et al., 2009). Additional formulation concerns Au nanoparticles capped by natural proteins, collagen (Aryal et al., 2006) or fibrin (Sastry et al., 2008), as well as by the nucleobase polymer (Gupta et al., 2006) and their deposition onto HAp. So obtained materials have good mechanical properties and they have been suggested for application in tissue engineering. It has been also shown that amino acid (aspartic acid)-capped Au nanoparticles are able to bind calcium ions and to act as a template for control of the crystallization of calcium phosphates (like hydroxyapatite) (Rautaray et al., 2005). None of these composites containing gold nanoparticles have been designed nor investigated for antibacterial activity.

HAp and Au have been considered as components for production of biocompatible surfaces. The coatings are formed by using depositing techniques (lithographic pattering or thin film deposition) and bonded to the surface by compression, electric arc spot welding or high temperature diffusion bonding method. The main purpose of these coatings is in formation of bioactive surface layer. They are planned to be used for

improvement of the interaction of medical products with cells. It is important for different biomedical devices such as implants, biochips, bioreactors, biosensors, etc. So obtained surfaces are also useful for production of cell substrates. They could contain bioactive agent within multi-functional implant device. This device comprises bioactive agents from the group of pharmaceuticals, therapeutic drugs, cancer drug, growth factor, protein, enzyme, hormone, nucleic acid, antibiotic, nanoparticle and biologically active material. The device is able to provide controlled release of the active agent by the application of external (electromagnetic or ultrasonic) field (Jin and Oh, 2008).

HAp and Au have also been included within the method for regulation of cellular function. Material system has core-shell structure and it coats the surface of another material. These core-shells are 50 μm to 50 mm in size and can be made of various materials including gold, metal, metal oxide, polymer, titanium dioxide, silver, carbon nanotubes, hydroxyapatite, quantum dots, crystals, salts, ceramic materials, magnetic materials and any combination thereof. Material system has been described as a surface coating or as a system for delivery of the drugs and bioactive substances. In the first case when material is used as coatings on the surface of medical devices and implants it has been specified that Au or HAp are used for the promotion of the tissue growth. If drug delivery is concerned, these systems contain at least one agent (protein, growth factor, antibody, amino acid, polymer, drug, hormone, nucleic acid, peptide, or enzyme) linked to the nanoparticle. It has been specified that the cellular function that can be regulated by so developed stimulating agent made of nanoparticle linked with mentioned agent(s) is bone growth (Biris et al., 2010).

For the first time HAp/Au composite has been designed as materials with antibacterial activity by Vukomanović and co-workers (Vukomanović et al., 2012c). Activation of the Au-component for action against bacterial has been achieved by surface functionalization using different amino and/or thiol molecules (such as amino acids). So-obtained materials had high antibacterial activity and high compatibility with human cells which make them “green”, human and environmental friendly substitutions for Ag-containing antimicrobials.

Procedures developed for formation of HAp/Au are different variations of deposition procedure (deposition of HAp onto previously synthesized gold/protein matrix or deposition of Au on previously formed HAp). This approach usually results in particles agglomeration and low stability of Au nanoparticles attached onto HAp or vice versa. Application of sonochemical method, developed for formation of antibacterial HAp/Au, when different functionalizing molecules were also used as reduction and stabilizing agents produced stable HAp/Au composite. Material was formed of Au nanoparticles with functionalized surface which were attached onto HAp plate-like carriers. Particles were well distributed onto HAp surface and without signs of agglomeration (Vukomanović et al., 2012c).

1.5 Mechanisms of antibacterial activity of noble metals

1.5.1 Natural antibacterial activity of silver

Silver is a member of noble metals with natural ability for activity against bacteria. It has the strongest antibacterial activity among all inorganic materials that possess this property. Mechanism of its action is not completely clear, however the most of the up-to-date results are suggesting following three mechanisms which are illustrated in Figure 9: (i) free Ag-ions mechanism- uptake of free Ag-ions by bacteria cell that induce disruption of ATP production and damage of DNA which prevent its replication; (ii) mechanism of

generation of reactive radicals- ROS production by Ag-ions and Ag nanoparticles that induce oxidative stress and (iii) mechanism of cellular membrane disruption by Ag-nanoparticles (Marambio-Jones and Hoek, 2010).

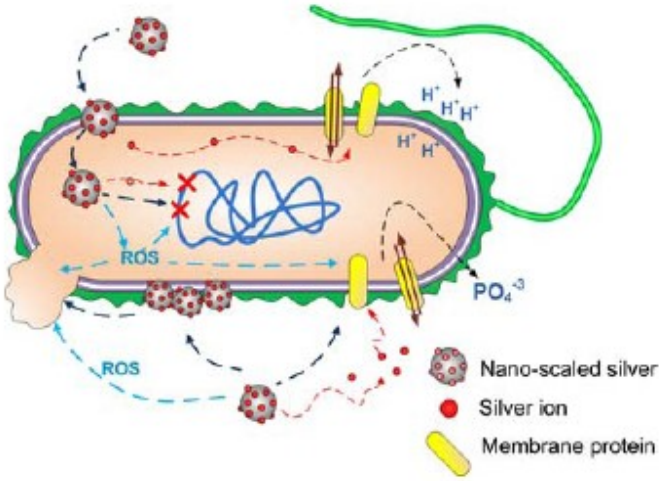

Figure 9: *Schematic illustration of the proposed mechanisms of antibacterial activity of silver (Marambio-Jones and Hoek, 2010).*

1.5.1.1 Free-Ag-ions mechanism

Materials containing Ag-ions (without presence of Ag nanoparticles) are one of the sources for free-Ag-ions mechanism of antibacterial activity. Some of the examples are materials with Ag-ions doped inside the structure of other material (as AgHAp) (Figure 10) and materials with Ag-ions adsorbed onto the surface of other material by interactions with polar groups (such as Ag^+ interacting with surface OH^- groups of HAp within HApAg or HApAg/TiO_2 composite) (Figure 11). In both cases materials are able to release Ag-ions which are the major source of antibacterial activity (Rameshbabu et al., 2007; Hwang et al., 2008; Mo et al., 2008; Shirkhanzadeh et al., 1995). For Ag-ions adsorbed/immobilized onto HAp surface proposed mechanism for their release concerned their diffusion or ion-exchange (Shirkhanzadeh et al., 1995). For Ag-doped HAp materials precise mechanism for Ag-release was not proposed, however it may be presumed that physiological conditions (pH, ionic strength, metabolites etc.) are able to influence desorption of adsorbed Ag-ions from the surface or partial dissolution of HAp which release doped Ag-ions.

Another source of Ag-ions responsible for the free-Ag-ions mechanism of antibacterial action is dissolution of Ag nanoparticles. Two different reactions have been proposed for oxidative dissolution of Ag nanoparticles under physiological conditions. First mechanism proposes involvement of hydrogen peroxide. It was suggested that increased concentration of H^+ ions and presence of H_2O_2 in mitochondria are able to induce oxidative dissolution of Ag nanoparticles inside cell in accordance with reaction presented by Eq. 1 (AshaRani et al., 2009). The reaction was proposed for toxic effect in eukaryotic cells and it was hypothesized that the same method silver uses for activity against bacteria (Marambio-Jones and Hoek, 2010).

$$2Ag + H_2O_2 + H^+ \longleftrightarrow 2Ag^+ + 2H_2O \qquad E^0=0.17\ eV \qquad (1)$$

$$2Ag + O_2 + H_2O \longleftrightarrow 4Ag^+ + 4OH^- \qquad (2)$$

The second mechanism proposed oxidative dissolution of Ag nanoparticles by oxygen

in accordance with the Eq. 2. It was speculated that Ag nanoparticles are oxidized because of the change of the colour of their dispersion after aging during a week. After separation of Ag nanoparticles, measurements revealed presence of low concentration of Ag-ions in solution which corresponded to 2.2% of the totally dispersed Ag nanoparticles (Choi and Hu, 2008).

Therefore, free Ag-ions are formed by: (i) release of Ag-ions from another material or (ii) dissolution of Ag nanoparticle. It was suggested that so-formed Ag-ions may interact with bacteria in several different ways. Majority of them are associated with possibility for interaction of Ag-ions with macromolecules (enzymes, proteins, nucleic acids) resulting in blocking of their normal functions. Some of the illustrative examples are: (i) interaction of Ag-ions and enzymes of the respiratory chains (such as NADH dehydrogenase) that decoupled respiratory chain from ATP synthesis; (ii) binding the Ag-ions on transport proteins in the membrane (Lok et al., 2006) that prevent normal transport of ions (such as transport of PO_4^{3-}) (Schreurs and Rosenberg, 1982) and (iii) induction of the mutation of DNA due to the structural changes induced by attachment of Ag-ions (Yang et al., 2009). Structural and conformational changes of macromolecules induced by attachment of Ag-ions are associated with cellular shrinkage, detachment of the cellular wall and/or its degradation and rupture and condensation of DNA (Jung et al., 2008).

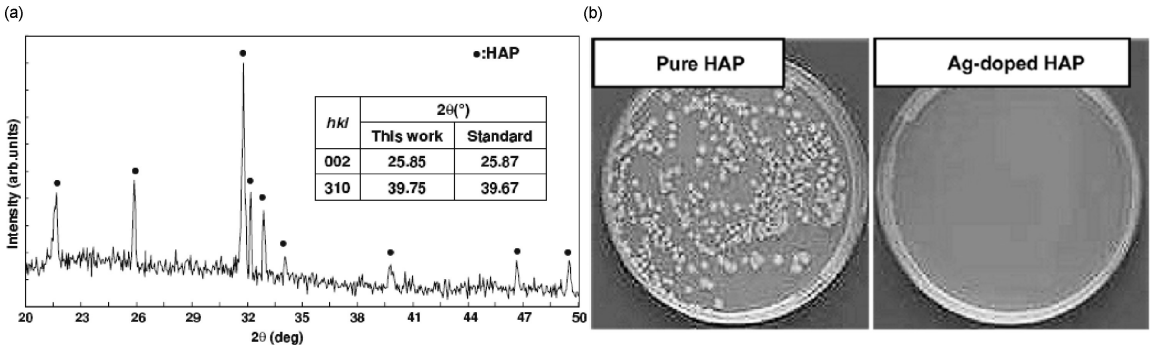

Figure 10: *XRD pattern of Ag-doped HAp without presence of Ag-nanoparticles (a) and corresponding antibacterial activity (b) (Hwang et al., 2008).*

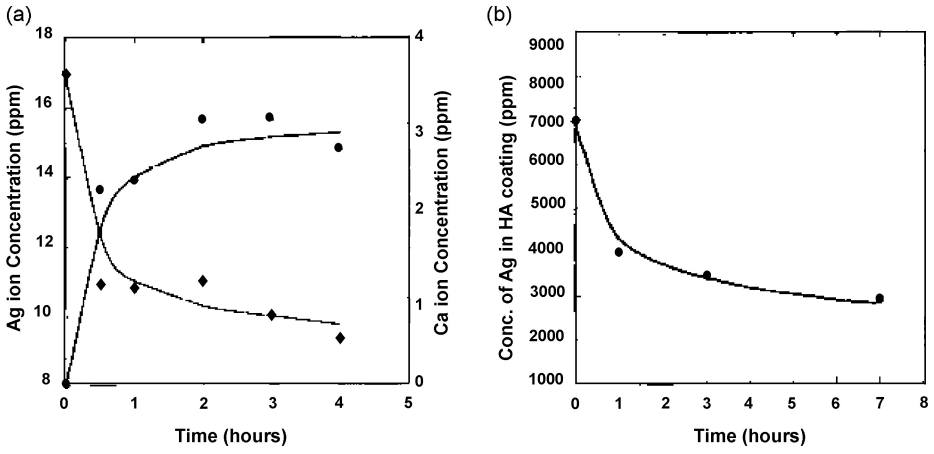

Figure 11: *Absorption and immobilization of Ag-ions into HAp by Ca-replacement (a) and release of the adsorbed/immobilized Ag ions under physiological conditions (b) (Shirkhanzadeh et al., 1995).*

1.5.1.2 Mechanism of generation of reactive radicals

Ability for production of reactive radicals by silver was detected in eukaryotic cells, which was associated with silver toxicity (detailed description in the next chapter). Accordingly it was proposed that similar effect may be associated with antibacterial activity of silver (Marambio-Jones and Hoek, 2010).

Investigations performed on Ag-ions loaded zeolites, confirmed that different reactive radicals are involved in antibacterial activity. It has been detected that superoxide anions, hydrogen peroxide, hydroxyl radicals and singlet oxygen are involved (Inoue et al, 2002). Usage of the scavengers of these radicals decreased antibacterial activity of material. Moreover, two independent investigations confirmed a critical role of dissolved oxygen in antibacterial activity of Ag-ions. In the absence of oxygen, antibacterial activity could not be obtained (Inoue et al, 2002; Yoon et al. 2008). Observed effect was completely in contradiction with previously described mechanism of free Ag ions. If oxygen is required, antibacterial activity cannot be explained by natural affinity of Ag-ions to attach macromolecules and to destroy their structure.

Kim et al. detected formation of reactive Ag-radical and correlated it with antibacterial activity of tested Ag nanoparticles (Figure 12a, b). When antioxidants were added the same activity against bacteria was completely lost (Figure 12c). These results lead them to conclusion that antibacterial activity of Ag nanoparticles is related to reactive radicals formed by dissolution of the surface layers of Ag nanoparticles. According to their opinion, Ag-radicals are able to attack extracellular side of bacterial membrane and to induce its damage (Kim et al., 2007). Accordingly, authors were suggesting that Ag nanoparticles and Ag-ions have different antibacterial mechanism. Ag ions get inside cell while Ag nanoparticles affect cellular surface. Results are important since they are confirming that antioxidants may be used as antidotes for silver-related toxicity.

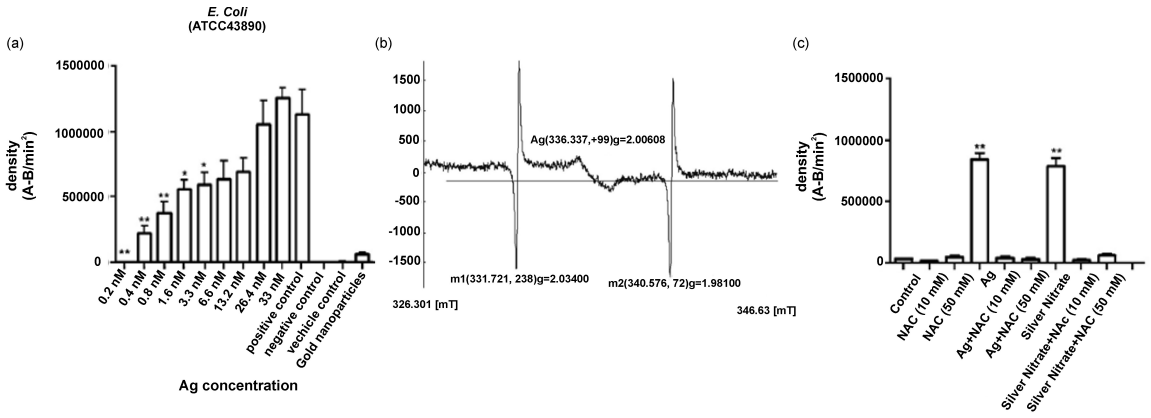

Figure 12: *Antibacterial activity of Ag nanoparticles against E. coli, ESR detection of ability of silver to form free radicals, complete loss of the antibacterial activity of silver by addition of antioxidant (c) (Kim et al., 2007).*

Further studies confirmed that besides Ag-ions, Ag nanoparticles also have ability to enter bacterial cell and to induce formation of reactive radicals inside it confirming the same mechanism. The question that remained unresolved was related to the fact that toxicity of Ag nanoparticles induced by distinct level of oxidative stress was higher than toxicity of some other material after induction the same level of oxidative stress (Choi at al., 2008). Explanation may be related to the more invasive type of the radicals induced by Ag or to another mechanism simultaneously involved together with ROS production.

1.5.1.3 Mechanism of cellular membrane disruption

TEM investigations confirmed that Ag particles have ability to attach the surface of the membrane as well as to enter inside cell (Figure 13a). It is not fully understood how these particles cross the membrane. Some researchers suggested electrostatic interactions between negatively charged bacterial surface and positively charged Ag nanoparticles (Raffi et al., 2008). However, this explanation was not able to explain crossing the membrane by negatively charged Ag nanoparticles. Another explanation was related to their interactions with the sulphur-sites in transporting proteins. Consequently proteins are damaged and/or cellular permeability is increased (Morones et al., 2005).

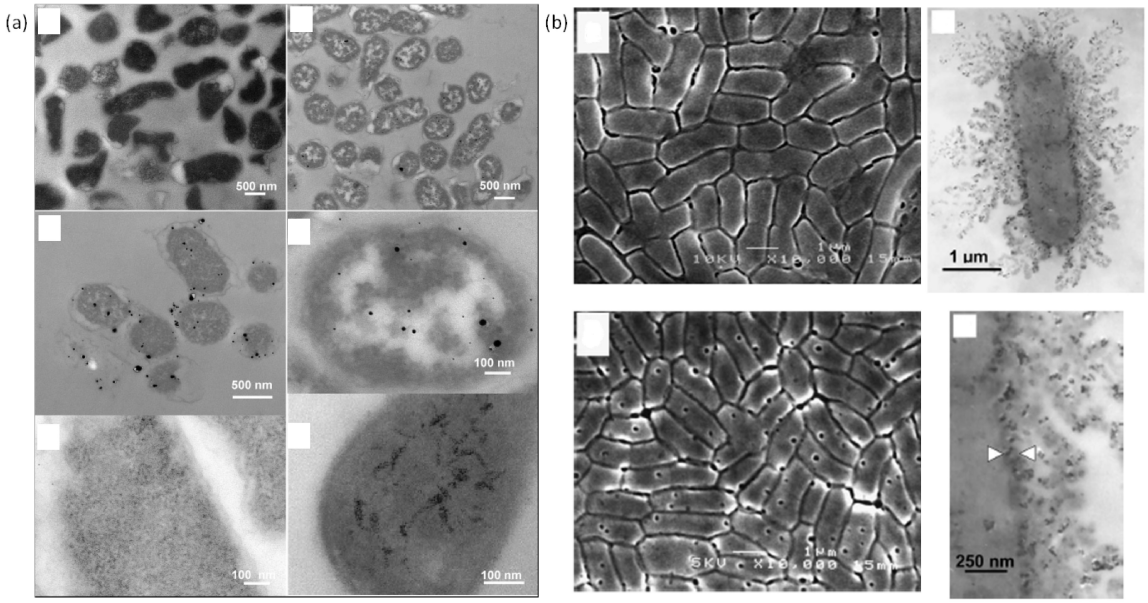

Figure 13: *Ag nanoparticles inside bacteria (Smetana et al., 2008) (a); pit-damages on the membrane of bacteria and adhesion of nanoparticles on the surface and their crossing over bacterial membrane (Sondi and Salopek-Sondi, 2004) (b).*

Regardless to the mechanism of their entrance inside cell, according to the literature, ability of Ag nanoparticles to induce formation of the damages in the bacterial membrane belongs to the additional mechanism which was assigned to Ag nanoparticles (Marambio-Jones and Hoek, 2010). Some researchers showed pit-shape damages (Figure 13b) in the membrane of Gram negative bacteria which were assigned to the activity of Ag nanoparticles (Sondi and Salopek-Sondi, 2004). Besides formation of these mechanical damages, they suggested influence of the Ag nanoparticles on permeability of the membrane by progressive release of membrane proteins and lipopolysaccharide (LPS) molecule. The mechanism is effective for Gram negative bacteria, however does not provide explanation for antibacterial activity of Ag against Gram positive bacteria (without LPS) and other pathogens.

Antibacterial activity of Ag nanoparticles was also affected by their size, shape and structure (Rai et al., 2009). Particles smaller than 10 nm have stronger activity in comparison to the activity of larger once. It was assigned to increased reactivity due to the quantum size effect. Moreover, smaller particles had larger surface area contacting bacterial membrane. For the shape it was observed that the most efficient antibacterial activity have truncated triangular particles with bacterial growth inhibition by 1µg, less active were sphere-like particles with inhibition by 12.5 µg and the least active were rod-like particles with the lowest efficacy and inhibition by 50-100 µg of powder. Contribution of the particle shape to antibacterial activity was assigned to the presence of

highly reactive (111) planes present at the surface of these structures (Figure 14) (Morones et al., 2005).

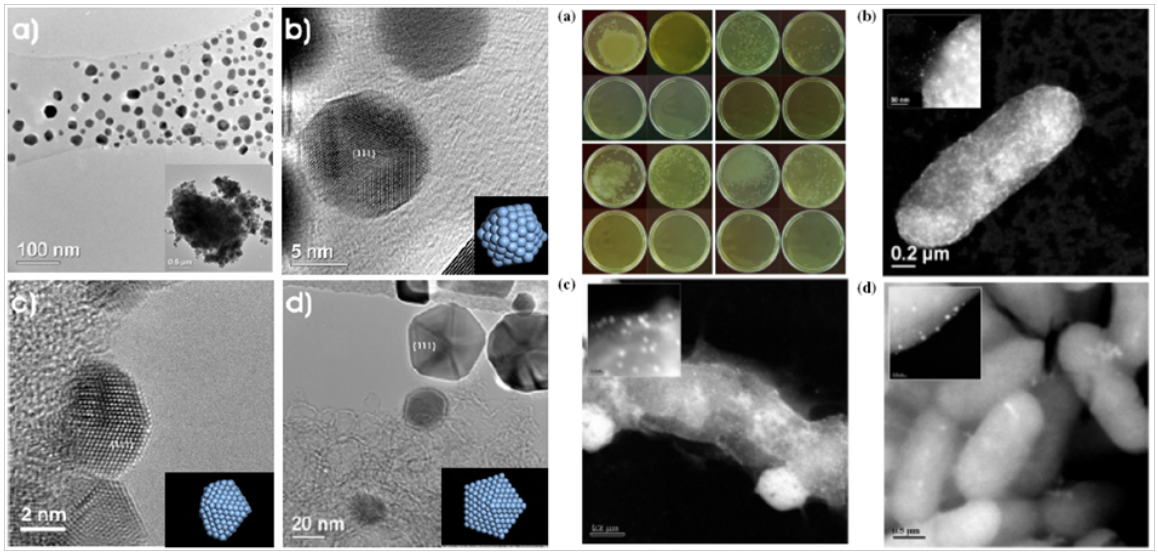

Figure 14: *Different shape, size and structure of Ag nanoparticles and their antibacterial activity and attachment onto the surface of bacteria (Morones et al., 2005).*

1.5.2 Synthetically-developed antibacterial activities of gold and platinum

Different from the silver, other noble metals, such as gold and platinum nanoparticles, are non-toxic. In the same time they are highly bioinert and do not possess natural antibacterial activity (Dreaden et al., 2012). It means that in the case of these metals this property needs to be designed.

One of the most perspective applications of Au nanoparticles is their usage in nanomedicine for controlled drug delivery. Many different medicines have been used for attachment onto Au nanoparticles in order to make more-efficient medicament. The majority of them correspond to anticancer drugs however some of them were also antibiotics. Au has been combined with vancomycin, ciprofloxacin and 5-fluorouracil (Dykman and Khlebtsov, 2012). According to the obtained results antibacterial activity of vancomycine was significantly improved after its bonding to colloidal Au (Gu et al., 2003). It was able to provide efficient activity even against vancomycin-resistant type of bacteria. Similar was obtained for nanoshell Au-ciprofloxacin (Rosemary et al., 2006). In some cases conjugation of a drug with Au nanoparticles provided them new therapeutic effect. The best example is attachment of 5-fluorouracil, antileukemic agent, onto Au nanoparticles (Selvaraj and Alagar, 2007). Formed conjugate showed interesting additional antibacterial and antifungal activity. There are also cases when Au nanoparticles were combined with antibiotics (ampicillin, streptomycin, gentamycin etc.) and any improvement of their antibacterial activity has not been achieved (Saha et al., 2007; Grace and Pandian, 2007). Data comparison revealed that improvement was obtained only in the case of stable, chemical attachment of antibiotic onto Au nanoparticles, otherwise improvement failed. As it has been shown for cefaclor (Rai et al., 2010), stable conjugation can be formed by reduction of Au-precursor by antibiotic when it remains attached onto formed nanoparticles. In that case obtained stable conjugates have high antibacterial activity.

Mechanism of improvement of antibacterial activity of so obtained Au-antibiotic

conjugates is unclear. In the case of Au-vancomycin mechanism of multivalence interactions between antibiotic molecule on the surface of Au nanoparticles and surface molecules of bacteria has been proposed (Figure 15). According to the experiences of the use of Au nanoparticles as carriers of other drugs, improvement in their activity was assigned to: (i) higher stability of drug molecule, (ii) improved solubility, and (iii) higher biodistribution since Au nanoparticles were able to take the drug directly to the cell and help it to cross the membrane and target cellular compartments (Ghosh et al., 2008).

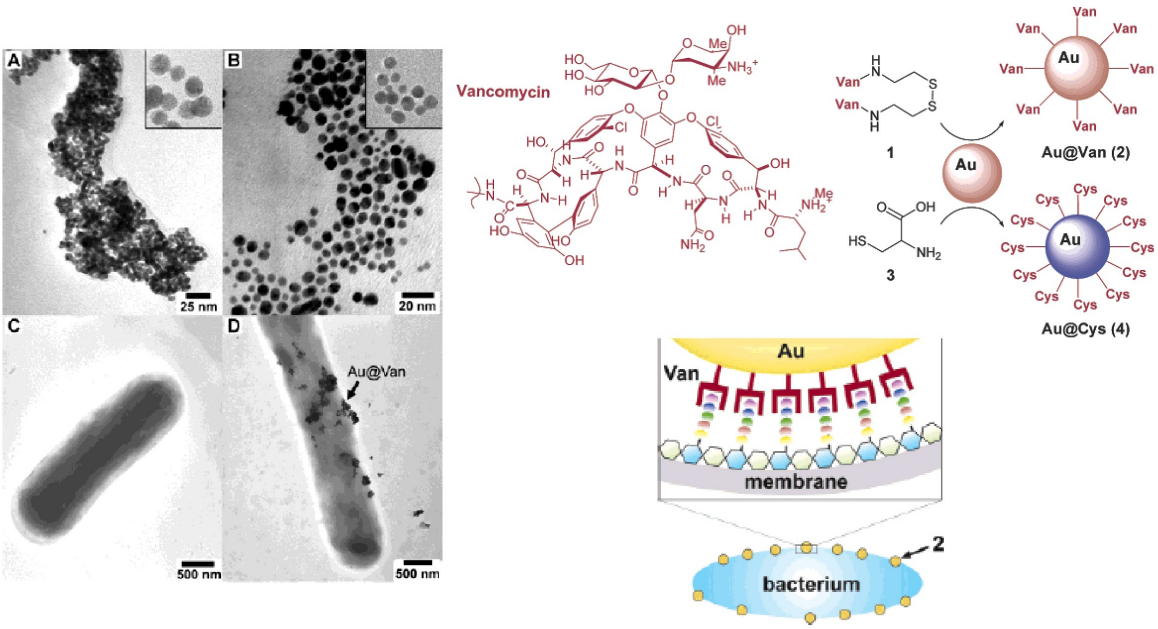

Figure 15: *Antibacterial activity of gold/vancomycin nanoparticles: morphology of nanoparticles, their attachment onto the surface of bacteria, functionalization of Au nanoparticles by antibiotic and proposed mechanism of antibacterial activity based on multivalent interactions (Gu et al., 2003).*

An example of the use of non-antibiotic substance which has antimicrobial property and which is used in alternative medicine for enhanced effect by combination with Au nanoparticles is gallic acid. This natural-sourced phenol is found in green tea, red vine and grapes. Beside antioxidant it possesses antimicrobial property. It was used for reduction and stabilization of Au nanoparticles. Resultant material had very strong antibacterial activity showing significant improvement of natural antimicrobial action of gallic acid (Moreno-Alvarez et al., 2010). Among non-antibiotic substances, branched polymers are also used to enhance its antimicrobial activity by attachment on Au nanoparticles. These polymers provided *in situ* reduction of Au nanoparticles and enabled them electrostatic stabilization (Zhang et al., 2008). Mechanism of increased antibacterial activity of so-formed structures was not proposed.

Antibacterial activity of Au was also developed by non-antibacterial agents without ability for antimicrobial activity. Formation of Au/C core-shell structures containing 200-nm sized carbon spheres with Au nanoparticles deposited on their surface enables antibacterial activity of material (Gao et al., 2010). Another example of achieving strong antibacterial activity of Au nanoparticles was their reduction and stabilization by different amino-substituted pyrimidines. Used molecules did not have antibacterial activity however their combination with Au nanoparticles resulted in formation of structure with strong antibacterial activity. During investigation of the mechanism of the action a few interesting points were revealed: (i) material was able to complex Mg^{2+} ions, (ii) it was able to prevent protein synthesis and (iii) it had ability for interaction with DNA.

Accordingly it was concluded that antibacterial activity was induced by the damage of the membrane due to the complexation of Mg-ions. After it succeeded in decreasing of the permittivity of the membrane, material crossed it and inside bacteria it induced prevention of protein synthesis and affected DNA (Zhao et al., 2010).

As it was shown by the firstly invented, natural-sourced antibiotic, Nature provides very good models for designing materials for the specific applications such as antibacterial activity. Starting from this idea, Au nanoparticles were synthesized using biosynthetic process where natural sources (plants, bacteria, honey or propolis) were used. This approach provided antibacterial activity to formed material. Efficiency of their action was low however they provided a good direction for possibility to use natural sources for designing antibacterial property of this metal (Mubarak Ali et al., 2011).

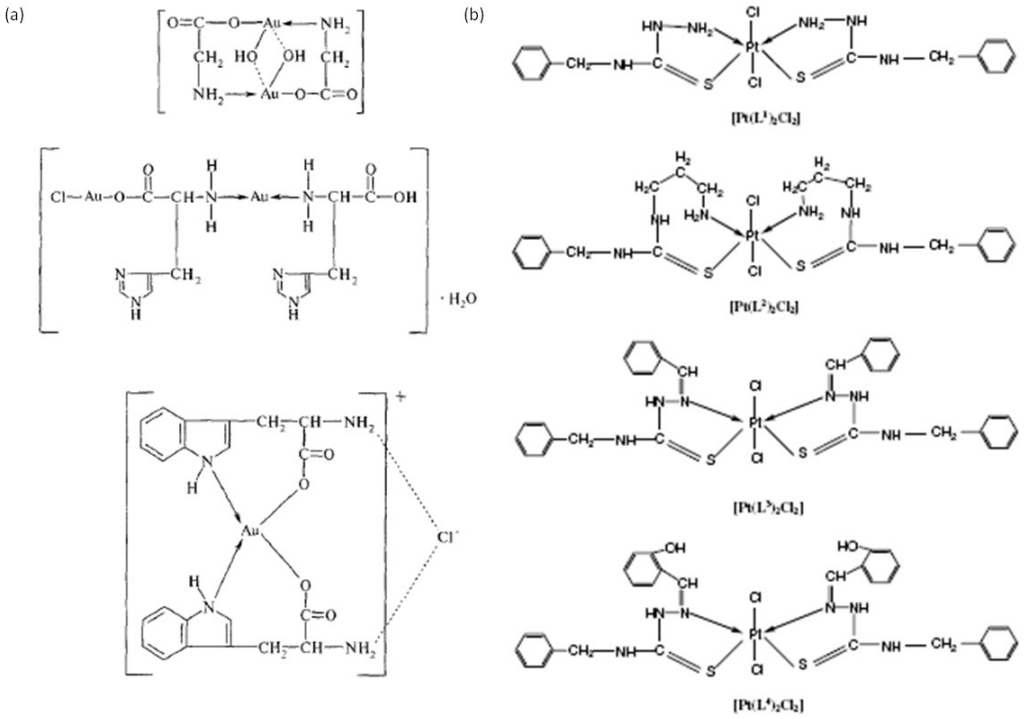

Figure 16: *Au-glycine, Au-histidine and Au-tryptophane complexes synthesized as new molecules with potential antibacterial activity (a) (Kazachenko et al., 1999); Pt-complexes with antibacterial activity (Mishra et al., 2006).*

Amino acids are biologically available molecules with groups which can allow their attachment onto the surface of Au nanoparticles. There is a possibility for formation of complexes between Au-ions and amino acids (Figure 16a). Synthesized materials were amorphous and did not contained Au nanoparticles. Among formed complexes Au-glycine and Au-tryptophan had antibacterial activity while Ag-histidine was inactive against bacteria. Mechanism of antibacterial activity of formed complexes was not analysed however *in vitro* toxicity investigation was performed in rats showing their enhanced compatibility (Kazachenko et al., 1999). In the case of Au nanoparticles, different amino acids were used either for their reduction or for stabilization of their surface after they have been formed by other reduction agents. These agents (like glutamic acid and histidine, (Polavarapu et al., 2008) or alanine and arginine (Koyama et al., 2008)) were attached on the surface of metallic nanoparticles after they have been formed using other reduction agents. Some of these amino acids were used for reduction of gold (aspartic acid, (Mandal et al., 2002), tryptophan, (Selvakannan et al., 2004), L-aspartate (Shao et al., 2004), as well as tyrosine, glycil-l-tyrosine and L-arginine

(Bhargava et al., 2005)) and this reaction was performed under increased temperature or pH of the system. None of these materials have been considered as materials with antibacterial activity.

Similar to the gold, platinum does not have natural ability for antibacterial activity (Shahidi and Ghoranneviss, 2011). Pt nanoparticles and Pt-complexes are frequently investigated as anticancer agents (Porcel et al., 2010). Some of the complexes of Pt (Figure 16b) are able to have antibacterial activity (Mishra et al., 2006). The major difficulty which may appear when complexes are entered inside organism is high possibility for their reduction by wide variety of metabolite products present in living surroundings and after formation of metallic nanoparticles antibacterial activity can be inactivated.

1.6 Toxicity of noble metals

A shift of nanoscience from the top-research topic to wide spread practical applications is nowadays reality. It means that nanoscience became part of everyday life. Unfortunately, the next step was asking the question- how much its safe is. There are huge number of materials with potential, unknown or known toxic influence to humans and their environment. Some of them are used in everyday practice.

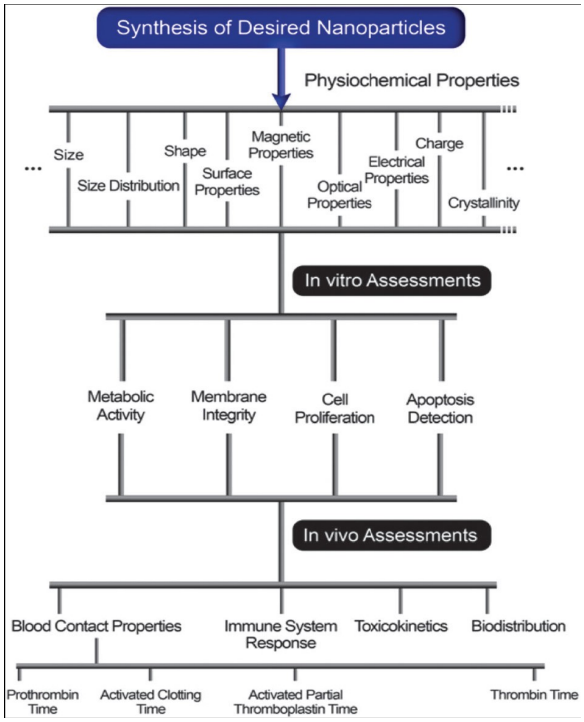

Figure 17: *In vivo and in vitro study of novel materials for nanotoxicity research (Sharifi et al., 2012).*

As illustrated in Figure 17, investigation of toxicity is a long-term procedure composed of large number of steps. First ones concern cellular and animal tests. Once obtained nanoparticles designed to have desired physicochemical properties (that need to be investigated in detail) are used for the next step associated with *in vitro* assessment in cells for analysis of the metabolite activity, proliferation, apoptosis and membrane integrity. The next step is investigation *in vivo* when animals are included. In that case blood contact, immune system response and biodistributions are firstly tested (Sharifi et al., 2012).

Fundamental investigations of the interactions of nanoparticles with cells, blood components, genetic material, proteins and tissues are essential for the future design of safety nanotechnologies (Sharifi et al., 2012).

1.6.1 Oxidative stress induction by different metals

Reactive radicals – reactive oxygen species (ROS) and reactive nitrogen species (RNS) – are normal components of the cellular metabolism. They may be produced as by-products of mitochondria electron transport (Figure 18a) with the major role in signalling process that leads other important segments of cellular life such as cellular growth and regulation of the redox state (Schafer and Buettner, 2001). Some other mechanism of their production concerns neutrophils and macrophage immune system defence against infections (Segal, 2005) as well as response of the organisms to irradiations (UV, X-ray, and gamma), pollutant form the environment and metals. However these types of species are known to have dual, beneficial and harmful, role in the living organism. The most important beneficial role of these species in the cell is subscribed to regulation of the aging process. However, overproduction of these types of radicals leads to inability of cell to regulate them, which leads to redox imbalance and formation of oxidative stress. High concentrations of ROS and RNS are able to induce damage in proteins, nucleic acids and lipids. Development of age-related diseases as arteriosclerosis, arthritis, neurodegenerative disorders and many other conditions are associated with accumulations of oxidative stress-induced damages formed during the life cycle. Frequent appearance of high-level oxidative stress can be highly dangerous. It has possibility to induce oncogenic stimulation and may provoke carcinogenity. Oxidative stress-induced cancers are usually associated with radical-formed DNA damages and formation of oxidative-DNA-lesions (Valko et al., 2006).

Free, uncomplexed metals in the organism are potential source of high toxicity since they have important role in ROS and RNS production. It has been shown that even essential transition metals such as iron, cobalt, copper, zinc and manganese which are present in the organism in the form of vital complexes involved in different metabolite and signalling processes, may escape these normal steps. Due to the rich coordination chemistry and redox potential, these metals are capable to change their state and to turn into chemical form undesired for the living organisms. These forms are able to induce a long sequence of modifications resulting in toxic consequences (Valko et al., 2005).

Many studies concerned metal-induced toxicity due to the production of reactive radicals. In general, metal-induced radicals result in modifications in DNA, lipid peroxidation and changes calcium and sulfhydryl homeostasis. According to the pathway of their toxicity metals are separated into several groups. First group belongs to copper (Cu), chromium (Cr), vanadium (V), iron (Fe) and cobalt (Co) which are involved in redox-cycling reactions. The second group belongs to mercury (Hg), cadmium (Cd) and nickel (Ni) which are binding directly to glutathione and sulfhydryl groups of proteins. Arsenic (As) belongs to the separated group with affinity for binding to the critical thiols and ability for formation of hydrogen peroxide (Valko et al., 2005).

The common property of these metals is ability to induce production of reactive radicals and to induce oxidative stress. As illustrated in Figure 18b common mechanism of their activity in this process involves Fenton reaction which concerns production of superoxide and hydroxyl radicals. The next step is induction of DNA damage and cancerogenesis. Metals have different pathways to induce this type of toxicity: Cd, As and Ni prevent DNA reparation; Ni and Cr are involved in base-modifications; Ni, Fe and Cu use cross-linking; Cd, Ni and Cr undergo scission and Cr, Na and Cd use depurination (Valko et al., 2005).

Zink has very interesting role in the organism. It has been shown that it has possibility to act as antioxidant and to suppress ROS production. It may protect proteins and enzymes from oxidation as well as to increase hydroxyl radical production from hydrogen peroxide. On contrary, its uncontrolled accumulation in cells has been associated with etiology of Alzheimer's disease, while Zn-induced stress and toxicity are in high contradiction with its antioxidant role (Valko et al., 2005).

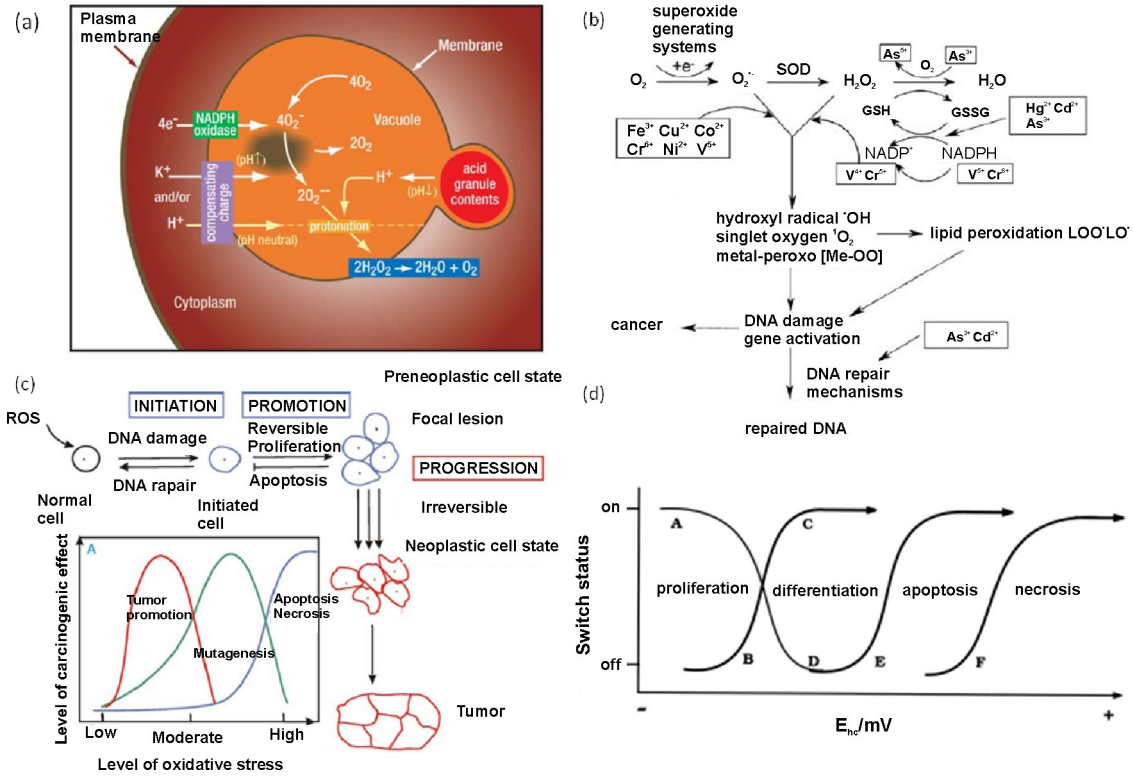

Figure 18: *Schematic illustration of oxidative stress: (a) activity of NADH oxidase (Segal, 2005), (b) the pathway of metal-induced oxidative stress (Valko et al., 2005), (c) model of carcinogenesis (Valko et al., 2006) and (d) redox-potential that moves cell through different stages of life cycle (Schafer and Buettner, 2001)*

There is very large number of redox couples involved in cell potential. Among others, glutathione-disulfide/glutathione couple (GSSG/2GSH) is considered to be the most abounded in the cell and to have the most important role in the normal cellular redox state. The change of the reduction potential (E_{hc}) of the cell shift it into different segments of life cycle (Figure 18d). During proliferation, E_{hc} has the most negative value. Gradual turn into more positive E_{hc} results in differentiation. In the same time proliferation is subsequently decreased. If E_{hc} is too positive, death signal is turned on and apoptosis as the normal step of cell life is initiated. This mechanism usually concern ordered removing of the cells that lost their ability to regulate redox potential and accordingly they lost their normal function. However, high value of E_{hc}, achieved by severe oxidative stress (toxicity) leads cell directly to necrosis. In this model, cancer has been considered as inappropriately shifted redox potential that results in imbalance between excessive proliferation and cell death forming tissue with more reducing environment (Schafer and Buettner, 2001). Carcinogenesis related to ROS may be described by three steps. Low-level ROS production induces reversible damages of initiation step. However, their frequent appearance may induce mutagenesis which is also reversible damage of promotion step. Further high-intensity, frequent ROS stress may induce necrosis and irreversible damages of progression step (Figure 18c). This model associates metal

toxicity with their cancerogenity (Valko et al., 2006).

1.6.2 Oxidative stress suppression by gold and platinum

The main production-site of reactive radicals, formed as a normal part of the cellular metabolism is in the mitochondria. This organelle possesses complexes I which has a role of proton pump and electron transport. This complex is an enzyme that transfers electrons form NADH to CoQ forming NAD^+ and $CoQH_2$. Besides, $CoQH_2$ is also made by mitochondrial complex II and electrons are transferred to succinic acid. It is a substrate of complex III and releases electrons to cytochrome c. In non-mitochondrial membranes CoQ has a role of antioxidant highly important in defence against oxidative stress (Hikosaka et al., 2008).

Platinum has potential to induce oxidation of NADH to form NAD^+ (Figure 19a, b) as well as to reduce CoQ into CoH_2 (Figure 19c, d). Since possibility to perform similar functions as mitochondrial complexes, after targeting in the adequate place in the membrane platinum is considered to be their potential substitution. It means that this metal is ready to induce control over the production of ROS species and to perform scavenge of their excessive formation.

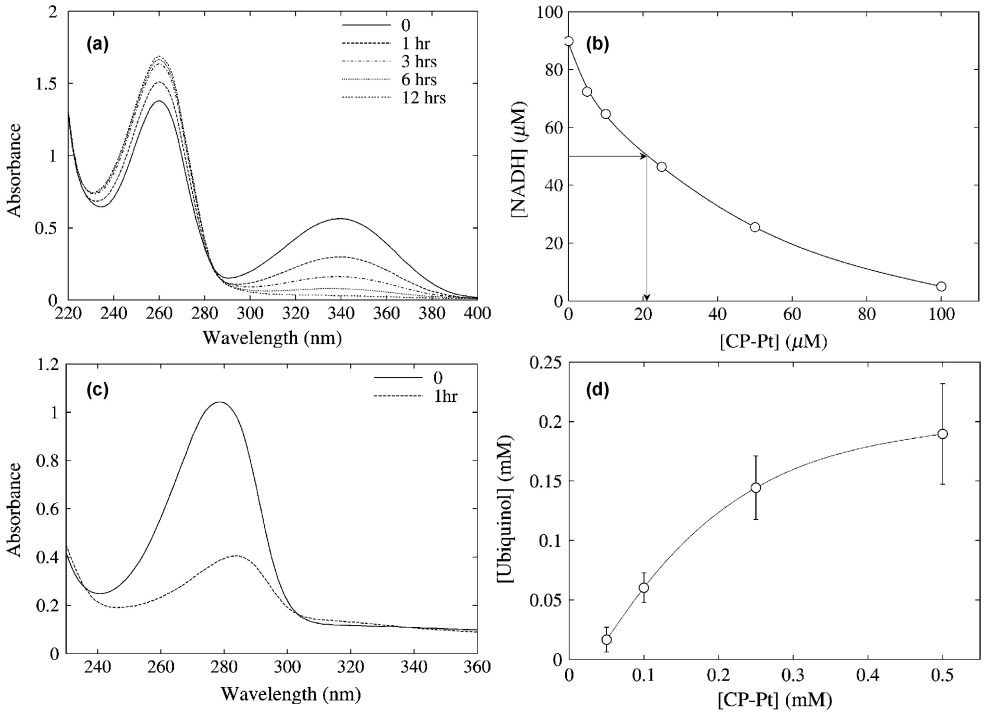

Figure 19: *Pt-induced oxido-reduction of NADH (a, b) and reduction of CoQ (c, d) (Hikosaka et al., 2008).*

Similar to platinum, it has been also confirmed that gold has the same possibility. Au nanoparticles were self-assembled onto sol-gel derived three-dimensional silicate network. So-formed structure was very efficient in catalysis of the reduction of NADH and formation of NAD^+ without usage of any electron transfer mediators (Raj and Jena, 2005). The formed structure (illustrated in Figure 20) has been investigated for dehydrogenase biosensor for detection of lactate and ethanol. The basic principle of the sensor was detection of the enzymatically-formed NADH by the formed Au-structure. It has been confirmed that Au has very high sensitivity and fast response for low concentrations of NADH resulting in its oxidation (Raj and Jena, 2005). Parts of the cellular system responsible for cellular respiratory process, transport hydrogen and

electrons and possess NADH. Possibility of Au nanoparticles to mimic behaviour of these molecules and to catalyse the same reactions is proposed to have important applicability in the field of biomedicine (Huang et al., 2005).

According to the presented literature data it could be expected that Au and Pt nanoparticles have potential to act as antioxidants *in vivo*. It means that they are able to suppress development of ROS and RNS species in the cell in the amount which may have toxic consequence and to have beneficial contribution to different stages of cellular life cycle.

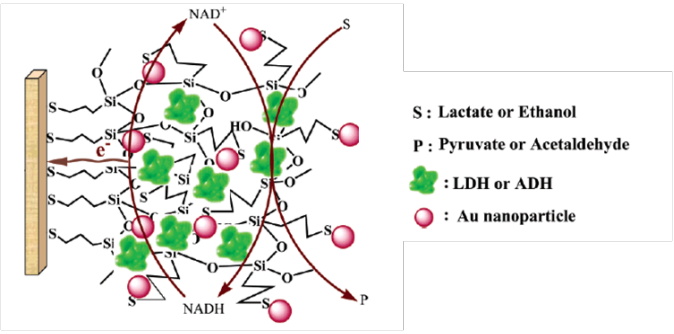

Figure 20: *Model for oxidation of NADH by Au nanoparticles (b) (Jena and Raj, 2006).*

1.6.3 Toxicity of silver

A majority of the commercially available products with an antibacterial component contain silver for this function. Despite its very high efficiency against bacteria, this material is highly toxic and harmful for humans and the environment. According to the U.S. Food and Drug Administration (FDA, 1997) and the Australian Therapeutics Good Administration (TGA, 2002), silver is unapproved for any application as an antibacterial agent in USA and Australia. Besides clear proofs of toxicity of this metal and its compounds their wide spread practical applications are alarming. One of the examples is recent approvement of the use of silver for correction of the food colour as additive released by EU Food Standard Agency under label E176 (EU FSA, 2010).

According to some investigations it has been pointed out that silver is non-toxic and that only very high concentrations are able to induce its toxicity. These investigations were promoting healthy side of this metal and supported its biomedical applications in the form of novel generation of antimicrobials (Rai et al., 2009).

Recently, high effort has been given to the identification, investigation and understanding of the origin of silver-related toxicity. It has been shown that Ag nanoparticles are able to induce morphological changes of cells and production of reactive radicals (such as peroxides and superoxides) that results in development of oxidative stress (Figure 21a, b). Consequently mitochondrial dysfunction is induced leading to cellular death. Investigation of ability of these particles to get inside cell showed homogeneous distribution of these particles within cell with ability to get inside all intercellular compartments including nucleus and micronucleus (Figure 21c). Furthermore, it has been shown that excessive production of reactive radicals by these nanoparticles is able to induce damage in DNA and to induce chromosomal aberrations leading to genotoxicity (Figure 21d, e) (AshaRani et al. 2009). This type of toxicity may have serious consequences which lead to carcinogenesis. All these highly serious indications of Ag toxicity were obtained for Ag nanoparticles which were capped by starch. It has been concluded that small concentrations are also prone to induce toxicity (AshaRani et al. 2009).

Besides concentrations it has been also shown that there are other factors able to affect toxicity of Ag nanoparticles. Physicochemical properties of Ag nanoparticles such as surface charge, their stability (binding and agglomeration potential) and the chemistry of their surface may affect cytotoxic effect of these particles. A contribution of these properties to toxicity was explained through their ability to dictate direct contact, transport and interactions of these nanoparticles and cells (Suresh et al, 2012). Accordingly it was presumed that formulation of more stable forms of Ag nanoparticles (within composites, layers, core-shells etc.) may contribute to regulation of their harmful effect to living organisms.

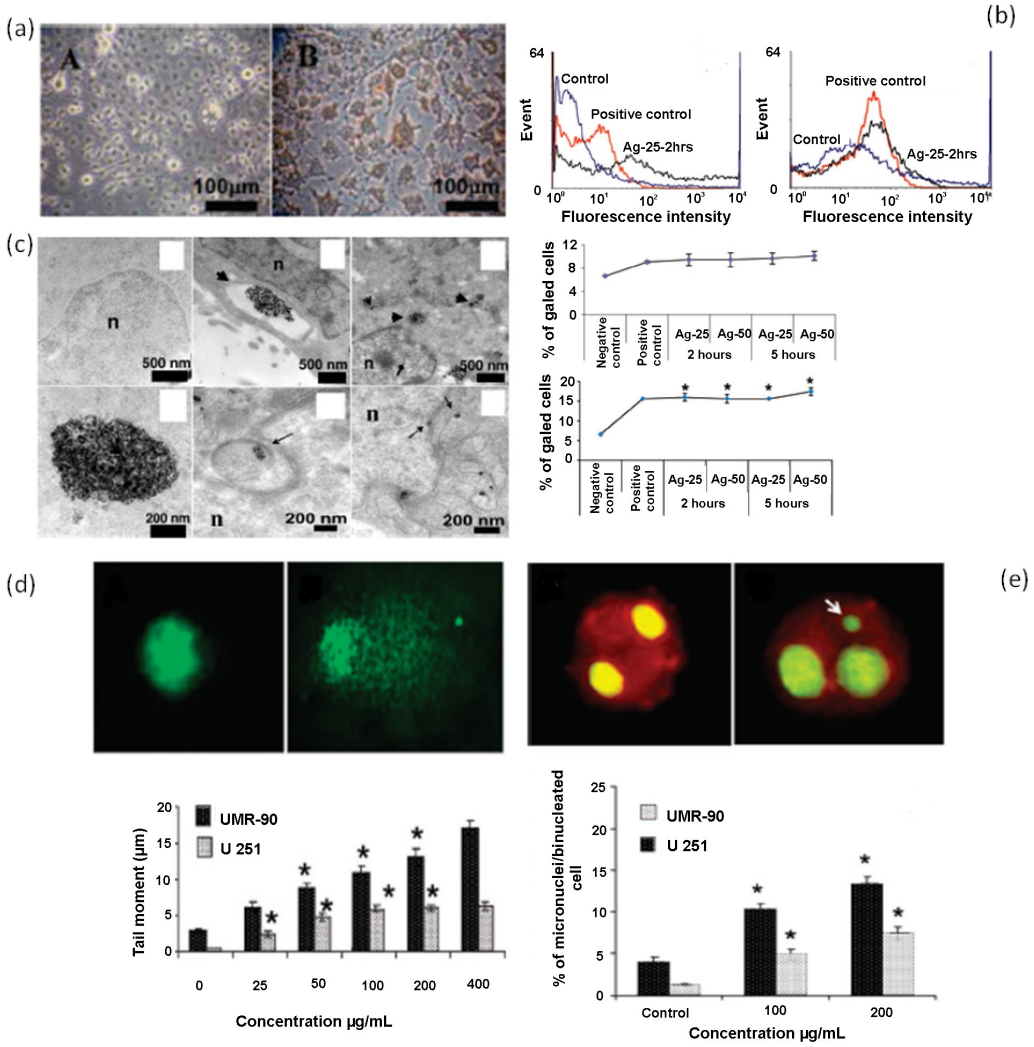

Figure 21: *Toxicity of Ag nanoparticles: (a) optical micrographs of U251 cells; (b) ROS production- detection of H_2O_2 in cells; (c) TEM images of nanoparticles inside cells; (d) Comet analysis of nucleus and (e) micronucleus analysis (AshaRani et al., 2009).*

1.6.4 Nano-size-related toxicity

Size, morphology and surface properties have important contribution to the toxicity of nanoparticles in general (Nel at al., 2006). It has been confirmed that this is especially important in the case of Ag nanoparticles. Recent investigations showed that size of Ag nanoparticles significantly contribute to development of cytotoxicity. Series of materials containing highly narrow size distribution of Ag nanoparticles were prepared to be used

as standards for investigation of size-dependant toxicity. These series contained sphere-like particles with size of 25 nm, 35 nm, 45 nm, 60 nm and 70 nm (Figure 22a). High precision in regulation of the size of these particles has been achieved by their capping using polyol method and stabilization by polyvinylpyrrolidone (PVP). So obtained systems were used for investigation of cell viability, apoptosis, necrosis and ROS production.

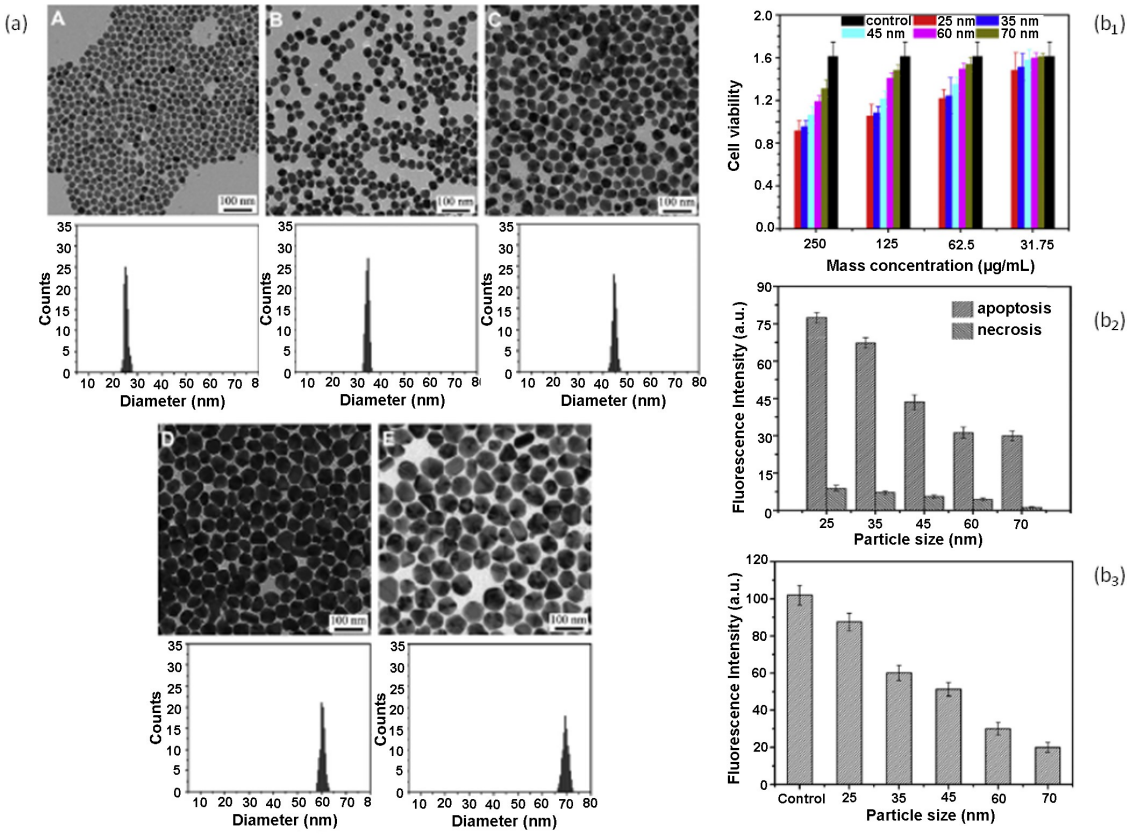

Figure 22: *Size-related toxicity of Ag nanoparticles: TEM images and corresponding size distributions of Ag nanoparticles (a); toxicity induced by different sizes of Ag particles- cell viability (b_1), apoptosis and necrosis (b_2) and ROS production (b_3) (Li et al., 2012).*

Cell viability investigations showed that particle size influenced viability of cells. However this contribution was in strong correlation with concentration. At lower concentrations (31.75 μg/ml) differences between toxic effect of smaller and larger particles was low and for all of them high cell viability has been obtained. Increasing of the concentration of particles decreased the percentage of death cells and made more significant difference between contribution of smaller and larger particles to cell death. For particles with diameters of 25 nm, the highest tested concentration (250 μg/ml) induced twice as low cell viability in comparison with the control (Figure 22b_1).

Similar results have been obtained for investigation of apoptosis and necrosis processes. Test was performed for the highest concentration (250 μg/ml) and for all of the investigated systems majority of the cells were in the stage of early apoptosis while lower fraction of them were in the stage of necrosis. It has been observed that increasing of the particle size affected the ratio of necrotic cells. Increasing the particle size decreases the ratio of necrotic cells.

ROS production was also investigated for the concentration of 250 μg/ml and results showed that it was affected by the size of investigated particles. Particles with the smallest size (25 nm) had ability to produce very high level of reactive radicals inside

cells. With increase of the particle size ability for production of these radicals was significantly decreased. For particles with 70 nm in diameter produced ROS was even four times lower (Figure 22b$_1$).

It was hypothesized that differences in toxic effect of Ag nanoparticles with different diameters was a consequence of higher contact area between smaller nanoparticles and cellular membrane that provided them higher possibility to enter the cell. Moreover, particles inside cells could be dissolved within acidic cellular compartments resulting in excessive development of Ag-ions inducing increase in ROS production (Li et al., 2012).

1.6.5 Comparative toxicity of noble metals

Stability of silver and all nanoparticles in general depends on the factors like size, shape, capping agents (if any), solution pH, ionic strength, specific ions and ligands and organic macromolecules- all able to affect their biodistribution (Marambio-Jones and Hoek, 2010). Consequently different routes of administrations (inhalation, intravenous, peroral, intraperitoneal etc.) may significantly contribute to their behaviour *in vivo* (Yildirimer et al., 2011).

Toxicity of Ag and Au nanoparticles has been intensively studied in many different conditions including various sorts of cell/animal models, different routes of administrations and different targeting organs/tissues as summarized in Table 3.

Inhalation of Ag nanoparticles was investigated in rats (Table 3). Results showed absence of any damages and pathological changes in lung after short-term exposure (Ji et al., 2007; Sung et al, 2011). However, exposure during the period of 13 weeks confirmed beginning of the pathogenesis, development of the alveolar inflammations and appearance of granulomatous lesions (Sung et al., 2008).

Dermal exposure performed under different conditions was investigated for both Ag and Au nanoparticles (Table 3). For Ag nanoparticles different cells were tested including human skin carcinoma. Results showed significant dose-dependent toxicity which was associated with ROS production and DNA fragmentations. These changes were notices even for the concentration of 6.25 μg/ml (Arora et al., 2008). Similar investigations were performed on Au nanoparticles. Their effect was tested on rat skin and results showed size-dependant permeability (Sonavane et al., 2008). For human dermal fibroblasts it has been observed that higher concentrations of Au-citrate capped nanoparticles decrease proliferation (Pernodet et al., 2006) while mouse fibroblasts apoptosis and necrosis have been induced only for very small particles with size of 1.4 nm (Pan et al., 2007).

Liver exposure was investigated mainly in animals for both Ag and Au nanoparticles (Table 3). Investigations of Ag nanoparticles were performed on zebrafish and rats and associated toxicity was result of particle accumulation and oxidative stress production (Choi et al., 2010; Lankveld et al, 2010). For Au nanoparticles all investigations were performed in mice. They were exposed to these particles up to 28 days and particles were administered to them per oral, intravenous (in tail) and intraperitoneal. Apoptosis was developed in the case of very small particles (smaller than 10 nm) and in the case of higher concentrations. Moreover, capping the surface by proteins or PEG improved cytocompatibility. If all three routes of administrations are compared, per oral (with systematic effect) was the most toxic while local one (in tail and peritoneum) were less toxic (Chen et al., 2009; Cho et al., 2009; Zhang et al., 2010b).

Table 3: *Ag and Au nanoparticles: toxicity for different cell/animal models and routes of administration (Yildirimer et al., 2011).*

Lung	Conjugation	Administration	Cells/animals	Outcome
Ag NP (Sung et al, 2010)		Inhalation, 750 μg/m^3, 4h/2weeks	Rats	No changes in lung function and body weight
Ag NP (Ji et al., 2007)		Inhalation 61 μg/m^3, 6h/4weeks	Rats	No changes in haematology and blood biochemical values
Ag NP (Sung et al., 2008)		Inhalation 515 μg/m^3, 6h/13weeks	Rats	Alveolar inflammations granulomatous lesions

Skin	Conjugation	Administration	Cells/animals	Outcome	Ref
Ag NP (Hsin et al., 2008)		50 and 100 μg/mL, 24h	Mouse fibroblasts	ROS-related apoptosis	
Ag NP (Arora et al., 2008)		0.76-50 μg/mL, 24h	Human skin carcinoma	for ≥6.25 μg/mL, DNA fragmentation	
Ag NP (Samberg et al, 2010)		0-1.7 μg/mL, 24h	HEK cells	Significant dose dependent decrease of viability	
Ag NP (Trop et al., 2006)		0.34-34 μg/mL, 14 days	Porcine skin	Focal inflammations NP localization in skin	
Au NP (Pan et al., 2010)		0.8-15 nm 24h	Melanoma cells Mouse fibroblasts	Small (1.4 nm) NP necrosis and apoptosis	
Au NP (Pernodet et al., 2006)	Citrate	0-0.8 μg/mL 14 nm; 2, 4, 6 days	Human dermal fibroblasts	Dose-dependent proliferation reduction	
Au NP (Sonavane et al., 2008)		15, 102, 198 nm	Rat skin	Size-dependent permeation through tissue	

Liver	Conjugation	Administration	Cells/animals	Outcome	Ref
Ag NP (Choi et al., 2010)		30 and 120 μg/mL 24h	Zebrafish	Oxidative-stress due Ag^+ apoptotic signals in liver	
Ag NP (Lankveld et al, 2010)		Intravenous 23.8, 26.4, 27.6 μg/mL 20, 80, 110 nm /5days	Rats	Size-related tissue uptake accumulation-related tissue toxicity	
Ag NP (Arora et al., 2009)		6.25-100 μg/mL 12.5-200 μg/mL 7-20 nm / 24h	Mouse fibroblasts and hepatocytes	NP entered cells inducing oxidative stress mediators production	
Au NP (Chen et al., 2009)	Immune Peptides	Intraperitoneal 8 kg/weight/week 3-100 nm, 4 weeks	Mouse	Naked NP: small-size death Surface-modified NP: improved compatibility	
Au NP (Cho et al., 2009)	PEG	Intravenous 0.17, 0.85, 4.26 μg/kg/ Weight, 13 nm, 7 days	Mouse	NP accumulation in liver and spleen, high-concentration apoptosis of hepatocytes	
Au NP (Zhang et al., 2010b)		per oral, intraperitoneal Intravenous, 14-28 days 13.5 nm, 0.14-2.2 mg/kg	Mouse	higher toxicity for oral and intraperitoneal and lower for tail vein injection	

Brain	Conjugation	Administration	Cells/animals	Outcome	Ref
Ag NP (Trickler et al., 2010)		6.15-50 μg/mL 25, 40, 80 nm/24h	Rat brain endothelial cells	Time and dose dependant increasing toxicity	
Ag NP (Costa et al., 2010)		10, 25, 50 μg/mL/1h	Rat tissue	Oxidative stress cell damage	
Au NP (Trickler et al., 2011)		0.8-50 μg/mL /24h 3, 5, 7, 10, 30, 60 nm	Rat brain endothelial cells	No toxicity except for 3-nm NP	
Au NP (Shukla et al., 2005)		Intraperitoneal/ 8days 40, 200, 400 μg/kg, 12.5 nm	Mouse	Low amount crossed brain barrier no neurotoxicity	

Brain exposure investigations are very important due to the fact that blood-brain-barrier (BBB) is very strong “filter” for the transport of any substances. However those who succeeded in crossing over it may cause significant damages. Tests of Ag nanoparticles were performed on rats and after exposure dose-dependent toxicity was

developed resulting in oxidative stress cell damages (Trikler et al., 2010; Costa et al., 2010). For Au nanoparticles, toxic reply was obtained only for those with 3-nm diameter. All others were non-toxic, low concentration was able to cross BBB and for those who crossed it neurotoxicity was not detected even after continuous exposure during 8 days (Shukla et al., 2005; Trikler et al., 2011).

Uptake of Au nanoparticles by cells is intensively studied. Obtained results agree that this function is strongly correlated with particle morphology (size, shape and agglomeration), surface properties (type of functionalization and charge), concentration of nanoparticles, cellular type, incubation conditions, selected media etc. (Dreaden et al., 2011). According to the very interesting study performed by Jiang and co-workers, uptake of antibody-functionalized Ag nanoparticles was analysed. Particles were spherical in shape and they were separated into groups depend on their size (2-100 nm) (Figure 23). The most efficient uptake was obtained for particles with 40-50 nm in size because they had the most optimal contacts with receptors on the cellular surface and they were entered inside cell by receptor-mediated endocytosis. In that case the highest cellular death was detected. It was not the case with smaller and larger particles which were mainly trapped on the extracellular side of membrane while Au nanoparticles without any functionalization showed no toxicity (Jiang et al., 2008).

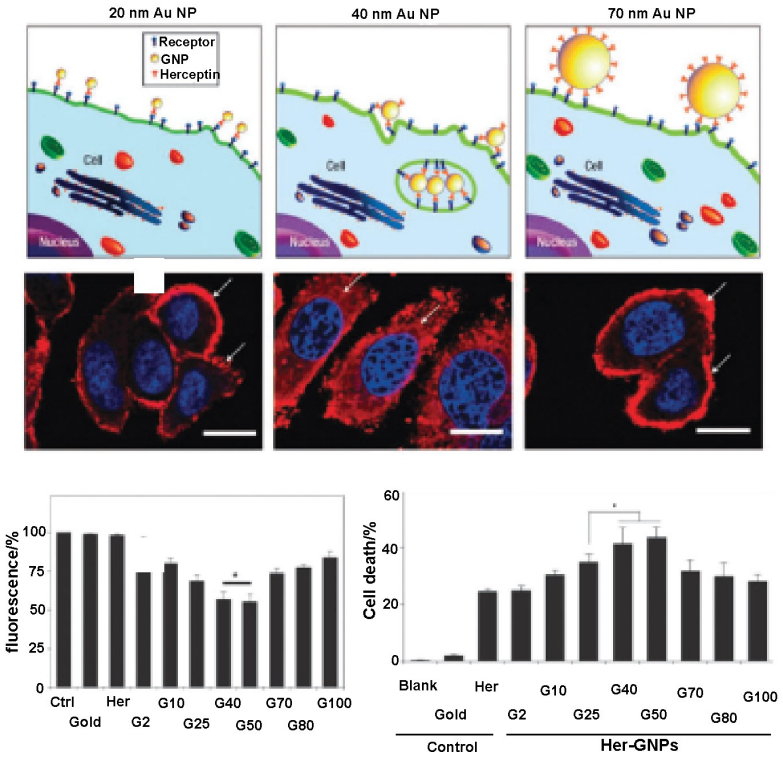

Figure 23: *Size-related toxicity of Au nanoparticles and method of their uptake by cells (Jiang et al., 2008).*

Recently, detailed investigation of the haemato-compatibility of noble metal nanoparticles with human erythrocytes (red blood cell) has been performed. Cells were tested for interaction with Ag, Pt and Au nanoparticles with mean diameters of 10 nm, 6 nm and 28 nm, respectively. The first signs of toxic effect of Ag nanoparticles to human erythrocytes were observed upon morphological changes (Figure 24). For normal cells which were not exposed to metal nanoparticles human erythrocytes had biconcave shape. After exposing to the different concentrations of Ag nanoparticles, human erythrocytes lost their concavity and started to swell and aggregate with the signs of heavy hemolysis.

In the case of Pt and Au nanoparticles exposed human erythrocytes remained their normal morphological characteristics. The similar was not observed for Ag-ions and $NaBH_4$ reduction agent. Results confirmed that obtained toxicity is solely a consequence of Ag nanoparticles. According to the measurements of the lipid peroxidation oxidative stress was determined. It was very interesting to observe that Ag-treated erythrocytes with all consequently developed changes and damages were further on toxic for healthy fibroblasts although they were separated from Ag nanoparticles. Unlike Ag nanoparticles which caused production of ROS and induced oxidative stress death of human erythrocytes, the same effect was not observed for Au and Pt nanoparticles. Au and Pt were unable to induce excessive ROS production, they did not induced cellular death or any change in morphology of these cells and consequently they were characterized as haematocompatible (AshaRani et al., 2010).

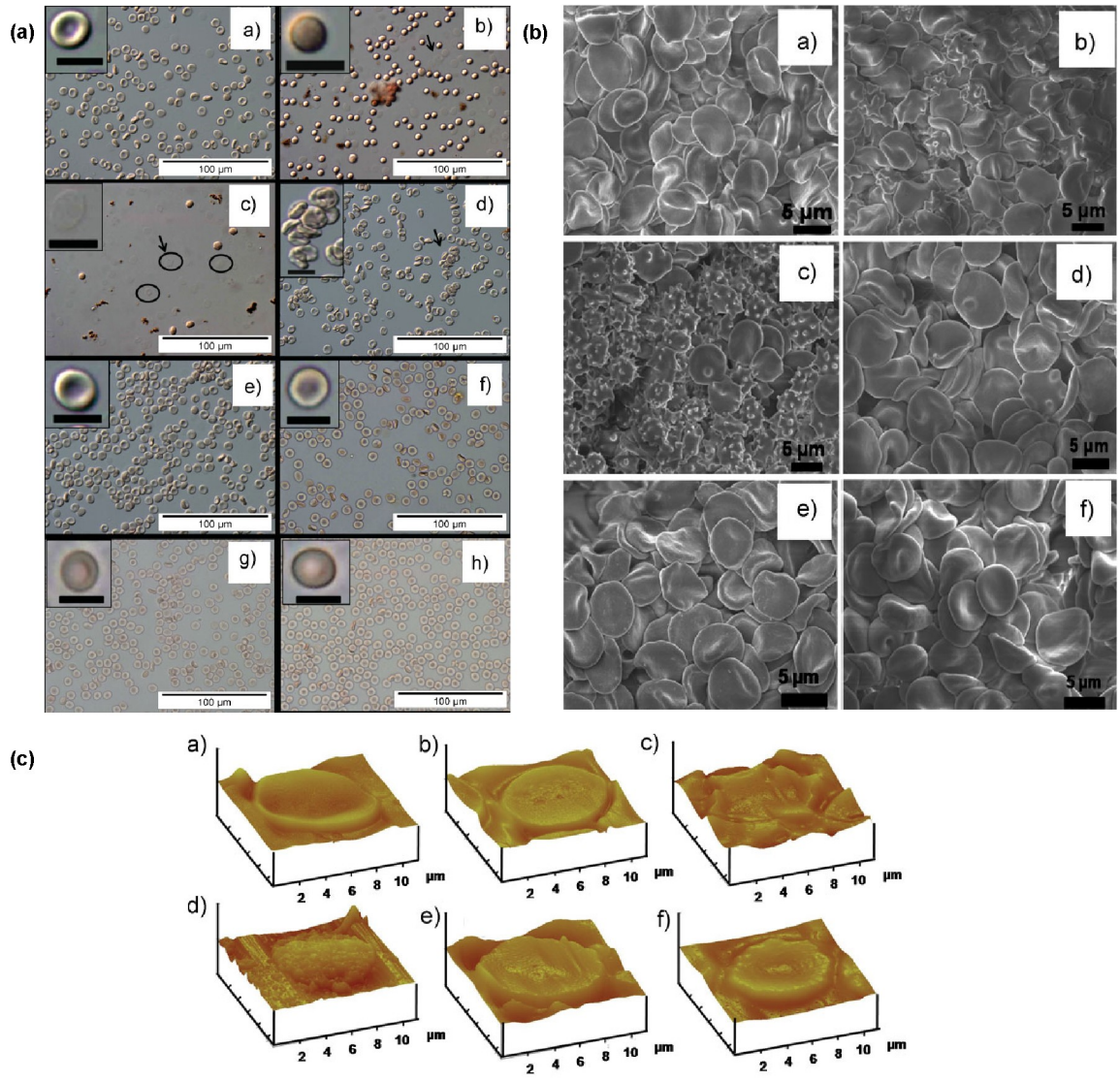

Figure 24: *Ag, Au and Pt toxicity: (a) Optical microscopy of red blood cells- normal (a), Ag-treated (b-d), Pt-treated (e), Au-treated (f), Ag-ion treated (g) and $NaBH_4$-treated (h); (b) Electron micrographs of red blood cells- normal (a), Ag-treated (b, c), Au-treated (d), Pt-treated (e) and PVA-treated (f); (c) AFM analysis of red blood cells- normal (a), Ag-treated (b–d), Au-treated (e) and Pt-treated (f) (AshaRani et al., 2010).*

Despite the fact that silver has very strong and nonselective activity against many different pathogens, its inability to make a difference between cells of pathogens and

other live cells is a serious lack of this metal. This property makes it toxic for human beings and their environment. Widespread application of this metal is the main reason for the urgent need to replace it with a “green” and human friendly substitute with at least the same properties as silver with respect to antibacterial activity. According to the toxicity investigations, other members of noble metals, platinum and gold could be good candidates for this purpose.

2 Aims and Hypothesis

2.1 Aim

The main goal of this dissertation is formation of material which will be suitable for biomedical application as material with minimized or eliminated hazard effects to human health.

For that purpose further goals should be reached:

(i) Optimization of homogeneous sonochemical method for formation of silver, gold and platinum nanoparticles and their composites with hydroxyapatite.

(ii) Determination of the influence of hydroxyapatite on the formation of noble metal nanoparticles.

(iii) Determination of the experimental conditions for formation regular size and shape of noble metal nanoparticles attached to the surface of hydroxyapatite.

(iv) Obtaining correlation among particle properties (morphology and structure) and applied precipitation and capping agents.

(v) Postulation of the reaction mechanism and mechanism of particle growth during the sonochemical synthesis of noble metal particles alone and within apatite composites.

(vi) Investigation of the release of the noble metal ions during the time spent in simulated physiological conditions in order to predict concentrations of ions which will be estimated in the body.

(vii) Investigation of the interactions of hydroxyapatite/noble metal composite particles with cells in order to determine the level of their cytotoxicity as well as investigation of their interactions with bacteria in order to test possibility to pronounce antibacterial action.

2.2 Hypothesis

The intention of this dissertation is to investigate formation of silver, gold and platinum nanoparticles and their composites with hydroxyapatite by the application of homogeneous sonochemical precipitation method.

Sonification of urea in aqueous solution at elevated temperature is able to provide its decomposition to carbon-dioxide and ammonia. Before final decomposition of urea, isocyanate ions are formed as intermediate compounds. Silver, gold and platinum are able to be complexed by these ions. We are suggesting that sonification of water solution of noble metal precursors containing urea which gradually decomposes can be applied for metal complexation. Obtained complexes have low temperature of decomposition and after thermal treatment noble metal nanoparticles can be formed. We are expecting that reaction mechanism can be modified by the application of noble metal precursors with different thermal and solubility properties. Consequently the used precursors can affect morphology and structure of resulted nanoparticles.

A reaction of sonochemical decomposition of urea can be controlled by ultrasonic parameters. This reaction results in subsequent increase of pH to the physiological value

(7.4). It has been already shown that this approach can be efficiently applied for formation of bone-like hydroxyapatite particles with rod- and plate- like shape. We assume that introduction of water solutions of noble metal precursors within the vessel during hydroxyapatite formation can be the way for composite formation. Noble metals will be complexed by isocyanates which can pronounce electrostatic interactions with hydroxyapatite surface (due to the presence of polar OH- groups onto its surface). After thermal treatment composite particles formed of noble metal nanoparticles attached to the surface of hydroxyapatite can be obtained.

Attachment of the noble metal complex onto the surface of hydroxyapatite prior to its reduction can contribute to the template role of hydroxyapatite in the mechanism of noble metal nanoparticles formation. For that reason different morphological and structural properties of noble metal particles formed alone and within apatite composites are expected.

Hydroxyapatite has an affinity to exchange many different cations (Hg, Cd, Pb, Co-ions etc.). According to the ionic radii of silver ions ($R(Ag^{2+})$=0.108 nm), gold ions ($R(Au^{3+})$=0.099 nm) and platinum ions ($R(Pt^{4+})$=0.077nm) compare to the ionic radius of cations in the hydroxyapatite ($R(Ca^{2+})$=0.099 nm), we expect that ions of noble metals can incorporate in apatite structure. Formation of Ca-deficient hydroxyapatite is associated with morphological changes which reduce aspect ratio of apatite rods. This ion incorporation can affect morphology of hydroxyapatite particles within its composites with noble metals.

Noble metals have an affinity to bind groups which contain nitrogen or sulphur onto its surface and to passivate it. These approaches might be able to provide control over the process of particle growth.

Besides many different methods, which are applied for the synthesis of noble metal nanoparticles, benefits of the application of homogeneous sonochemical precipitation method are related to contribution of ultrasonic effects together with controllable kinetics of decomposition of urea which increases local pH during precipitation. Physical effects of ultrasound, like homogenization, mixing, emulgation, together with chemical effects of ultrasound, such as formation of active radicals and active intermediate compounds, are able to affect morphological and structural properties of resultant materials.

Optimization of the conditions for homogeneous sonochemical precipitation method will allow us to form small- sized and regular- shaped noble metal particles attached to the surface of hydroxyapatite within composite.

It is expected that obtained composite will be able to pronounce antibacterial action and investigation of noble metal ions release in simulated physiological conditions can provide information suitable to predict this process.

3 Materials and Methods

3.1 Materials

3.1.1 Materials for composites formation

Hydroxyapatite has been synthesized using calcium nitrate pentahydrate ($Ca(NO_3)_2 \cdot 5H_2O$ (Sigma, Aldrich, Germany)) and ammonium dihydrogen phosphate ($NH_4H_2PO_4$ (Sigma Aldrich, Germany)) as Ca- and P- sources while urea ($(NH_2)_2CO$, (Alfa, Aesar, Germany)) provided homogeneous precipitation.

The formation of Ag nanoparticles and their composites with HAp was performed using silver nitrate ($AgNO_3$, T_m=212°C, T_b=444°C), silver acetate (CH_3COOAg, T_b=220°C) and silver lactate ($CH_3CH(OH)COOAg$, T_m=120-122°C) (Sigma Aldrich, Germany) as the silver precursors. For the preparation of Pt nanoparticles and their composites with HAp chloroplatinic acid hexahydrate ($H_2PtCl_6 \cdot 6H_2O$) (T_m=60°C, high solubility in water) and platinum(II)-2,4-pentanedionate ($C_{10}H_{14}O_4Pt$) (T_m=250°C, poor solubility in water) (Sigma Aldrich, Germany) were selected as sources of platinum while Au nanoparticles and their composites with HAp were prepared using gold-hydroxide ($Au(OH)_3$) (decomposes by heating, soluble in water), gold-acetate ($Au(CH_3COO)_3$) (decomposes by heating, slightly soluble in water) and chloroauric acid ($HAuCl_4$) (T_m=254°C, high solubility in water). Chemical reduction was performed using amino acids (*L*-arginine (*L*-2-amino-5-guanidinopentanoic acid; $C_{16}H_{14}N_4O_2$), glycine (aminoacetic acid, $H_2NCH_2CO_2H$) and *D*-histidine ((R)-2-amino-3-(4-imidazoly)-propionic acid, $C_6H_9N_3O_3$) and thiols and/or amines (thiourea/sodium borohydrate ($SC(NH_2)_2$)/$NaBH_4$, aniline ($C_6H_5NH_2$), 4(methylthio)aniline ($C_6H_5NH_2CH_3$), 5-bromopyridine-2-thiol (C_5H_4BrNS) (Sigma Aldrich, Germany).

All of the chemicals and reagents were of analytical grade. All of the experiments were performed using lab-made distilled water.

3.1.2 Materials for *in vitro* release of metal-ions

In vitro investigation of release of metal-ions from HAp/metal composites was performed in simulated body conditions provided by phosphate buffered solution (PBS) (1 tablet dissolved in 200 ml of water contains following concentrations of salts- 0.137 M sodium-chloride (NaCl), 0.01 M of phosphate buffer (Na_3PO_4/Na_2HPO_4/NaH_2PO_4) and 0.0027 M potassium-chloride (KCl)) (Sigma Aldrich, Germany).

3.1.3 Bacterial and cellular cultures

Antibacterial test were performed on two types of clinically isolated microorganisms- *Escherichia coli* as Gram negative and *Staphylococcus aureus* as Gram positive bacteria.

In vitro cytotoxicity tests were performed on human cells. Cells were purchased from European Collection of Cell Cultures. First model was human Caucasian foetal lung

fibroblasts cell line (IMR-90) (ECCAC catalogue no. 85020204). IMR-90 cells derived from lung tissue of a 16 week old female Caucasian foetus and were selected as a model of healthy human fibroblasts. Second model was human osteosarcoma (U-2 OS) (ECCAC catalogue no. 92022711) cell line. U-2 OS were selected as models of cancer-modified bone osteoblasts and they derived in 1964 from a moderately differentiated sarcoma of the tibia of a 15 year old girl.

Normal IMR-90 fibroblast cells were maintained in Eagle's minimal essential medium with Eagle's balanced salt solution (EMEM (EBSS)) supplemented with 2mM glutamine, 1% non-essential amino acids (NEAA), 10% foetal bovine serum (FBS) and 1% each of penicillin and streptomycin.

Osteosarcoma cells were maintained in McCoy's 5a medium with 1.5 mM glutamine, 10% PBS and 1% each of penicillin and streptomycin.

All cells were maintained under standard conditions in the incubator under atmosphere of air (95%) and CO_2 (5%) at 37°C.

3.2 Methods

3.2.1 Synthesis method

Composites of HAp with noble metals were synthesized using modified sonochemical homogeneous precipitation method (Vukomanović et al., 2011d). For that purpose two different routes of reduction of metallic part of the composite have been applied. In the first case reduction was thermal while in the second case it was chemical process performed using different reduction agents able to remain on the surface of metallic particles and to provide their functionalization.

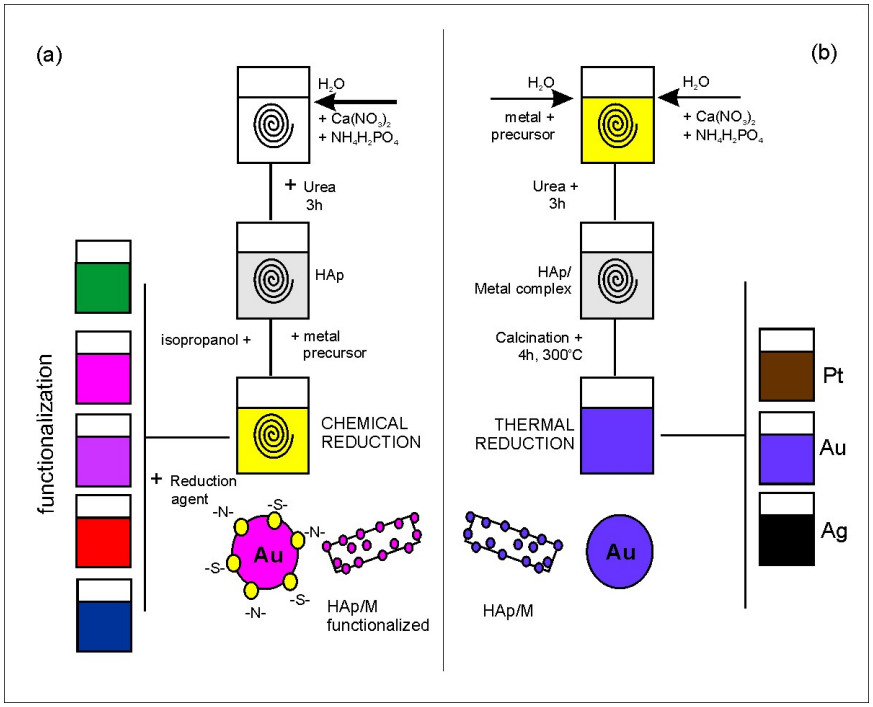

Figure 25: *Schematic illustration of experimental procedures for modification of sonochemical method coupled with chemical (a) and followed by thermal reduction of metallic part of the composite with HAp.*

3.2.1.1 Thermal reduction

The synthesis of the Ag, Pt and Au nanoparticles and their composites with HAp (HAp/Ag, HAp/Pt and HAp/Au) was performed using a modified sonochemical homogeneous-precipitation method followed by thermal reduction. For this purpose, aqueous solutions of metal precursors with different thermal properties and solubility in water were used. Precursors for silver were $AgNO_3$, CH_3COOAg and $CH_3CH(OH)COOAg$), for platinum they were $H_2PtCl_6 \cdot 6H_2O$ and $C_{10}H_{14}O_4Pt$ while $Au(OH)_3$, $Au(CH3COO)_3$ and $HAuCl_3$ were used as gold- sources. For the formation of the metallic particles, 50 ml of each of these solutions with concentration of 5 mg/ml were added to 100 ml of water, whereas in the case of the composites, the same volume of each of the solutions was added to 100 ml of a mixture of HAp precursors – water solutions of $Ca(NO_3)_2 \cdot 5H_2O$ and $NH_4H_2PO_4$ with a Ca/P ratio of 2. After the mixture of precursors was heated to $T_{max.}$=90°C, 10 ml of a 12 % solution of urea was added and the sonication was started. The following ultrasonic parameters were applied: ultrasonic field power, P=600W; frequency of the field, f=20 kHz; effective time of pulsed sonication, t=3h; and pulsation-to-relaxation time, on:off=02:01. When the sonication was finished, the samples were aged for 12h. The precipitates were separated from the mother liquid by centrifugation (4000 rpm) and then air dried. All of the powders were calcined for 4h at 300°C in an Ar/H_2 (96:4%) atmosphere. Selected calcinations temperature was also the temperature at which reduction was performed resulting in formation of metallic particles. In the case of silver and gold this temperature was 300°C while for platinum it was 400°C. After thermal reduction samples containing Ag turned into black, those containing Pt turned into dark brown and black while powders with Au had dark violet colour.

3.2.1.2 Chemical reduction

Affinity of gold surface to bond amines and thiols was used for development of the second type of modification of sonochemical homogeneous precipitation method coupled by chemical reduction. In the first step HAp has been synthesized without addition of metal-precursors, using a mixture of water solutions of $Ca(NO_3)_2 \cdot 5H_2O$ and $NH_4H_2PO_4$. These solutions were placed into Suslick reactor and heated to the maximal temperature of 90°C. After reaching the temperature, 10 ml of 12-% aqueous solution of urea has been added and sonication was initiated. Following parameters were used: time of sonication t= 3h, pulse on:off = 02:01s, amplitude 80%, power P=600W and frequency f=20 kHz. In the second step, HAp (c=1.5 mg/ml) has been separated from motherliquid and re-dispersed into isopropanol solution in water ($c=2 \cdot 10^{-2}$ ml/ml) using ultrasonication (time of sonication t=10 minutes, pulsation-to-relaxation periods on:off=02:01, T=25°C, power P=600W, frequency f=20 kHz and amplitude A=80%). After dispersion period was finished, 50 ml of aqueous solution of chloroauric acid ($HAuCl_4$) (c=0.8 mg/ml) were added. This step was followed by addition of 50 ml of aqueous solution of selected reduction agent/functionalization ($n_{(HAuCl4)} : n_{(functionalization)} = 1 : 1$ mol/mol). During the last two steps sonication was performed using the following parameters: pulsation-to-relaxation periods on:off=02:01, T=25°C, power P=600W, frequency f=20 kHz, amplitude A=80% and time of sonication that depended on selected functionalization. For amino acid sonication time was t=15 minutes, for thoiurea/$NaBrH_4$, aniline and its derivate t=5 minutes and for bromopyridine-2-thiol it was t=30 minutes. Obtained precipitates were separated from supernatant by centrifugation (15 minutes at 5000 rpm) and air-dried on glass slides. Powders were purple, red, violet, grey, and dark green depend on the reduction agent.

All the experiments were performed using an Ultrasonic Processor for High Volume Applications VCX 750, Newtown, Connecticut, USA.

3.2.2 Methods for characterization of materials

3.2.2.1 Powder X-ray diffraction (XRPD)

Identification of the crystalline phases formed after each step of sonication procedure on the way to the formation of silver, gold and platinum particles with and without HAp was performed using XRPD method. Samples were recorded with a Bruker AXS D4 Endeavor diffractometer at room temperature in the 2θ range from 2° to 70° with a step size of 0.02° and a time of 2 s/step. Data were analyses using Eva software package.

3.2.2.2 Fourier infrared spectroscopy (FTIR)

FTIR spectroscopy was used for qualitative analysis of the samples and investigation of the existence of the physical or/and chemical interactions among the phases. Method was used for identification of the complexes formed during the process of sonochemical formation of metals and their composites with HAp as well as for identification of the interactions between them. For that purpose potassium/-bromide (KBr) technique has been applied and spectra were recorded in transition mode. Samples were mixed with KBr in the molar ratio 1:1, homogenized and pressed into disk. The same method was used for identification of the organic species on the surface of metallic particles bonded during chemical reduction process when they were functionalized. In that case attenuated total reflectance (ATR) technique has been applied. FTIR spectra were recorded on a Spectrum One (Perkin Elmer) FTIR spectrometer in the spectral range between 4000 and 400 cm^{-1} with a spectral resolution of 4 cm^{-1}.

3.2.2.3 UV/VIS spectrophotometry (UV/VIS)

UV/VIS spectrophotometry allowed investigation of the optical properties of HAp and their changes after formation of composites with noble metals. Ability of composites to absorb the light from UV and visible range of electromagnetic spectrum were investigation depend on the different types of surface functionalizations. Absorption spectra were measured on UV-VIS spectrophotometer (UV-VIS-NIR spectrophotometer Shimadzu UV-3600) in the range between 200 and 800 nm with a spectral resolution of 0.1 nm.

3.2.2.4 Inductively coupled plasma atomic emission spectrometry (ICP AES)

ICP AES was used as quantitative analysis method which provided information on the total content of noble metals within the composites. Samples were prepared by dissolving in 1 M solution of hydrochloric acid. Measurements were performed using an inductively coupled plasma atomic emission spectrometer (ICP AES) (Thermo Jarrell Ash, model Atomscan 25) equipped with an ultrasonic nebulizer (Cetac, model U-6000 AT).

3.2.2.5 X-ray photoelectron spectroscopy (XPS)

Elemental composition analyses of the surface and profile of HAp composites with noble metals were carried out on the PHI-TFA XPS spectrometer, exciting the sample's surface by X-ray radiation from an Al-monochromatic source. The survey and narrow-scan spectra of the emitted photoelectrons were taken at 187 eV and 29 eV. The depth-profile analyses were performed by sequential sputtering of the sample and removing the layers with an argon ion beam (sputtering velocity ~1.7 nm min^{-1}). The XPS analyses were performed after every five sputter cycles (5-min duration). The data were processed with the Multipak program, version 8.1.

3.2.2.6 Surface charge measurements

The surface charge was measured by z-potential using a Zeta-Plus Analyser (Brookhaven Instruments, USA). The measurements were performed for HAp/Ag composites obtained using nitrate, acetate and lactate precursors obtained by thermal reduction as well as for HAp/Au composites obtained by thermal reduction and by chemical reduction using amino acids (glycine, arginine and histidine) and synthetic amines/thiols (thiourea, aniline, 5(bromo-piridine-2-thiol and 4(methylthio)-aniline) The samples were suspended in a diluted sodium chloride solution (1 mM) at pH=7.0. All measurements were done in triplicate.

3.2.2.7 Field emission scanning electron microscopy (FESEM)

The morphological analysis of noble metal nanoparticles and their composites with HAp was performed using a SUPRA 35 VP Carl Zeiss field-emission scanning electron microscope (FESEM). Method was used for investigation of the influence of different precursors, contribution of HAp as a template as well as contribution of reduction agents as capping agent to the morphological properties of metal nanoparticles. All samples were dispersed in water, deposited into the polycarbonate membrane by vacuum filtering and coated by thin layer of carbon to prevent charging.

A stereological analysis was used for obtaining of the distribution of particle size and determination of the mean value of their diameters. A method is based on statistical analysis of 2D projections of the particles from SEM images. Quantification of morphological parameters was performed on approximately 550–700 particles using an image analyzer (Image Tool Win 3.0 Software).

3.2.2.8 Transmission electron microscopy (TEM)

Transmission electron microscopy using a JEOL JEM-2100 was employed for the further morphological analysis of the as-synthesized metallic nanoparticles and their composites with HAp. The structural characteristics were determined by high-resolution electron microscopy (HRTEM) and selected-area electron diffraction (SAED). All samples were dispersed in water and drop-wise added to the copper grid.

3.2.3 Method for investigation of photocatalytic activity

Method used for determination of photocatalytic activity of HAp composites was based on testing of materials' ability to induce degradation of organic dyes after activation by adsorption of the light from UV and VIS range of electromagnetic spectrum.

A water solution of methylene blue (2.67 x 10-5 M; 10 mg/l solution) was used as pollutant, non-degradable dye. A 7 ml of dye solution was mixed with 13 mg of tested powders. The mixtures were kept in dark overnight to ensure reaching of the adsorption-desorption balance. In the following step, mixtures were incubated in reactor in the position where irradiated area of samples was 5 cm in diameter and the working distance between the sample and the lamp was 8 cm. The UV irradiation was carried out using the fluorescence Blacklight Blue Lamps L18-73 (3.5 W; λ=300-400 nm) and the VIS irradiation was carried out using the LED Parathom PAR 16 (5 W) provided by Osram. After distinct periods of time, a 700 µl of dye solution were selected for spectrophotometric measurements (UV-VIS-NIR spectrophotometer Shimadzu UV-3600) and determination of the dye concentration. Obtained data were used for monitoring and measurement of kinetics of photocatalytically induced degradation process of non-degradable dye. The procedure was applied for analysis of HAp/Pt composites synthesized using H_2PtCl_6 and $C_{10}H_{14}O_4Pt$ precursors while commercial photocatalyst

P25, which is a mixture of rutile and anatase phase of TiO_2, was tested as a reference.

In gaseous media the photocatalytic activity was determined by monitoring the degradation of isopropanol as model organic substance which can be oxidized into acetone upon irradiation with UV or VIS light in the presence of a photocatalyst. The photocatalytic oxidation of the isopropanol into acetone and subsequent oxidation of acetone was followed with the calculated area of the characteristic bands for isopropanol and acetone, at 951 cm^{-1} and 1207 cm^{-1}, respectively, measured by a FTIR spectrometer (Perkin Elmer BX II).

3.2.4 Tests of antibacterial activity

3.2.4.1 Disk diffusion test (Kirby-Bauer method)

The disk diffusion test, known as Kirby-Bauer method, is a standardized method for investigation of antibiotic susceptibility. A basic principle of the method is diffusion of the chemical from the disk through the surrounding medium around the disk. Medium (usually Meuller-Hinton agar) contains selected microorganisms. In the case when they are susceptible to diffused substance, they will not grow in the area around disk. This area is known as zone of inhibition. Infiltration of the substance around disk depends on various conditions as solubility and molecular size of the substance, its concentration, pH of the medium, temperature and atmosphere as well as the time of exposure. Method used for investigations of different potential antibacterial agent tested under the same conditions provides good conditions for comparison of their efficacy.

Table 4: *Criteria for evaluation of the results of disk diffusion test: indexing of the parameters and definition of the level of toxicity of investigated substance (Schmalz, 1988).*

Zone index	Description of the zone
0	No zone around disk nor under it
1	Zone under disk
2	Zone less than 0.5 cm around disk
3	Zone between 0.5 and 1.0 cm around disk
4	Zone more than 1.0 cm around disk
5	Zone over the whole surface
Lysis index	**Description of the zone**
0	No changes
1	Less than 20% of the zone covered by the change
2	Between 20 and 39% of the zone covered by the change
3	Between 40 and 59% of the zone covered by the change
4	Between 60 and 80% of the zone covered by the change
5	More than 80% of the zone covered by the changes
Response index (zone index/lysis index)	**Description of the zone**
(0/0)-(0.5/0.5)	Non-toxic
(1/1)-(1.5/1.5)	Slightly toxic
(2/2)-(3/3)	Middle toxic
≥(4/4)	Intensively toxic

Described test has been used for investigation and quantification of susceptibility of HAp composites with silver, gold and platinum determined under the same conditions and their comparison. Composites were with and without surface functionalization and they were tested for ability to inhibit growth of *E. coli* as Gram negative and *S. aureus* as

Gram positive model.

Tests were performed under the following conditions: agar dissolved in saline solution was poured into a Petri dish in the volume of 30 ml per plate; *E. coli* and *S. aureus* were collected during the phase of logarithm growth and their suspension in media broth (1 OD) was plated on agar with a wet cotton swab; HAp/Ag, HAp/Pt and HAp/Au composites prepared under different conditions were compacted into 8-mm disks containing 10% of active (metallic) substance; disks made of HAp formed under the same conditions used for the synthesis of composites were used as negative controls; thus obtained disks were put on the surface of the agar plates with bacteria, they were turned upside down and incubated at 37 °C for the next 24h.

Zones of inhibition of bacteria growth were photographed for the future evaluation according to the criteria defined in Table 4.

3.2.4.2 Phase contrast microscopy

Phase contrast microscopy based on the difference in refractive indexes of the light after the transmission through different media is useful tool in biology since it provides fast, *in situ* observation of live and dead cells without additional treatment. After investigation of the susceptibility of HAp/Ag, HAp/Pt and HAp/Au composites to *E. coli* and *S. aureus*, areas around the disks were observed by optical microscope (Olympus BX series) using phase contrast technique in order to observe existence and size of the zones of inhibition of bacteria growth.

3.2.4.3 Fluorescence microscopy

In the case of materials which confirmed susceptibility to analyzed bacteria, detection of dead and live bacteria and their distribution on the surface of the disks and within the zone of inhibition were investigated using fluorescence microscopy.

The fluorescent Live/Dead BacLight bacterial viability kit (Molecular Probes, Inc.) consisting of two dyes: SYTO 9 and propidium iodide (PI) was used for labelling. SYTO 9 is the green fluorescent nucleic acid stain which stains the nucleic acids of both living and dead bacteria. PI is a red fluorescent nucleic acid stain, which does not enter bacteria that have intact cell membranes and thus only stains bacteria that have damaged membranes. It means that after labelling live bacteria fluoresce in green whereas dead bacteria fluoresce in red (Ericsson et al., 2000).

E. coli and *S. aurous* were coherently grown in 24-well plates with agar and disks made of bacteria susceptible composites were put on their surface. After 24-hour incubation at 37°C, disks were removed and water solution of the two solid-phase components of the Live/Dead Backlight kit was added. After incubation in the dark for 30 min samples were inoculated.

The analysis of the fluorescently labelled bacteria was performed using an inverted research microscope Olympus IX81 with a motorized fluorescence attachment. The emission signal was filtered using U-N49002 (green fluorescence) and U-M41002 (red fluorescence) filter cubes. The objective 100× (oil immersion, N. A. 1.35) was used together with an additional intermediate optical lens. Micrographs were taken with Hamamatsu CCD camera ORCA-R2 and Olympus Cell F software was used to evaluate the specific labelling signal.

3.2.4.4 Antibacterial test during VIS irradiation

Antibacterial test of photocatalytically active materials measures their ability to influence growth of bacteria after activation by light. Test was used for investigation of photocatalytically-induced antibacterial activity of HAp/Pt with two different surface

functionalizations.

300 µl of agar containing no composite (negative control), 0,5 mg/ml HAp/Ag (positive control) or 2, 4 or 6 mg/ml HAp/Pt composites synthesized using H_2PtCl_6 and $C_{10}H_{14}O_4Pt$ precursors, was poured in duplicates into a 24-well plate. *E. coli* suspension (1 OD) was plated on agar with a wet cotton swab. Wells were incubated at 37 °C under direct VIS light (without a lid) for the first 3 h and then with a lid for the next 18h. The total number of cells was determined using Live/Dead Baclight viability and counting kit (Molecular Probes). To collect bacteria, agar surface was washed with 300 µl 0.9% NaCl. 10 µl of 6-fold diluted bacterial suspension, 0.75 µl of SYTO9 and 0.75 µl of PI were added to 977 µl of 0.9% NaCl and incubated for 15 min. Then 10 µl of microsphere suspension (1.0 x $10e^8$ beads/ml) was added and samples were analyzed with a FACSCalibur (Becton Dickinson) flow cytometer. The acquisition was stopped when 1000 events were acquired in the beads region. The concentration of cells was calculated as follows: [(# events in bacteria region) x (dilution factor)] / [(# of events in bead region) x 10 e^{-6}].

3.2.4.5 Minimum inhibitory and minimum bactericidal concentrations (MIC and MBC) tests

Dilution tests are methods for the quantitative measurement of antibacterial activity used for precise determination of the influence of different concentrations of investigated substance to bacterial growth. A method can be conceptualized in two ways: (i) agar dilutions- when a distinct concentration of the active substance in broth is added to the plates with different concentrations of bacteria and (ii) broth micro dilutions- when different concentrations of antimicrobial agent are added to the same concentration of bacteria in agar plates. In any case, the lowest concentration of the tested substance able to induce visually-detectable inhibition of bacterial growth is minimal inhibitory concentration (MIC). The lowest concentration of the substance which is able to prevent the growth of bacteria after subculturing in agar plates without antimicrobial agent is the minimum bactericidal concentration (MBC). Method is widely used in comparative analysis of novel antimicrobial agent (EUCAST, 2000; Andrews, 2001).

MIC test. HAp/Ag, HAp/Au and HAp (as negative control) were dispersed in growth medium to form stock solutions (4 mg/ml). These solutions were subsequently diluted by addition of distinct volumes of growth medium to form series of solutions with different concentrations of each material. Series contained solutions in the range of 0.0-6.0 mg/ml. 1000 µl of each solution was mixed with the same volume of both bacterial cultures (*E. coli* and *S.aureus*) Dispersions containing different concentrations of materials and constant concentration of bacteria (OD~1) were incubated overnight in 15-ml centrifuges in shaking water bath at 37°C to detect MIC.

MBC test. After overnight incubation, a 200 µl of all dispersions were separated. One half of this volume was plated on agar in Petri dishes (Ø=10 mm) using a wet cotton swab while another one was mixed with 1.9 µl of fresh medium. They were additionally incubated overnight at 37C to determine MBC.

All analyzed concentrations for each material were tested in twice. Statistical analysis of results was done by Student's t-test. Sigma plot software version 11.0 was applied for processing of the data and differences have been considered as significant at p-value below 0.05.

3.2.4.6 Method for SEM and TEM investigation of bacteria

Electron microscopy methods provide possibility for investigation of the morphological and ultrastructural properties of prokaryotic cells as well as their interactions with surroundings. Because of the soft carbon-based structure and a large content of water preparations of these sorts of samples require special procedures in order to preserve them from high-vacuum-induced damage (Stadtländer, 2007).
Morphological and structural properties of E. coli and S. aureus were analyzed after exposure of bacteria to HAp/Ag and HAp/Au/arginine composites. A 15 mg of each materials are compacted into disks (Ø=8 mm). Disks were kept overnight on bacteria plated in agar at 37°C. Sampling of bacteria exposure to materials was performed from the area of the zone of inhibition near to the surface of the disks while negative references were bacteria grown in the healthy colony far from the disk.

SEM investigation of the surface structure of bacteria requires following basic steps involved in their preparation- surface cleaning, stabilizing the sample with a fixative, rinsing, dehydrating, drying, mounting the specimen on a metal holder, and coating the sample with a layer of a material that is electrically conductive (Bozzola and Russell, 1992).

(i) Surface cleaning. Cleaning of the surface is important because of the detachment of unnecessary deposits. The best way for cleaning is a use of the solution with the pH, temperature and osmotic strength close to the medium in which bacteria were analysed. HAp/Ag and HAp/Au composites were carefully rinsed three times for 10 minutes using 0.1 M phosphate buffer solution (pH=7.4) at room temperature through millipore filter.

(ii) Stabilizing the sample with a fixative. Stabilization has been done using 1.5% solution of glutaraldehyde in 0.1M PBS buffer. Samples deposited on millipore filter or agar plates were kept in aldehyde solution in a closed Petri dish overnight at the temperature of 4°C. Samples were rinsed by PBS solution (three times for 10 min at 4°C), post-fixed using 1% aqueous solution of osmium-tetra oxide for 1 hour and once again rinsed by distilled water.

(iii) Dehydrating. This process allows the water inside the biological samples to be slowly exchanged by liquids with lower surface tensions. This step is usually performed in gradient solutions of acetone or ethanol. In this case, samples were immersed in 50%, 70%, 90% and 100% ethanol solution and finally in 100% acetone during the intervals of 20 min for each solution.

(iv) Drying. Samples were dried using critical point drying method in CPD030 dryer (Balzers) using liquid carbon-dioxide as transition medium.

(v) Mounting the specimen on a metal holder and its coating with a layer of a material that is electrically conductive. In this case coating was performed by platinum in 050 sputter coater (BAL-TEC).

TEM investigation of ultrastructure of bacteria requires following major steps- cleaning, primary fixation, rinsing, secondary fixation, dehydration, infiltration with a transitional solvent, infiltration with resin and embedding, and sectioning with staining. The last three steps are different compare to the procedure described for SEM sample preparation (Bozzola and Russell, 1992) at room temperature is sufficiently long period for efficient infiltration.

(i) Infiltration with resin and embedding. Epoxy resin (Spurr) is mixed with acetone (1:1 v/v) and bacteria are immersed into the mixture for 1 h. After that the samples were transferred in fresh resin and kept overnight at room temperature in order to reach infiltration. The next day, specimens transformed again pure resin and left during the next 2 hours for embedding. Polymerization of resin was performed in oven at 60°C for 72 h.

(ii) Sectioning with staining. Dry specimens were sectioned into thick slides (~60 nm) using diamond knife on UltracutS (Leica) and stained by uranyl-acetate and lead-citrate (Bozzola and Russel, 1992).

3.2.5 Method for *in vitro* investigation of release of metal-ions

In vitro methods for investigation of biomaterials during aging in simulated physiological conditions are design to test some of their properties important for practical application and to use the data to predict their compatibility and suitability for the real, *in vivo* conditions. Investigation of release of metal- ions from HAp/Ag and HAp/Au composites was performed using *in vitro* simulated physiological conditions which were conceptualized as simulation of chemical and physical level. First level of simulation of these conditions concerns chemical simulation. Method is based on keeping the composition, concentrations and acidity of the release- medium as much similar as it is possible to the real *in vivo* conditions. For that purpose there was a need for use of the mixture of the salts solutions with concentrations and acidity at the level that correspond to their level in the mammalian blood plasma. Concerning the difference of the pH and salt concentration in extracellular and intracellular environments, method includes possibility for their variation in order to predict their influence. The second level of simulation concerns physical conditions. Dynamics provided by the natural circulation of the liquids in living systems is included within this level of simulation. It is presumed that usage of the mean value of adult human pulse (which is approximately 60 beats per minute) can be taken as a reference. Additional direction within the physical level of physiological conditions simulation is a temperature. Method uses 37°C as an average temperature of the living organism.

For investigation of release of Ag- and Au- ions from HAp/Ag and HAp/Au composites chemical level of simulation of physiological conditions was reached using PBS buffer solution which is able to ensure neutral pH (at the value of 7.4) as well as solutions with increased acidities which were maintained by hydrochloric acid to the slightly acid (pH=5.4) and strongly acid (pH=3.4) values. Dynamical conditions and constant temperature were ensured by the use of shaking water bath (Memert, WNB 7–45, Germany). Powders of HAp/Ag and HAp/Au functionalized with arginine were divided into three series of samples for each composite. These three series contained release media with the three different pH values. All series contained five samples which corresponded to the number of investigated periods of time during which a distinct quantity of ions has been released. Every sample contained 10 mg of HAp/Ag or HAp/Au composite powder dispersed in 10 ml of release medium. The total release of the ions was investigated during the period of ten days. After every two days of investigated period, release of the ions has been stopped, cuvettes were centrifuged (4000 rpm), liquids and powders were separated and stored in dark for further characterization.

Quantities of the Ag and Au ions released under described conditions were determined using previously described ICP AES (Thermo Jarrell Ash, model Atomscan 25) method. Quantification was performed from release media without additional preparation. Powders remained after aging of the materials in releasing mediums are dried and powders are investigated for phase composition. For that purpose above described XRPD (Bruker AXS D4 Endeavor diffractometer) method has been applied.

3.2.6 Sterilization method

Materials used for investigation of the cytotoxicity were compacted into disks with diameters of 8 mm. These disks were further on sterilized using γ sterilization method.

Samples were irradiated in ^{60}Co radiation chamber under normal condition (in air atmosphere and room temperature). Sterilization was performed using irradiation rate of kGy/h and total absorbed dose of 25 kGy. These parameters are in accordance with the standard for sterilization of the medical devices- E552.

3.2.7 Methods for *in vitro* investigation of cytocompatibility

Viability tests are vital for investigation of the toxicity of materials especially those who were newly developed since they have ability to show how living cells react on their presence. This is the way for prediction of the possible reaction of living organism after incorporation of the same sort of material.

Annexin V/ propidium-iodide (PI) assay. In the case of living cells phosphatidylserine, which is a phospholipid component of cellular membrane, is present on its inner, cytosolic side (Figure 26a). The earliest event which indicates apoptosis of live cells is translocation of this phospholipid to the outer, surface side of cellular membrane by the action of flippase. At this moment cellular membrane is still compact and poses only the change in its structure (Figure 26b). Annexing V has high affinity to bond phosphatidylserine which provides ability for detection of both very early and late phases of cellular death. PI is impermeable dye which can get inside cell only in the case when its cellular membrane is ruptured which is the case of dead, necrotic cells. Chemically, it is a chelating agent with affinity to bond nucleic acids (Figure 26c). Simultaneous staining with annexin V and PI provides ability for making a difference between necrotic and apoptotic cells.

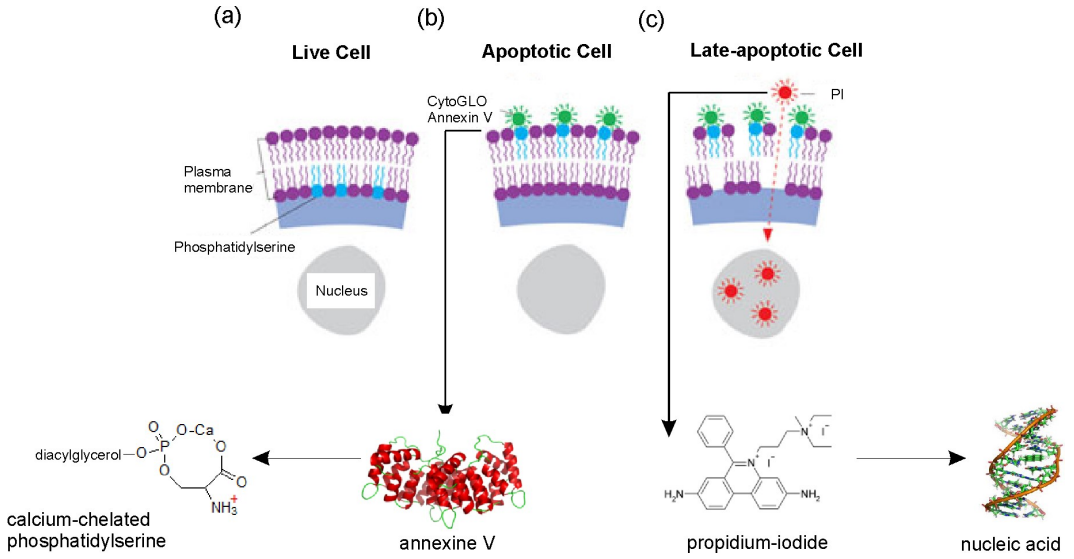

Figure 26: *Schematic illustration of the principle used for fluorescence labelling of O-2 osteoblast and IMR-90 fibroblast cells for detection of apoptosis and necrosis during investigation of cytotoxicity induced by HAp composites with noble metal nanoparticles (Apoptosis).*

Apoptosis and necrosis were investigated for U-2 osteoblasts and IMR-90 fibroblasts. Cells are dispersed in McCoy's 5a and EMEM media, respectively and grown in 24-well plates. HAp/Ag and HAp/Au composites with different types of functionalization of the surface were dispersed in the same type of media and added to the cellular cultures at different concentrations. After 24-hours-exposure to materials, cells were harvested and washed by PBS buffer solution. In the following step they were stained by annexin v/PI according to the procedure provided by the manufacturer (Annexin V Apoptosis Detection Kit, BD Pharmingen, NJ).

Measurements of the labelled cells were performed using a FACSC (Becton Dickinson) flow cytometer. The acquisition was stopped when 1000 events were acquired in the beads region. The concentration of cells was calculated as follows: [(# events in bacteria region) x (dilution factor)] / [(# of events in bead region) x 10 e^{-6}].

Optical microscopy was used to investigate changes of the morphological properties of cells depend on the concentration of HAp/Ag and HAp/Au composites.

4 Results

HAp/metallic composites were formed using calcium-phosphate bioceramic and noble metal metallic components by the application of a novel sonochemical approach. The main intension was to develop new type of biomaterials which will be able to provide high efficacy in action against Gram positive and Gram negative bacteria as well as high level of compatibility with human cells.

Development of these novel materials with advanced characteristics and high potential for improved biomedical application was structured through: (i) designing of the physicochemical properties of these materials and activation of their noble-metal component, (ii) investigation of antibacterial activity of developed materials and (iii) analysis of the influence of so formed materials to human cells. Silver as known antibacterial agent very efficient against bacteria and very toxic for human was used as a reference.

4.1 Characterization of hydroxyapatite/metal composites

A first step in development of HAp/metallic composites was to design their physicochemical properties and to activate their metallic component. Materials were synthesized using sonochemical approach which was appropriately optimized in order to reach modification in materials potentially effective against bacteria. During this process the special attention has been oriented to the surface, morphological and structural properties.

4.1.1 Hydroxyapatite/silver composites

During the synthesis of HAp/Ag composites sonochemical method was optimized in order to reach combination of different forms of silver as centres for antibacterial activity. The idea is based on high effectiveness of Ag-ions, stronger action of Ag nanoparticles compare to the Ag bulk and long-term action which can be reached in the case when particles are embedded or strongly attached to the surface of the carrier. So obtained material was used as positive control of antibacterial action as well as a positive control of toxicity.

4.1.1.1 Formation of hydroxyapatite/silver composites

Phase composition

HAp/Ag was synthesized by two-step process consisted of sonochemical synthesis followed by calcinations at elevated temperature in inert atmosphere. Ag-precursors with different thermal properties are used in order to optimize particle growth. Their processing without HAp phase was used to analyze template role of bioceramic part of the composite.

The phase identification showed that the sonochemically synthesized Ag particles using nitrate (Figure 27a) as a precursor were single phase; it reveals diffraction peaks

that correspond to the structure of the cubic silver (Ag 3C) (JCPDS No.: 4-0783). The Ag nanoparticles synthesized using acetate (Figure 27b) and lactates (Figure 27c) show two phases with diffraction peaks that correspond to the structure of both cubic (Ag 3C) and hexagonal silver (Ag 4H) (JCPDS No.: 87-0598). During the synthesis process, after the sonication of nitrate, silver isocyanate (AgNCO) (JCPDS No.: 72-1637) was detected and the reduction of the silver did not start (Figure 28a). In contrast, the sonication of the acetate and lactate resulted in the formation of both AgNCO and Ag 3C. This means that when precursors with a lower decomposition temperature were applied the reduction of the Ag was initiated during the sonication stage.

The phase identification of the HAp/Ag composites obtained using nitrate (Figure 27d), acetate (Figure 27e) and lactate (Figure 27f) as the Ag precursors showed three-phase systems containing Ag 3C and Ag 4H together with hexagonal HAp ($Ca_5(PO_4)_3OH$) (JCPDS No.: 9-0432). The presence of Ag 4H in all three cases indicates that the HAp contributes to the growth of this phase during the reduction process. There is also a decrease in the intensity and a broadening of the diffraction maxima of the HAp, indicating that its structure and crystal growth were also affected by the formation of the composite. The applied homogeneous precipitation method was previously developed for the synthesis of HAp, (Jevtić et al., 2008) but during the synthesis of HAp/Ag, the HAp was immediately obtained only after the sonication when the nitrates were applied as sources of silver. In the case of acetates and lactates the sonication resulted in the formation of a Ca-deficient octacalcium phosphate (OCP) ($Ca_8(PO_4)_6 \cdot 5H_2O$) phase (JCPDS No.: 26-1056) (Figure 28b) (Cheng, 1987) and after a thermal treatment it was transformed into the HAp. Having in mind that HAp has a high ion-exchange ability (Badrour et al., 1998; Ternane et al., 2000; Dorozhkin, 2010) the observed changes indicate the increased incorporation of Ag ions into the apatite structure, depending on the type of Ag precursor.

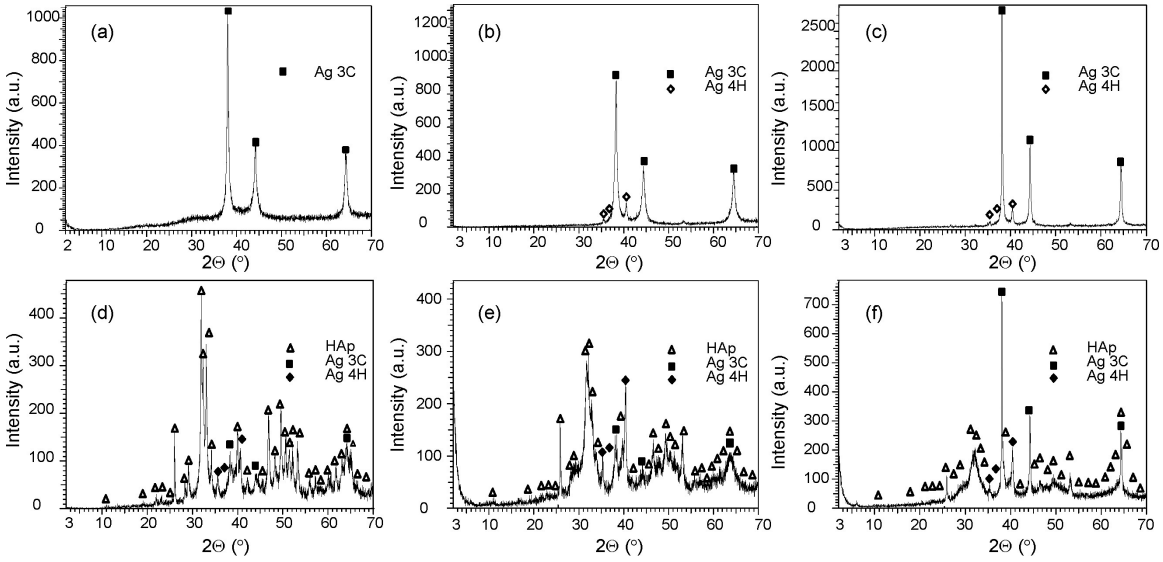

Figure 27: *XRD patterns of: Ag obtained from nitrate (a), acetate (b) and lactate (c) precursors after calcination at 300°C; HAp/Ag composite obtained from nitrate (d), acetate (e) and lactate (f) silver precursors after calcination at 300°C.*

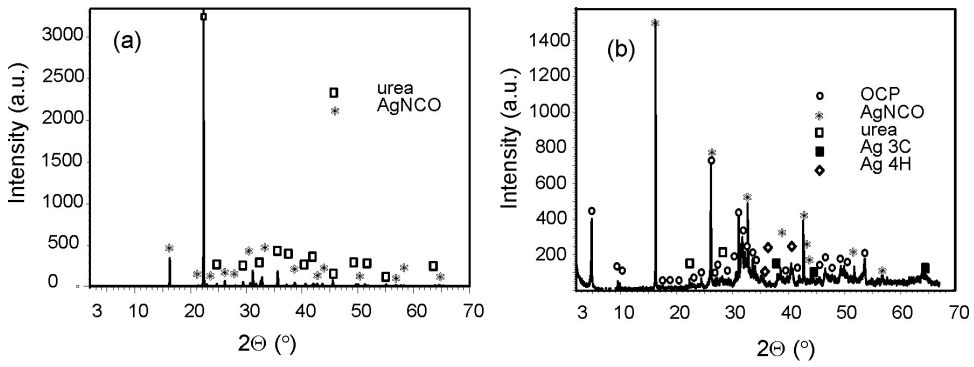

Figure 28: *XRD patterns of urea and AgNCO formed using nitrate Ag-precursor before the calcinations and OCP, AgNCO, urea and Ag obtained before the calcination using acetate Ag-precursor (h).*

Physical and chemical interactions

The contribution of the HAp to the process of the formation of Ag particles within the HAp/Ag composites was analyzed from the point of view of possible physical and/or chemical interactions between them using FTIR spectrometry. The comparative spectra of the HAp and the systems obtained using nitrates, acetates and lactates as silver precursors after the sonication (Figure 29a), after removing the AgNCO and the remaining urea (Figure 29b), and after the calcination at 300°C (Figure 29c), were used for this purpose.

After the sonication, the characteristic bands of the remaining urea were detected at 3446 and 3345 cm^{-1}, which corresponds to the stretching vibrations of the N-H groups; at 1625 cm^{-1}, corresponding to the N-H bending vibrations; at 1681 cm^{-1}, due to the vibrations of the C=O group bonded to the amine; as well as at 1464 and 1385 cm^{-1}, belonging to the C-N stretching vibrations, (Stewart, 1957; Smith, 1999; Madhurambal et al., 2010) together with a broad band at 2156 cm^{-1}, which could be assigned to the vibration of the isocyanate group (Schmidt et al., 2009) from the AgNCO (Figure 29a). The wide band in the range between 3700 and 2600 cm^{-1}, as well as the band at 1642 cm^{-1}, belongs to the vibrations of the H_2O molecules (Jevtić, et al., 2008; Jevtić et al., 2009). After the urea and AgNCO were removed, all the spectra showed bands that are characteristic of Ca-phosphate. The spectra belonging to the systems obtained without silver and using silver nitrate show bands typical of carbonated HAp (bands of PO_4^{3-} appear at 472 (υ_2), 583 (υ_4), 601 (υ_4), 961 (υ_1), 1032 (υ_3) and 1108 (υ_3) cm^{-1}; peaks at 874 (υ_2), 1415 (υ_3) and 1455 (υ_3) corresponding to the vibrations of CO_3^{2-} and the bands of OH^- ions at 3573 and 632 cm^{-1}), (Jevtić, et al., 2008; Jevtić et al., 2009) the main difference being that the spectra that belong to the system obtained with silver show the absence of any sharp bands at around 3573 cm^{-1} and 632 cm^{-1} that correspond to the stretching and libration modes of the OH- ions, respectively (Figure 29b). A similar situation was observed in the case of the HAp/Ag inorganic-inorganic hybrid obtained by the reduction of Ag ions using the electron transfer from the OH groups of the apatite surface (Arumugam et al., 2007). On the other hand, the spectra of the composites obtained using the acetate and lactate precursors show the bands characteristic for OCP: the P-OH bending modes from HPO_4 and PO_4 are detected at 1296 and 1193 cm^{-1}, the vibrations of P-O in the HPO_4 and PO_4 groups at 1126, 1110, 1058, 1040, 1023, 962, 628, 603, 560, 471 and 452 cm^{-1}, the P-OH stretching of the HPO_4 groups are at 914 and 874 cm^{-1} and the P-OH stretching mode of the HPO_4 is at 525 cm^{-1} (Mandel and Tas, 2010).

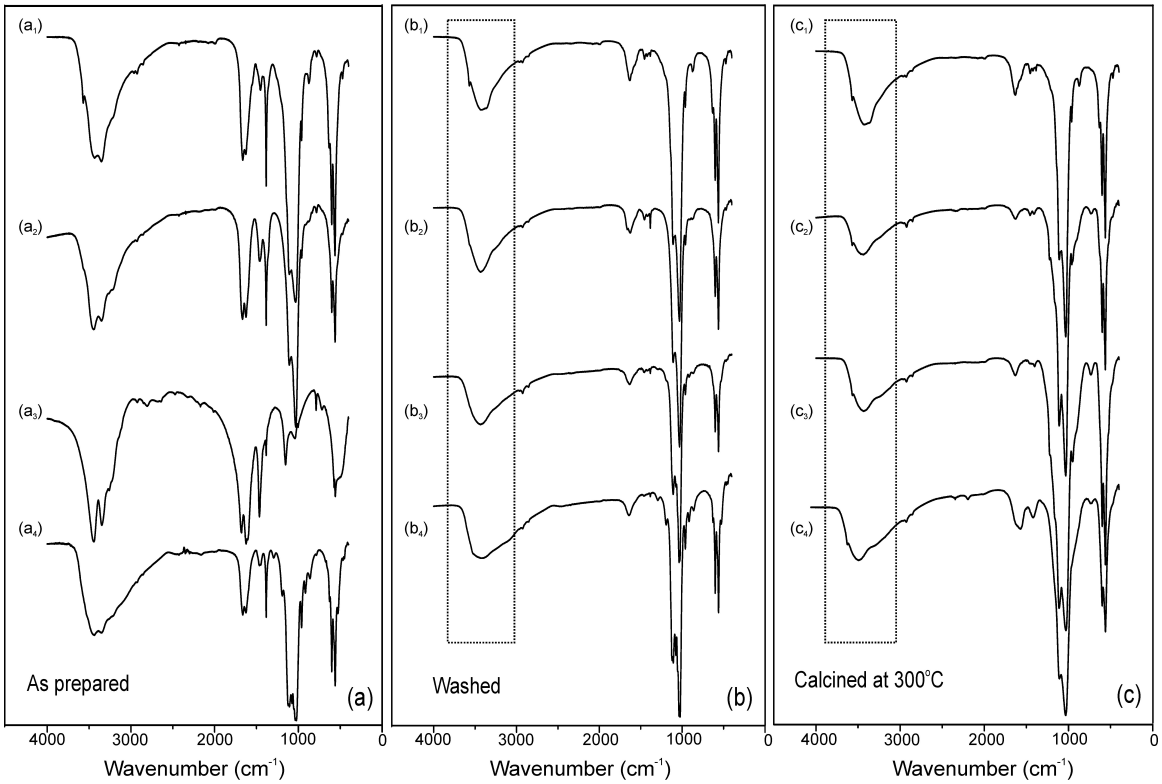

Figure 29: *FTIR spectra of HAp (1) and HAp/Ag obtained from the nitrates (2), acetates (3) and lactates (4): as prepared (a), washed with water (b) and calcined at 300°C (c).*

After the calcination at 300°C, which resulted in the reduction of the silver, and a sharp band that corresponds to the stretching mode of the OH- ions (3573 cm^{-1}) appeared, the band that corresponds to the libration mode of these ions was absent, indicating the existence of the interactions that prevented this type of vibration (Figure 29c). These results show that negative, polar OH- groups on the surface of the HAp are involved in the mechanism of the formation of metallic Ag within the HAp/Ag composite and that they are able to ensure the stabilization of Ag particles, preventing their further growth. The influence of pH on the stability of the Ag colloid particles was already shown: after the addition of the acid they tend to aggregate and grow, while a decreased acidity, as a consequence of the addition of a base, prevents their aggregation and keeps them dispersed (Sondi et al, 2003). This mechanism can be applied in the HAp/Ag system and it can provide an explanation for the difference in the particle sizes of the Ag obtained with and without the HAp, as well as the smaller particle size obtained when the nitrates were used as the silver precursor compared to that obtained when using acetates and lactates. This shows the templating role of the surface of the HAp that stabilized the Ag particles within the composite. Moreover, it has been observed that the resolution of the bands that correspond to υ_2, υ_3 and υ_4 of the vibrations of the PO_4^{3-} group was decreased in the systems that contain silver originating from the following range of silver precursors: from nitrates, through acetates, to lactates. According to the literature, the decreased resolution of the bands that correspond to the phosphate vibrations in the apatite is a consequence of a decreased crystallinity (smaller crystal size and/or more strain) (Pleshko et al., 1991) and can be associated with an increased incorporation of the ions into the apatite structure (Landi et al., 2005; Liao et al., 2007; Mayer et al., 1997). This is in accordance with the XRD patterns of the HAp/Ag (Figure 27d,e,f), which show a decreased intensity and a broadening of the main diffraction maxima (2θ = 30-35°) corresponding to the apatite structure, starting from the system obtained using nitrates (Figure 27d) to the one obtained using lactates (Figure 27f). These changes can be

connected with the incorporation of silver ions into the HAp (similar to the incorporation of Mg^{2+}-ions and carbonates into apatite) (Landi et al., 2005; Liao et al., 2007; Mayer et al., 1997).

4.1.1.2 Surface properties of hydroxyapatite/silver composites

The XPS spectra of the surface of HAp bioceramics and the HAp/Ag composites obtained using different silver precursors (Figure 30a) reveal the signals of calcium, phosphorus and oxygen, as well as the signal of carbon corresponding to the carbonates from the sonochemically synthesized HAp (Jevtić et al, 2008). The composite spectra show additional signals that correspond to silver. The elemental composition at the surface of these samples was similar, showing a slight decrease in the Ca/P ratio in the HAp/Ag composites compared to that in the HAp. Moreover, in the HAp/Ag obtained using the lactate precursor we observed an increasing trend for the surface Ag content, compared to that in the composites obtained using nitrates and acetates (Table 5). If we compare these values related to the silver at the surface with the total amount of silver in the composites (Table 5), it is clear that there is a difference in the quantity assigned to the incorporation of silver into apatite (in ionic and particulate form).

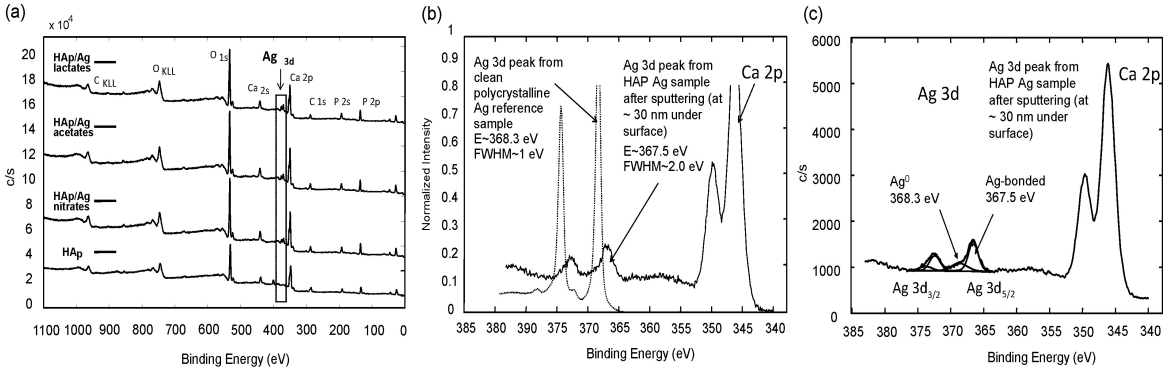

Figure 30: *XPS spectra of the surface of the HAp and HAp/Ag obtained from different silver precursors (a); spectrum of HAp/Ag obtained after sputtering: comparison with the spectrum of silver reference (b) and de-convoluted peaks corresponding to metallic (Ag^0) and bonded silver (c)*.

Table 5: *Quantitative analysis of the Ag within the HAp/Ag composites obtained using different silver precursors.*

Precursor	Total silver content (ICP analysis) wt.%	Surface silver content (XPS analysis) wt.%
Ag-nitrate	5.2	4.3
Ag-acetate	7.0	4.3
Ag-lactate	7.8	4.4

A depth-composition analysis was performed on the HAp/Ag composite and it showed a uniform distribution of elements along the profile. The high-resolution spectrum of the HAp/Ag obtained after sputtering, at approximately 30 nm under the surface, showed a signal with a maximum at 367.5 eV and a full width at half maximum (FWHM) around 2.0 eV. The comparison with the position of the maximum and FWHM values of a pure polycrystalline Ag reference sample (E~368.3 eV and FWHM~1 eV) showed a shift to a lower binding energy as well as a broadening of the Ag 3d peak in the profile of the HAp/Ag (Figure 30b). According to the literature, an anomalous negative shift in the

binding energy of the Ag 3d peak (with the value between 0.1 and 0.8 eV) occurs when the oxidation state of the silver is increased (Weaver and Hoflund, 1994). The different peak shape and the different binding energy of the Ag peak in the HAp/Ag profile spectrum, compared to the Ag reference, show that the profile contains Ag in more than one oxidation state. By means of the curve-fitting procedure, the Ag 3d double peak was decomposed into two doublets: one having Ag $3d_{5/2}$ at 367.5 eV (Ag-bonded) and the other had Ag $3d_{5/2}$ at 368.3 eV (Ag-metallic). This shows that the smaller portion of Ag is in the metallic state, whereas the larger portion is bonded in the other state (1+ or 2+) (Figure 30c). As was already mentioned, the apatite structure has the capacity to provide a variety of exchanges of both cations and anions. According to the literature data, there is a possibility to incorporate Ag within the apatite structure. As an example, there is the possibility to form lead-silver apatite ($Pb_8Ag_2(PO_4)_6$) (Ternane et al., 2000) as well as to incorporate silver into the Ca-apatite structure (Rameshbabu et al., 2007). The presence of both metallic and ionic Ag in the profile of the HAp/Ag, together with the change of the Ca/P ratio compared to that in pure HAp, indicates that, along with the metallic Ag attached to the surface of the HAp and/or embedded into the HAp plates, an amount of Ag is also present in the HAp structure. This is in accordance with the assumption that the decreased crystallinity and the increased strain are a consequence of the incorporation of silver ions within the HAp structure according to the results of the XRD and FTIR analyses.

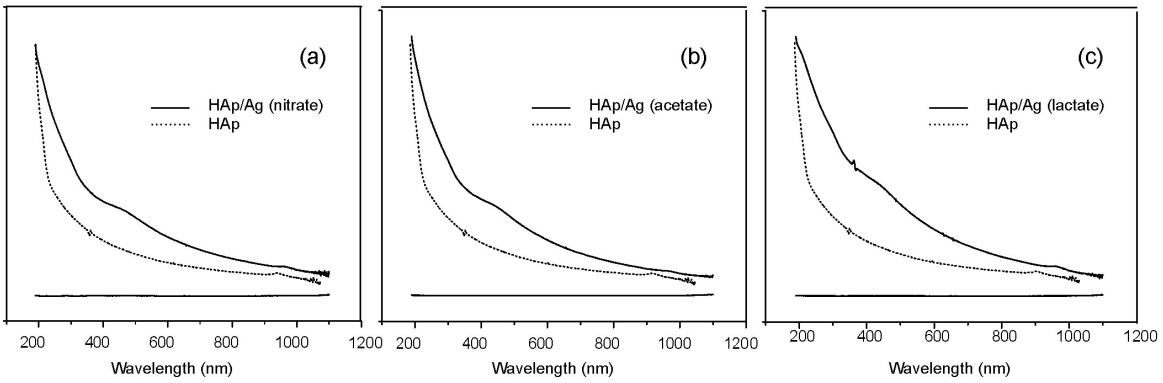

Figure 31: *UV/VIS spectra of HAp/Ag composites synthesized using nitrate (a), acetate (b) and lactate (c) silver precursor. Dotted line corresponds to the spectrum of HAp.*

According to the analysis of the absorption of the light form UV/VIS region, formed composites are showing absorption maxima around 456 nm superimposed to absorption of HAp in this region (Figure 31). These maxima are consequence of the excitation of the surface plasmon oscillations of silver nanoparticles within composites. Compare to single, spherical silver nanoparticles with SPR absorption around 410 nm (Bhui et al., 2009; Choi et al., 2007), within the HAp/Ag composite this maximum is red shifted due to the influence of dielectric constant of contacting HAp phase.

Table 6: *Zeta potential of HAp/Ag composites obtained using different silver precursors.*

Material	Zeta potential (mV)
HAp/Ag form nitrate	-15
HAp/Ag from acetate	-14
HAp/Ag from lactate	-13

Charge of the surface of HAp/Ag composites obtained using different Ag-precursors was investigated by analysis of the zeta-potential. Results obtained after reduction of silver nitrates, acetates and lactates and formation of composites are summarized in Table 6. In all three cases particles had negative zeta potentials with very similar magnitudes.

4.1.1.3 Morphological properties of hydroxyapatite/silver composites

The morphological analysis of the Ag obtained from the nitrates (Figure 32a,b,c), acetates (Figure 32d,e,f) and lactates (Figure 32g,h,i) showed an axial alignment of the nanoparticles obtained during the growth process. This type of growth is a consequence of the rod-like shape of the pre-formed silver isocyanate particles. After thermal reduction, the small, sphere-like Ag nanoparticles (Figure 32b) obtained from these rods were grown in the direction determined by the shape of the rods. In the case of acetates (Figure 32d) and lactates (Figure 32g), this axial alignment was also observed, but partially disturbed by the sonochemically initiated reduction of the silver, which acted as the nucleation seeds for further growth during the thermal reduction.

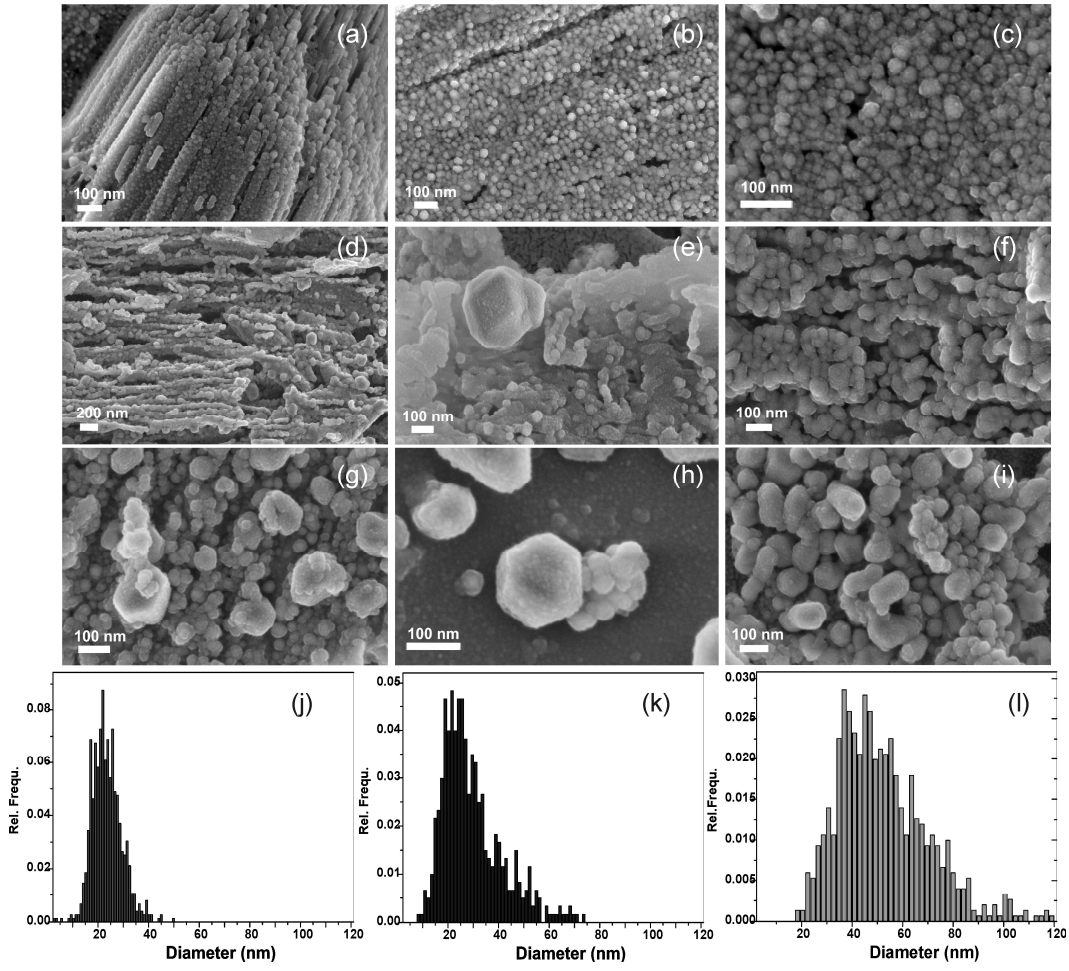

Figure 32: *FESEM micrographs of Ag nanoparticles obtained using nitrate (a, b, c), acetate (d, e, f) and lactate (g, h, i) silver precursors and the corresponding size distributions of the sphere-like particles (j, k, l).*

In the case of the nitrate precursor, all of the Ag particles were sphere-like (Figure 32c), while in the case of the acetate and lactate, both hexagonal (Figure 32e,h) and spherical particles (Figure 32f,i) were observed. The distribution and the mean size of the sphere-like nanoparticles for the three precursors are different, showing broadening of the size distribution and increasing of the mean value of the Ag particle sizes obtained from

the nitrates (D_{mean}=23 nm (Figure 32j)), acetates (D_{mean}=30 nm (Figure 32k)) and lactates (D_{mean}=52 nm (Figure 32l)).

Figure 33a shows a bright-field TEM image of the Ag nanoparticles synthesized using the lactate precursor. In comparison to the Ag nanoparticles obtained from the nitrate precursor, the Ag nanoparticles prepared from the lactate (and acetate) exhibited a broader size distribution.

The SAED pattern of the Ag nanoparticles obtained from the lactate precursor indicates the coexistence of Ag nanoparticles with cubic and hexagonal crystal structures (Figure 33b). Ag nanoparticles with both structures were obtained in all three systems. The larger Ag nanoparticles appear to consist of smaller, differently oriented, subunits, as can be seen in Figure 33c. These polycrystalline nanoparticles exhibit a hexagonal crystal structure (Figure 33d). These observations are in agreement with the hypothesis made on the basis of the XRD phase composition analysis and confirm the different growth mechanisms resulting from the sonochemically induced pre-nucleation.

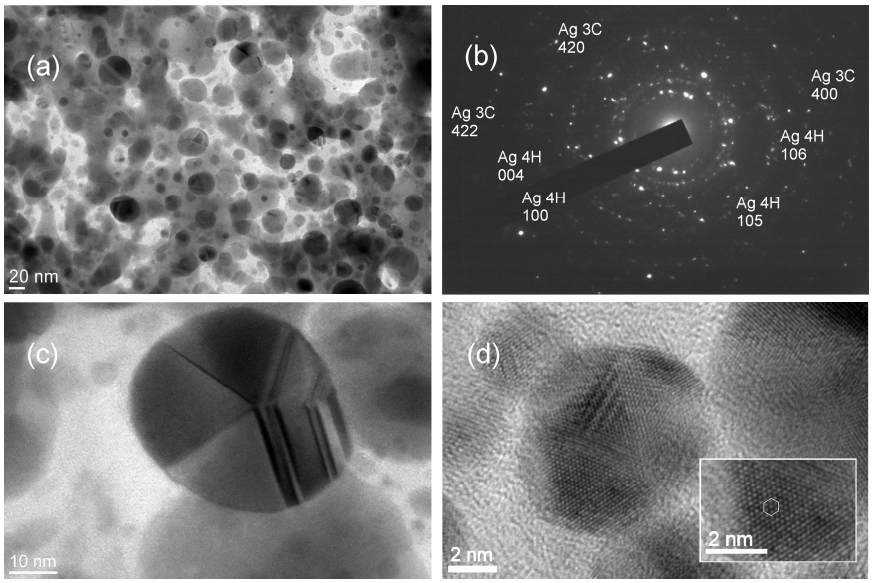

Figure 33: *Bright-field TEM images of Ag nanoparticles obtained from lactates (a) and the corresponding SAED pattern with indexed reflections of 3C and 4H Ag (b), polycrystalline, larger particles (c) with hexagonal structure (d)*.

The morphological properties of the HAp/Ag obtained from the nitrate (Figure 34a,b,c), acetate (Figure 34d,e,f) and lactate (Figure 34g,h,i) silver precursors generally show the formation of plate-like and/or rod-like HAp particles with spherical and hexagonal Ag particles attached to their surfaces. As far as the morphology of the HAp within the HAp/Ag composites obtained using different Ag-precursors is concerned, it was observed that the application of the nitrate precursor resulted in rod-like particles that were significantly reduced in size, compared to the mixed plates and rods of the HAp obtained using acetates and lactates. The obtained morphology can be explained if we correlate it with the phase composition during the synthesis process. It is clear that in the case of the nitrate precursor of silver, the HAp was formed in the solution as a result of an increased pH that was high enough to allow its precipitation; this process was followed by intensive mixing induced by the sonication and these conditions resulted in the formation of rod-like particles. On the other hand, after the formation of the OCP using acetates and lactates, the formation of the HAp took place at an increased temperature (300°C) during the process of calcination without mixing; it provided different conditions for the crystal growth, which resulted in a change of the shape and the size of the resulting particles.

As for the morphology of the Ag particles attached to the surface of the HAp, it was observed that the particles obtained from the nitrates (Figure 34c) had considerably smaller dimensions compared to those obtained from the acetate (Figure 34f) and lactate (Figure 34i) precursors. Figure 35a shows a bright-field TEM image of the Ag nanoparticles synthesized from the nitrate on the surface of the HAp. The size of the Ag nanoparticles estimated directly from the TEM image reveals the formation of Ag nanoparticles smaller than 10 nm. A typical SAED pattern of the HAp/Ag composite in Figure 35b indicates the presence of phases with the crystal structure of HAp and silver. However, the similar characteristic *d*-spacing lengths of the cubic and hexagonal crystal structures of the silver nanoparticles and the presence of reflections that correspond to the HAp hinder an accurate differentiation between the cubic and hexagonal Ag nanoparticles in the HAp/Ag composite. The Ag particles formed within the composite using acetates and lactates were larger (up to 30 nm) and showed a broader size distribution. Along with the spherical particles, the hexagonal particles could also be observed; they showed an axial, chain-like direction of growth (Figure 34e,i).

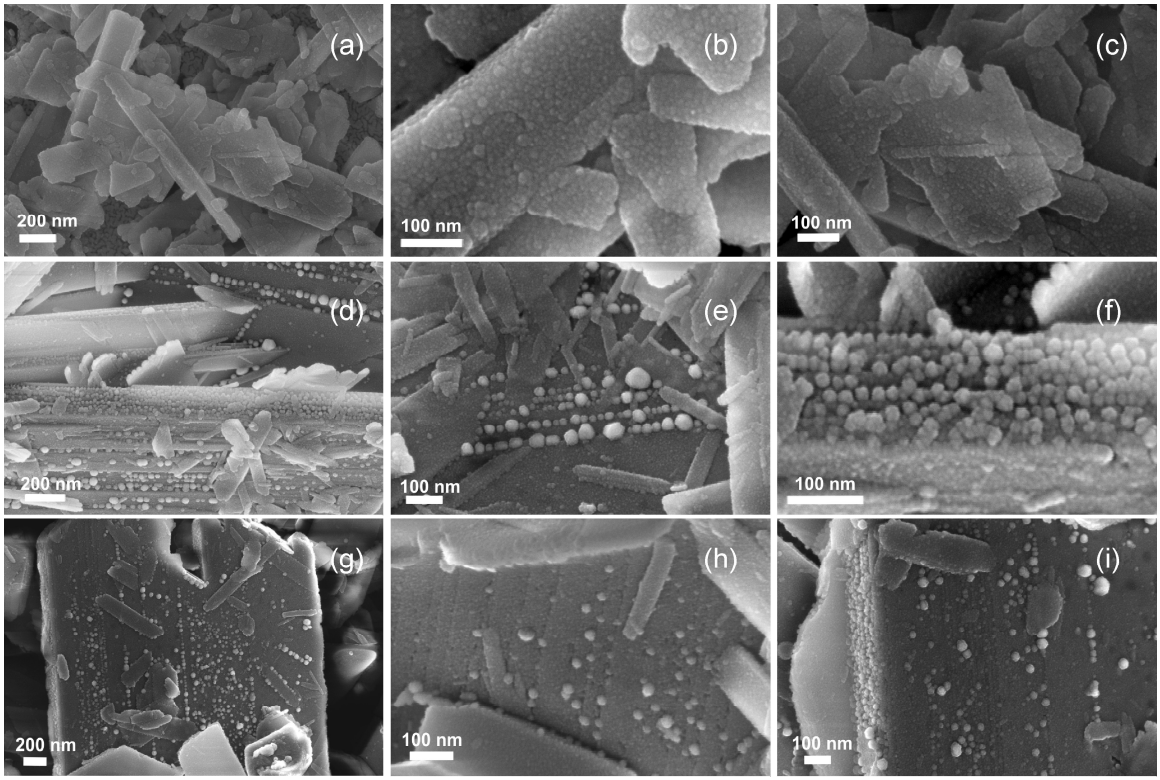

Figure 34: *FESEM micrographs of HAp/Ag nanocomposites obtained using nitrates (a, b, c), acetates (d, e, f) and lactates (g, h, i) as the silver precursors.*

A TEM analysis showed that these Ag particles are connected to the HAp plates (Figure 35c,d). Moreover, along with the larger particles, which were up to 30 nm in size, smaller ones with a diameter up to 5 nm were also detected and they were templated into the HAp plates (Figure 35e,f).

It is interesting to note that if we compare the sizes of the Ag particles obtained with and without the HAp the size of the Ag particles is significantly reduced within the composite. This means that, independent of the type of silver precursor, the HAp plays a distinct role in the process of the growth of these nanoparticles, preventing their small dimensions.

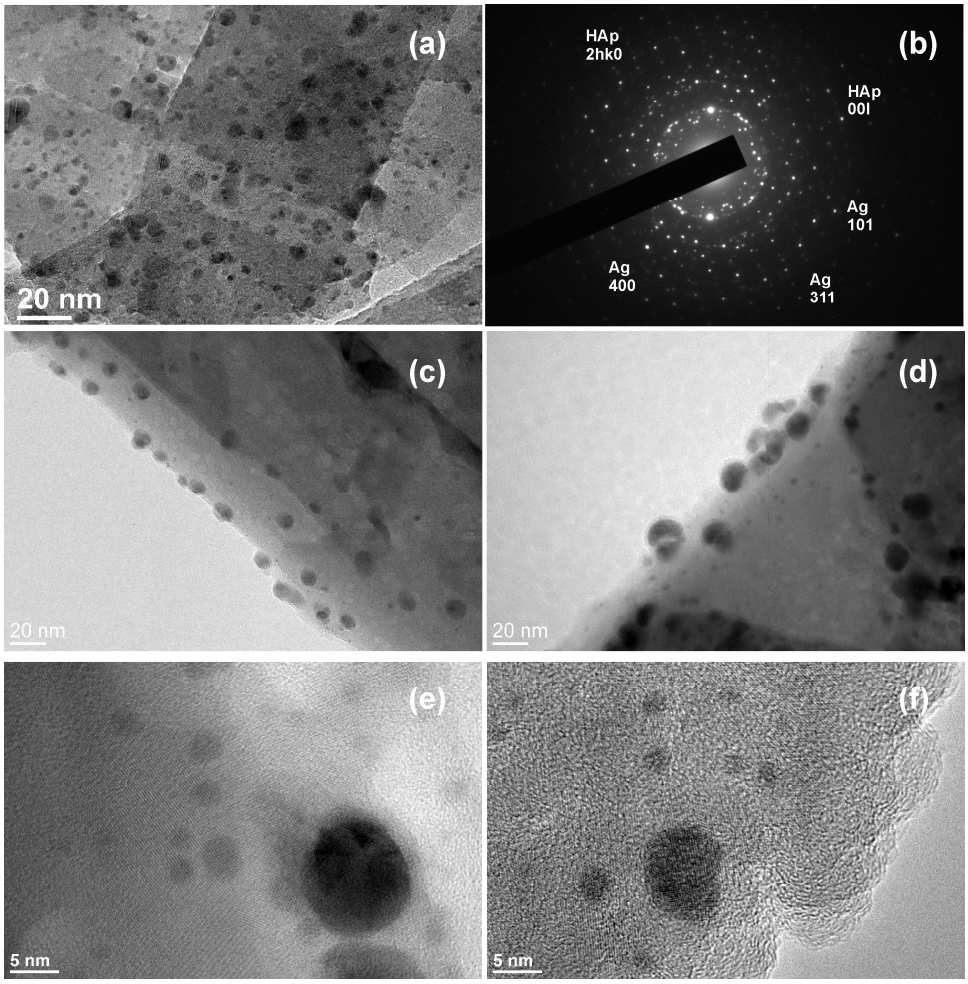

Figure 35: *TEM images of the HAp/Ag nanocomposite obtained from nitrates (a), corresponding SAED pattern (b) and Ag particles obtained using acetates and lactates attached on the edge of the HAp plates (c, d) and within the HAp plate (e, f).*

4.1.2 Hydroxyapatite/platinum composites

HAp/Pt is a novel composite material. Metallic component of this material is platinum noble metal which is highly bioinert and with very low reactivity. These properties make it a perfect choice from the standpoint of toxicity. However, unlike HAp/Ag, it does not have natural ability to suppress growth of bacteria. As it was already mentioned, in the case of this material there is a need for activation of the metal component in order to reach activity against bacteria.

Low reactivity of Pt does not provide a lot of possibilities for chemical modifications; however ability of this metal to storage electrons gives opportunity for its activation by photons. If HAp/Pt composite is observed as a composite of a semiconductor and metal there is a way for the activation of its photocatalytic activity. The basic idea for the activation of metallic component within HAp/Pt composite in order to form novel bio-photocatalyst was assumed to be effective for degradation of non-biodegradable organic pollutants and reaching antibacterial activity.

4.1.2.1 Formation of hydroxyapatite/platinum composites

HAp/Pt composites were synthesized by the same two-step process consisted of sonochemical synthesis followed by calcinations at elevated temperature in inert

atmosphere which was previously used for formation of HAp/Ag material (Vukomanović et al., 2011d). Sonochemical method was optimized by the selection of Pt-precursors. Unlike inertness of metallic Pt, its compounds and ions have ability for adsorption onto surface with polar groups. This was used for selection of Pt-precursors with different thermal properties in order to investigate their contribution to the growth of Pt nanoparticles as well as their abilities to adsorb onto the HAp surface. Both, Pt nanoparticles growth and adsorption of Pt-ions/compounds are important for photocatalytic activity of composite. Template role of bioceramic part for formation of Pt nanoparticles was investigated by processing of the precursors without HAp phase and comparison of the morphological properties to the once obtained within composite (Vukomanović et al., 2012b).

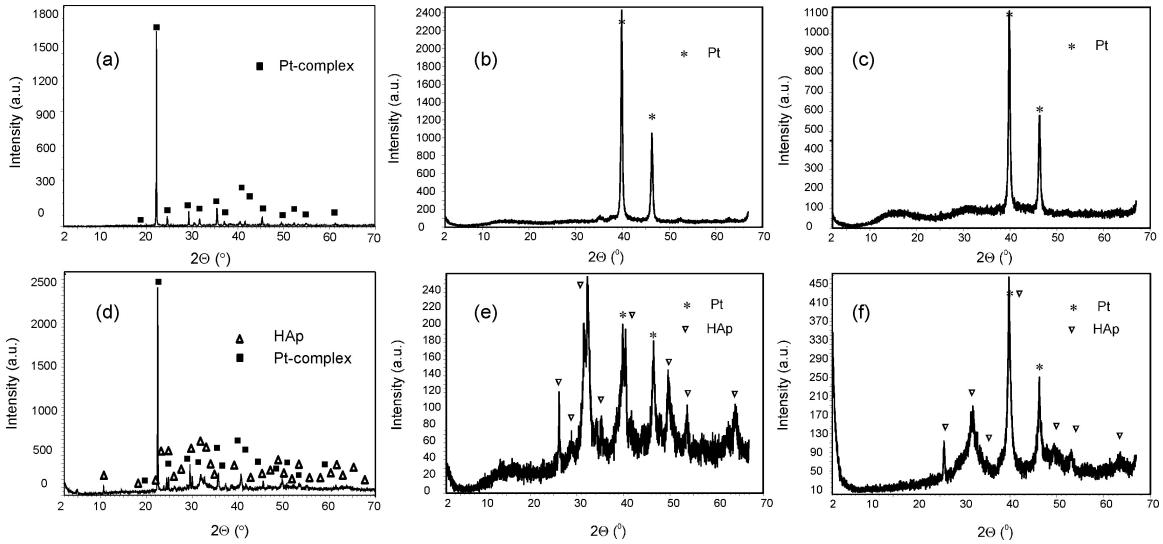

Figure 36: *XRD patterns of: urea-complex formed before calcination (a) and Pt obtained using H_2PtCl_6 (b) and $C_{10}H_{14}O_4Pt$ (c) after calcinations; urea-complex and HAp (d) and HAp/Pt composites obtained by using H_2PtCl_6 (e) and $C_{10}H_{14}O_4Pt$ (f) after calcination*.

Pt nanoparticles and their composites with HAp were formed using homogeneous precipitation method using two different Pt- sources - $H_2PtCl_6 \cdot 6H_2O$ and $C_{10}H_{14}O_4Pt$. Sonochemical step resulted in formation of platinum-urea complex (Figure 36a) which was reduced during the next thermal treatment stage. Phase identification revealed a crystalline phase corresponding to the structure of cubic platinum (JCPDS No.: 87-0646) in the case of both precursors (Figure 36b,c). During formation of the composites precipitation of hydroxyapatite took place along with formation of platinum-urea complex (Figure 36d). The following thermal step provided reduction of a complex and formation of HAp/Pt composites (Figure 36e,f) (JCPDS No.: 87-0646 and JCPDS No.: 9-0432). Under applied conditions, neither sonochemically formed radicals nor apatite polar OH-groups were strong enough to initiate Pt reduction. Formation of Pt was one-stage, slow thermal reduction process.

It was also observed that there is a decrease in the intensity and a broadening of the diffraction maxima corresponding to the Pt particles formed within the composites for both Pt-precursors. These changes indicate influence of the HAp to the crystal growth of Pt particles as components of the composites (Vukomanović et al., 2012b).

4.1.2.2 Surface properties of hydroxyapatite/platinum composites

During sonochemical formation of HAp/Pt composite optical properties of HAp have been modified. According to the UV/VIS analysis broad absorption of HAp was

superimposed to the additional absorption maxima (Figure 37a,b). Their comparison to absorption spectra of Pt precursors revealed matching and they were assigned to absorptions of $[PtCl_6]^{2-}$ (Figure 37a) and $C_{10}H_{14}O_4Pt$ (Figure 37b) remained after formation of the composite. The same matching of the position of the absorption maxima occurred also for the spectra of the HAp/Pt/urea-complex formed before Pt-reduction. One part of the complex was reduced during the slow thermal reduction while another remained in material. Stability test was performed using supernatants obtained by dispersing of the HAp/Pt composite synthesized using H_2PtCl_6 and separation of the solid part by centrifugation. Absorption of the $[PtCl_6]^{2-}$ions was not detected. The same procedure was applied for the composite obtained using second precursor. In this case adsorption of $C_{10}H_{14}O_4Pt$ was detected after removal of dispersed solids despite much lower solubility in water compare to hexachloroplatinum ions (Vukomanović et al., 2012b).

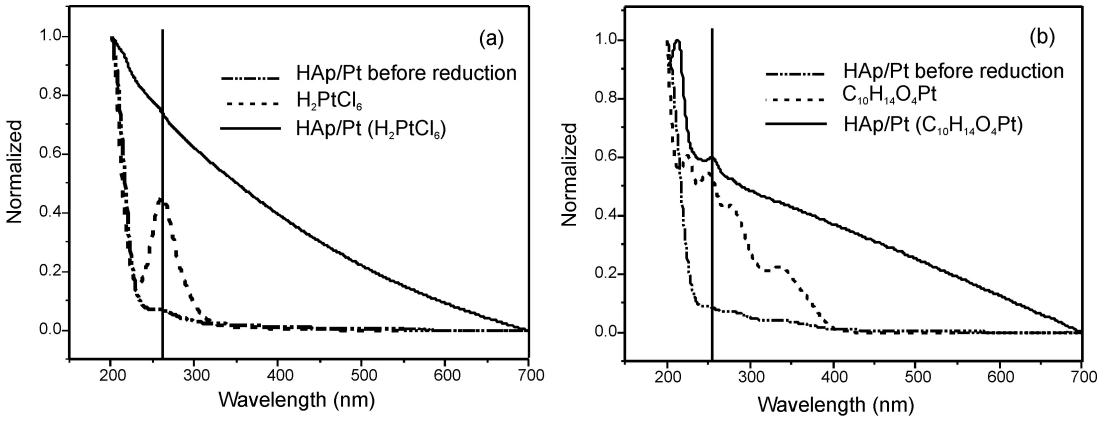

Figure 37: *UV/VIS spectra of: HAp/Pt before and after reduction using H_2PtCl_6 precursor (a) and HAp/Pt before and after reduction using $C_{10}H_{14}O_4Pt$ precursor (b).*

Apatite has highly adsorptive surface with the presence of polar OH groups and a specific structure capable for various ion-exchanges. It means that there are conditions for the irreversible adsorption of hexachloroplatinum ions on their surface. Similar was observed on the surface of TiO_2 when hexachloroplatinum ions were chemisorbed onto the surface by reaction with OH groups (Burgeth and Kisch, 2002) and the same mechanism is applicable for HAp. In the case of $C_{10}H_{14}O_4Pt$, lower stability shows reversible adsorption indicating possibility for physical interaction between polar surface OH groups of HAp and C=O groups of $C_{10}H_{14}O_4Pt$ (Vukomanović et al., 2012b).

4.1.2.3 Morphological properties of hydroxyapatite/platinum composites

Application of homogeneous sonication method followed by thermal reduction resulted in formation of plate-like (Figure 38a,b) or submicrometer-sized sphere-like (Figure 38c,d) Pt nanostructures. The shape of these structures depended on the type of initially used Pt-source. Since inability of sonication to induce reduction of Pt-sources these nanostructures were formed during slow-rate thermal stage by decomposition of Pt-urea complex. This slow reaction was performed without mixing and presence of any templating agent which were good conditions for intensive agglomeration of formed nanoparticles and their ingrowths into larger structures.

During formation of the composites situation was different. In that case adsorption of the HAp/Pt-urea complex onto the surface of HAp took place during sonication step. Consequently Pt-complex was stabilized before reduction process. In this case apatite had a role of a substrate with templating effect which influenced growth and stability of Pt particles formed during thermal reduction. The effect is similar to the case when HAp

composite with silver has been formed using this method (Vukomanović et al., 2011d). So-obtained Pt particles were attached onto the surface of apatite plates. In this case morphological properties of formed composites were strongly dependent on selected Pt-source.

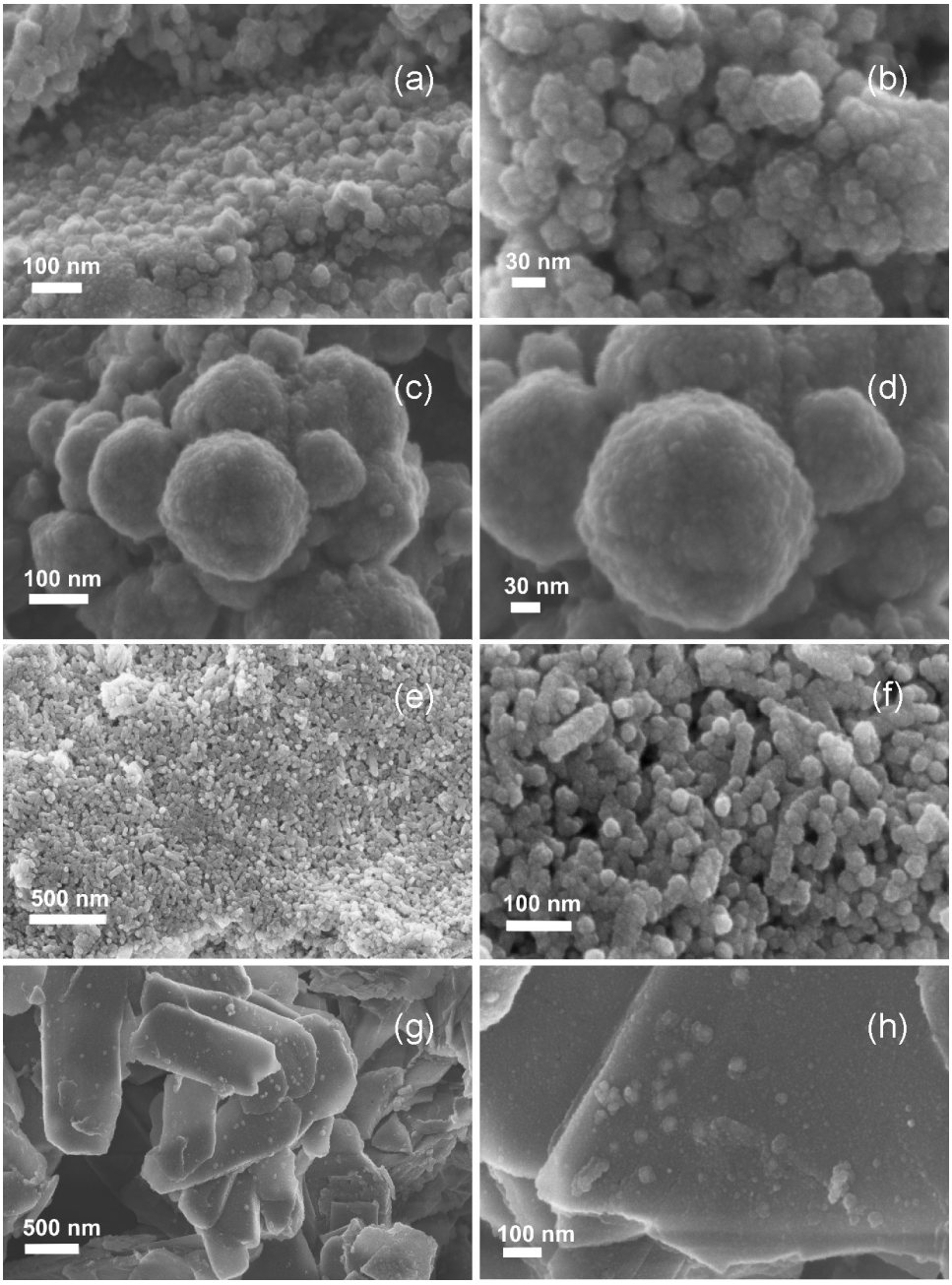

Figure 38: *FESEM micrographs of Pt particles obtained using platinum $C_{10}H_{14}O_4Pt$ (a, b) and H_2PtCl_6 (c, d) precursor and HAp/Pt particles obtained using $C_{10}H_{14}O_4Pt$ (e, f) and H_2PtC_{l6} (g, h) precursors.*

In the case of $C_{10}H_{14}O_4Pt$ significant amount of Pt particles were attached onto the surface of apatite plates (Figure 38e,f) compared to the layer of Pt particles attached onto the apatite surface formed using $H_2PtCl_6 \cdot 6H_2O$ (Figure 38g,h). Moreover, particles formed using $C_{10}H_{14}O_4Pt$ are nanostructured rods up to 100 nm in length and 20 nm in width (Figure 38e,f). These rods are aggregates of Pt nanoparticles intensively agglomerated and deposited onto apatite surface (Figure 39a,b). Smaller Pt particles within these structures are a few nanometer-sized spheres while larger ones are well-

crystallized, partially aggregated single crystal cubes up to 10 nm in size (Figure 39c,d).

In the case of formation of composite using H_2PtCl_6, Pt particles deposited onto HAp surface were able to preserve their identity. These particles were spheres with diameters from a few nm to 30 nm (Figure 39e,f), with well-defined shape and without a presence of agglomeration (Figure 39g,h).

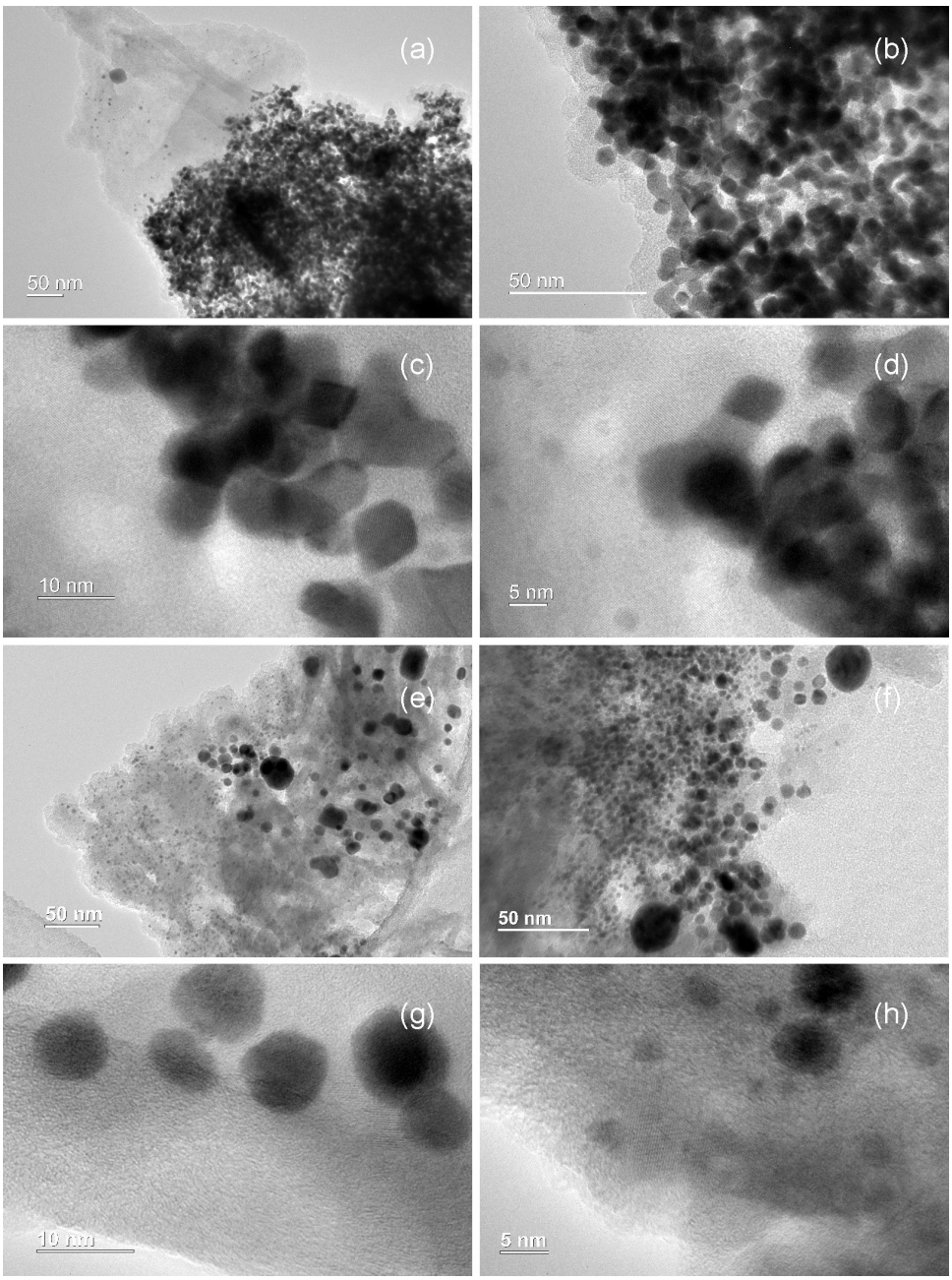

Figure 39: *TEM micrographs of HAp/Pt particles obtained using $C_{10}H_{14}O_4Pt$ (a, b, c, d) and H_2PtCl_6 (e, f, g, h) as platinum-precursor.*

Similar to the results of XRD and UV/VIS analyses, existence of the interactions between Pt-complex and HAp and template role of HAp in the process of slow thermal reduction of Pt and formation of composite were additionally revealed through their contribution to the morphology of Pt particles obtained after reduction of the complex with and without the presence of HAp. Sonochemically synthesized HAp has preferential growth along c-axis (Jevtić et al., 2008). According to its structure, polar OH groups are oriented normally to this direction. The last is one of the main reasons for lateral

connections of the HAp rods and their ingrowths into the plate-like, micrometer-sized structures (Jevtić et al., 2008). These plates have reactive, polar groups present on their surface. As it was already observed Pt-complexes are adsorbed on the surface of HAp.

According to the lower stability it was proposed that complex formed using $C_{10}H_{14}O_4Pt$ is physically adsorbed onto HAp which directly affected morphology of Pt particles formed after reduction and allowed intensive agglomeration. Stability of the complex formed using $[PtCl_6]^{2}$-ions was higher since they have possibility for chemisorption onto HAp and after reduction so-formed Pt particles were non-agglomerated (Vukomanović et al., 2012b).

According to the TEM images of the both HAp/Pt composites metallic Pt particles were closely attached to the surface of HAp. On the other hand, similar to the case of HAp/Ag, smaller particles of Pt are embedded within micrometer-sized apatite plates. Incorporation of the small Pt particles (with the size below 5 nm) into the HAp plates is indication of attachment of the Pt-complexes to the HAp during its growth in sonication step. In the moment of thermal reduction, Pt-complexes were present at the surface as well as within HAp plates which resulted in formation of both attached and embedded Pt nanoparticles (Vukomanović et al., 2012b). These close contacts between semiconductor and metallic nanoparticles are highly important for photocatalytic activity because they are associated with ability for transition of the electrons (Carp et al., 2004).

4.1.3 Hydroxyapatite/gold composites

The next HAp-based composite material which was designed for antibacterial activity consisted Au as noble metal component. Similar to the platinum in HAp/Pt composite, Au component within HAp/Au composite does not have natural ability for antibacterial action. It means that there is a need for development of a strategy for its activation.

Like platinum, gold is also bioinert metal with low reactivity. However, it has high affinity to bond nitrogen- and sulphur- containing groups including amines and thiols to its surface. It means that there is a possibility for variety of organic molecules to be attached onto the surface of Au particles in order to functionalize them. In the same time a large number of natural-sourced molecules, including nucleic acids, proteins, amino acids, growth factors, enzymes etc., contain amino or/and thiol groups. This property provides wide network of opportunities for their modification in order to develop distinct properties required by some special need in the field of biomedicine. Accordingly, activation of the Au composite within HAp/Au composite was performed using natural- and synthetic- sourced functionalizing molecules.

4.1.3.1 Formation of hydroxyapatite/gold composites

Phase composition

Formation of HAp/Au composites was performed by two different modifications of sonochemical method. In the first case, reduction of metallic particles was performed thermally using two-step process- sonochemical synthesis followed by calcinations at elevated temperature. The same method was used for the synthesis of HAp/Ag and HAp/Pt composites (Vukomanović et al., 2011d; Vukomanović et al., 2012b). In the second case, reduction of metallic particles was performed chemically and it was followed by simultaneous functionalization of formed Au particles (Vukomanović et al., 2012c). Both cases were used for the synthesis of Au particles with and without HAp.

A first step in investigation of the formation of Au alone and within HAp/Au composites using different reduction approaches was performed by identification of the phases (Figure 40). According to the XRD measurements after sonochemical synthesis

followed by thermal treatment one crystalline phase corresponding to the structure of cubic gold (JCPDS No.: 4-0784) was identified for both, $Au(CH_3COO)_3$ and $Au(OH)_3$ gold-precursors. In this case, Au-precursors were added to the system in the first step and formation of gold phase started during sonication along with formation of gold-urea complex (Figure $40a_1$). This complex was completely transformed into Au phase during thermal treatment. Initiation of the precipitation of Au nanoparticles during sonochemical synthesis and their further growth and formation of well-crystalline, large metallic particles during the thermal step may explain appearance of a high-intensity, sharp maxima.

The second approach to the synthesis of Au particles was chemical reduction using amino acids- (glycine, arginine and histidine (Figure $40a_{2-4}$)) as well as using synthetic-sourced amines and thiols (thiuorea/$NaBH_4$, 5(bromo-piridine-2-thiol), aniline and 4(methilthio) aniline) (Figure $40a_{4-8}$). In all three cases, except for thiourea/$NaBH_4$, one crystalline phase corresponding to the cubic gold (JCPDS No.: 4-0784) has been identified. For thiourea/$NaBH_4$ very stable Au-urea-thiourea complex has been formed which was unable to be reduced even with a strong reduction agent such as $NaBH_4$. In the case when Au-phase has been formed, this process was very fast single step reduction and growth of so formed particles was different compare to the long-lasting thermal reduction. Consequently, diffraction maxima of chemically obtained Au particles were much broader and with lower intensities. Within these Au particles obtained by chemical reduction there are also differences in diffraction maxima depend on the reduction agents meaning that each of them had a specific role in their formation and growth.

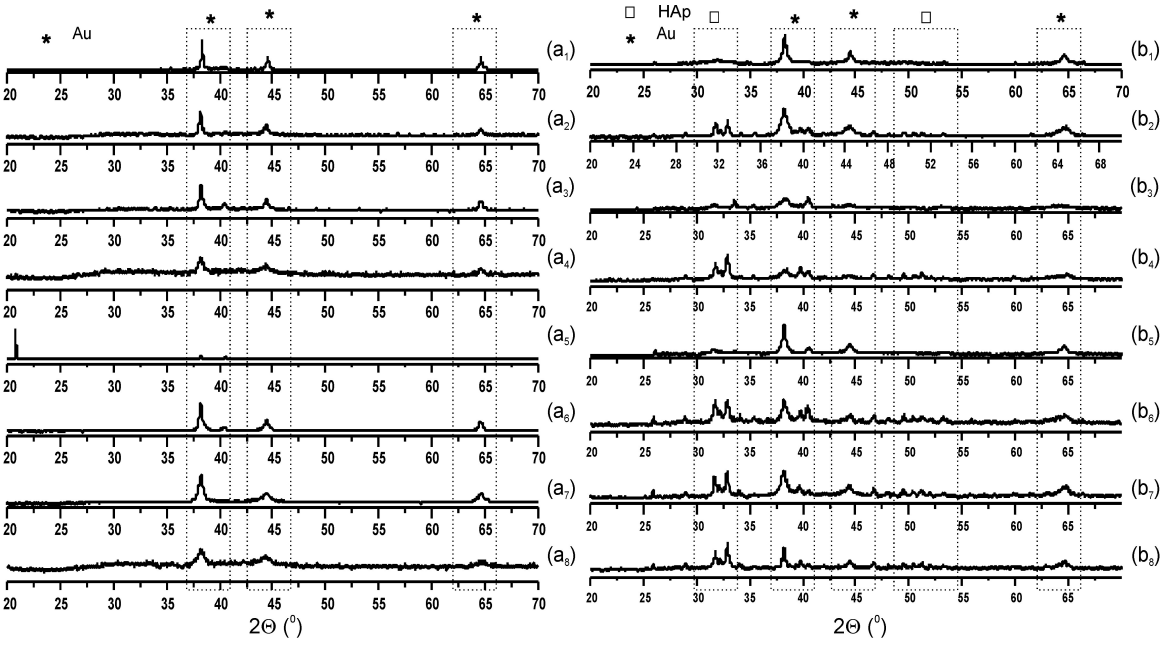

Figure 40: *XRD patterns of Au nanoparticles (a_{1-8}) and HAp/Au composites (b_{1-8}) where Au has been obtained: by thermal reduction and by chemical reduction using amino acids (glycine, arginine, histidine), thiourea/$NaBH_4$ and aromatic amines and/or thiols (5(bromo-piridine-2-thiol), aniline and 4(methylthio) aniline), respectively.*

When the first, thermal reduction step has been used for formation of HAp/Au composite, in the presence of calcium- and phosphate- sources together with Au-precursors, homogeneous sonochemical method resulted in co-precipitation of gold-urea complex, metallic gold and hydroxyapatite phases. After thermal reduction, two phases corresponding to the cubic gold and hexagonal hydroxyapatite (JCPDS No.: 9-0432) were identified for both, $Au(CH_3COO)_3$ and $Au(OH)_3$ indicating formation of HAp/Au

composite (Figure 40b_1). There is a significant broadening of diffraction maxima corresponding to the low crystalline HAp phase within HAp/Au composite which may be explained through incorporation of Au-ions within HAp similar to the case when HAp/Ag composites has been formed.

During formation of HAp/Au composites using chemical reduction when HAp was formed alone and then Au-sources followed by reduction agents were added the same phase composition corresponding to the cubic Au and hexagonal HAp phases were identified (Figure 40$b_{2\text{-}8}$). Formation of HAp/Au composites was succeeded for all reduction agents including thiuorea/$NaBH_4$. In all cases diffraction maxima of Au within composites were broader compare to single-phased Au indicating contribution of HAp to the growth of Au phase and decrease of its crystallite size. In these systems, HAp phase had higher crystallinity compare to the HAp obtained by thermal reduction since chemical reduction was fast process and there were no conditions for incorporation of Au-ions within apatite structure. Once again, the system obtained using thiuorea/$NaBH_4$ was an exception resulting in formation of low crystallinity HAp phase.

Independent research when HAp urea and thiourea has been processed revealed that there is an influence of thiourea to the HAp structure. Similar to the processing of Au when stable Au-urea-thiourea complex was formed during the synthesis of composite, formation of Ca-urea-thiourea complex occurred. Higher preference for formation of Ca-complex compare to the formation of Au-complex allowed reduction of Au-precursor and formation of Au particles while formed Ca-complex influenced formation and crystallization of HAp phase.

Total quantity of gold within materials obtained using chemical reduction by amino acids and synthetic amines and thiols was determined by ICP analysis and results are summarized in Table 7.

Table 7: *Quantitative analysis of the Au-content within HAp/Au composites.*

Composite	Total gold content (ICP analysis) wt.%
HAp/Au/glycine	21.5
HAp/Au/arginine	15.7
HAp/Au/histidine	14.9
HAp/Au/5(bromo-piridine-2-thiol)	17.9
HAp/Au/aniline	21.5
HAp/Au/4(methylthio)aniline	26.0

Physical and chemical interactions

Physical and/or chemical interactions among components of HAp/Au composites formed by chemical approach using amino acids or synthetic amines/thiols for reduction of Au-component were investigated using FTIR spectrometry. Chemical structures (a_1-f_1) and FTIR spectra of pure reduction agents (a_2-e_2) as well as spectra of HAp/Au composites obtained by these reduction agents for the case of amino acids (glycine (a_3), arginine (b_3) and histidine (c_3)) or synthetic amines/thiols (thiourea (d_3), 5(bromo-piridine-2-thiol) (f_3), aniline and 4(methylthio)aniline (f_2) are presented in Figure 41. All composite spectra are compared with the spectrum of pure HAp presented by dotted line.

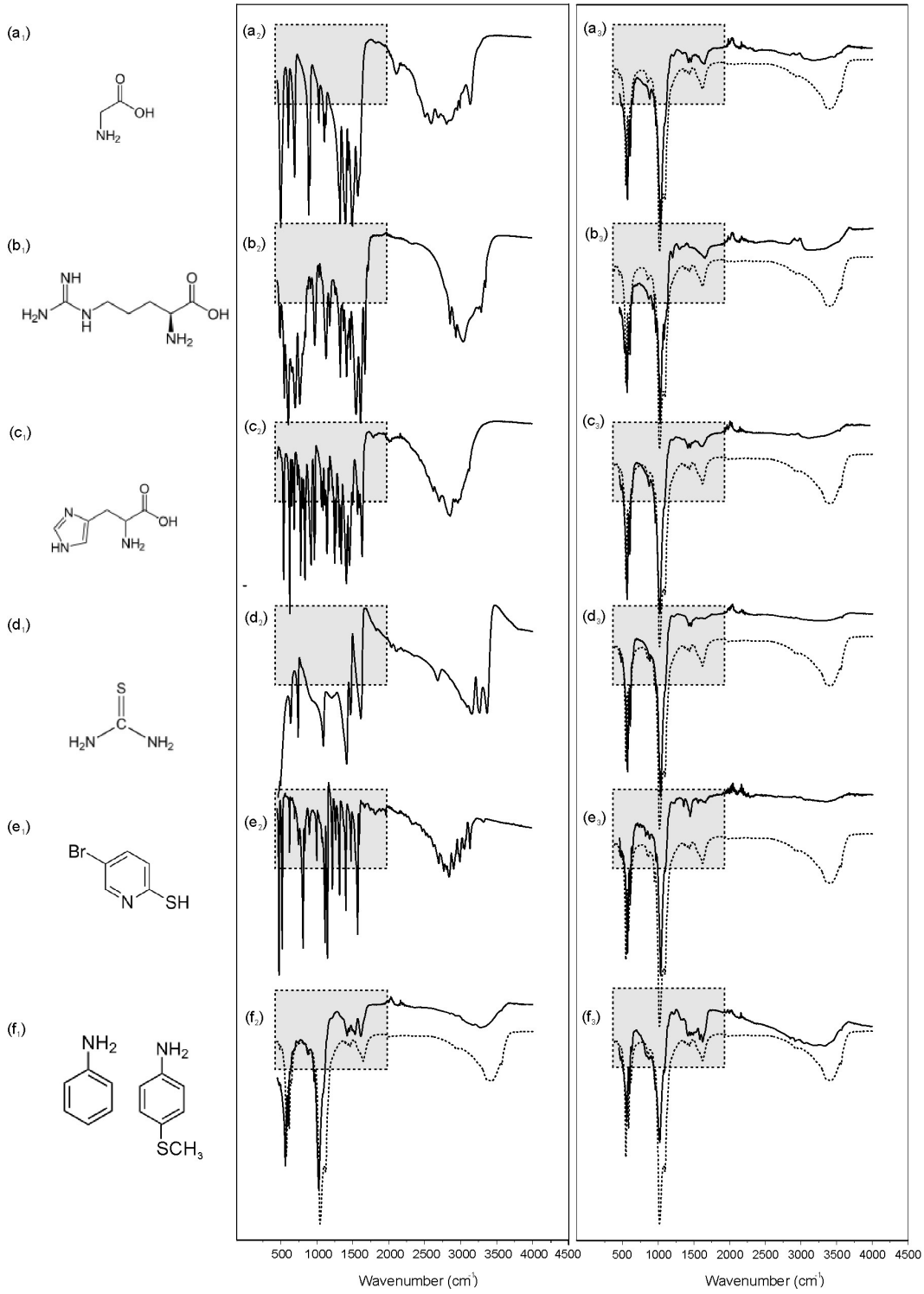

Figure 41: *Structural formula of reduction agents (1) and FTIR spectra of reduction agent and HAp/Au composites functionalized by them (2,3), where Au has been obtained: by chemical reduction using amino acids (glycine, (a) arginine, (b) hystidine (c)), thiourea/$NaBH_4$ (d) and aromatic amines and/or thiols (5(bromo-piridine-2-thiol (e)), aniline and 4(methylthio) aniline (f)). Dotted line is FTIR spectrum of HAp.*

Typical spectra of carbonated HAp formed by sonochemical method contains bands of PO_4^{3-} at 472 (υ_2), 583 (υ_4), 601 (υ_4), 961 (υ_1), 1032 (υ_3) and 1108 (υ_3) cm^{-1}; peaks at 874 (υ_2), 1415 (υ_3) and 1455 (υ_3) corresponding to the vibrations of CO_3^{2-} and the bands of OH^- ions at 3573 and 632 cm^{-1} (Jevtić, et al., 2008; Jevtić et al., 2009). HAp/Au composite spectra contains all these bands due to the apatite components with the main

difference related to the decreasing and broadening of the band at around 3573 cm^{-1} and 632 cm^{-1} that correspond to the stretching and libration modes of the OH- ions, respectively. Rod and plate-like HAp have preferential growth along c-axis with OH groups present on the surface of the formed plates. Observed changes indicate existence of interactions which allow HAp to attract Au nanoparticle on its surface using its surface polar OH groups which provides it a templating role and a formation of the composite. Additionally, in the region of the "finger prints" between 500 and 2000 cm^{-1} (marked by the grey squares) existence of the low-intensity bands which were superimposed to the spectrum of HAp was observed. These are regions of intensive vibrations of the groups of molecules used for reduction process suggesting their attachment onto Au component of HAp/Au composites. This suggestion was also supported by significant decrease of the bands of these molecules in the region between 2500 and 3500 cm^{-1} that correspond to the range of stretching vibrations of amino- and thio-groups (Stewart, 1957; Smith, 1999). According to the literature, molecules containing these groups use sulphur or nitrogen to bond to the surface of metal atoms (Yang, 2003a; Polavarapu, 2008). This type of bonding prevents or decrease degree of liberty for vibration of these groups inducing broadening, lowering of the intensity and shifts of the bands that are assigned to their vibrations (Smith, 1999; Polavarapu, 2008).

4.1.3.2 Surface properties of hydroxyapatite/gold composite

Characterization of the surface and investigation of the surface chemistry of functionalized materials was performed on HAp/Au/thiourea using photoelectron spectroscopy (Figure 42). XPS spectra of polycrystalline pure Au reference (Figure 42a) and HAp/Au synthesized without thiourea (Figure 42b) were used as a references, while functionalization of materials was investigated on Au/thiourea (Figure 42c,d) and HAp/Au/tiourea (Figure 42e,f) obtained by chemical reduction using $NaBH_4$ as well as by thermal reduction at 300°C. Binding energy values (BE) for spin-orbit doublets of gold in Au and HAp/Au materials are summarized in Table 8. Additionally, BEs of gold and sulphur doublets of as well as singlets of nitrogen from HAp/Au composite are presented in Table 9.

Table 8: *Binding energy values for Au4f spectra and assigned oxidation states for gold in Au and HAp/Au materials with and without thiourea functionalization obtained by chemical and thermal reduction procedure.*

Sample	Au $4f_{5/2}/4f_{7/2}$ doublet (I)	Au $4f_{5/2}/4f_{7/2}$ doublet (II)	Au $4f_{5/2}/4f_{7/2}$ doublet (III)	Au $4f_{5/2}/4f_{7/2}$ doublet (IV)
Au		84.6±0.5 eV		
Reference		88.2±0.5 eV		
Au/thiourea	83.3±0.5 eV	84.5±0.5 eV		
($NaBH_4$)	87.1±0.5 eV	88.4±0.5 eV		
Au/thiourea		84.1±0.5 eV	85.3±0.5 eV	87.9±0.5 eV
(300°C)		88.3±0.5 eV	89.2±0.5 eV	92.0±0.5 eV
HAp/Au	83.7±0.5 eV			
Reference	87.4±0.5 eV			
HAp/Au/thiourea	83.7±0.5 eV		85.1±0.5 eV	
($NaBH_4$)	87.4±0.5 eV		89.0±0.5 eV	
HAp/Au/thiourea	84.0±0.5 eV	84.7±0.5 eV	85.6±0.5 eV	
(300°C)	87.7±0.5 eV	88.4±0.5 eV	89.3±0.5 eV	
Oxidation state	**Au(0)**	**Au(0)**	**Au(1+)**	**Au(3+)**

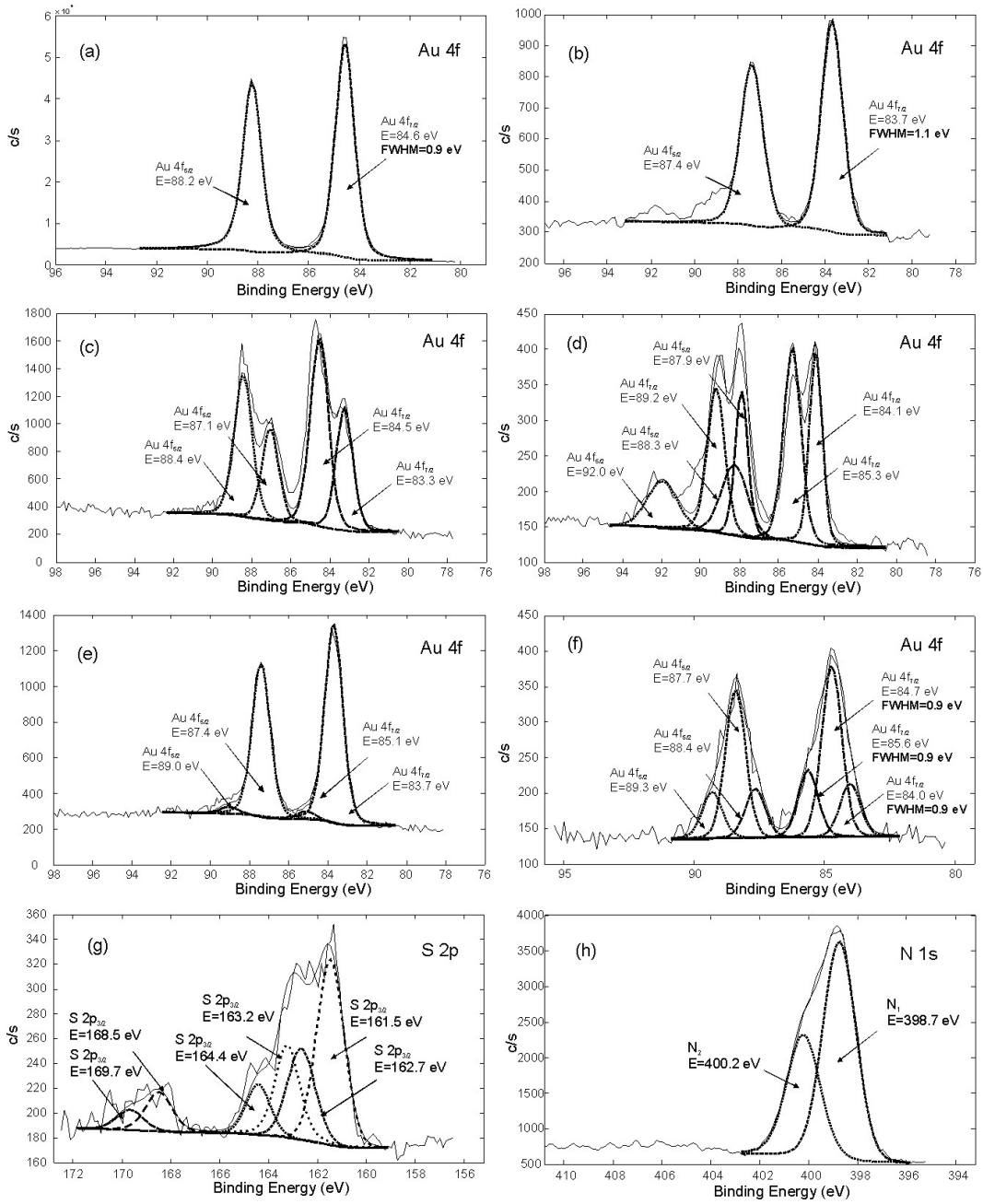

Figure 42: *High resolution XPS spectra of: polycrystalline Au reference (a); Au spectra of -HAp/Au (b) Au/thiourea/$NaBH_4$ (c), Au/thiourea (d), HAp/Au/tiourea/$NaBH_4$ (e) and HAp/Au/thiourea (f); S and N spectra of HAp/Au/thiourea (g, h).*

An Au4f spectrum of pure Au reference with elemental gold possesses a doublet corresponding to $Au4f_{7/2}$ and $Au4f_{5/2}$ peaks positioned at 84.6 and 88.2 eV with a FWHM value of $Au4f_{7/2}$ peak of approximately 0.9 eV. In the case of Au/thiourea obtained by chemical reduction using $NaBH_4$, two pairs of doublets, each of them with FWHM values similar to Au reference, were observed. The first doublet had peaks at 84.5 and 88.4 eV while the peaks of the second were shifted for -1.3 eV and they were present at 83.3 and 87.4 eV. Compare to the Au reference, first doublet corresponded to the clean elemental gold. According to the literature, the second doublet also belongs to elemental gold while shifts indicate surface adsorptions similar to the case of 2D and 3D Au self-assembled monolayers (SAMs) obtained with adsorbed thiol surfactants (Bourg et al., 2000). In this case there is no Au-S bond since detected gold has elemental state and the shift is due to the physical interactions between Au(0) and -S- (Table 8). In the second case, when

thermal reduction was applied, an Au4f spectrum showed three doublets. A doublet at the lowest energy belonged to the pure elemental gold with BE values similar to those of the Au reference. The other two doublets at higher BE at (85.3/89.2 eV and 87.9/92.0 eV for $Au4f_{7/2}$/$Au4f_{5/2}$) corresponded to oxidized gold with +1 and +3 oxidation states (Casaletto et al., 2006) and they are forming bonds which could be assigned to surface-complexes.

For HAp/Au composite without functionalization, component of Au4f were located at 83.7 and 87.4 eV. They had negative shift compare to the Au reference. Similar effect has been observed in the case of Au on different oxide materials (TiO_2, SiO_2, CeO_2) (Casaletto et al., 2006) and it was explained as a contribution of the substrate. In this case observed shift confirms surface interaction/adsorption onto HAp and templating role of this material within composite.

As for the HAp/Au composites without surface functionalization, in the case of composites with functionalized surface one doublet corresponding to the spin-orbit components of Au4f have been detected. In contrast to the case of HAp/Au without functionalization when FWHM value of $Au4f_{7/2}$ peak was approximately 1.1 eV, for both other materials when HAp/Au/thiourea was formed chemically or after thermal treatment, this peak had significantly higher value (1.4 and 2.0 eV) and irregular, non-symmetric shape which is an indication of the presence of a higher number of components. They have been fitted for separation by deconvolution process by using a constant distance of 3.7 eV and constant intensity ratio of 1.33 between spin-orbit components of the Au4f doublets. The procedure provided two Au4f doublets for HAp/Au/thiourea obtained chemically using the fast $NaBH_4$-reduction as well as three component of HAp/Au/thiourea obtained by the slow thermal treatment under H_2-reducing atmosphere.

The first doublet of HAp/Au/thiourea formed by reduction using $NaBH_4$ was positioned at the same values of BE as for the HAp/Au and corresponded to the Au(0) templated by HAp. Another one, which was significantly lower in intensity, had peaks at 85.1 and 89.0 eV which belong to the oxidized surface-complexing Au(+1). Obtained results are suggesting formation of Au-metallic particles presented onto the HAp template with the surface monolayer of oxidized Au involved into functionalization process. Similar was obtained for HAp/Au/thiourea using thermal reduction. However, in this case there was additional Au doublet with peaks at 84.7 and 88.4 eV corresponding to the pure elemental gold (as for the Au reference) which indicated presence of Au particles which were not under templating-influence of HAp support. In general, results are suggesting chemical reduction as much efficient process for formation of the composite with functionalized surface of metallic particles which are templated by oxide support.

As opposite to the HAp/Au, XPS spectra of HAp/Au/thiourea contained maxima with BEs of nitrogen and sulphur. It allowed investigation of the composite functionalization from the side of thiourea as functionalizing molecules present on the surface of HAp/Au which provided more in-depth information's about this process.

Investigation of the high-resolution S2p spectra indicated existence of three pairs of doublets corresponding to the $S2p_{3/2}$ and $S2p_{1/3}$ spin-orbital components (Figure 42g). The peaks of the doubles were presented at 161.5/162.7 eV, 163.2/164.4 eV and 168.5/169.7 eV (Table 9). The two doublets at lower energies are assigned to S-bearing negative charge with oxidation state of 2-, while the third is oxidized S with 4+ or 6+ states. For metal-thoiurea systems, the first doublet corresponds to bond between metal and S atom of thiourea molecule while the second belongs to S=CN(R) bond between S and C in free thiourea adsorbed onto metallic surface (Quinet et al., 2010). The precise role of the third component is unclear and it could be expected that it belongs to sulphates incorporated into or adsorbed onto HAp structure either to the formation of the salt of formamidine sulphuric acid which is a product of thiourea oxidation (Hoffmann and Edwards, 1977).

Table 9: *Binding energy values for Au4f, S2p and N1s spectra, and assigned oxidation states for HAp/Au composite material functionalized by thiourea.*

Au $4f_{5/2}/4f_{7/2}$ doublets	Oxidation state	S $2p_{1//2}/2p_{3/2}$ doublets	Oxidation state	N 1s singlet	Oxidation state
84.0±0.5 eV	Au(0)	163.2±0.5 eV	S(2-)	400.2±0.5 eV	N(3+)
87.7±0.5 eV	**Au**··S=CN- HAp template	164.4±0.5 eV	Au··**S**=CN-		Au··S=C**N**-
85.6±0.5 eV	Au(1+)	161.5±0.5 eV	S(2-)	389.7±0.5 eV	N(3+)
89.3±0.5 eV	**Au**-S-C-N	162.7±0.5 eV	Au-**S**-C-N-		Au-S-C-**N**-
84.7±0.5 eV	Au(0)	168.5±0.5 eV	S(4+/6+)		
88.4±0.5 eV	pure	169.7±0.5 eV			

Region which corresponds to the N1s had broad single peak with the shoulder at higher value of energy indicating two different superimposed components which were separated using deconvolution process (Figure 42h). These singlets were present at 389.7 eV and 400.2 eV (Table 9). In the literature first one is assigned to the thiourea bonded to the metal by chemisorbtion process while the second is ascribed to the free thiourea at the metal surface (the most probably by physisorbtion) (Quinet et al., 2010).

Accordingly, results are showing that at the surface of HAp/Au there are: (i) Au-S-C-N- bonding which belongs to thiourea chemisorbed on Au particles as well as (ii) Au···S=C-N- formation due to the physisorption of free thiourea molecules onto the Au particle surface.

Table 10: *Zeta potential of HAp/Au composites with and without functionalized surface of Au nanoparticles.*

Material	Zeta potential (mV)
HAp/Au	-14
HAp/Au/Glycine	-22
HAp/Au/Arginine	-2
HAp/Au/Histidine	-21
HAp/Au/Thiourea	-8
HAp/Au/5(bromo-pyridine)-2-thiol	-21
HAp/Au/aniline	0
HAp/Au/4(methylthio) aniline	+7

Surface charge of HAp/Au composites obtained by thermal reduction (without functionalization) and composites obtained by chemical reduction using amino acids (glycine, arginine and histidine) as well as by synthetic amines and thiols (thiourea, 5(bromo-pyridine)-2-thiol and aniline and 4(methylthio) aniline) was investigated based on the zeta potential (Table 10). Composite particles had different magnitudes of zeta-potential as a result of the modification of their surface chemistry obtained by functionalization. HAp/Au without functionalization had negative zeta potential with the magnitude very similar to HAp/Ag composites. However, HAp/Au with functionalizations showed significant variations of surface charge in comparison to pure

HAp/Au. Attachment of thiourea to Au nanoparticles by formation of Au-S bonds caused presence of positive amino groups at the surface that decreased the magnitude of negative charge of HAp-surface within composite. Similar decrease of the magnitude of the negative charge of HAp was detected for 4(methylthio) aniline, aniline and arginine. In the case of glycine, histidine and 5(bromo-pyridine)-2-thiol the magnitude of negative charge of HAp was increased. It was a contribution of negative groups (COO^- in the case of amino acids and Br^- for the thiol) present on the surface of Au particles as part of HAp/Au composite.

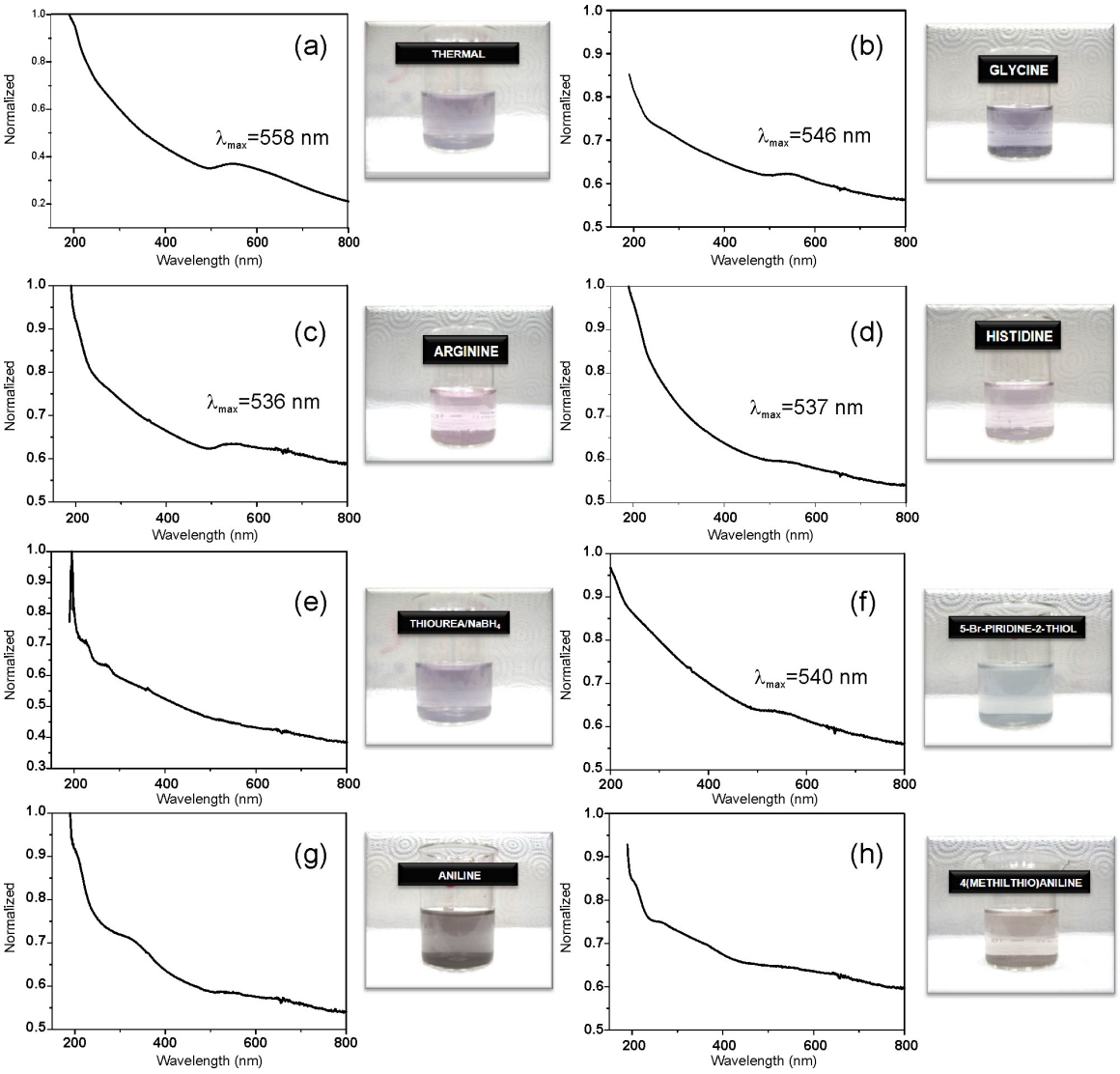

Figure 43: *UV/VIS spectra and corresponding aqueous dispersions of samples in water for HAp/Au composites obtained by thermal reduction (a) and chemical reduction using amino acids (glycine (b), arginine (c), histidine (d)), thiourea/$NaBH_4$ (e) and aromatic amines and/or thiols (5(bromo-piridine-2-thiol) (f), aniline (g) and 4(methylthio)aniline (h).*

UV/VIS absorption spectra of HAp/Au composites obtained by thermal reduction as well as by chemical reduction using amino acids and synthetic amines and thiols together with their dispersions in water are presented in Figure 43. Formation of HAp/Au composites using thermal or chemical reduction containing different surface functionalizations resulted in precipitation of purple, red, violet, blue or grey precipitates. These colourful water dispersions indicated formation of nanosized metallic phase within HAp/Au composite with different size, shape and/or level of agglomeration. Colour of

noble metal nanoparticles depends on their absorption in visible region which is referred to surface plasmon resonance effect. This effect occurs when there is a resonance of the frequency of the photon of light with the frequency of collective oscillation of conducting electrons of metal (Schasfoort and Tudos, 2008). Mention phenomenon is characteristic for nanoparticles and depends on the size, shape and agglomeration of metallic nanoparticles showing sensitivity to their changes (Jain et al., 2007). It means that the change of these properties of nanoparticles could be detected by the shift or by the broadening of this band. It was also already mentioned that surface plasmon resonance of metals is strongly dependant on dielectric constant of their surroundings (Brandl et al., 2005). Formation of composite between metallic nanoparticles and dielectric material induce changes at metallic-dielectric interface which is followed by decrease of plasmon excitation energy and results in red shift of resonant surface band of isolated metallic nanoparticles. Similar is for surface coatings and functionalizations. Increment of the value of dielectric constant of material results in increased red shift of resonant surface band of metallic part of the composite (Choi et al., 2007). HAp/Au obtained by thermal reduction had absorption maximum at 558 nm. Its value is significantly shifted in comparison to the maximum of isolated Au nanoparticles which usually appears at 520 nm (Rautaray et al., 2005). In the case of composites obtained by chemical reduction using amino acids absorption maxima are at 546 nm, 537 nm and 536 nm for glycine, arginine and histidine, respectively. These maxima are blue-shifted compare to the thermal reduction because of the contribution of the surface functionalizations to their size, shape and level of agglomeration as well as to dielectric constant of their surroundings. Similar contribution was observed for composite particles obtained by chemical reduction using synthetic amines and thiols. Resulting nanoparticles had absorption maxima at 540 nm for 5(bromo-pyridine)-2-thiol, while for aniline, 4(methylthio)aniline and thiourea/$NaBH_4$ these absorption maxima had low intensity. In the case of synthetic amines and thiols absorption maxima of these reducing agents bonded to the Au nanoparticles as surface functionalizations were detected in UV/VIS spectra as maxima superimposed to absorption of HAp/Au composite. This was not the case for amino acids used for reduction and functionalization of Au within composite with HAp due to their transparency for UV/VIS light which is intrinsic property of all amino acids (Narayan Bhat and Dharmaprakash, 2002).

4.1.3.3 Morphological properties of hydroxyapatite/gold composite

Morphological properties of Au particles obtained after thermal reduction in inert atmosphere as well as after chemical reduction using amino acids (glycine, arginine and histidine) and synthetic amines and thiols (thiourea/$NaBH_4$, 5(bromo-pyridine)-2-thiol, aniline and 4(methylthio)aniline) are presented in Figure 44. In all cases when Au particles were formed, applied method resulted in their high instability which was reflected through intensive agglomeration and ingrowths into larger structures present as sub-micrometer sized aggregates.

After thermal treatment system showed the highest level of instability for both, $Au(CH_3COO)_3$ and $Au(OH)_3$, gold precursors (Figure 44a,b). Reduction of pre-formed complex by decomposition at high temperature in inert medium provided formation of Au particles which were ingrown into larger structures.

In the case of chemical reduction morphological properties were different. Using of the amino acids for reduction and functionalization of Au particles resulted in formation of irregular, highly agglomerated spheres. However, among all particles obtained by chemical reduction these ones had the lowest particle size. Size and size distribution of so formed Au particles decreased starting from the glycine over arginine to histidine (Figure 44c,d,e).

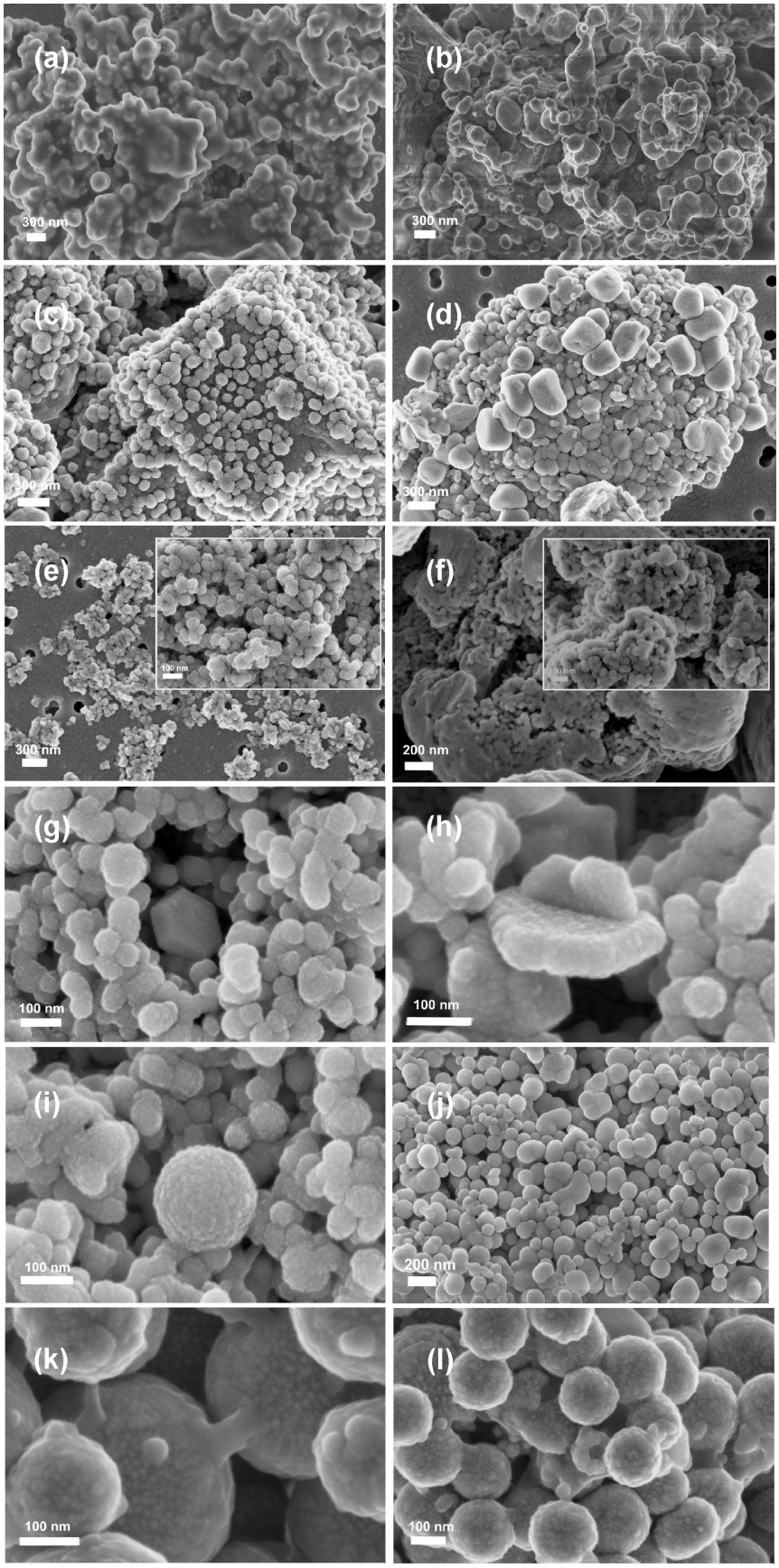

Figure 44: *FESEM micrographs of Au particles obtained by thermal (a, b) and chemical reduction using amino acids (glycine (c), arginine (d), histidine (e)), thiourea/$NaBH_4$ (f) and aromatic amines and/or thiols (5(bromo-piridine-2-thiol (g, h, i)), aniline (j) and 4(methilthio)aniline (k, l).*

Fast reduction of gold which was provided by the application of thiourea/$NaBH_4$ as system for functionalization and reduction resulted in formation of small, metallic particles similar to those formed by histidine. However, surface functionalization was not sufficient for compensation of the surface charge and these particles were also intensively agglomerated (Figure 44f). Particles which were formed by the application of others synthetic amines and thiols showed higher level of stability. In the case when 5(bromo-pyridine)-2-thiol was used formed particles had two different morphologies- smaller ones were spheres up to 100 nm in diameter while the larger ones were hexagons up to 200 nm in length and around 50 nm in width (Figure 44g,h). Application of aniline and 4(methylthio)aniline allowed formation of 200-nm sized spheres (Figure 44i, j, k, l). In the case of 4(methylthio)aniline these particles were nanostructured hollow spheres with the core formed of small Au nanoparticles a few nanometres in size. These spheres have visible "necks" formed between particles because of the intensive collision during sonication when energy was transferred and melting took place at the point of impact (Figure 44k,l).

Observed differences in morphology of Au particles formed by thermal and chemical reductions are direct consequence of the mechanism of their formation and conditions for their growth. Seeds for thermally reduced particles were formed during sonication step and they grew during the slow processing at elevated temperature. In contrast, chemical reduction provided fast reduction which took place along with sonication and intensive mixing. Differences obtained in morphology of particles formed by chemical reduction depended on the properties of reduction agents and their ability to affect shape and size of formed particles after attachment onto their surface. These results showed that surface functionalizations were able to affect growth of these particles however did not have ability to prevent their nanometre size and they grew to submicrometre-sized dimensions.

In the case of formation of HAp/Au composites morphological properties of Au particles were significantly improved for both, thermal reduction and for chemical reduction using amino acids (Figure 45). Reached improvements concern significant reduction in particle size, narrower size distribution and decrease or absence of agglomeration.

In the case of thermal reduction, Au particles formed using acetate (Figure 45a_{1-3}) and hydroxide (Figure 45b_{1-3}) gold precursor resulted in formation of Au particles attached onto the surface of HAp rods and finely distributed on it which allowed their stabilization and prevented agglomeration and ingrowths into larger structures. According to TEM images these particles were spheres with diameters in the range between 10-30 nm. Observed metallic particles were polycrystalline and with the presence of twin-boundary defects which indicate their growth process.

Very similar morphology formed of apatite plates with small Au particles attached onto their surface was observed for the particles obtained after chemical reduction using amino acids. The main difference reached in this case was a shift of particle size distribution of spherical Au particles which had diameters in the range from a few to 15 nm with significant share of particles with the size of 1-2 nm. For glycine (Figure 45c_{1-3}) and histidine (Figure 45e_{1-3}) there was a low degree of aggregation which was completely absent in the case of Au particles obtained using arginine (Figure 45d_{1-3}).

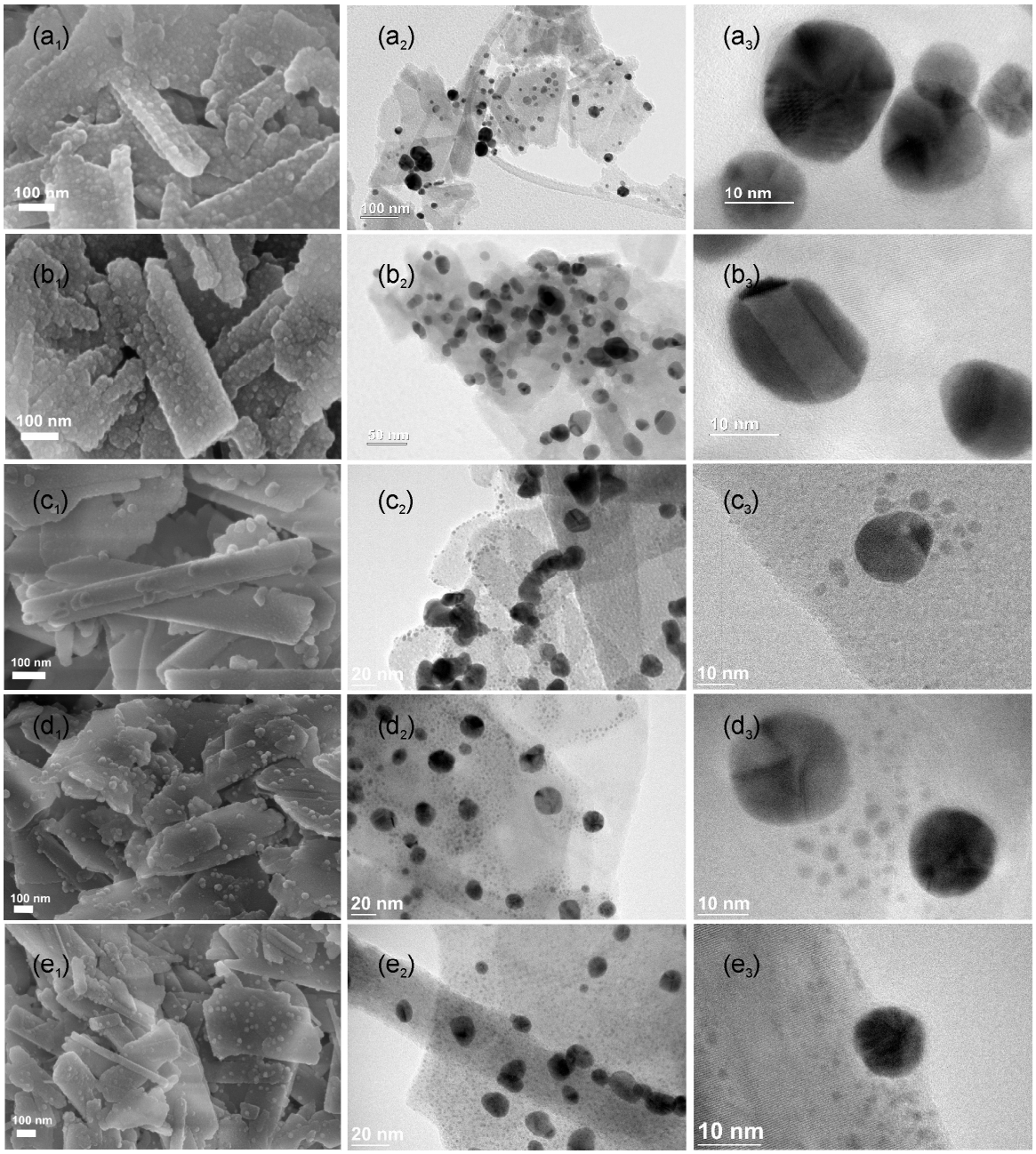

Figure 45: *Morphological properties of HApAu particles obtained by thermal reduction (a_{1-3},b_{1-3}) and chemical reduction using amino acids (glycine (c_{1-3}), arginine (d_{1-3}), histidine (e_{1-3}))*

Application of synthetic amines and thiols for reduction and functionalizaton of Au particles within HAp/Au composites had different contribution to morphological properties. In the case of thiourea/$NaBH_4$ system, formed particles were still aggregated with a very low content of them attached onto apatite plates (Figure 46a, b). For 5(bromo-piridine-2-thiol) Au particles were 1-3-nm in size dots very finely distributed onto the surface of HAp plates (Figure 46c, d). Once again the largest particles were obtained for aniline and 4(methylthio)aniline reduction agent (Figure 46e, f) when Au particles were 50-100 nm in size. They were partially attached onto HAp plates and rods and partially presented as isolated phases and agglomerated.

In all composites HAp had a template role and succeeded in prevention of Au particle growth and decreased a degree of their agglomeration compare to the pure Au particles formed by the same method.

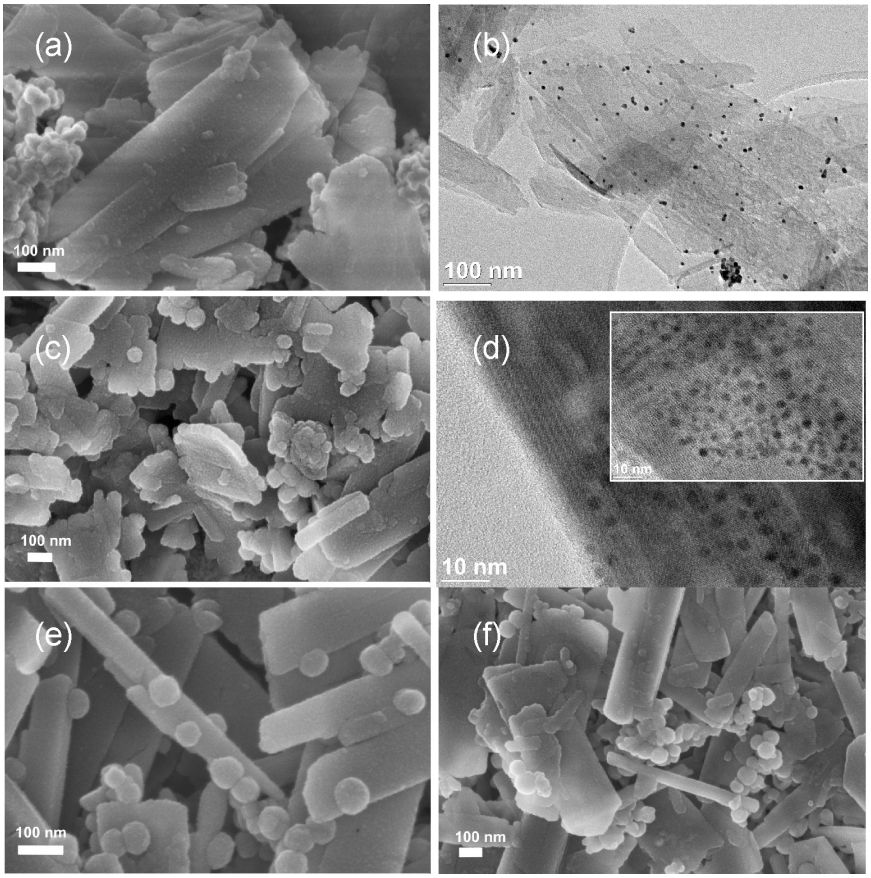

Figure 46: *Morphological properties of HAp/Au particles obtained by chemical reduction using thiourea/$NaBH_4$ (a, b) and aromatic amines and/or thiols (5(bromo-pyridine-2-thiol (c, d)), aniline (e) and 4(methylthio)aniline (f).*

4.2 Investigation of antibacterial activity of hydroxyapatite/metal composites

HAp/metal composites were synthesized in order to form novel materials which would be able to have strong effect on prevention of the growth of bacteria. The main strategy for their formation concerned the usage of gold and platinum nanoparticles as building blocks of these newly designed materials and different approaches have been used in order to activate them. Formed materials contained nanosized metallic nanoparticles attached onto the surface of apatite carriers. It was presumed that activation of so formed structures could be achieved by carefully selected surface functionalizations. Developed materials were tested for activity against two sorts of bacteria.

4.2.1 Antibacterial activity of hydroxyapatite/silver composites

As one of the well-known and widely used metal with natural ability to have action against very broad classes of pathogens, silver was used as a starting point for development of novel group of antibacterial materials. In this case functionalization was not used however formation of nanoparticles attached or embedded within apatite carriers as well as incorporation of silver ions within apatite structure was the way for reaching a high activity of finally–formed material. Resulted material was used as a positive control and a reference for the next steps performed in these investigations.

4.2.1.1 Disk diffusion test for antibacterial activity of HAp/Ag composites

A first step in investigation of the ability of formed HAp/Ag composites for the activity against bacteria was performed using disk diffusion test. Materials were tested for activity against *E. coli* as representative of the group of Gram negative (Figure 47a) and *S. aureus* as representative of the group of Gram positive (Figure 47b) bacteria. HAp/Ag composites with 1%, 5% and 10% of metal-content were tested while pure HAp was used as a negative control (Figure 47 1-4). All disks were incubated on the surface of agar plates with *E. coli* and *S. aureus* for 24 hours at the temperature of 37°C.

Results showed that all silver-containing materials were able to form a distinct level of inhibition of the growth for the both types of tested bacteria. Around the disks with HAp zones of inhibition of the growth of bacteria could not be detected. In the case when silver was present, formation of the rings around disks was observed which was indication of suppression of bacterial growth in their surroundings.

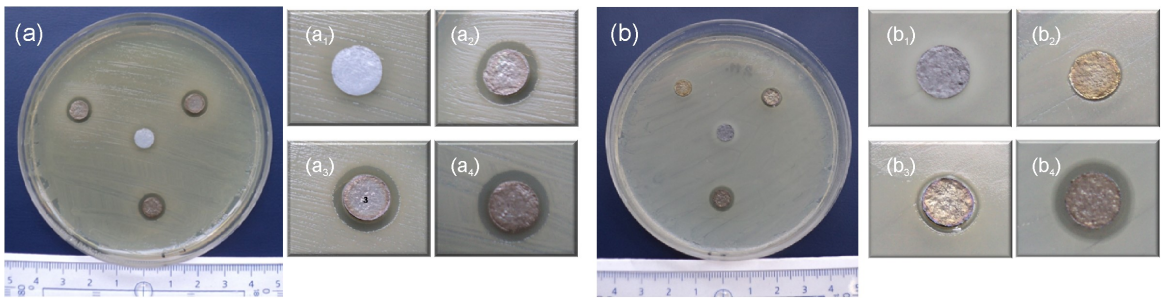

Figure 47: *Disk diffusion test for the growth of E. coli (a) and S. aureus (b) near disks made of HAp (1) and HAp/Ag composites with 1% (2), 5% (3) and 10% (4) of silver.*

Disk diffusion test is standardized method for investigation of antibacterial activity with pre-defined criteria for evaluation of results. These criteria include the width as well as clarity of the zone of inhibition, which appears around/under disks as reliable parameters for description and interpretation of the toxicity results (Schmalz, 1988).

The regions around disks obtained after 24-hours aging with bacteria were inoculated by phase contrast microscopy method (Figure 48) in order to evaluate results. In the case of *E. coli*, around the disk with pure HAp there was a thin layer of bacteria with modified density however, appearance of the inhibition zone was not detected (Figure 48a_1). In contrast, the case of HAp/Ag composites inhibition zone appeared, it was clear with modification of the density of bacteria along the zone more than 80% diameter less than 0.5 cm. Inhibition zones formed due to the diffusion of antibacterial silver through agar medium showed concentration-dependence. The higher content of silver in material resulted in higher defending concentration and greater width of the rings around tested disks (Figure 48a_2,a_3,a_4). Obtained results showed 0.5/0.5 response index for HAp and 2/5 response index for HAp/Ag and according to the Schmalz criteria (Schmalz, 1988) (Table 4) their action against *E. coli* was evaluated as “not toxic” and “middle toxic”, respectively.

In the case of *S. aureus*, there were no changes in the density of bacteria around or below the disk formed of pure HAp (Figure 48b_1). In this case response index was 0/0 and according to the Schmitz criteria material was classified into “not toxic” group. For HAp/Ag composites formed zones of inhibition of bacterial growth were lower in diameter compare to the zones obtained for previously described bacteria and they were not clear. In this case there was a gradual change of the density of bacteria around disks. Similar to the previous case, observed changes showed dependence upon the concentration and gradually increased with the increase of silver content (Figure 48b_2, b_3, b_4). Investigated material had lower impact to the growth of *S. aureus*. Response index of these materials was 2/3 and they are also classified into the group of “middle toxic” materials for the growth of *S. aureus*. However, it was not clear whether these bacteria were dead or not and it was not easy to determine the boundary of the zone of the lysis.

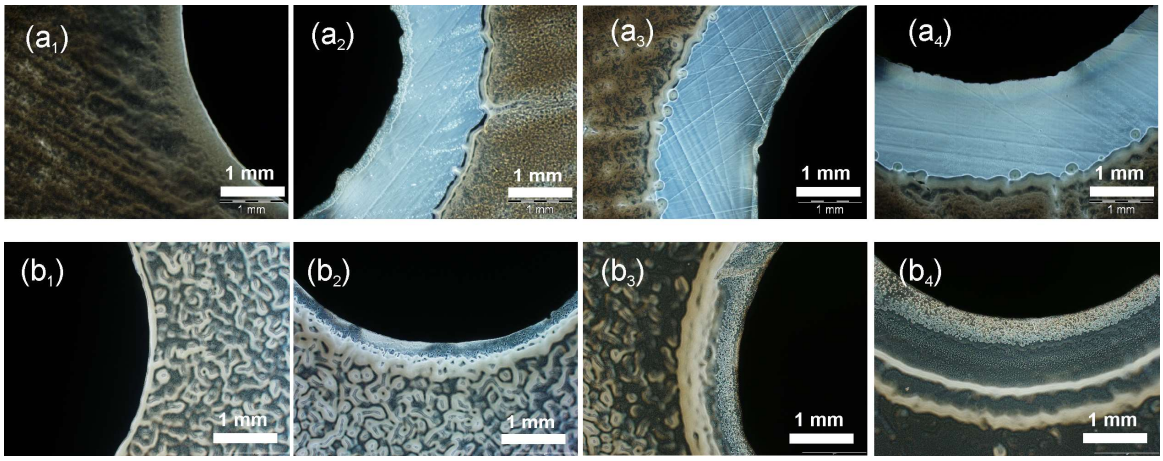

Figure 48: *Phase contrast images of the growth of E. coli (a) and S. aureus (b) near the surface of HAp (1) and HAp/Ag composites with 1% (2), 5% (3) and 10% (4) of silver.*

In the next step, regions around disks obtained after analysis of the diffusion of silver through agar medium and its influence to the bacteria were additionally investigated for precise distinguishing of living and dead bacteria along the region around disks. Separation was performed by fluorescence labelling using SYTO 9 and PI. SYTO 9 is a green fluorescence dye permeable through cellular membrane and able to attach nucleic acids of both dead and living cells. PI is red fluorescence dye which is non-permeable

through intact cellular membrane and with ability to get inside cells and attach to their nucleic acids only in the case when their membrane is mechanically destroyed, which is the case when they are dead. Labelling and observation of dead and living bacteria were performed *in situ*. This approach for investigation of antibacterial action was performed on pure HAp and HAp/Ag composite with 10% of silver and tests were performed for both, *E. coli* and *S. aureus*.

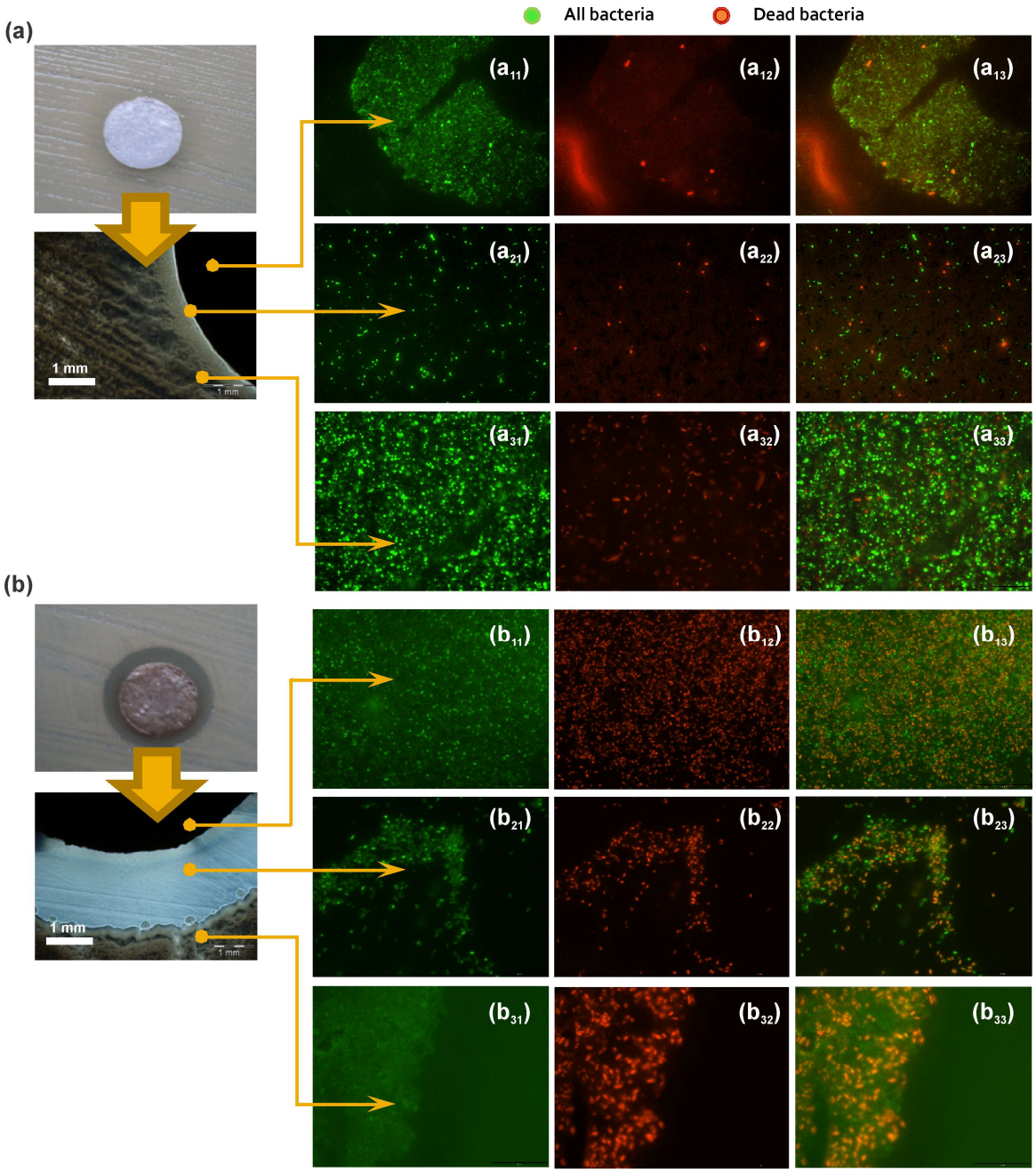

Figure 49: *E. coli fluorescence detection of dead (orange) and all (green) bacteria for HAp (a) and HAp/Ag (with 10% of silver) (b) for the regions corresponding to the surface of disks (11-13) and zone of inhibition close (21-23) and far(31-33) of the disk surface.*

In the case of *E. coli*, for the pure HAp this type of labelling of the region below and around the disk showed dominant green fluorescence (Figure 49a$_{11, 21, 31}$) indicating that majority of bacteria were alive. Only a few of them showed orange colour indicating dead bacteria (Figure 49a$_{12, 22, 32}$). In general, as confirmed by disk diffusion, material was non-toxic for bacteria (Figure 49a$_{13, 23, 33}$). For HAp/Ag situation was completely opposite

since only a part of bacteria showed only green (Figure 49b$_{11, 21, 31}$), while a large number of them showed orange fluorescence (Figure 49b$_{12, 22, 32}$) for all three investigated regions indicating existence of the large number of dead bacteria (Figure 49b$_{31, 32, 33}$).

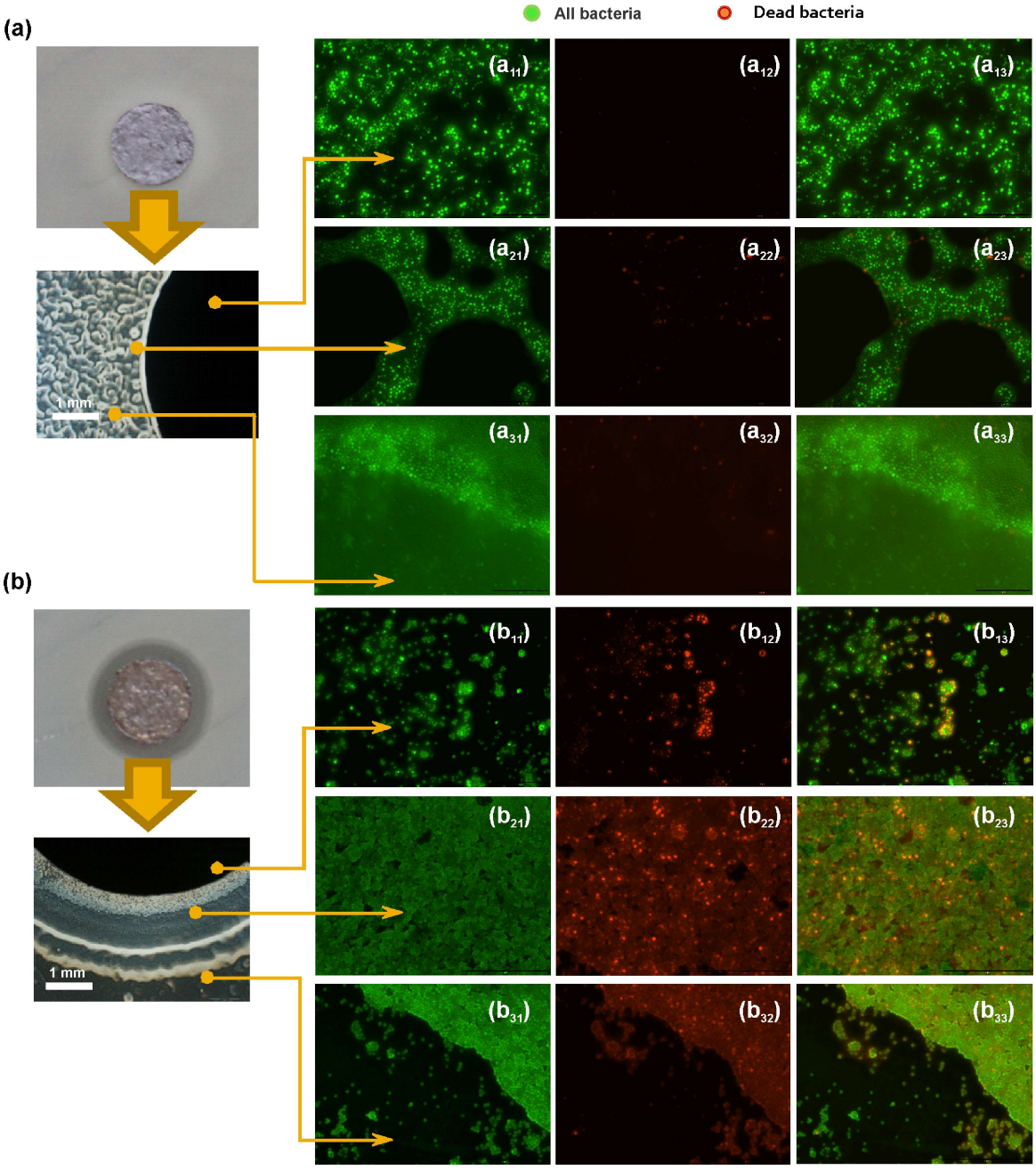

Figure 50: *S. aureus fluorescence detection of dead (orange) and all (green) bacteria for HAp (a) and HAp/Ag (with 10% of silver) (b) for the regions corresponding to the surface of disks (11-13) and zone of inhibition close (21-23) and far (31-33) of the disk surface.*

When the same method was used for investigations of these materials in the case of *S. aureus* situation was similar (Figure 50). Testing the HAp for interactions with this type of bacteria showed that all of them were labelled in green (Figure 50a$_{11–33}$) which indicated growth and existence of healthy colony near the surface of the disk which was not affected by the material. Testing the material with 10% of silver confirmed existence of dead bacteria within the ring which corresponds to the zone of inhibition (Figure 50b$_{11–33}$). In this way it was proven, that previously detected gradual change of the density of bacteria within the zone of inhibition contains a large part of dead bacteria.

4.2.1.2 Minimal growth-inhibitory concentrations (MIC) and minimal bactericidal concentrations (MBC) of HAp/Ag composites

Quantification of antibacterial action of HAp/Ag composite was determined using MIC and MBC methods. Tests were performed for both representatives corresponding to Gram positive and Gram negative bacteria. During this type of testing, composite powder was finely dispersed within medium containing bacteria, which provided better contact between bacteria and material and did not depended only on the diffusion of silver through the medium as it was in the case of disk diffusion method.

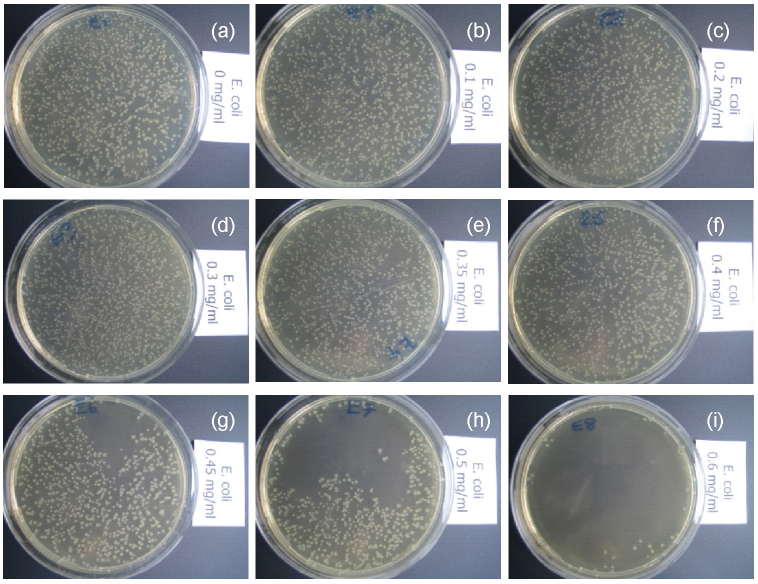

Figure 51: *Abilities of different concentrations (0 mg/ml (a), 0.1 mg/ml (b), 0.2 mg/ml (c),0.3 mg/ml (d), 0.35 mg/ml (e), 0.40 mg/ml (f), 0.45 mg/ml (g), 0.5 mg/ml (h) and 0.6 mg/ml (i)) of HAp/Ag (with 10% of silver) to inhibit growth of E. coli.*

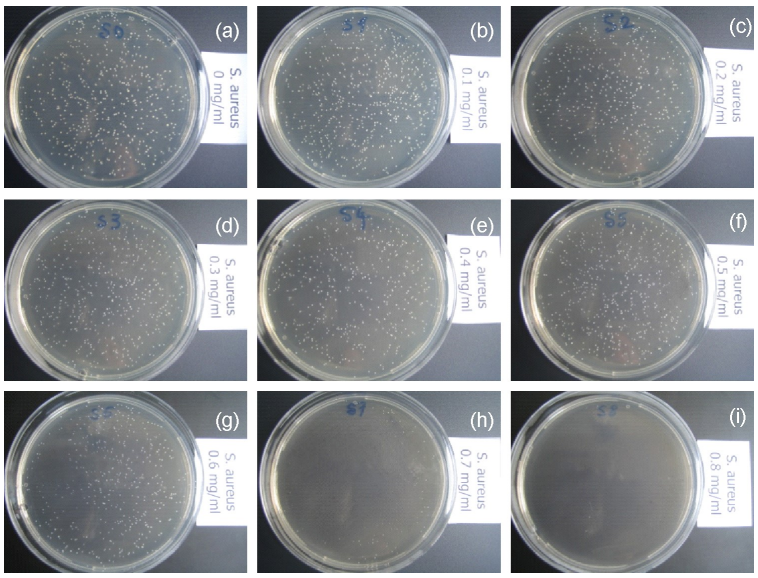

Figure 52: *Abilities of different concentrations (0 mg/ml (a), 0.1 mg/ml (b), 0.2 mg/ml (c),0.3 mg/ml (d), 0.40 mg/ml (e), 0.50 mg/ml (f), 0.60 mg/ml (g), 0.70 mg/ml (h) and 0.80 mg/ml (i)) of HAp/Ag (with 10% of silver) to inhibit growth of S. aureus.*

MIC concentration of HAp/Ag composite was firstly determined for *E. coli* as

representative of Gram negative bacteria. Series containing dispersions of different concentrations of this material in medium were tested for ability to inhibit a growth of bacteria. After aging during the period of 24 hours at 37°C it was determined that the minimal concentration of this material able to provide inhibition of the growth of this sort of bacteria was in the range between 0.6-0.7 mg/ml (Figure 51).

In the next step, the same method was used for testing of the *S. aureus* as representative of gram positive bacteria. The series containing dispersions of different concentration of HAp/Ag powder in medium with bacteria showed that 24-hour aging provides inhibition of bacterial growth for the concentration of composite in the range between 0.7-0.8 mg/ml (Figure 52).

MIC concentrations of HAp/Ag for both types of tested bacteria were similar and slightly higher for *S. aureus* as a representative of Gram positive bacteria. These two sorts of bacteria basically differ in cell wall structure which makes *S. aureus* commonly more resistant to antibacterial agents.

Material was also tested for concentration, which had bactericidal effect on these two sorts of bacteria. After 24-hour aging with dispersions of different concentrations of HAp/Ag power in media containing bacteria, a small sample of medium was replaced into fresh medium to investigate their ability for the further growth. Concentration of material which affected bacteria in such a manner that their further growth was prevented was bactericidal.

HAp/Ag had ability for bactericidal influence to both sorts of bacteria. In the case of *E. coli* bactericidal concentration of composite was 0.8 mg/ml while this concentration for *S. aureus* was 1.25 mg/ml (Figure 53). Both bactericidal concentrations were around 40-50% higher than bacteriostatic once.

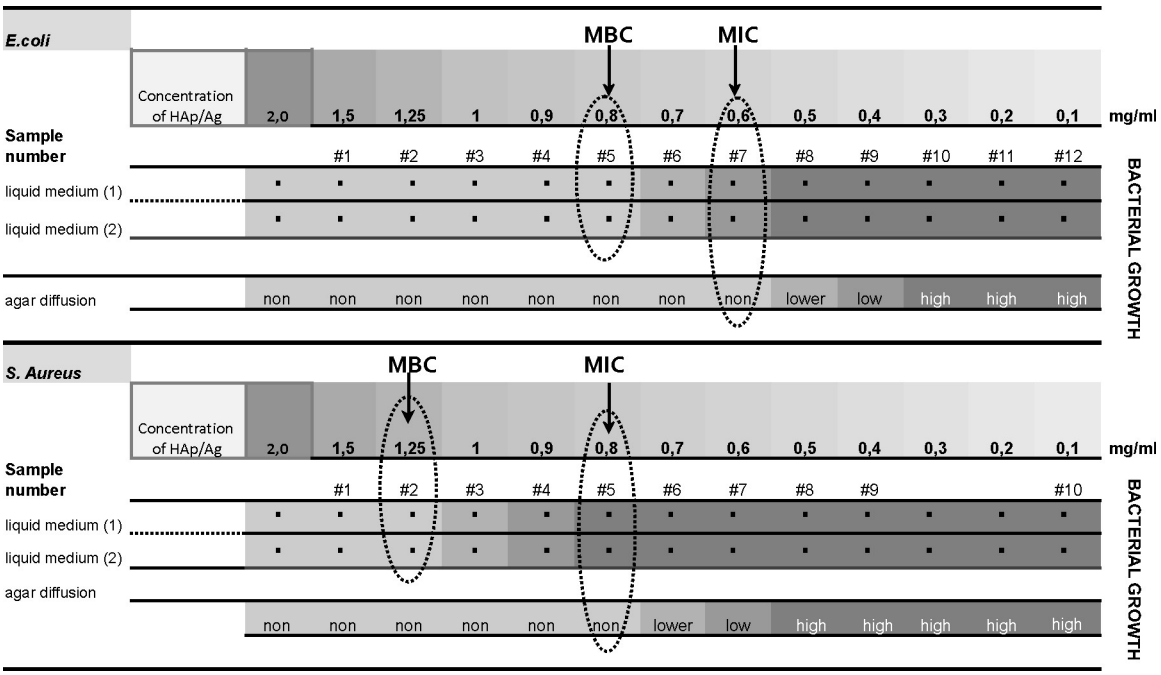

Figure 53: *Minimal concentrations of HAp/Ag composite with 10% of silver able to induce growth inhibition (MIC) and bactericidal effect (MBC) to E. coli and S. aureus.*

4.2.1.3 Morphological changes in bacteria induced by HAp/Ag composite

Antibacterial activity of HAp/Ag composite was also tested from the standpoint of ability

to induce morphological changes in bacterial wall. Morphological analysis was performed for two different cases which differed in the contact of materials with bacteria. A first case concerned disk diffusion when morphology of bacteria present in the zone of inhibition of the growth were analysed. In this case eventually obtained morphological changes are assigned to the influence of diffuse silver. The second case included investigation of the morphological properties of bacteria aged within medium with dispersed composite powder. Tests were performed for *E. coli* and *S. aureus* bacteria.

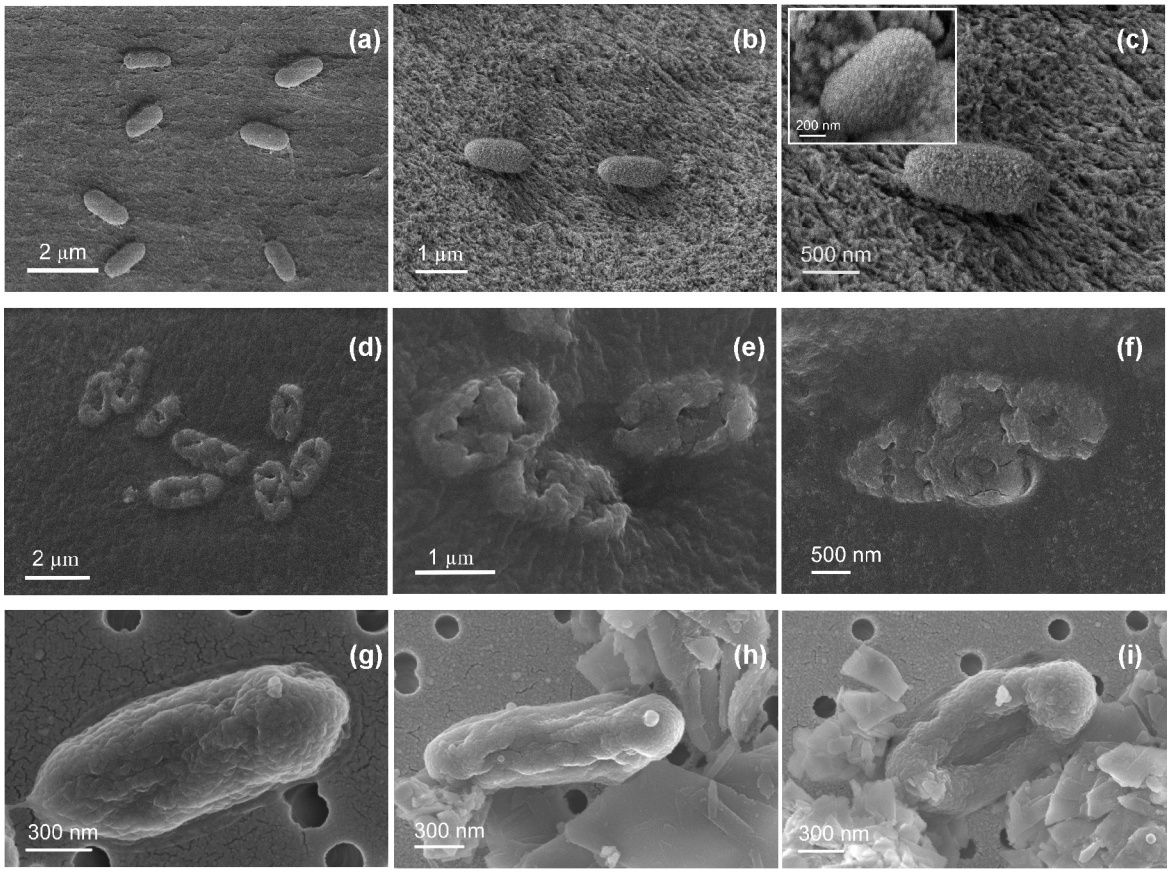

Figure 54: *SEM images of healthy E. coli bacteria (a, b, c) and modified bacteria from the zone of inhibition around disk made of HAp/Ag composite (d, e, f) as well as comparison of healthy bacteria in agar (g) and in presence of HAp (h) with modified bacteria mixed with HAp/Ag composite (i).*

Morphological properties of the surface of *E. coli* are presented in FESEM micrographs in Figure 54. When morphology was investigated for disk diffusion, positive control were bacteria present in the agar far from the disk. These healthy bacteria which are rod-like in shape and 1-2 μm in length possess compact rough surface (Figure 54a, b, c). Bacteria which were tested for morphological changes induced by silver were sampled from the zone of inhibition present around the disk. These bacteria were exposed to diffuse silver during 24-hours. Compare to the compact healthy bacteria, investigation of the morphological properties of those influenced by silver revealed that they had completely damaged bacterial wall (Figure 54d, e, f) and collapsed morphology.

The second case concerned morphological properties of bacteria from the dispersion of material in the growing medium. In this case there was a higher contacting surface between bacteria and material. A first reference were bacteria dispersed inside medium without material (Figure 54g) while the second reference corresponded to the dispersion of HAp within medium (Figure 54h). Bacteria obtained from these two negative probes had similar morphology which means that HAp did not had any influence to bacterial

wall. Investigation of the bacteria obtained from the dispersion of growth medium with HAp/Ag composite showed high level of a wall damage which was similar to the wall damage of bacteria from the zone of inhibition. It should be mentioned that in this cased preparation procedure additionally affected bacterial morphology.

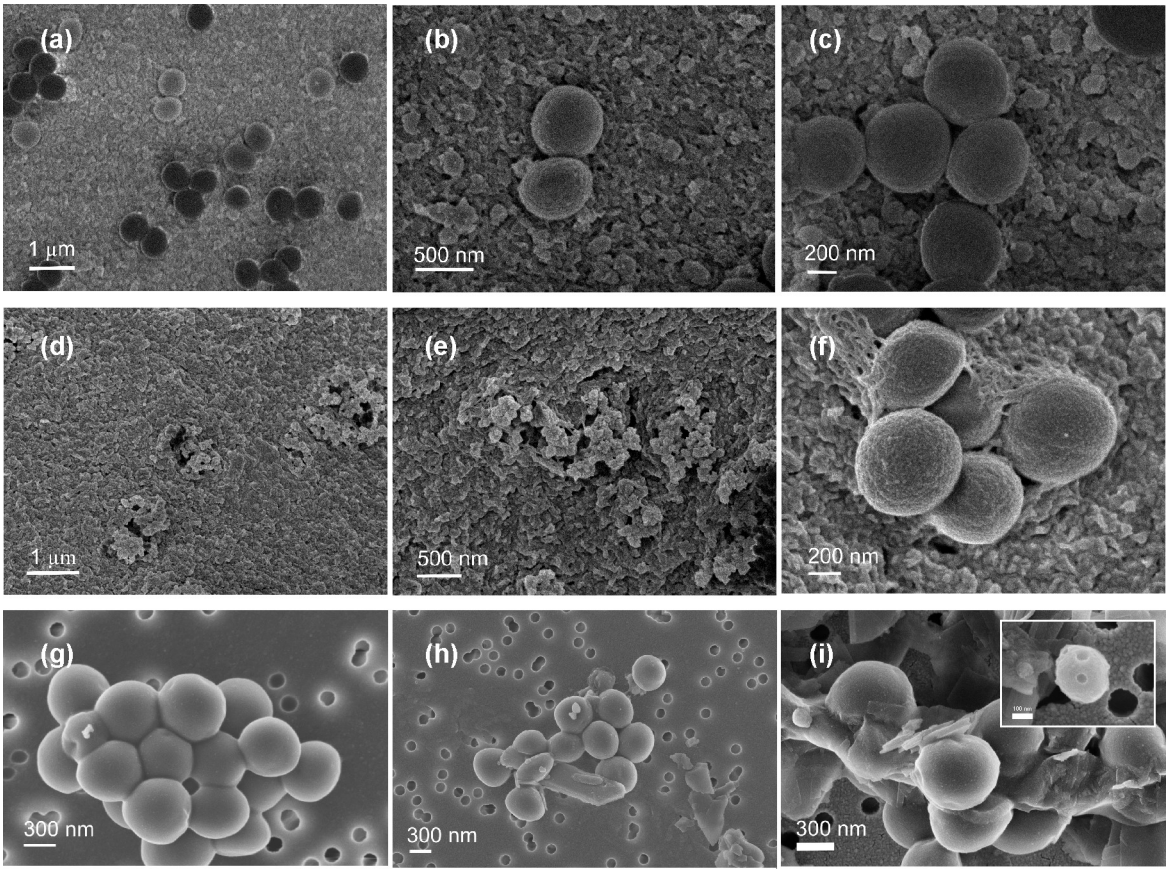

Figure 55: *SEM images of healthy S. aureus bacteria (a, b, c) and modified bacteria from the zone of inhibition around disk made of HAp/Ag composite (d, e, f) as well as comparison of healthy bacteria in agar (g) and in presence of HAp (h) with modified bacteria mixed with HAp/Ag composite (i).*

In the case of *S. aureus*, the same investigations of morphological properties of bacteria from the zone of inhibition as well as from dispersions with bacteria were performed (Figure 55). In the first case, morphology of healthy bacteria far fromm the disk was negative control. These bacteria were sphere-like in shape and 200-500 nm in size (Figure 55a, b, c). When bacteria were selected from the region which corresponded to the zone of the inhibition where they were in direct contact with diffuse silver, some of them had completely disrupted bacterial wall with lost integrity of the shape. There was also a group of others which kept their size and shape but they had a sort of network which was formed around them (Figure 55d, e, f). This network could be assign to the protein mucus formed as a beginning of formation of a biofilm (Donlan and Costerton, 2002) which has a protective role in bacteria, especially *S. aureus.*

In the second case when dispersions were tested, two negative probes containing only bacteria and bacteria dispersed with pure HAp had morphology without any visible changes in bacterial wall (Figure 55g, h). Bacteria from dispersions with HAp/Ag showed mechanical damages of the wall which were in the form of surface ruptures or in some cases bacteria were cut in two parts and in close contact with material (Figure 55i).

4.2.2 Antibacterial and self-cleaning activities of hydroxyapatite/platinum composites

Ability of platinum to contribute to development and increase of the efficacy of semiconductor for photocatalytic activity was an inspiration for formation of HAp/Pt composite. So far HAp has been the most frequently analyzed as bioactive ceramics applicable in reparation and reconstruction of bone tissue. If this material is looked as semiconductor which can be activated by ultraviolet light for activity in degradation of organic molecules there is a novel direction for its development. It was assumed that formation of HAp composite with Pt nanoparticles, by the procedure which will be able to provide attachment of Pt-complex onto HAp surface, will be able to contribute to increase the efficiency of development of self-cleaning ability of this material. Ability for materials for self-cleaning is associated with their antibacterial activity induced due to the photocatalytic degradation. Design of the material in such a manner that its activation could be initiated by visible light implies possibility for antibacterial activity with harmless impact to human health.

4.2.2.1 Quantification of photocatalytic and antibacterial activities of HAp/Pt composites during light-irradiation

Both composites, HAp/Pt (H_2PtCl_6) and HAp/Pt ($C_{10}H_{14}O_4Pt$), were irradiated by ultraviolet (UV) (Figure 56a, b) and visible (Vis) (Figure 56c, d) light and their ability to induce degradation of non-degradable dye was monitored spectroscopically. For that purpose, methylene blue has been used as a model of pollutant, non-degradable azo dye and both materials showed ability to provide its degradation after irradiation by two different ranges of electromagnetic spectrum. Results were compared with commercial photocatalyst (P25) used as a reference.

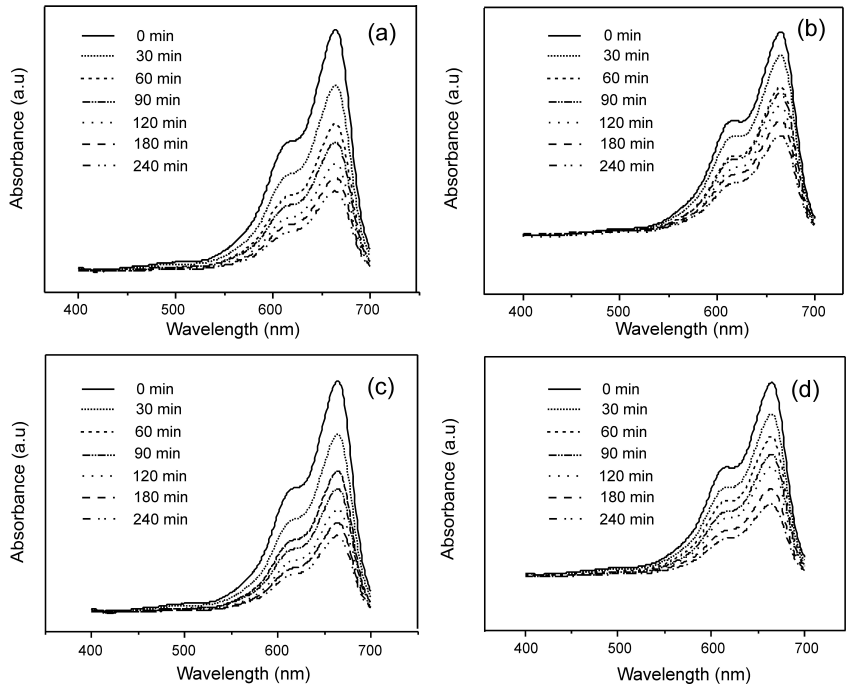

Figure 56: *UV/VIS spectra of methylene blue during degradation induced by- HAp/Pt (H_2PtCl_6) (a) and HAp/Pt ($C_{10}H_{14}O_4Pt$) (b) both irradiated by UV light as well as HAp/Pt (H_2PtCl_6) (c) and HAp/Pt ($C_{10}H_{14}O_4Pt$) (d) both irradiated by visible light.*

After irradiation of HAp/Pt (H_2PtCl_6) and HAp/Pt ($C_{10}H_{14}O_4Pt$) by UV light materials induced gradual drop of relative concentration of the dye with the time and showed photo-induced activity. Degradation rates of these two materials were similar and slightly faster for the first one with chemisorbed hexachloroplatinum ions (Figure 57a). Both materials had lower degradation rates compare to the degradation rate of commercial P25 (Figure 57a). Photocatalytical degradation of non-degradable azo-dyes usually follows Langmuir-Hinshelwood model and degradation reaction could be described by first-order kinetic mechanism (Park, 2010). Rate constants were calculated from the slopes of the curves of the ln(co/c) change with time (Figure 57b). Their values for HAp/Pt (H_2PtCl_6) and HAp/Pt ($C_{10}H_{14}O_4Pt$) were $3.92 \cdot 10^{-3}$ min^{-1} and $2.82 \cdot 10^{-3}$ min^{-1}, respectively and they are significantly lower compare to the value of reaction constant of P25 which was $9.826 \cdot 10^{-2}$ min^{-1}.

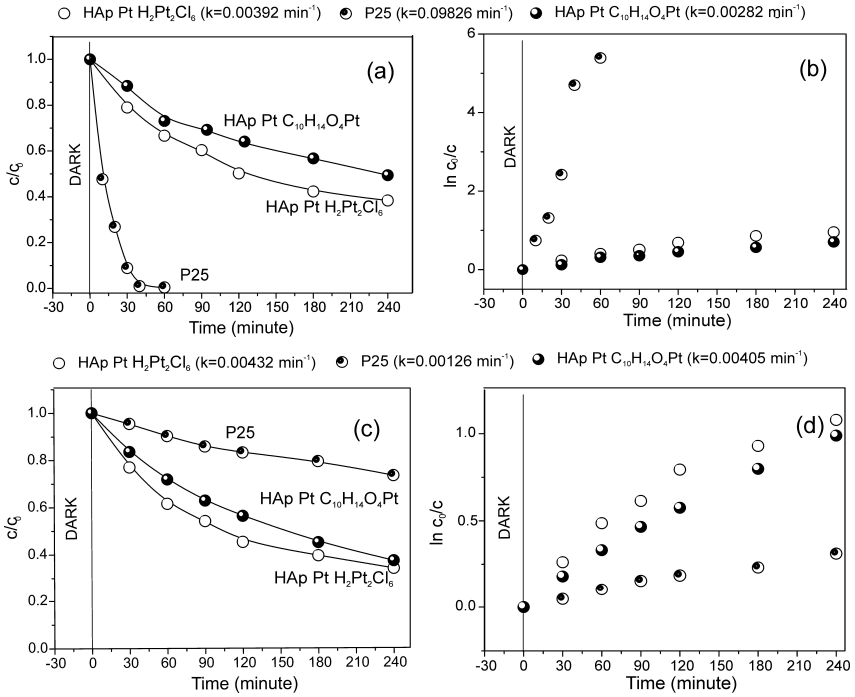

Figure 57: *Kinetics of the dye degradation for HAp/Pt (H_2PtCl_6) (c), HAp/Pt ($C_{10}H_{14}O_4Pt$) and commercial TiO_2 (P25) all three irradiated by UV light (a, b) and the kinetics of degradation of the dye induced by the same materials irradiated by visible light (c, d) with corresponding reaction constants.*

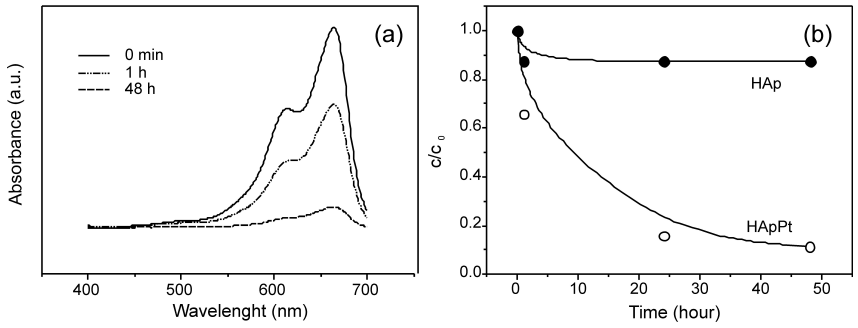

Figure 58: *Dye degradation in the presence of HAp/Pt (H_2PtCl_6) composite: UV/VIS spectra (a) and comparison of the absence of degradation in the presence of HAp and its appearance in the case of the presence of the composite with Pt after materials has been kept in the dark.*

In the case when materials were irradiated by VIS light situation was opposite. While P25 had very low activity and slow degradation rate, both composites showed higher photo-induced activity with significantly higher degradation rate (Figure 57c). Once again degradation rate of HAp/Pt (H_2PtCl_6) was slightly higher in comparison to the degradation rate of HAp/Pt ($C_{10}H_{14}O_4Pt$) (Figure 57c). Composite had rate constants $4.32 \cdot 10^{-3}$ min^{-1} and $4.05 \cdot 10^{-3}$ min^{-1} while the constant of the P25 was more than three times lower and its value was 1.26 10^{-3} min^{-1}(Figure 57d). Degradation rates reached by activation of the composites by irradiation with VIS light are higher compare to the ones reached after activation by UV light.

Kinetic parameters of investigated processes showed the major differences depend on: (i) the applied spectrum of irradiation light and (ii) the type of material. It was also interested to observe that HAp composites with Pt were able to induce degradation of the dye in the dark. Investigation of the UV/VIS spectra of HAp/Pt (H_2PtCl_6), which was kept in the dark, showed gradual decrease of absorption maxima of the dye due to its degradation (Figure 58a). Kinetics showed that this process was slower in comparison to the rate of degradation activated by UV or VIS light. Moreover, if abilities of HAp and its composite with Pt to induce degradation of the dye are compared it is obvious that only composite was able to induce this process in the dark (Figure 58b). It means that presence of Pt nanoparticles within composite is responsible for this activity.

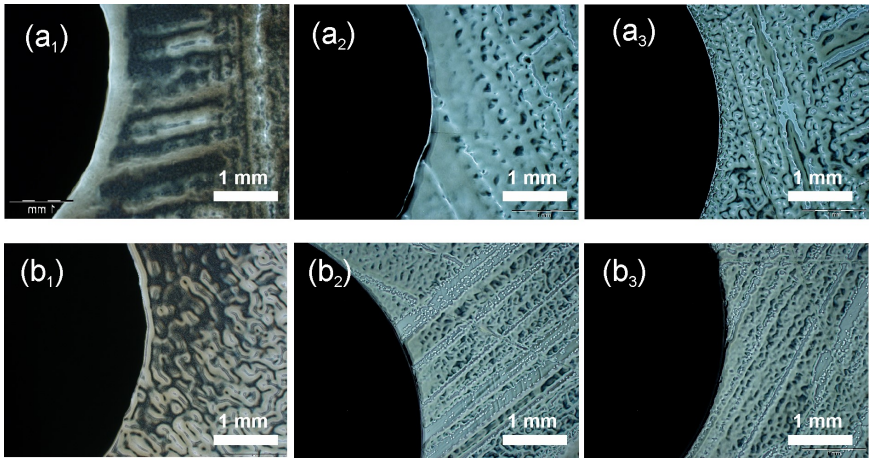

Figure 59: *Phase contrast images of the growth of E. coli (a) and S. aureus (b) near the surface of HAp (1), HAp/Pt (H_2PtCl_6) and HAp/Pt ($C_{10}H_{14}O_4Pt$) without irradiation.*

In the next step, materials formed of HAp as bioceramic and Pt as metallic part with two different types of functionalizations of HAp surface which had strong photocatalytic activity were investigated for antibacterial activity. Investigations were performed in dark as well as after irradiation.

Firstly their influence to bacteria was investigated by classical approach without irradiation by light. It means that materials were tested in dark without ability for intensive photocatalytic activity. For that purpose disk diffusion method was applied and HAp was used as negative control. Tests were performed for both types of bacteria, *E. coli* and *S. aureus,* and in both cases disks were unable to induce any zones of inhibition of bacterial growth. After they have been analysed using phase contrast microscopy (Figure 59), it was observed that similar to the pure HAp (Figure 59a_1, b_1) bacteria were able to growth close to the surface of the disks for both composites (Figure 59$a_{2,3}$, $b_{2,3}$).

It was suspected that photocatalytic activity of materials in dark was too low to affect bacterial growth. Therefore, the tests were repeated and antibacterial activity was tested once again when material were irradiated with VIS light. As it was already shown in this case materials had the strongest photocatalytic activity. However results were similar. In order to increase the contact with bacteria, materials were used in the form of dispersions (Figure 61a, b). For the negative control *E. coli* was grown in absence of any photocatalytically active material, while HAp/Ag composite was used for the positive control. The second reference was used because Ag-component has a potential to increase the photocatalytic activity of material (Malagutti et al., 2009) and in the same time it has natural ability to induce very strong antibacterial action (Marambio-Jones et al., 2010). Results showed that HAp/Pt materials were unable to decrease bacterial growth in the level that might be expected on the basis of their strong activity for degradation of the dye. Compared to the strong antibacterial activity of HAp/Ag, the HAp/Pt materials was very weak. It is important to understand that in this case natural antibacterial action of Ag has been superimposed to its photocatalytic activity induced by irradiation using VIS light. In contrast, Pt in HAp/Pt materials does not have a natural ability for antibacterial action, so the observed effect on the bacterial growth was mediated only through the photocatalytic action and consequently it was significantly lower. Nevertheless, compared to the negative control HAp/Pt has exerted some inhibitory effect on bacterial growth and it may be expected that further optimization could increase its antibacterial activity. Accordingly it was concluded that strong photocatalytic activity does not necessarily implies the same effectiveness for antibacterial activity and there is a need for additional process in order to reach sufficient level of antibacterial action.

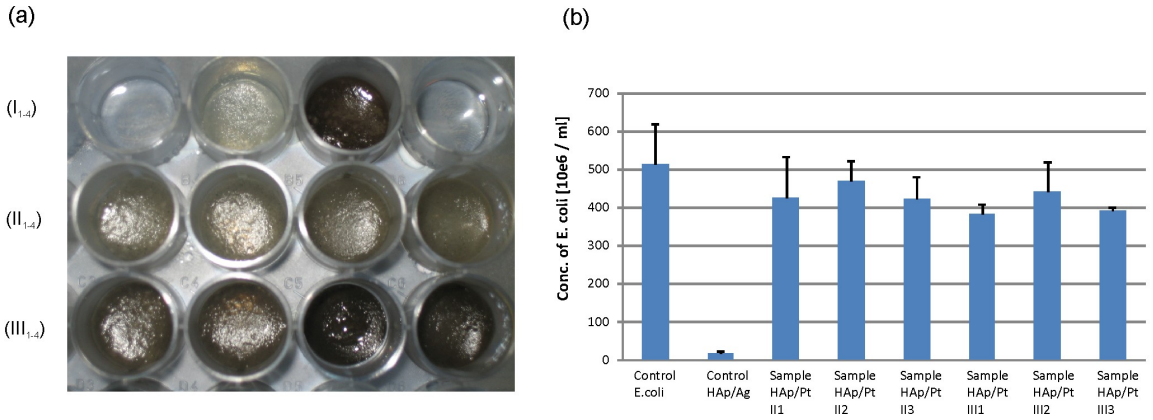

Figure 60: *E. coli irradiated by visible light: (a) photographs of- bacteria in agar (I_{1-2}) and HAp/Ag (I_{3-4}) as controls, bacteria with HAp/Pt (H_2PtC_{l6}) (II_{1-4}) and bacteria with HAp/Pt ($C_{10}H_{14}O_4Pt$) (III_{1-4}); (b) results of antibacterial test performed on mentioned materials.*

4.2.3 Antibacterial activity of hydroxyapatite/gold composites

Another approach used for formation of antibacterial agent based on HAp/metal-based composite contained Au nanoparticles. Activation of gold within HAp/Au composite for antibacterial activity was performed by attachment of different natural- and synthetic-sourced molecules onto the surface of its nanosized particles. In this case affinity of gold for interaction and formation of covalent bonds with thiols and amines was used. This approach showed significant success in increase of activity of some antibiotics (such as vancomycin) and it has been shown that their activity could be increased up to 40% when they were delivered attached onto Au nano-carriers. In this case selected functionalizations were not antibacterial agents but they contained groups able to provide attachment onto gold on one side and attachment and transport through the membrane of bacteria on other side. It was expected that used surface functionalization will be successful in achievement of antibacterial activity of so formed materials.

4.2.3.1 Disk diffusion test for antibacterial activity of HAp/Au composites

HAp/Au composites formed of apatite plates with Au nanoparticles attached on their surface with amino acids and synthetic amines and/or thiols bonded to the surface of Au particles were investigated for antibacterial activity starting from disk diffusion method. Disks containing 10% of functionalized Au component were aged overnight at 37°C with two types of bacteria- *E. coli* and *S. aureus* grown in agar medium. Parallel tests were performed on HAp without Au component processed with the same type of molecules used for functionalization of this component. All material used for functionalization of Au components were also tested for the action against bacteria under the same conditions and using the same methods which were applied for investigation of the composites.

First group of materials which were tested for antibacterial activity using disk diffusion test belonged to materials with amino acids (Figure 61). *E. coli* and *S. aureus* were applied for testing of HAp/Au composites functionalized by amino acids (Figure 61a_1, b_1), HAp processed with amino acids (Figure 61a_2, b_2) and pure amino acids used for functionalization (Figure 61a_3, b_3).

According to the obtained results it has been observed that all composites containing Au functionalized by amino acids- HAp/Au/glycine (Figure 61a_{11}, b_{11}), HAp/Au/arginine (Figure 61a_{12}, b_{12}) and HAp/Au/histidine (Figure 61a_{13}, b_{13}) confirmed ability for antibacterial action against tested bacteria since in all of these cases formation of zones of inhibition of bacterial growth around disks was detected. Another important thing which was observed concerned appearance of red coloration which was gradually widespread around disk. Detected red colour within zone of inhibition confirmed ability of Au nanoparticles to diffuse in agar and to participate in the process of suppression of the bacterial growth.

Importance of Au component in reaching of antibacterial activity of the composites was confirmed by the investigation of HAp/amino acids systems for action against *E. coli* and *S.aureus* (Figure 61a_2, b_2). In the case of all three systems- HAp/glycine (Figure 61a_{21}, b_{21}), HAp/arginine (Figure 61a_{22}, b_{22}), and HAp/histidine (Figure 61a_{23}, b_{23}) tested showed absence of the zone of inhibition of bacteria around disks which confirmed their inability for antibacterial action.

Investigation of pure amino acids showed the same trends for both type of bacteria (Figure 61a_3, b_3). Glycine, arginine and histidine were compacted into disks containing 100% of amino acids which were tested for the activity against bacteria. After aging in agar media, disks were completely dissolved and the whole quantity of amino acids diffused in the surrounding area. However, in spite of a very high concentration of tested substances, they were able to induce very small zones of inhibition of bacterial growth. In

the case of *E. coli* diameters of formed zones decreased starting from glycine (Figure 61a$_{31}$), over arginine (Figure 61a$_{32}$), to histidine (Figure 61a$_{33}$), while in the case of *S. aureus* glycine (Figure 61b$_{31}$), and arginine (Figure 61b$_{32}$), showed zone of inhibition while for histidine (Figure 61b$_{33}$) it was not observed.

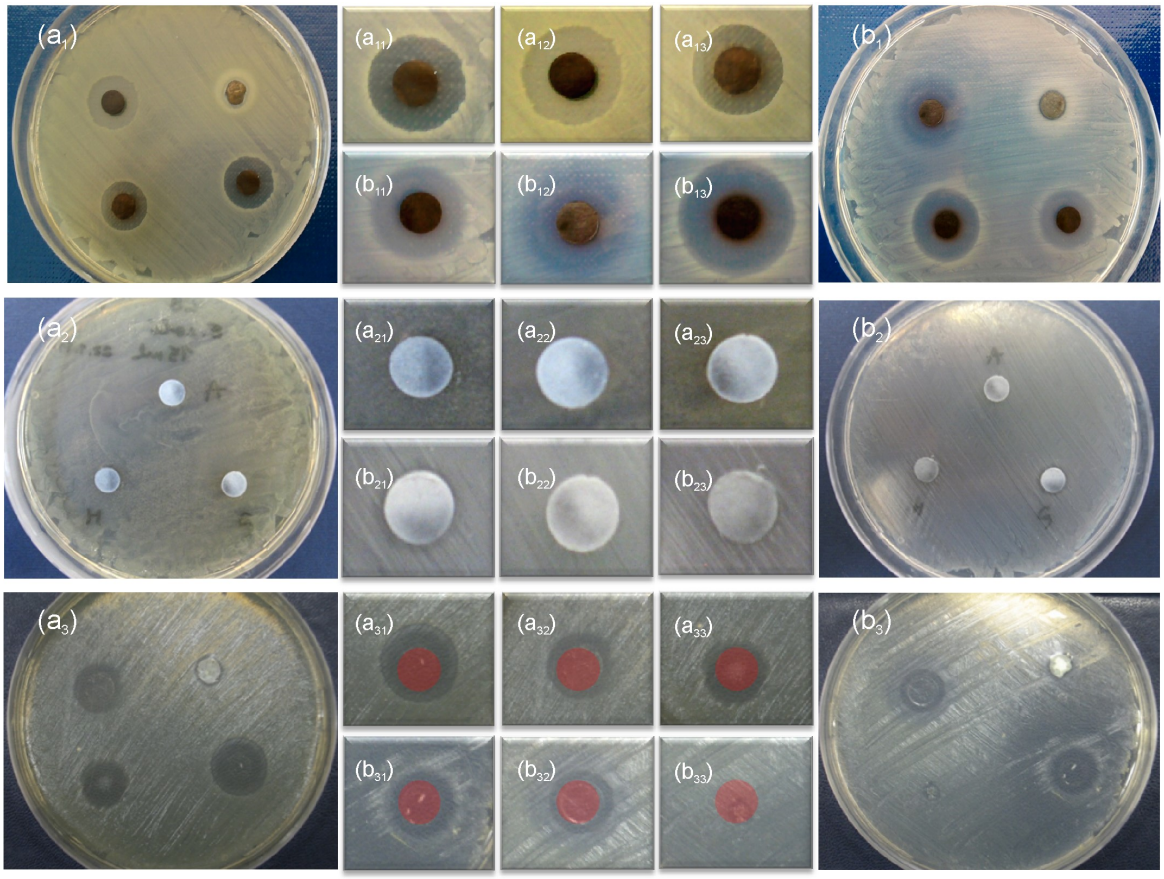

Figure 61: *Disk diffusion test for the growth of E. coli (a) and S. aureus (b) near the surface of: functionalized HAp/Au composite (1)(HAp/Au/glycine (11),HAp/Au/arginine (12) and HAp/Au/histidine (13)); HAp (2) processed by amino acids (HAp/glycine (21), HAp/arginine (22) and HAp/histidine) (23); and pure amino acids (3) (glycine (31), arginine (32) and histidine (33)) used for functionalization.*

Investigated group of materials containing amino acids showed that HAp/Au composite functionalized by these molecules is able to have activity against bacteria. Concerning inability of amino acids to have antibacterial activity, inactivity of HAp processed with these amino acids for the action against bacteria, as well as inability for the formation of Au nanoparticles using amino acids without presence of HAp, antibacterial activity of composites with amino acids onto Au surface is assigned to the joint activity of all three components of developed material.

Zones of inhibition of bacterial growth induced by composites functionalized by amino acids were inoculated by phase contrast microscopy (Figure 62) and disk diffusion results were evaluated according to the Schmitz criteria (Schmitz, 1988). Absence of the inhibition of the growth of *E. coli* in the presence of pure HAp/Au without any functionalization and development of these zones for HAp/Au/glycine, HAp/Au/arginine and HAp/Au/histidine are presented in Figure 62a$_1$–a$_4$, respectively. In contrast to the growth of bacteria close to the surface of the disk made of pure HAp/Au, in the case of functionalized composites zones of inhibition were developed and they were clear. For

glycine- and histidine-containing composites zones were narrower and clear so they had zone-to-lysis index 2/5 while for the composite with arginine zone was wider and clear, its zone-to-lysis index is 3/5. According to Schmitz, all three composites are evaluated as "middle toxic" for tested bacteria. In the case of *S. aureus*, compare to the HAp/Au with bacteria grown to the edge of the disk, composites with glycine, arginine and histidine showed clear zones of inhibition of bacterial growth. Diameters of the zones increased form glycine over histidine to glycine. In all three cases zone-to-lysis index was 2/5 and composites were evaluated as "middle toxic".

Regardless to the performed evaluation, diameters of the zones of inhibition showed highest activity of HAp/Au/arginine compare to all other materials and for both types of tested bacteria.

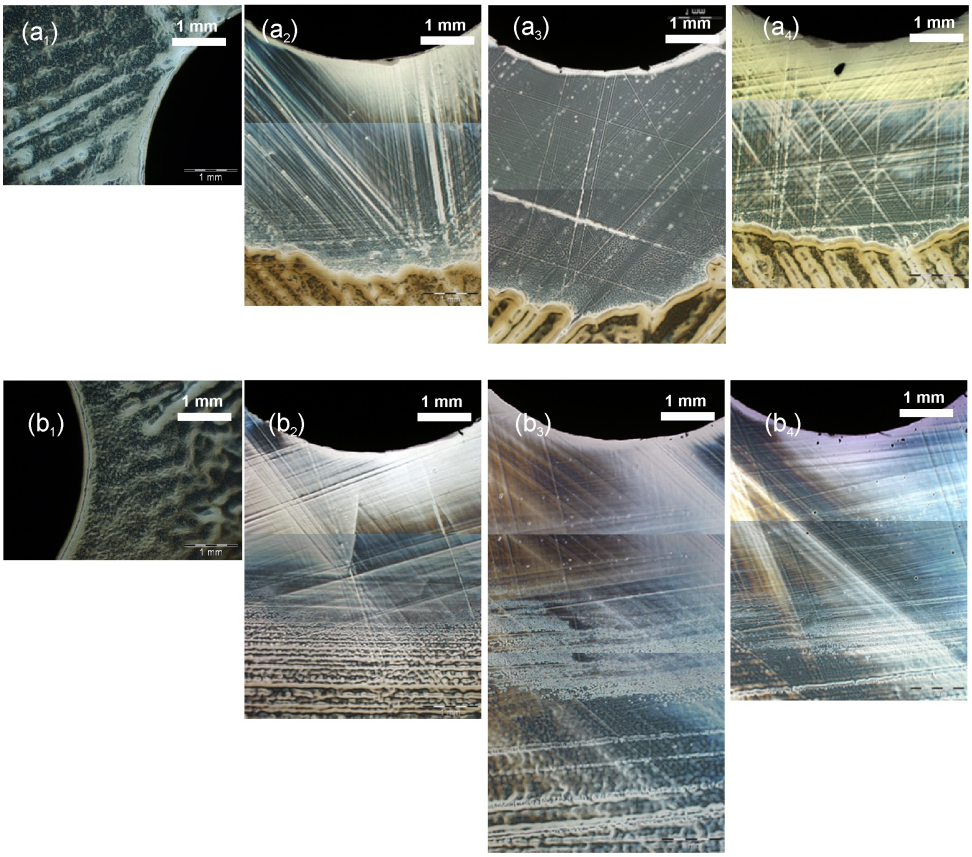

Figure 62: *Phase contrast images of zones of inhibition of the growth for E. coli around HAp/Au composite obtained by thermal reduction (without functionalization) (a_1), HAp/Au/glycine (a_2), HAp/Au/arginine (a_3) and HAp/Au/histidine (a_4) as well as for inhibition of the growth of S. aureus around pure HAp/Au (b_1) and the same composites containing glycine (b_2), arginine (b_3) and histidine (b_4) functionalizations.*

The same analysis was performed on the second group of materials which were functionalized using synthetic amines and/or thiols (Figure 63) and investigated for the action against *E. coli* (a) and *S. aureus* (b). Tested materials contained HAp/Au composites functionalized with amines and/or thiols (Figure 63a_1, b_1), HAp processed with amines and/or thiols (Figure 63a_2, b_2) as well as pure amines and/or thiols used for functionalization (Figure 63a_3, b_3).

Results showed that for both types of bacteria composite with thiourea did not have clear zone of inhibition and only the change of the density around disks was detected (Figure 63a_{11}, b_{11}). In all other cases when 5(bromo-pyridine)-2-thiol (Figure 63a_{12}, b_{12}), aniline (Figure 63a_{13}, b_{13}) and 4(methylthio)-aniline (Figure 63a_{14}, b_{14}) were used for

functionalization of Au within HAp/Au composites, inhibition zones appeared.

In the case of HAp processed with the same type of amines and/or thiols used for composites after testing of activity against *E. coli* zone of inhibition has not appear for any of tested composites (Figure 63a_{21}–a_{24}). For *S. aureus* the same results were repeated (Figure 63b_{21}–b_{23}) except for HAp/5(bromo-pyridine)-2-thiol when zone of inhibition appeared (Figure 63b_{24}).

Synthetic organic molecules containing amines and thiols used for functionalizations of Au component within HAp/Au composites were also tested for antibacterial activity against *E. coli* and *S. aureus* (Figure 63a_3, b_3). In contrast to the very low activity within HAp/Au composite and inactivity in HAp, after dissolution and diffusion of a large quantity of material pure thiourea had ability to form zone of inhibition of the growth for both types of bacteria (Figure 63a_{31}, b_{31}). A similar situation occurred for 5(bromo-pyridine)-2-thiol (Figure 63a_{32}, b_{32}), while aniline and 4(methylthio)pyridine did not showed any activity against tested bacteria.

Similar to the amino acids, results of antibacterial activity of materials functionalized by amines and/or thiols showed that all three components- bioceramic carrier, metallic nanoparticles and organic surface functionalizations are important to reach this activity. Exception was 5(bromo-pyridine)-2-thiol which was able for antibacterial action in the case when Au component was absent. However this activity of HAp/5(bromo-pyridine)-2-thiol was about 50% lower compared to the composite with the same functionalization.

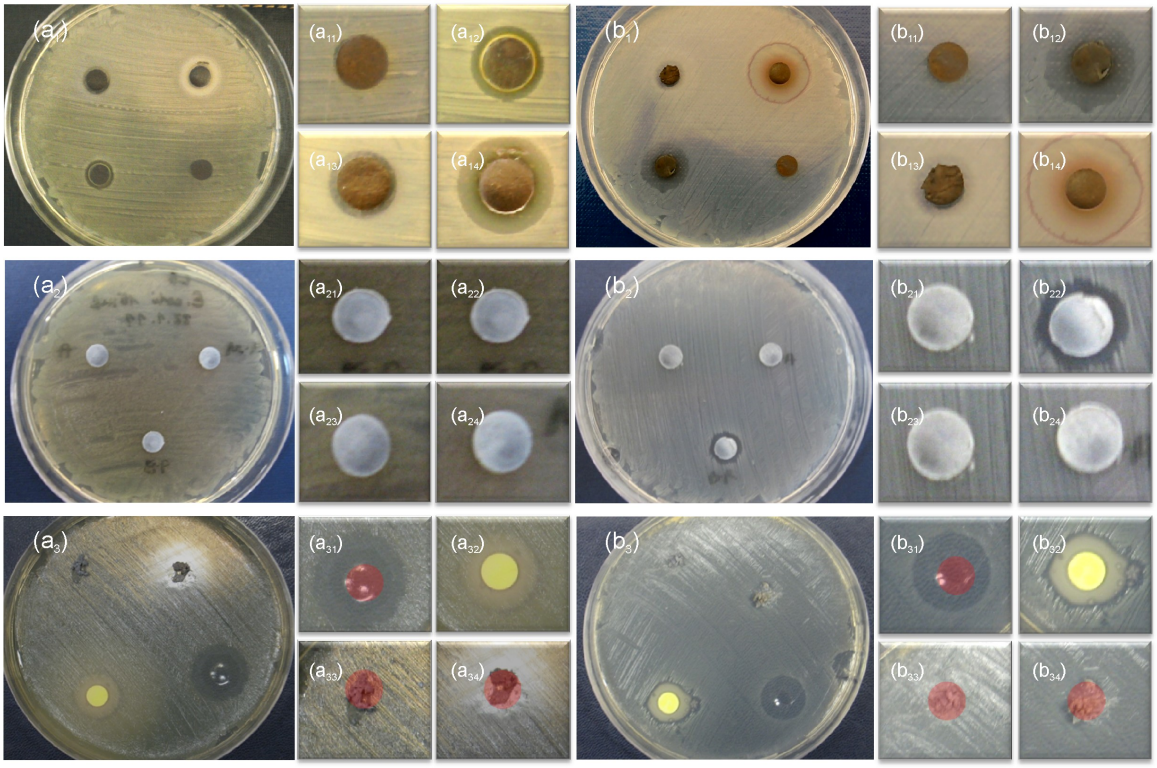

Figure 63: *Disk diffusion test for the growth of E. coli (a) and S. aureus (b) near the surface of: functionalized HAp/Au composite (1) (HAp/Au/thiourea (11), HAp/Au/5(bromo-piridine-2-thiol (12), HAp/Au/ aniline (13) and HAp/Au/4(methylthio)-aniline (14)); HAp (2) processed by amines/thiols (HAp/thiourea (21), HAp/5(bromo-piridine-2-thiol (22), HAp/aniline (23) and HAp/4(methylthio)-aniline (24)); and pure amines/thiols (3) (thiourea (31), 5(bromo-piridine-2-thiol (32), aniline (33)) and 4(methylthio)-pyridine (34) used for functionalization.*

Similar to the group of materials with amino acids the next step in investigation of the results of disk diffusion test of the group of materials with synthetic amines and/or thiols was inoculation using phase contrast microscopy. Method was used for analysis of developed zones of inhibition of bacterial growth around disks consisted of composites for both types of bacteria- *E. coli* (Figure 64a) and *S. aureus* (Figure 64b).

Inoculation of the regions around disks showed that similar to the HAp/Au without functionalization, HAp/Au with thiourea did not have any, or had very low influence to the growth of bacteria. According to the Schmitz, responding index of this material for *E. coli* is 0/0 while for *S. aureus* it is 0.5/0.5 since there is a slight change of the bacterial density around disk (Figure 64a_2, b_2). In both cases material can be classified as "non-toxic" for tested bacteria. For all other composites functionalized by 5(bromo-piridine-2-thiol (Figure 64a_3, b_3), aniline (Figure 64a_4, b_4) and 4(methylthio)aniline (Figure 64a_5, b_5), zones have been developed for both types of bacteria. While they were narrow for *E. coli*, for *S. aureus* they were wider but not clear along all the surface of the zone. For composites with these three types of surface functionalizations, response index was 2/3 for *E. coli* and 2/4 for *S. aureus* and they were classified into "middle toxic" group for tested bacteria.

Compare to the HAp/Au without any functionalization, in the case of all other materials obtained using chemical reduction when functionalization by reduction agents took place a distinct level of activation of Au component for the action against bacterial growth has been achieved. The most efficient activation has been reached by functionalization by naturally- sourced amino acids, especially arginine which showed high activity against both types of bacteria.

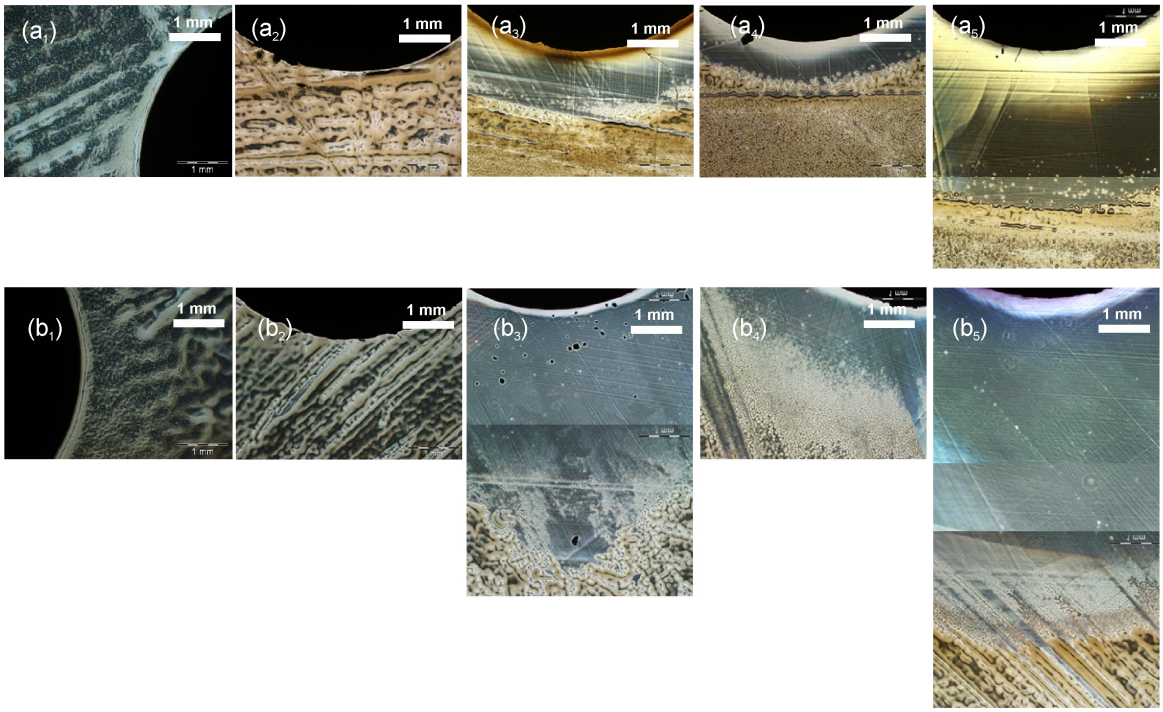

Figure 64: *Phase contrast images of the zone of inhibition of the growth of E. coli (a) and S. aureus (b) near the surface of HAp/Au composites obtained by thermal reduction (without functionalization) (1) and by chemical reduction and with functionalization by amines/thiols (HAp/Au/thiourea (2), HAp/Au/5(bromo-piridine-2-thiol (3), HAp/Au/ aniline (4) and HAp/Au/4(methylthio)-aniline (5)).*

4.2.3.2 Fluorescence labelling test for antibacterial activity of HAp/Au composites

The next step in investigation of the antibacterial activity of HAp/Au composites with different types of functionalizations attached onto the surface of Au nanoparticles was investigated using fluorescence labelling. For that purpose, SYTO 9 green fluorescence and PI red fluorescence dyes were applied. Similar to the investigation of HAp/Ag composites, this type of analysis of antibacterial activity provided ability for distinguishing of the live and dead bacteria after they have been labelled by fluorescence dyes.

This type of investigation was performed on HAp/Au composites functionalized by amino acids. They were selected among all other composites obtained by modification of the surface using other molecules since results of disk diffusion test revealed that functionalization of HAp/Au composites by this group of agents provides the strongest action against both types of tested bacteria. Disks made of HAp/Au composites with amino acids on the surface were aged on agar with bacteria during the period of 24 hours. After aging bacteria were labelled *in situ* and fluorescence microscopic method was used for detection and separation of dead and live bacteria based on their colour.

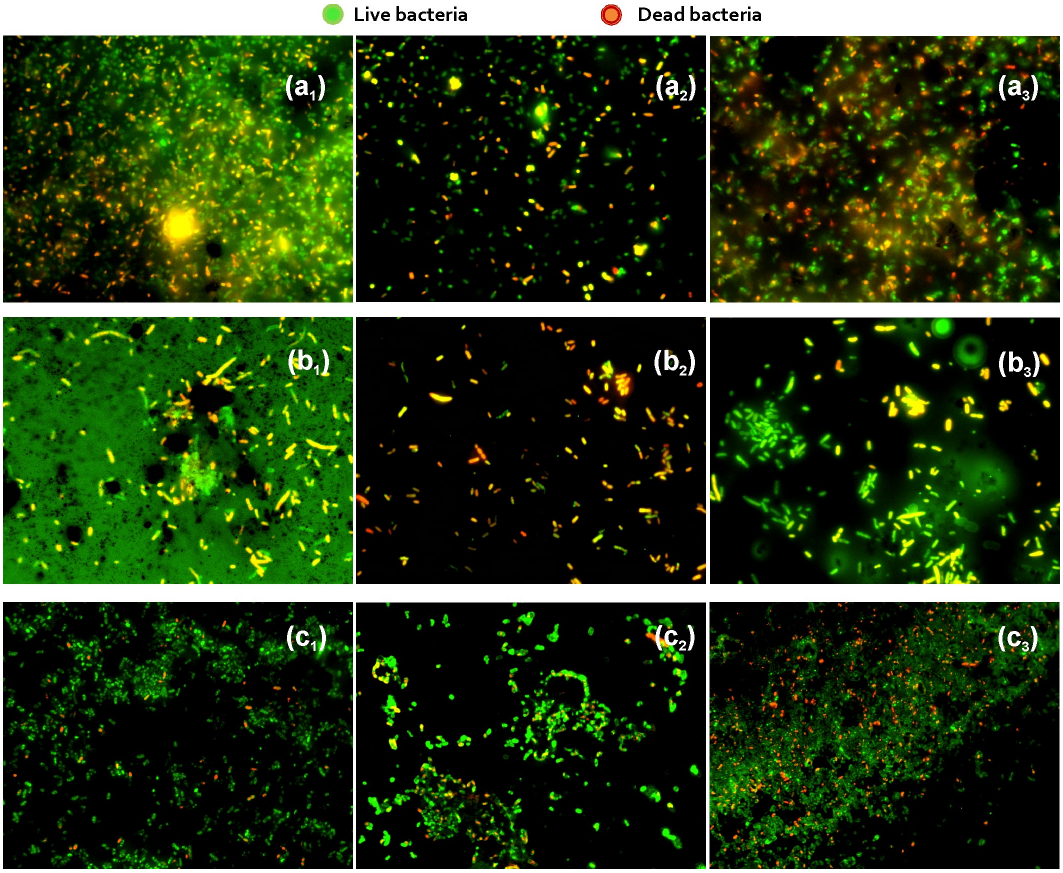

Figure 65: *E. coli fluorescence detection of dead (red) and live (green) bacteria for HAp/Au composites functionalized by glycine ($a_{1\text{-}3}$), arginine ($b_{1\text{-}3}$) and histidine ($c_{1\text{-}3}$).*

Investigation of antibacterial activity of HAp/Au with amino acid functionalization tested for activity against *E. coli* is summarized in Figure 65. Aging of the disks containing HAp/Au/glycine (Figure 65$a_{1–3}$), HAp/Au/arginine (Figure 65$b_{1–3}$) and HAp/Au/histidine (Figure 65$c_{1–3}$) with *E. coli* and labelling by fluorescence dyes revealed different regions with dead and live bacteria. It was observed that regions near and under

the surface of the disk contained decreased density of bacteria and significant areas with red coloration belonging to dead gram negative bacteria.

Investigation of the materials' interaction with *E. coli* as gram negative bacteria was followed by their investigation of their interactions with *S. aureus* as gram positive bacteria (Figure 66). It was observed that all three types of functionalizations in HAp/Au/glycine (Figure 66$a_{1–3}$), HAp/Au/arginine (Figure 66$b_{1–3}$) and HAp/Au/histidine (Figure 66$c_{1–3}$) are capable to provide large areas of dead (orange-labelled) bacteria near the surface of the disks as well as in the region below them. This was particularly observed in the case of composite functionalization using glycine and arginine. In all cases decrease of the density of bacteria was detected which indicated decrease in their growth near the disks and it was also observed that they were present in small groups rather than in larger colonies. Their growth into large colonies is typical for them in the case when there is no agent with antibacterial activity. This means that their presence into smaller groups is an indication of the presence and influence of agent able to induce some modification in their life cycle.

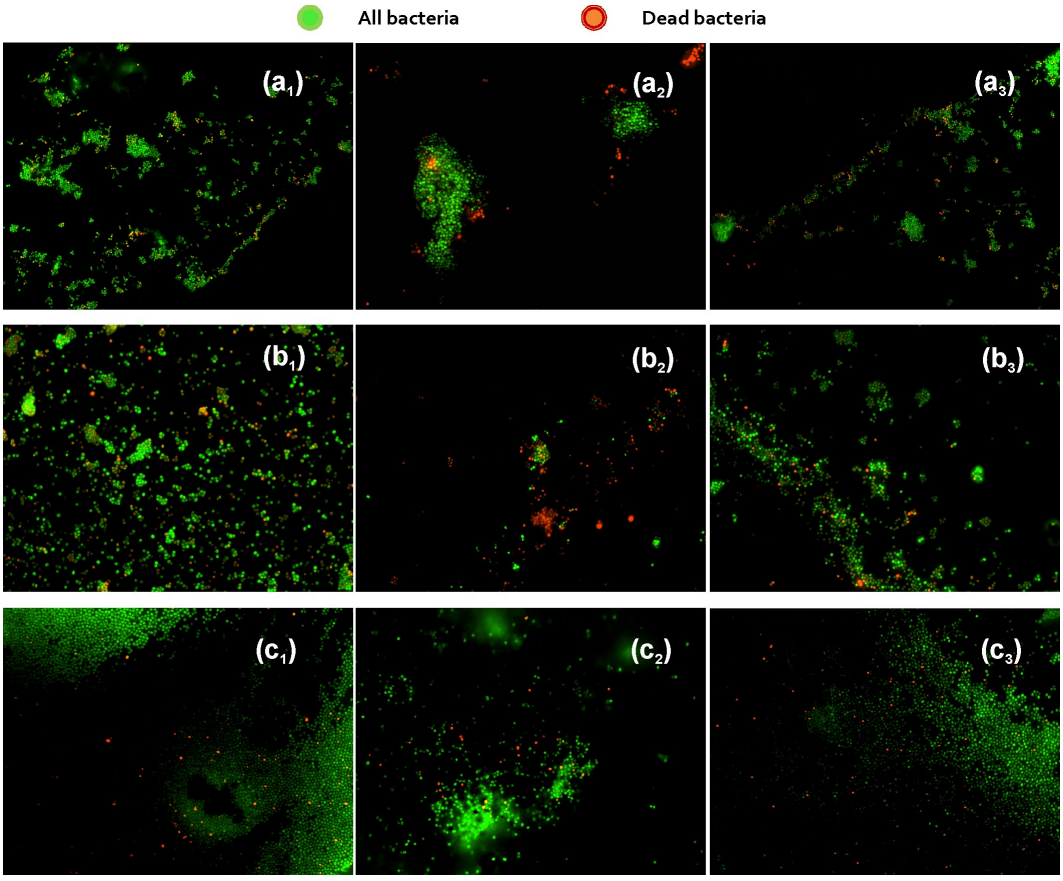

Figure 66: *S. aureus fluorescence detection of dead (red) and live (green) bacteria for HAp/Au composites functionalized by glycine (a_{1-3}), arginine (b_{1-3}) and histidine (c_{1-3}).*

4.2.3.3 Minimal growth-inhibition concentrations (MIC) and minimal bactericidal concentrations (MBC) of HAp/Au composites

Quantification of antibacterial effect of novel composites made of HAp/Au with functionalized surface was performed using methods for determination of minimal growth-inhibition and bactericidal concentrations. All powders were dispersed in growth media with bacteria and aged overnight at 37°C at different concentrations. Tests were performed for all materials functionalized using amino acids (glycine, arginine and histidine) and synthetic amines and/or thiols for *E. coli* and *S. aureus*.

An example of the influence of the change of bacterial growth as a consequence of the gradual increase of the concentration of powder within growth medium is illustrated for HAp/Au functionalized using 4-bromo-pyridine-2-thiol as synthetic amine and thiol. Bacteria used for testing of antibacterial effect of this material corresponded to *S. aureus*. Concentration of the powder was increased up to 6.0 mg/ml. It was observed that prevention of the growth of bacteria started with dispersion containing 0.5 mg/ml of material in agar medium and further increase of the concentration of the composite within agar prevented bacterial growth. The concentration of 0.5 mg/ml was minimal concentration of HAp/Au functionalized by 4-bromo-pyridine-2-thiol able to inhibit a growth of *S. aureus*.

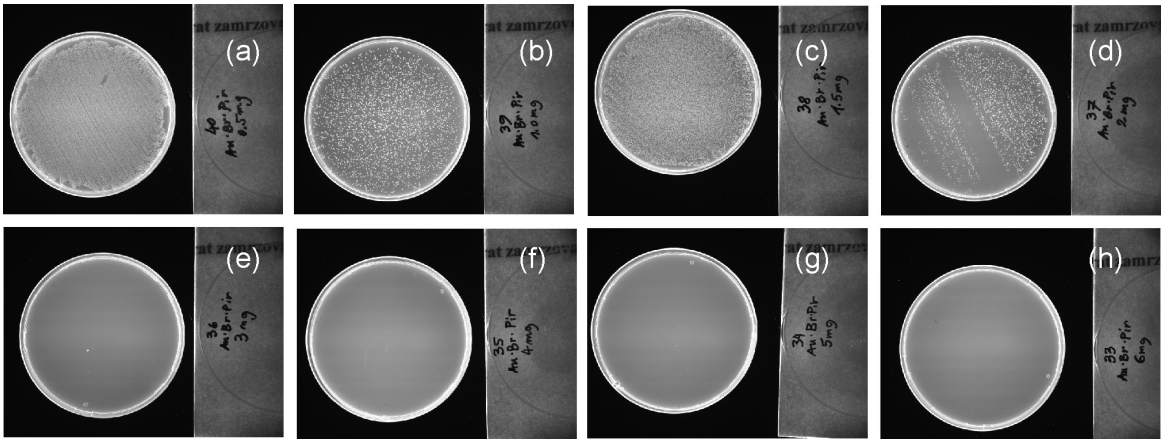

Figure 67: *Ability of different concentrations (0.5 mg/ml (a),1.0 mg/ml (b), 1.5 mg/ml (c), 2.0 mg/ml (d),3.0 mg/ml (e), 4.0 mg/ml (f), 5,0 mg/ml (g) and 6.0 mg/ml (h)) of HAp/Au/4-bromo-pyridine-2-thiol to prevent re-growth of S. aureus.*

In the next part of quantitative analysis of antibacterial action of HAp/Au with 4-bromo-pyridine-2-thiol concerned re-growing the bacteria that were inhibited during the first segment of investigation. It means that samples containing medium with bacteria from plates containing 0.5 mg/ml, 1.0 mg/ml, 1.5 mg/ml, 3.0 mg/ml, 4.0 mg/ml, 5.0 mg/ml and 6.0 mg/ml were transferred to the fresh agar medium and their growth was observed after the aging during additional 24 hours 37°C in (Figure 67). For 0.5 mg/ml dispersion of composite bacteria had spread confluent growth over the whole surface of the plate while concentrations of 1.0 and 1.5 resulted in colony growth. At concentration of 2 mg/ml, decrease of the growth of bacteria was observed and some areas were out of bacterial growth while other contained colonies. Samples containing concentrations of 3.0 mg/ml, 4.0 mg/ml, 5.0 mg/ml and 6.0 mg/ml material in agar prevented re-growth of bacteria. It means that concentration of 3 mg/ml was determined as minimal bactericidal concentration of this material for *S. aureus*.

The strongest influence to bacterial growth was detected for HAp/Au composites functionalized by amino acids. Obtained results together with the effects obtained for distinct concentrations of tested materials are summarized in Figure 68. In the first step materials were tested for interaction with *E. coli.* It was revealed that HAp/Au composite functionalized by glycine had the strongest effect to the inhibition of the growth of this type of Gram negative bacteria. According to the obtained results, concentration of 0.3 mg/ml was high enough to prevent growth of this type of bacteria while lower concentrations of 0.1 mg/ml and 0.2 mg/ml allowed their growth. Similar results were also obtained for HAp/Au composite functionalized by arginine. For this material concentration able to inhibit bacterial growth was slightly higher in comparison to functionalization by glycine and it was 0.4 mg/ml. HAp/Au functionalized by histidine had the highest concentration able to inhibit bacterial growth among all tested composites functionalized with amino acids and for this material it was 0.6 mg/ml. This value is still very good since it corresponds to the concentration of HAp/Ag to inhibit growth of this type of bacteria. It means that glycine and arginine were one and a half and two times more efficient for inhibition of the growth of *E. coli* compare to the same composite containing silver. Results were in a very good correlation with disk diffusion tests.

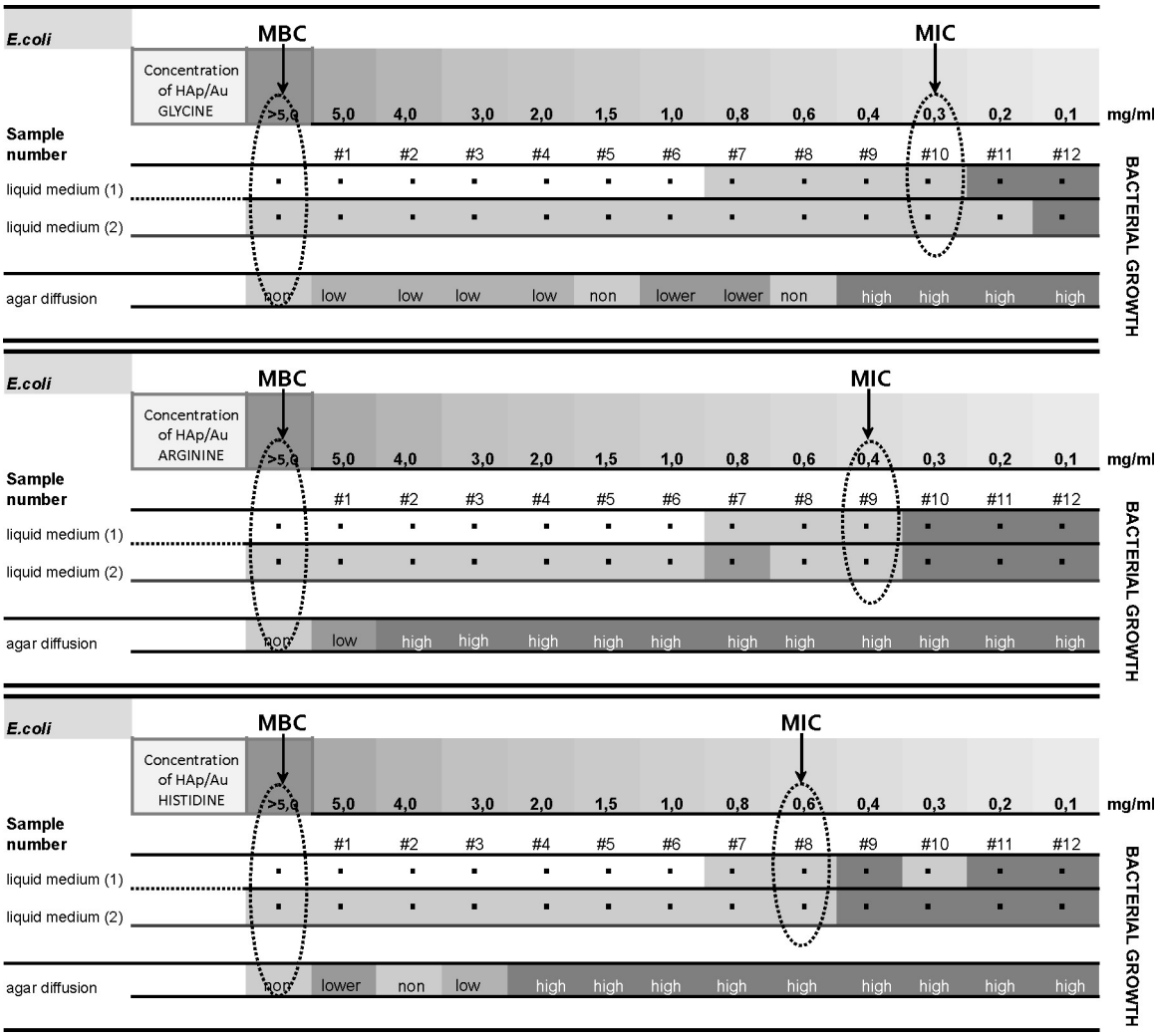

Figure 68: *Minimal concentrations of HAp/Au composite functionalized by glycine, arginine and histidine able to induce growth inhibition (MIC) and bactericidal effect (MBC) to E. coli.*

When the same materials were tested for re-growth in order to determine bactericidal concentrations, it was determined that for all three types of functionalizations concentrations higher than 5 mg/ml were required to prevent this effect. It means that these materials have pronounced bacteriostatic effect while their bactericidal ability is lower.

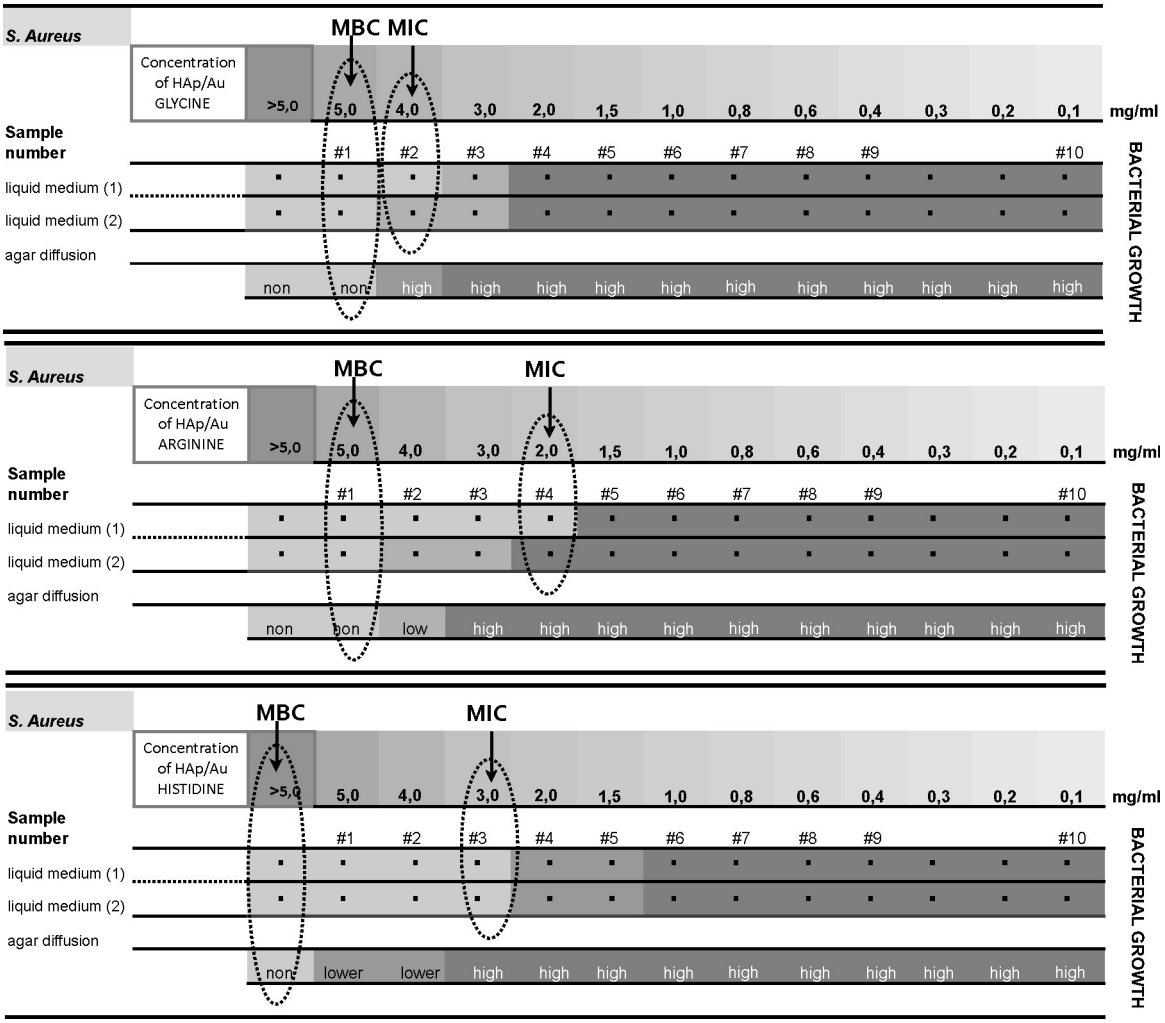

Figure 69: *Minimal concentrations of HAp/Au composite functionalized by glycine arginine and histidine able to induce growth inhibition (MIC) and bactericidal effect (MBC) to S. aureus.*

In the next step, materials were tested for quantitative antibacterial effect to *S. aureus* using the same MIC and MBC tests. Influence of gradual increase of the concentration of materials functionalized by different types of amino acids to the growth of this type of bacteria is presented in Figure 69. In this case concentration of materials needed for inhibition of bacterial growth were higher since this type of bacteria belongs to the group of Gram positive bacteria which are more resistive sort. In the case of HAp/Au functionalized by glycine MIC concentration was 4 mg/ml and it was close to the bactericidal concentration which prevented bacterial re-growth and had a value of 5.0 mg/ml. For HAp/Au composite functionalized using arginine MIC concentration was significantly lower and it was 2 mg/ml while its MBC concentration was 5.0 mg/ml. In the case of HAp/Au composite functionalized with histidine MIC was in the middle of values obtained for the last two materials and for this material inhibition of bacterial growth was achieved by concentration of 3 mg/ml while MBC concentration was higher than 5 mg/ml.

Obtained results revealed that material functionalized by arginine was the most efficient in inhibition of this type of bacteria. It was followed by histidine while glycine had the lowest efficacy. The same order of efficacy against *S. aureus* was obtained during disk diffusion test. MIC and MBC tests of these materials showed that higher concentrations are required to inhibit growth of *S. aureus* compare to HAp/Ag composite. Tests also showed that similar to their effect on Gram negative bacteria, materials had bacteriostatic effect as dominant influence on Gram positive bacteria while their ability for bactericide influence was lower.

Concerning the ability for highly efficient influence to the growth of both types of bacteria it was also observed that among all investigated materials HAp/Au composite functionalized by arginine was the most efficient one.

4.2.3.4 Photocatalytic ability of HAp/Au composite

According to the above presented results functionalized HAp/Au composites were able for intensive antibacterial activity. The strongest action against both types of tested bacteria was reached for functionalization using arginine. For the purpose of determination of the mechanism of its action, this material was tested for ability to induce photocatalytic activity.

Photocatalytic tests applied for analysis of HAp/Au were performed by two reactions-methylene blue and isopropanol degradation. Tests were performed in gas and liquid phase. Liquid phase photocatalytic activity was tested in the same manner as for the HAp/Pt composites. It means that investigation of ability for methylene-blue degradation in liquid phase has been employed (Figure 70a). Additional method used for this material was gas-phase activity for decomposition of isopropanol vapour (Figure 70b). In the case of liquid phase, results showed very slow kinetics of dye degradation with the constant of reaction rate at $3.9 \cdot 10^{-4}$ min^{-1} which was more than ten times lower than for the HAp/Pt composite. The same was obtained for gas phase investigations. Accordingly, results showed that both tests of photocatalytic activity of HAp/Au were negative and material failed in ability to be excited by VIS photons which will allow it formation of reactive radicals.

Based on these results, in contrast to HAp/Ag and HAp/Pt which have possibility for formation of reactive radicals as a consequence of light-activation, HAp/Au did not have this property which means that its antibacterial action is driven by some other mechanism.

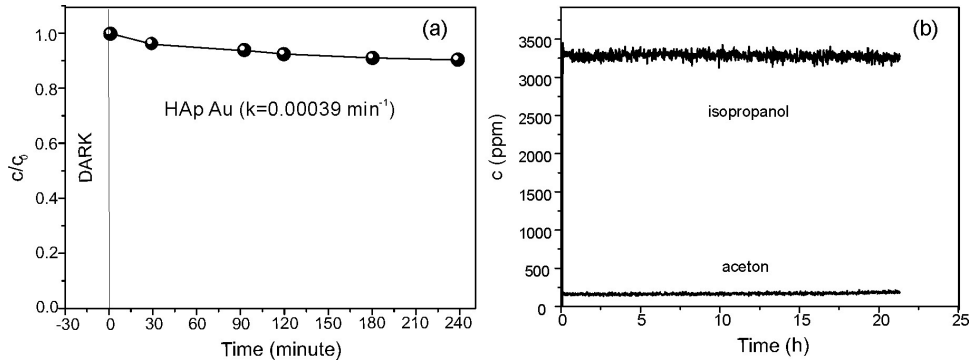

Figure 70: *Photocatalytic activity of HAp/Au/arginine irradiated by visible light investigated by dye degradation (a) and decomposition of isopropanol gas phase (b).*

4.2.3.5 Morphological changes in bacteria induced by HAp/Au composites

Concerning the highest efficacy of antibacterial effect which was obtained using HAp/Au composite functionalized by arginine it was selected for investigation of the influence on morphological properties of bacteria. Changes in the morphology induced by the action of this antibacterial material were investigated in the case of *E. coli* and *S. aureus*.

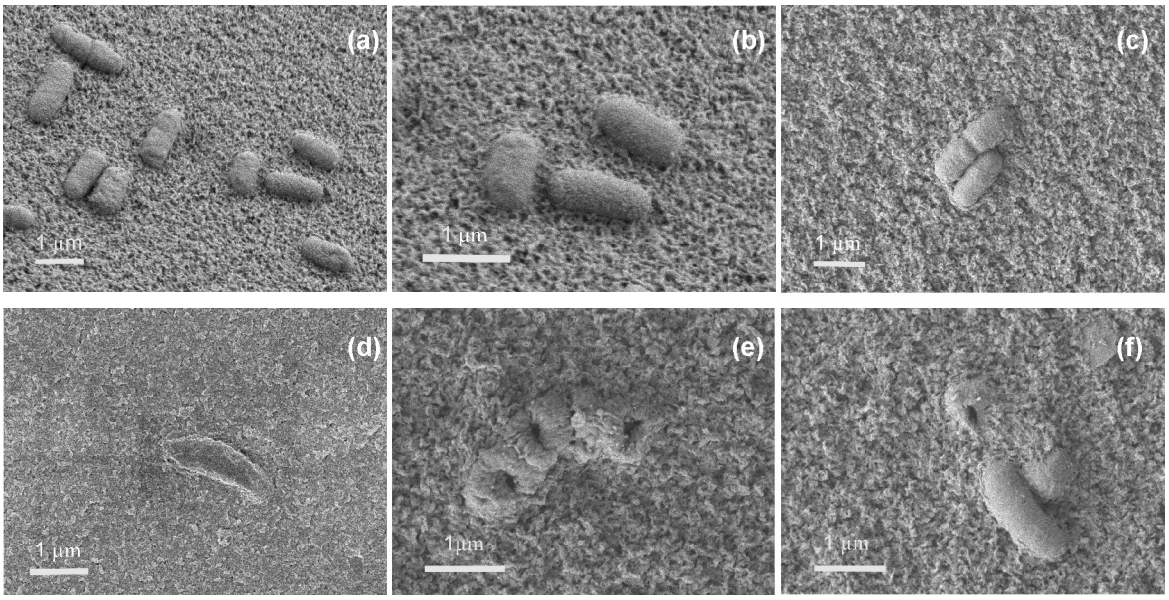

Figure 71: *Morphological properties of E. coli in agar without presence of composite (a, b, c) and in agar with the presence of HAp/Au composite functionalized with arginine (d, e, f).*

Morphology of the surface of *E. coli* obtained after its aging with HAp/Au/arginine in comparison to the morphology of the surface of bacteria grown without presence of material is presented in Figure 71. For the case when material was not present, healthy bacteria had rod-like shape and they were around 1 µm long (Figure 71a, b). The only morphological changes detected in these bacteria corresponded to the normal segments of their life cycle which include division and growth which were detected based on the appearance of the distinctive narrowing along the cell division plane (Figure 71c). For the case when bacteria were aged with material, changes of morphology indicated cellular disruption due to the contribution of antibacterial agent. Shape of bacteria was changed and they were wrapped into coils, shrinked and with folded surface of the outer membrane (Figure 71d, e, f). Obtained morphological changes did not reveal any visible mechanical perforations of the membrane, like those observed in the case of HAp/Ag material. In this case observed changes indicated losing the integrity of the membrane most probably because of the structural changes in the peptidoglycan layer.

The last was confirmed after observations of the bacteria sections using transmission electron microscopy. In the case of healthy bacteria rod-like bacteria contained compact and smooth inner and outer membrane layers (Figure 72a, b). In the case of bacteria which were affected by HAp/Au/arginine composite, their cells had disrupted integrity of the outer membrane. Instead of the compact smooth surface it turned into wrinkled layer with clearly observable sphere-like nanosized particles presented on the surface as well as inside the cell (Figure 72c, d).

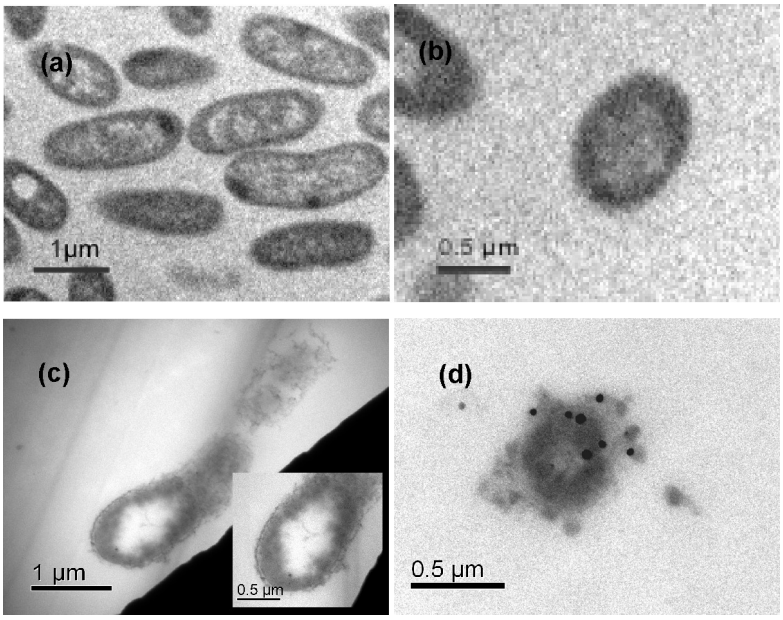

Figure 72: *TEM images of E. coli in agar without presence of composite (a, b) and in agar with the presence of HAp/Au composite functionalized with arginine (c, d).*

Morphological changes induced by HAp/Au composite with the surface functionalized by arginine were also tested for *S. aureus* as a representative of gram positive bacteria. According to the analysis of the surface healthy bacteria were sphere-like in shape, with diameters between 200 and 500 nm and with the smooth surface (Figure 73a, b, c). In comparison with them, in the case of bacteria aged with material shape and size were very similar and without obvious structural or integrity changes. In the case of these bacteria affected by HAp/Au/arginine it was interesting to note existence of a network around bacteria. Its development could be assigned to the protein, mucosa layer excreted by bacteria or to the disrupted outer peptidoglycan layer (Figure 73d, e, f). Changes were very similar to HAp/Ag, however without presence of any mechanical disruptions at the bacterial membrane.

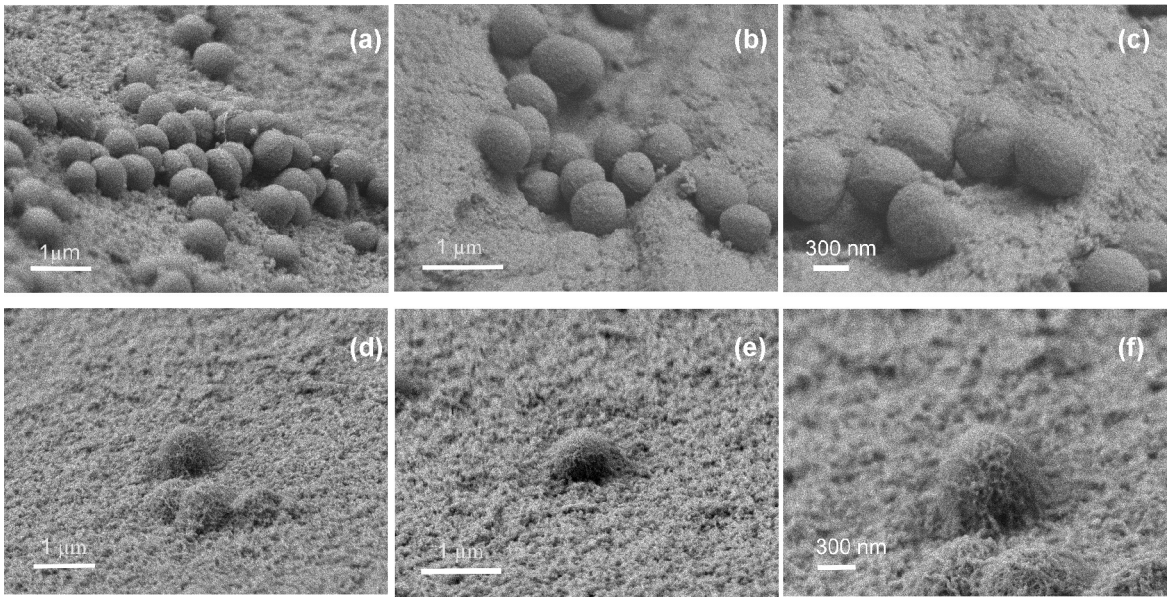

Figure 73: *SEM images of S. aureus in agar without presence of composite (a, b, c) and in agar with the presence of HAp/Au composite functionalized with arginine (d, e, f).*

Observation of the sections of bacteria using TEM revealed compact structure made of smooth surface membrane surrounding cytoplasm (Figure 74a). Detected bacteria were also in the phase of division and a pale ring at the middle corresponds to the protein division (Figure 74b). In the case of bacteria which were influenced by HAp/Au/arginine composite cellular wall was significantly disrupted and its integrity was damaged by the material. Contact among the outer layer of the bacterial wall and plate-like HApAu composite particles was observed together with the Au nanospheres detected inside bacteria (Figure 74c). In some cases bacteria completely lost their typical sphere-like shape and in that case very high concentration of Au nanoparticles was detected inside them (Figure 74d).

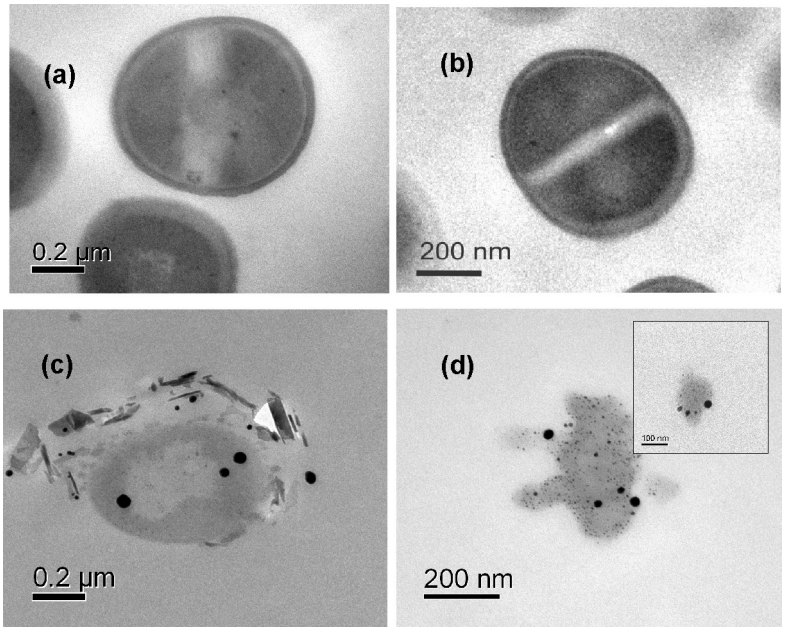

Figure 74: *TEM images of S. aureus in agar without presence of composite (a, b) and in agar with the presence of HAp/Au composite functionalized with arginine (c, d).*

4.3 Investigations of *in vitro* release of metal-ions and compatibility of hydroxyapatite/metal composites with human cells

During development of a novel material environmental friendly approach is a very important issue. It means that complete optimization of its design is achieved only in the case when its abilities meet both, performance and ecological standards.

Development of a material with potential application in the field of biomedicine is associated with required investigation of its biocompatibility as a highly important issue. This type of investigation concerns long lasting procedure which has a large number of levels including *in vitro* investigations performed on cells, *in vivo* investigations on animals and preclinical and clinical investigation on humans. These steps are interconnected, with alternating order and they exclude each other. It means that material with toxic influence to cells will not be concerned for investigations in animals or for further tests in humans which explains importance of the first step related to investigation of compatibility of material with cells.

4.3.1 *In vitro* release of metal-ions from hydroxyapatite/metal composites

Materials which had ability for satisfied activity against bacteria were further on selected for *in vitro* investigations of possible interactions with living surroundings. For these type of analysis following materials were selected: (i) HAp composite with silver as a material which contain metallic component with natural ability for antibacterial action and ability for strong toxic influence and (ii) HAp composite with gold functionalized by arginine as a material with stronger antibacterial activity compare to all so far developed materials as well as a material build upon natural components.

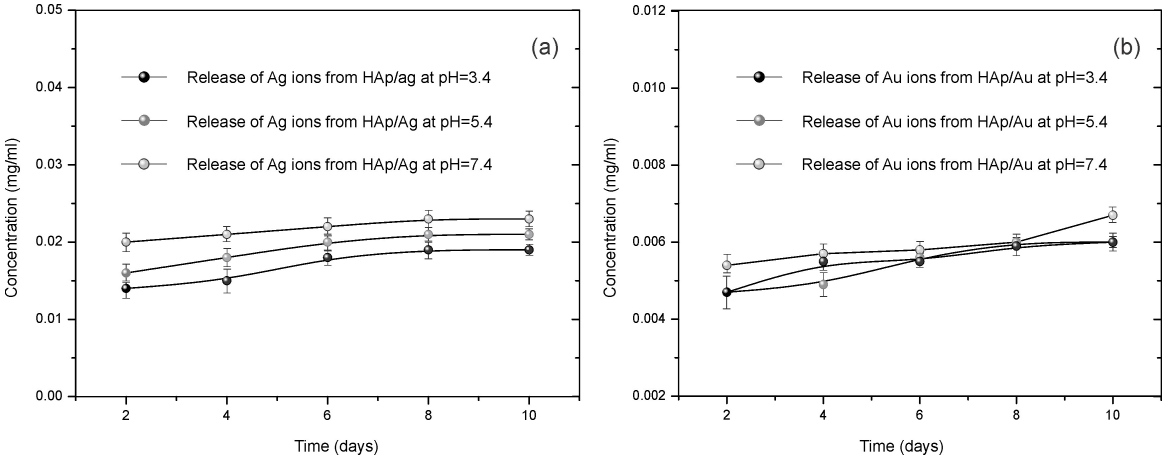

Figure 75: *In vitro release of Ag- and Au- ions from HAp/Ag (a) and HAp/Au/arginine (b) composites after aging in media with different acidity during the time interval of ten days.*

Prediction of the possible interactions of these materials with environment is investigated upon their ability to release metallic ions. These abilities of HAp/Ag and HAp/Au/arginine composites were tested in simulated physiological conditions which were ensured using PBS buffer with the concentration of salts equal to their concentration

in blood plasma. It was used as ion-release liquid medium. All samples were kept at 37°C in shaking water bath to simulate dynamic conditions present *in vivo*. Besides physiological pH which is 7.4, media with additional two pH values were tested. These media were able to provide slightly acidic and strongly acidic environments. Materials were kept under these conditions during the period of ten days. Concentrations of ions released from these materials were investigated from the media using ICP analysis and results are summarized in Figure 75. It should be noticed that graphs presented in Figure 75 a and b have different scales of y-axes.

In the case of HAp/Ag composite the initially-released concentration of Ag-ions was highest for the medium at pH=7.4 and it was decreased with decrease of pH (Figure 75a). Besides, it was observed that for medium with pH=7.4 concentration which was released in the beginning was kept almost constant during the time while at acidic environment it had increasing trend with the time of aging in this type of medium. The concentrations of released Ag-ions were in the range between 15μg/ml and 25μg/ml.

For HAp/Au composite with arginine as surface functionalization situation was completely different (Figure 75b). In this case for all three media with three different acidities, initially released concentrations of Au-ions were almost identical and abilities for release of Au-ions with the time were very low and almost identical for all three cases. It means that increase of the acidity did not have significant influence to the process of ion-release from these samples. The concentrations of released Au-ions were in the range between 4μg/ml and 7μg/ml which is about four times lower compare to composite with silver.

Along with investigation of the ability for release of metallic ions from HAp/Ag and HAp/Au composites, phase composition of remained powders was also analyzed. This type of analysis was performed using XRD method and resulted diffractograms with assigned phases are summarized in Figure 76.

Investigation of phase composition obtained in the case of powders of HAp/Ag kept in media with different pH values revealed ability of media to change material (Figure 76a_1, b_1, c_1). In all three cases when media had different pH values, together with the phases corresponding to the structures of HAp, cubic and hexagonal Ag (which were also present in starting material) a phase corresponding to the structure of silver-chloride (AgCl) was identified. It means that after release of Ag-ions within these media there were conditions for their precipitation and formation a novel phase with unknown characteristics. It means that, due to the chemical reactivity of silver, material showed instability in simulated physiological condition which can be potentially dangerous for its biomedical application. An AgCl is known as highly insoluble salt of silver ($K_{sp}=1.6\cdot10^{-10}$). Its precipitation under physiological conditions has potential to induce accumulation of silver in organism and to induce its toxicity.

The same principle was used for investigation of HAp/Au composite with arginine functionalization. In this case identified phases corresponded to HAp and Au structures and were the same as for the starting material (Figure 76a_2, b_2, c_2). Formation of any additional phase containing gold was not detected,, which means that under all three conditions material was stable. This stability can be assign to low chemical reactivity of gold. However, it should be taken into considerations that one additional phase was formed as a consequence of the presence of material and it was sodium-chloride (NaCl). This salt has very good solubility in water. However presence of HAp/Au influenced its saturation and there is a possibility that it had a nucleating role in the process of precipitation of this salt.

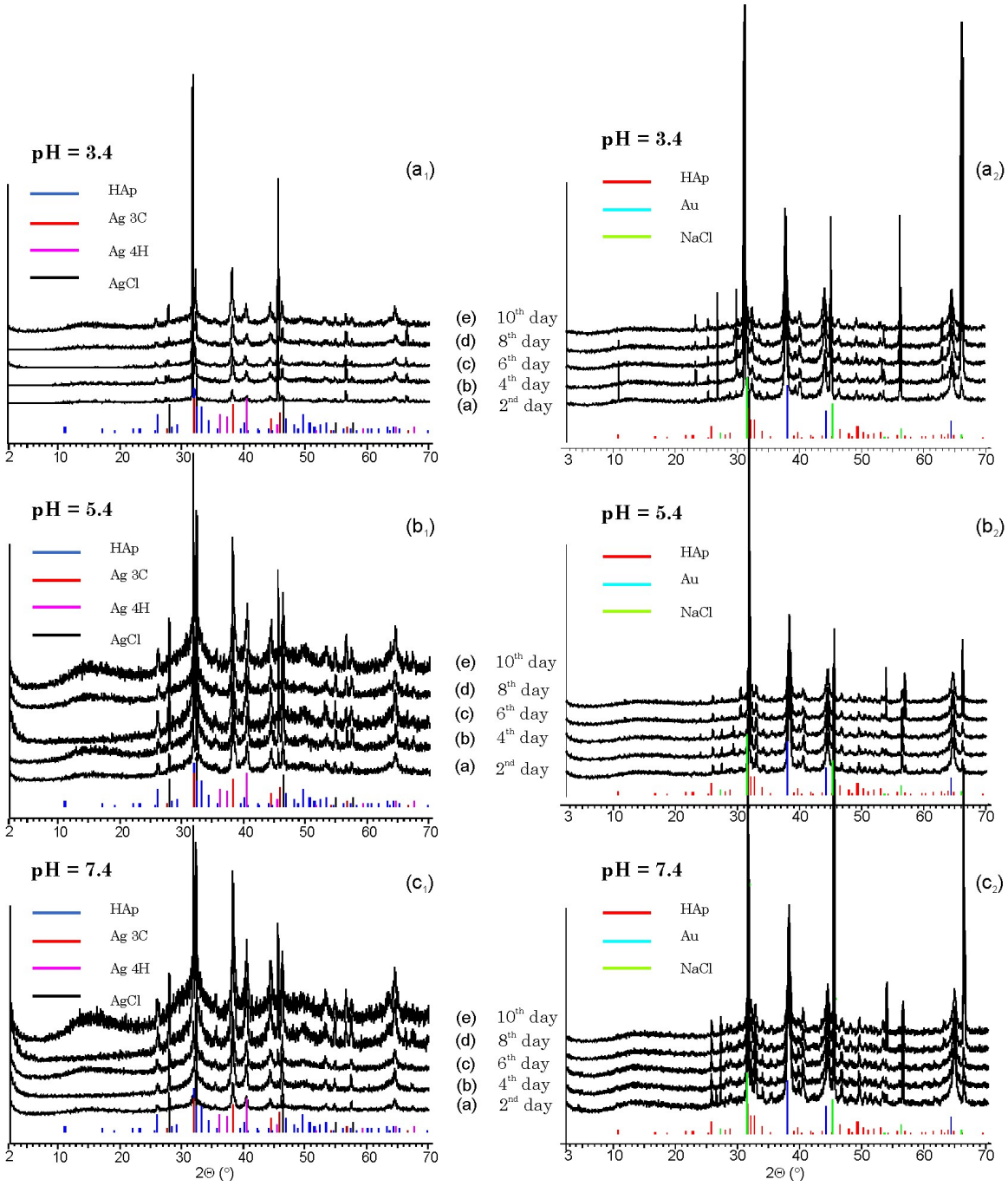

Figure 76: *Phase composition obtained after aging of HAp/Ag (1) and HAp/Au/arginine (2) composites in media with pH value 3.4 (a), 5.4 (b) and 7.4 (c) during the time interval of ten days.*

4.3.1.1 Quantification of cytocompatibility of hydroxyapatite/metal composites

In the last segment of investigation of developed apatite/metallic composites with ability for intensive antibacterial activity were tested for toxic effect. Toxicity of these materials was tested *in vitro* and for that purpose two types of human cells were used. First group of tested cells were human osteosarcoma cells, bone cells modified with cancer, and the second group belonged to human foetal lung fibroblasts. Cells were exposed to HAp/Ag composite which contain silver as known toxic agent and to newly developed HAp/Au

composites with a surface functionalized by amino acids. In the case of the composites with gold, formed composites contained natural building blocks: HAp as a bioactive ceramics able to stimulate growth of bone tissue, Au as inert material and amino acids which are essential for every living organism. However activation of these materials by surface functionalization provided development of a novel property related to their activity against bacteria. It consequently implied a new question regarding their toxicity.

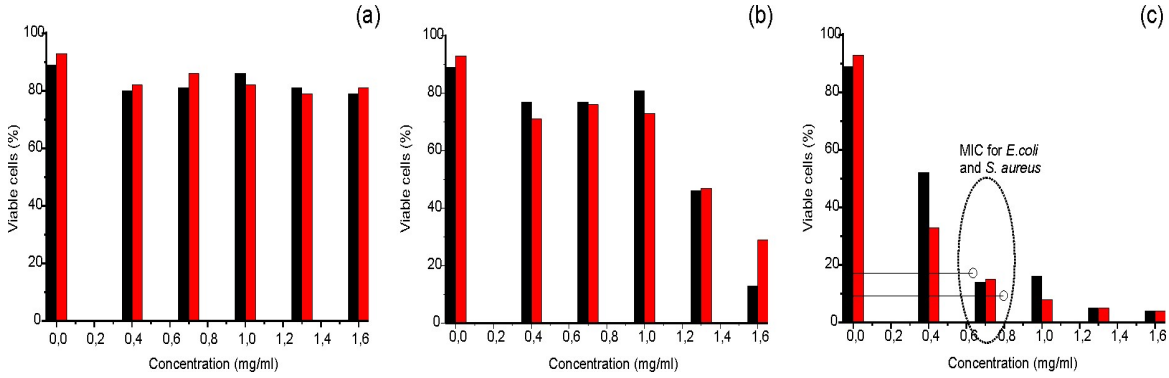

Figure 77: *Cytotoxicity of HAp/Ag with 1% (a), 5% (b) and 10% (c) of silver-content for U-2 OS- human osteosarcoma cells (red and black bars- the same measurements repeated in twice).*

During investigations of the toxicity of HAp/Ag to human osteosarcoma cells materials with different contents of silver were analyzed for toxic respond. In this case composites with 1%, 5% and 10% of silver were tested and all of them were compared to the pure HAp made by the same synthesis route. Interaction between cells and composites were quantitatively presented as a percentage of survived (viable) cells obtained after overnight exposure to the gradually increased concentrations of composites. Obtained results are summarized in Figure 77 for HAp/Ag with 1% (a), HAp/Ag with 5% (b) and HAp/Ag with 10% (c) of silver component.

It was observed that material with the lowest content of silver (HAp/Ag 1%) (which was tested in five different concentrations from the range between 0.4-1.6 mg/ml) had very low toxicity and showed almost the same compatibility with cells as it was obtained for pure HAp (Figure 77a). In this case around 80% of tested cells were viable.

Further investigations were performed on material with higher content of silver (HAp/Ag 5%) and it was tested for the toxicity of the same concentrations selected from the range between 0.4 and 1.6 mg/ml. Results showed high percentage of survival cells for lower and significant drop of their number for higher concentrations of this material (Figure 77b).

In the last step, material with the highest concentration of silver was tested (HAp/Ag 10%). After investigation of the same concentrations as for the previous two cases this materials showed significant toxicity with a very low percentage of viable cells (Figure 77c).

Obtained results show concentration-dependence toxicity induced by HAp/Ag composite. However, in these groups of concentrations those which correspond to MIC and MBC concentrations, able to prevent bacterial growth and to have bactericidal impact on them, are applicable for antibacterial activity and have to be selected for toxicity assessment. In the case of HAp/Ag MIC concentrations able to inhibit growth of *E. coli* and *S. aureus* are marked on the viability graph and it can be observed that for these concentrations viability of U-2 OS cells is lower than 20% which is an indication of very high toxicity. The same tests were repeated for human lung foetal fibroblast cells. Obtained results were very similar showing intensive toxicity of MIC concentrations.

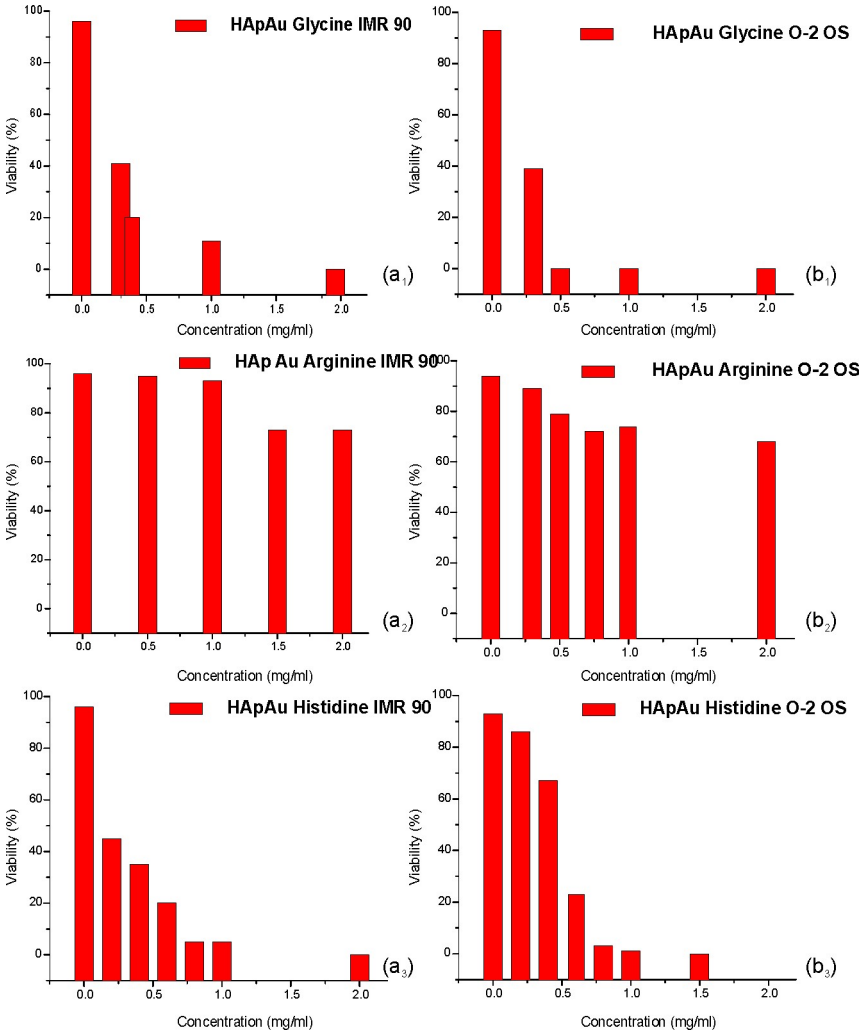

Figure 78: *Cytotoxicity of HAp/Au functionalized by glycine (1), arginine (2) and histidine (3) for MRC-90 human foetal lung fibroblasts (a) and U-2 OS- human osteosarcoma cells.*

The same method was used for investigation of toxicity of HAp/Au composites functionalized with amino acids (Figure 78). Materials with glycine (1), arginine (2) and histidine (3) functionalizations were tested for the influence on U-2 OS (a) and IMR-90 (b) cancer modified and healthy human cells. All investigated materials are tested for different concentrations within the range from 0-2.0 mg/ml including lower concentrations with smaller steps (up to 1 mg/ml) and higher concentration (2 mg/ml).

Unlike arginine functionalization, which showed very high compatibility with both cell types, in the case of glycine and histidine functionalizations, results of toxicity testing were opposite to the expectations. It means that apart from the selection of natural-sources building components these materials showed concentration-related toxicity. At low concentrations materials were non-toxic; however increase of concentration decreased a number of survived cells. Both materials have very low MIC concentrations for *E. coli* (0.3 and 0.4 mg/ml, respectively) and for these concentrations the percentage of survived cells is high. However, they have high MIC concentrations for *S. aureus* and for these concentrations they are toxic. These results imply possibility for their safe usage

only for suppression of growth of gram negative bacteria such as *E. coli*.

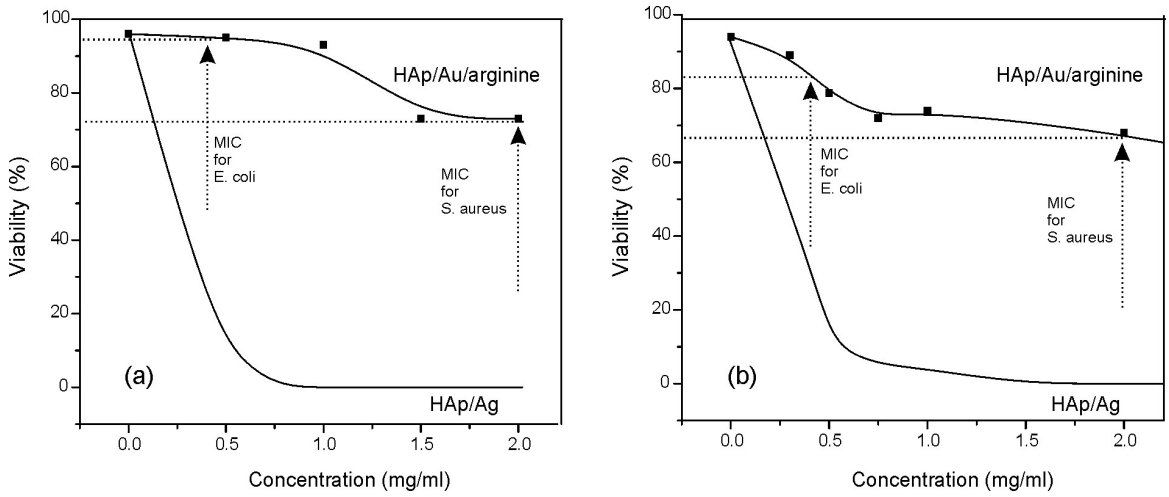

Figure 79: *Comparison of the level of survived human cells after aging with HAp/Au/arginine and HAp/Ag with 10% of silver for two types of cells- healthy MRC 90 foetal lung fibroblasts (a) and cancer modified U-2 OS human osteosarcoma cells (b).*

In the case of the third type of functionalization, when arginine was attached onto HAp/Au, material showed optimal characteristics which were in accordance with its design. Natural selection of building blocks in this case provided very high antibacterial activity which was accompanied with very good compatibility with human cells and absence of toxicity. Comparison of toxicity results for HAp/Au with arginine and for HAp/Ag composites for both, U-2 OS and IMR-90 human cells, is presented in Figure 79.

In contrast to HAp/Ag, after exposure to U-2 OS and IMR-90 human cells HAp/Au functionalized with arginine showed very high level of compatibility. In the case of this material both cell types showed very high level of viability after interaction with material for the whole range of investigated concentrations (0-2 mg/ml) and viability was higher than 70%.

As indicated in Figure 79 if MIC concentrations of HAp/Au/arginine for *E. coli* and *S. aureus* are concerned, viabilities that correspond to them for both cell types are significantly high. In the case of U-2 OS cells, viabilities are higher than 90% for MIC of *E. coli* and higher than 70% for MIC of *S. aureus*. For the second type of cells, IMR-90, viabilities obtained for MIC concentrations of composite for *E. coli* and *S. aureus* are around 80% and 70%, respectively. These values confirmed non-toxicity of tested material and strongly suggest its further investigations in animals.

4.3.1.2 Morphological properties of human cells in contact with hydroxyapatite/metal composites

Compatibility of hydroxyapatite/metal composites with two types of human cells, osteosarcoma cancer modified bone cells and fibroblasts from foetal lung, is additionally investigated from the standpoint of morphological changes in cells. Composite powders were dispersed in growth media with cells at different concentration and after exposure during the period of 24 hours they were inoculated.

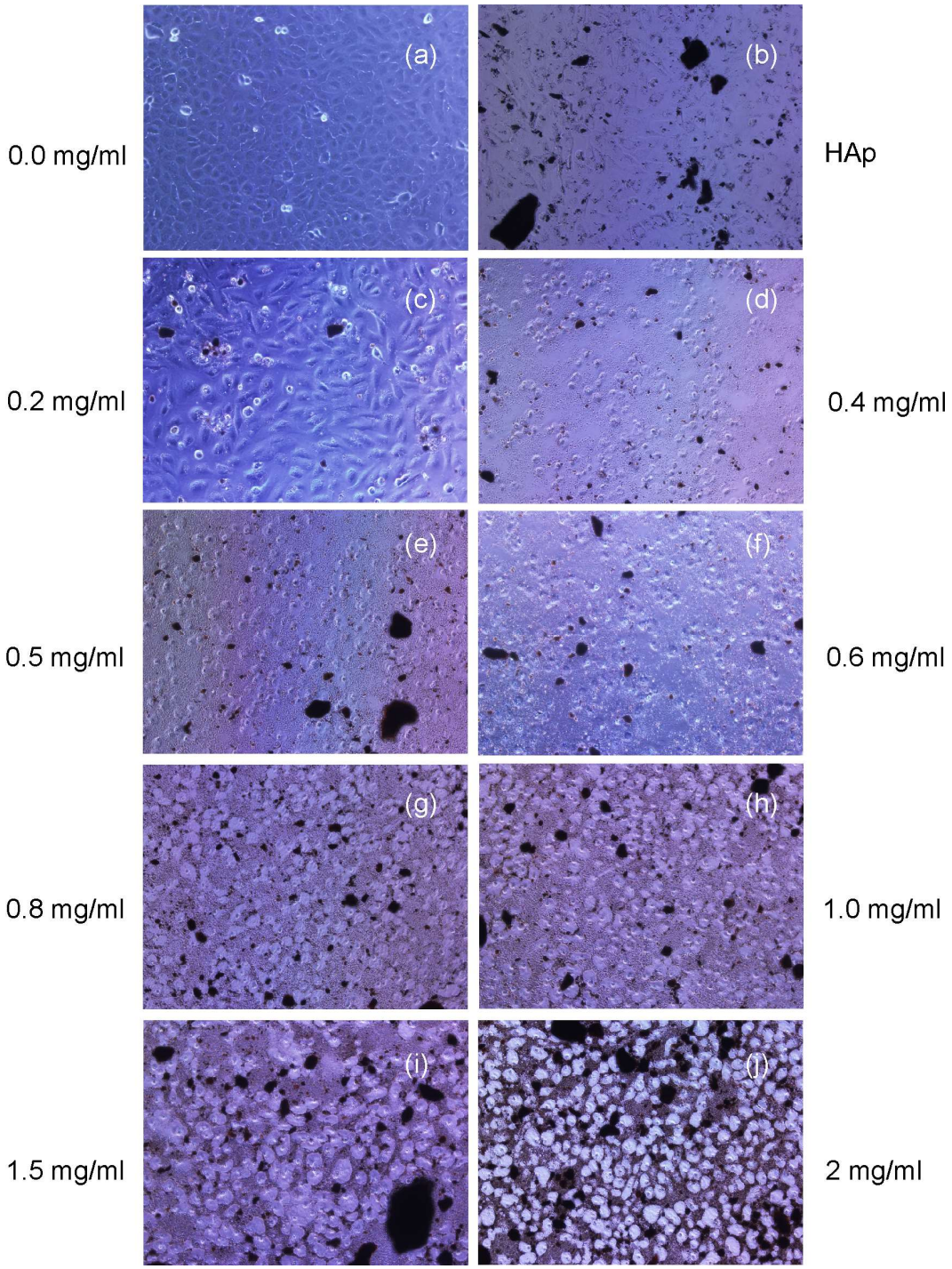

Figure 80: *Morphological changes of U-2 osteosarcoma cancer-modified human cells developed as a result of toxicity obtained after exposure to very low concentrations of HAp/Ag composite with 10% of silver (black fields).*

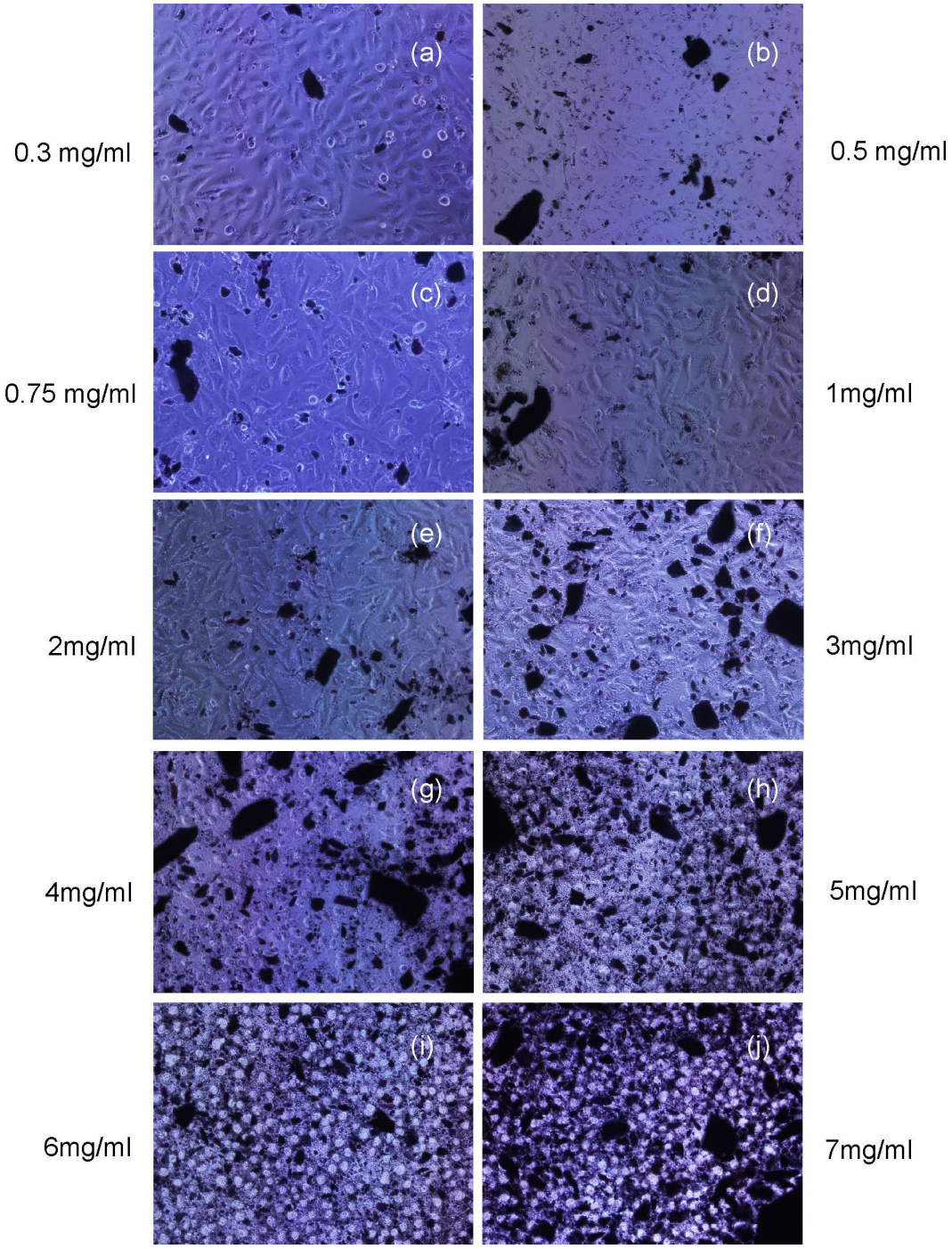

Figure 81: *Morphological changes of U-2 osteosarcoma cancer-modified human cells developed as a result of toxicity obtained after exposure to very high concentrations of HAp/Au/arginine composite (black fields).*

Figure 80 summarizes morphological properties of pure U-2 OS cells aged without material (a), morphological properties of cells aged with pure HAp without any metallic content (b) as well as morphology of the cells exposed to HAp/Ag composite (c-j). HAp/Ag composite with 10% of silver was tested after dispersion within growth media in several different concentrations: 0.2 (c), 0.4 (d), 0.5 (e), 0.6 (f), 0.8 (g), 1.0 (h), 1.5 (i) and 2.0 (j) mg/ml. Normal U-2 osteosarcoma concerned spindle-shaped cells which were observed in the case of pure cells without material and for cells with HAp. When HAp/Ag was present cells start to change their morphology and turned into floating cells, sphere-like in shape, known as “ghost” cells (AshiRani et al., 2009). These morphological changes were obtained even for 0.4 mg/ml of the composite. It should be mentioned that

this concentration of composite contains only 40 µg/mL of Ag-content (10%) which indicated that apoptosis could be induced by very low concentration of material. At higher concentrations of 0.8 mg/ml (which are about MIC concentrations of this composite) cells turned into swollen, interconnected and fused structures which clearly indicated necrosis.

The same method was used for investigation of the morphological influence of HAp/Au/arginine to the morphology of U-2 OS cells. As shown in Figure 81, morphology of these cells was investigated after their exposure to wider range of concentrations of composite including higher values and tested concentrations were 0.3 (a), 0.5 (b), 0.75 (c), 1.0 (d), 2.0 (e), 3.0 (f), 4.0 (g), 5.0 (h), 6.0 (i) and 7.0 (j). In this case cells had regular morphology of normal healthy cells up to the 4.0 mg/ml which is two times higher than MIC concentration of this material for *S. aureus*. For 5 mg/ml and higher concentrations cells showed morphology which is an indication of necrosis process. The same level of necrosis has been reached by almost fivefold lower concentration of HAp/Ag. It indicate that HAp/Au/arginine has five-time higher compatibility.

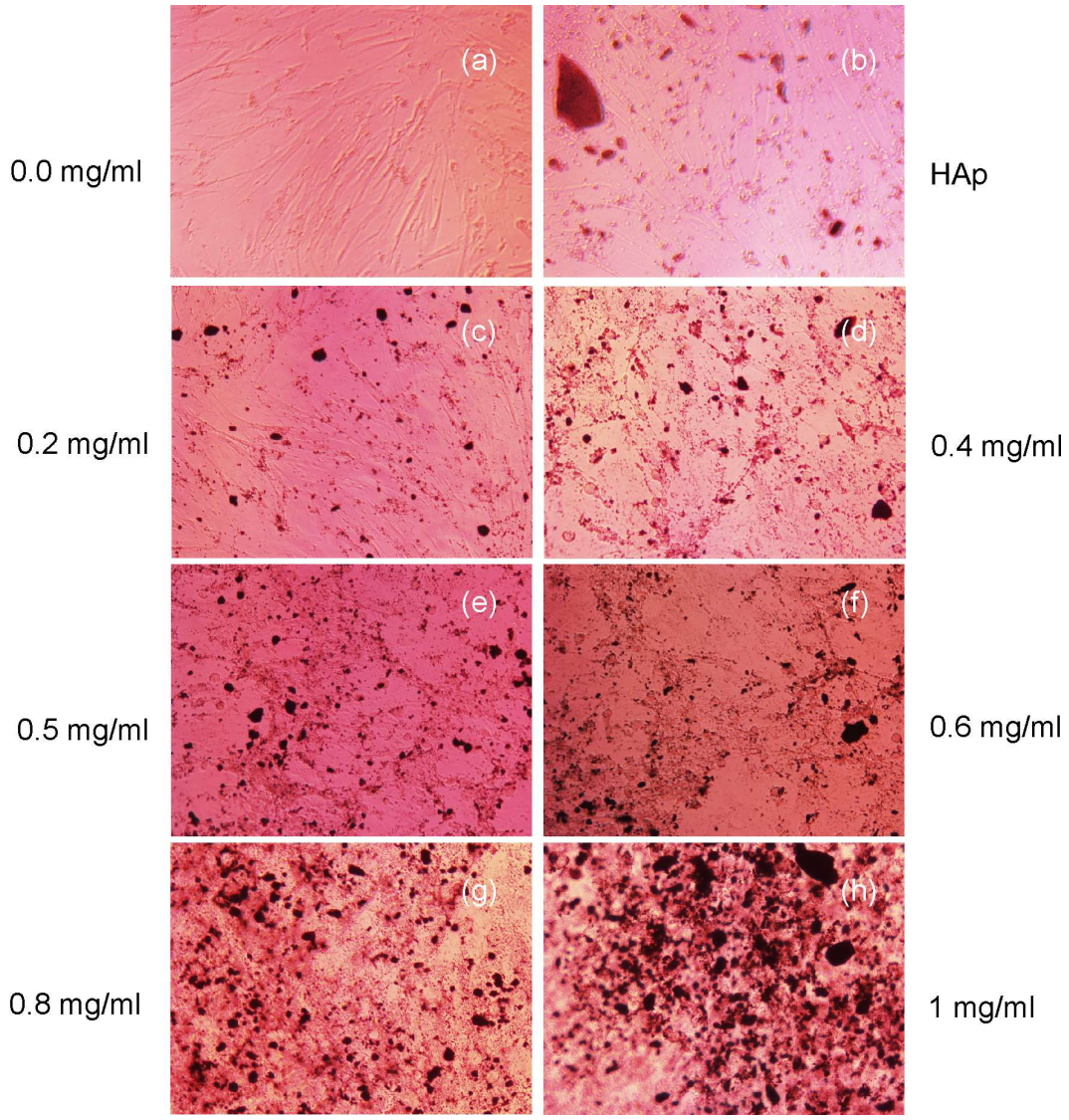

Figure 82: *Morphological changes of IMR-90 foetal lung fibroblast human cells developed as a result of toxicity obtained after exposure to low concentrations of HAp/Ag composite (black fields).*

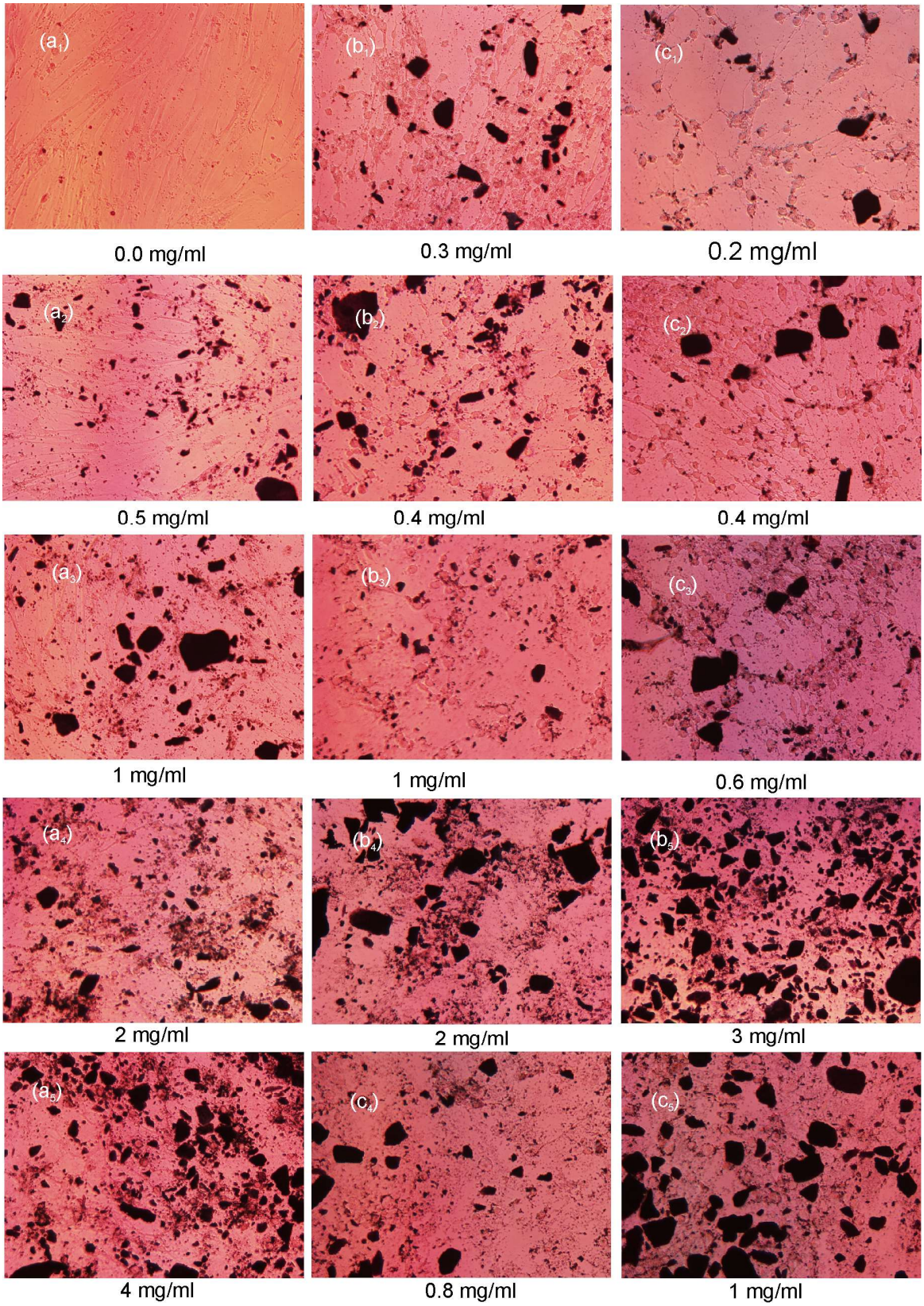

Figure 83: *Morphological changes of IMR-90 foetal lung fibroblast human cells after aging with different concentrations of HAp/Au composite (black fields) functionalized by amino acids (arginine (a), glycine (b) and histidine (c)).*

The second type of investigated cells was IMR-90 as type of healthy human cells. HAp/Ag and HAp/Au/arginine composites were tested for interaction with them and ability to induce their morphological changes. Obtained results were very similar to the previously tested cancer-modified cells.

Firstly, influence of HAp/Ag on morphology of IMR-90 was tested (Figure 82). Normal IMR-90 cells are elongated, fibrous (a).The same morphology corresponds to the cells aged with pure HAp (b) as well as with low concentration (0.2 mg/ml) of HAp/Ag composite. At higher concentrations (0.4, 0.5, 0.6, 0.8 and 1.0 mg/ml) fibre-like morphology of cells turned into granular which indicated apoptosis process. Once again low concentration of material induced first signs of toxicity. The most important observation was that this concentration is only half of the MIC concentration of HAp/Ag. It led us to the conclusion that Ag-material is even more toxic to human then to bacteria cells.

IMR-90 cells were further on tested for the influence of HAp/Au composites functionalized by amino acids (Figure 83). Tested cells were exposed to different concentrations of composites which had arginine ($a_{2\text{-}5}$), glycine ($b_{1\text{-}5}$) and histidine ($c_{1\text{-}5}$) functionalizations. For glycine and histidine, morphological changes of IMR-90 cells were induced at low concentrations and they showed development of granular shapes which are indications of toxicity. However, after exposure to arginine functionalized material, morphological properties of IMR-90 cells remained unchanged for lower concentrations including its MIC concentrations against both types of bacteria. The same granular type of the morphological changes was observed only for the higher concentrations of this material. It means that HAp/Au/arginine has some kind of “smart” mechanism which provides it selectivity and enables stronger action against bacteria.

Morphological investigations indicated good correlations with quantitative analysis of toxic influence of HAp/metallic composites confirming optimal characteristics when toxicity is concerned in the case of HAp composite with gold as metallic part and surface functionalization by arginine amino acid.

5 Discussion

5.1 Hydroxyapatite/metal composites and their physicochemical properties

Homogeneous precipitation method was developed for formation of HAp/metal-based composites formed of apatite bioceramic and noble metal metallic part. The main goal of formation of the composites was development of novel, environmental and human-friendly materials with antibacterial activity suitable for biomedical application. Schematic illustration of designed materials is presented in Figure 84.

During development of these materials, HAp has been used as bioceramic carrier of metallic nanoparticles. It was selected because of the following properties: (a) hydrophilic surface with the presence of reactive/interactive polar groups, (b) tuneable electronic properties due to the structure capable for different types of modifications (incorporation of different ions inside apatite structure, formation of composites with nanoparticles attached on the surface or their ingrowths inside material and/or complexation of the surface by attachment of organic molecules that provides ability for formation of additional hybridized level within forbidden layer) and (c) bioactivity that activate cellular life-cycle, support cellular attachment and stimulate healing process (Dorozhkin, 2009; Nishikawa, 2007; de Araujo et al., 2010). These outstanding properties make this biomaterial suitable for different types of modifications that can be directed to achievement of the properties useful in engineering of materials for specific biomedical applications.

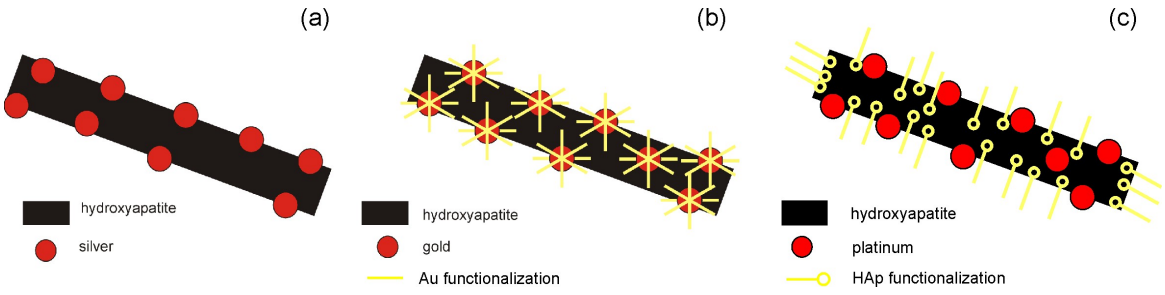

Figure 84: *Illustration of the properties of HAp/metal composite formed by sonochemical method.*

Developed materials had metallic components that were design to be a centre of antibacterial activity. They were selected from the group of noble metals. Unlike other metals, members of this group have very high resistance for corrosion and low ability to induce allergic reaction in live organism which are properties very important for *in vivo* conditions (Wiesenfeld, 1984; Brook, 2006). Silver has very strong, natural ability for antibacterial activity (Rai et al., 2009) that was one of the reasons why this material has been selected as a centre of antibacterial activity within HAp/Ag composite. However, ions and nanoparticles of this metal are highly toxic which made formed composite very

useful negative reference. Platinum and gold are inert, with low solubility and low toxicity (AshaRani et al., 2010). Special strategies have been developed for the activation of these metals in order to design antibacterial activity. Strong affinity of sulphur-containing and nitrogen-containing groups to bond gold was used for activation of Au nanoparticles, while modulation of HAp electric properties by the application of combination of Pt-complexes and Pt nanoparticles was used for activation of this metal. The main similarity with HAp/Ag was to achieve at least the same antibacterial properties while the main difference was to decrease it's toxically response.

Accordingly, sonochemical method was used for formation of HAp/Ag composite containing unmodified Ag nanoparticles (Figure 84a), HAp/Au composite with functionalized surface of Au nanoparticles (Figure 84b) and HAp/Pt composite with Pt nanoparticles and Pt-ions used for functionalization of the surface of HAp (Figure 84c).

5.1.1 Hydroxyapatite/silver composites

During development of the homogeneous precipitation method for the synthesis of HAp/Ag composite it was important to achieve strong connection among formed nanoparticles and HAp carriers by their attachment onto the surface of HAp and by their incorporation within HAp carriers. The main purpose of such structure was to prevent "rinsing effect" related to detachment of nanoparticles from the carrier. This step should decrease Ag-nanoparticles-induced toxicity. Besides, one part of the silver was incorporated within HAp structure in the form of Ag-ions. It was expected that HAp structure will be able to stabilize them and to prevent their uncontrolled release. As a result formed material contained two different sources of antibacterial activity- Ag nanoparticles and Ag-ions.

Optimization of the homogeneous precipitation method for the synthesis of Ag nanoparticles and their composites with HAp was performed using Ag-precursors with different thermal properties. The type of the Ag-precursor influenced the structure, as well as the morphological properties and the growth rate of the silver nanoparticles. Mechanism of formation of these materials by the application of high-intensity ultrasonic field was investigated in more details.

Under the applied sonochemical conditions, the silver acetates and lactates were partially reduced due to the lower temperature of the thermal decomposition, compared to the silver nitrate. Another part of the silver precursor was able to react with the products of the thermal decomposition of urea to form AgNCO. The formation of Ag nanoparticles after the sonication provided a pre-nucleated precipitation during the thermal reduction in an Ar/H_2 atmosphere. This means that an amount of Ag was formed through the reduction of AgNCO, while the other was grown onto sonochemically formed Ag seeds. These two growth mechanisms resulted in the formation of Ag nanoparticles with cubic and hexagonal crystal structures and different morphological properties (Figure 85a). In the case of the silver nitrate (with a higher decomposition temperature) only one mechanism of Ag-particle formation occurred (mechanism II in Figure 85a) and the silver was reduced only during the thermal treatment. The Ag nanoparticles formed as the final outcome had a cubic structure and they were spherical in shape with a significantly reduced size, compared to the two-step growth mechanism, because of the absence of any pre-nucleated growth. According to the literature, it has been observed that it is possible to form two different (cubic and hexagonal) structures of nanoparticles, depending on the type of synthesis method and that the mechanism of synthesis contributes to the formed structure (Weaver and Hoflund, 1994). Additionally, it was observed that seed-mediated growth (when fine metal particles allow further crystal growth) results in the formation of a variety of shapes and structures (Sau et al., 2010). It has been described that these

structural and morphological parameters are in a close relationship with the rate of the reduction process in such a manner that a slower reduction results in a non-spherical shape, and the preferential growth and assembly in different, non-usual structures (Wetli et al., 1997; Tan et al., 2003; Harfenist et al., 1997). Cavitation bubbles and hot spots formed during the sonication are able to lead to extreme parameters (temperature and pressure) and highly reactive radicals capable of providing a rapid reduction of the precursors with a low temperature of decomposition (Suslick et al., 1996). At the same time, the kinetics of the thermal decomposition of AgNCO is a slow process (Schmidt et al., 2009). These two sources for the formation and growth of Ag particles explain the main reason for the obtained shapes and structures.

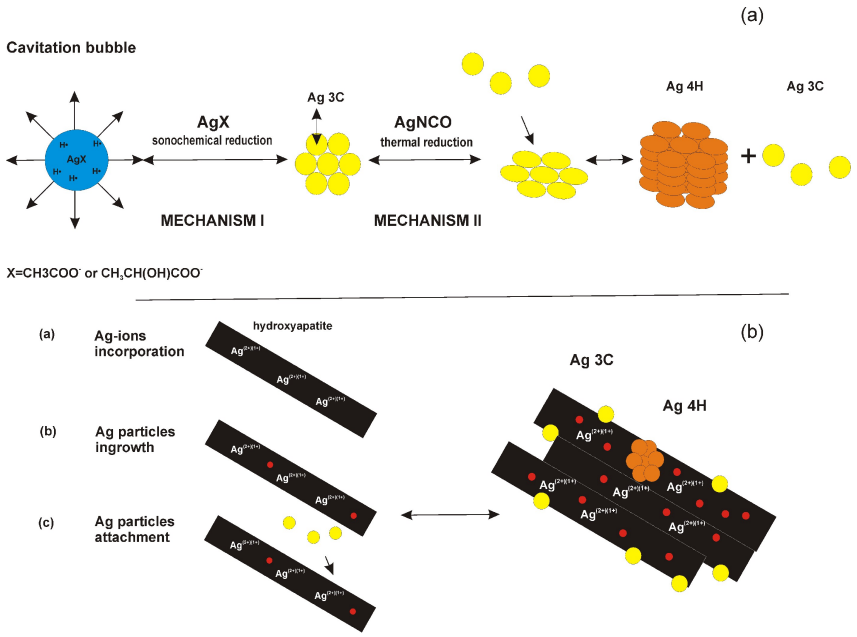

Figure 85: *Schematic illustration of the proposed mechanisms for formation of Ag nanoparticles and HAp/Ag composites by the application of homogeneous sonochemical precipitation method.*

In the case of the HAp/Ag composites, the mechanism of particle formation is more complex and consists of three steps: (a) the incorporation of Ag-ions into the HAp structure, (b) the in-growth of Ag particles into the Ca-phosphate plates and (c) the attachment of Ag particles onto the surface of the Ca-phosphate plates, and/or the final formation of the HAp. The first segment associated with the initiation of the precipitation of Ca-phosphate depends on the type of the selected silver precursor. In contrast to the formation of the HAp immediately after the sonochemical synthesis, when silver nitrate was used (similar to the case when silver ions are not applied), (Jevtić et al, 2008) in the case of the acetate and lactate precursors, OCP was formed. In that case, the pH of the solution was low and it resulted in the precipitation of OCP as the most stable phase. At the same time, one part of the Ag ions was incorporated into the formed Ca-phosphate structure (Figure 85b). Similar to mechanism I in the Ag-particle formation (Figure 85a), the initiation of the precipitation of Ca-phosphate provided nucleation sites for the formation of Ag particles, which was the driving force for their sonochemical reduction in the case of all three Ag precursors. During the preferential growth of the Ca-phosphate plates, these Ag particles remained in-grown inside them, which prevented their further growth (Figure 85b). After the thermal treatment, AgNCO was reduced and the formed

Ag particles were attached onto HAp plates, which resulted in the formation of both cubic and hexagonal Ag structures (Figure 85b). A significant difference in the size of the Ag particles attached to the surface of the HAp, depending on the selected silver precursor, is assigned to the role of surface OH- groups in the process of the Ag formation. As was already mentioned, in the case of the nitrate silver precursor, the HAp was formed after the sonochemical synthesis and its surface OH- groups enabled interactions with the Ag ions. After they were reduced during the thermal process, these interactions ensured their stabilization and they remained attached to the surface of the HAp. Their growth took place due to the reduction of AgNCO; however, they could not aggregate due to the templating role of the surface of HAp. In the case of the lactate and acetate precursors, the OCP was transformed to HAp and the reduction of Ag occurred during the thermal treatment. The surface stabilization of the Ag by the OH-groups did not occur and the formed particles were physically deposited. In this case, the conditions were more favourable for their aggregation and growth into larger particles.

The interactions of the ultrasonic waves with the liquid/liquid and liquid/solid medium result in the development of physical and chemical effects like the homogenization, intensive mixing, dispersing, the formation of reactive radicals, deagglomeration etc. These effects contribute to the major advantages of sonochemistry over other methods associated with the ability to: (i) increase/control the rate of chemical reactions, (ii) allow the formation of non-typical products and drive chemical reactions that do not take place under normal conditions and (iii) influence the morphological and structural properties of the material in a non-convenient manner (Suslick et al., 1996; Bang and Suslick, 2010). During the formation of Ag nanoparticles and their composite with HAp by the application of the sonochemical approach tasks (i) and (iii) have been achieved. It has been already discussed that compared to classical homogeneous precipitation using urea as the precipitation agent, sonochemical homogeneous precipitation ensures the formation of monophase HAp with two enhancements: (i) the reduction of time for the formation of monophase HAp and (ii) the reduction of the dimensions of crystals, which have a controlled morphology and structure (Jevtić et al., 2008). These enhancements can be assigned to an increased rate of urea degradation during the process of sonication due to the intensive mixing and local heating of the liquid medium to significantly high temperatures caused by cavitation. The last phenomenon is very important for the formation of AgNCO, since faster urea degradation leads to a faster formation of AgNCO – which certainly affects the morphology of the grown crystals – compared to the classical precipitation method and the formation of this material after heating at 80°C without sonication (Nour and Rady, 1991). Consequently, sonochemically formed parallel oriented AgNCO nanorods are able to affect the morphology of the Ag particles obtained in the next thermal reduction step. Moreover, in some cases an amount of silver was sonochemically reduced and Ag seeds were formed. In these cases, sonochemically obtained pre-nucleation provided conditions for the growth of another, hexagonal Ag phase with geometrically more regular particle shapes. It has been reported that the co-precipitation of Ag with Ca-phosphates may result in the formation of an additional silver-phosphate (Ag_3PO_4) phase (Rameshbabu et al., 2007). However, the subsequent decomposition of urea during sonication increases the pH to the region in which Ca-phosphates and AgNCO are the only stable phases preventing the formation of Ag_3PO_4.

5.1.2 Hydroxyapatite/platinum composites

As it was already mentioned platinum is a metal without natural ability to affect bacterial growth (Shahidi and Ghoranneviss, 2011). In contrast to the very low solubility and high inertness of the metallic form of this metal, Pt-complexes are biologically active (Brook, 2006). The best example is cisplatin as a member of a large group of platinum complexes with *cis*-geometry known as highly efficient anticancer-agents (Kostonova, 2006). Pt-complexes are able to interact with cells, preferentially to nucleic acids, and in some cases they were developed in the form which was middle-intensity-active against bacteria (Mishra et al., 2006).

The main strategy for the activation of metallic part of the HAp/Pt composite for the activity against bacteria concerned formation of biophotocatalyst with the structure which will be able for intensive photocatalytic activity. Illustration of the strategy is presented in Figure 86. During development this type of material it was taken into account that: (i) HAp is a semiconductor with ability for modulation of electric properties (Aronov et al., 2007a; Aronov et al., 2007b), (ii) Pt-ions are very reactive and have tendency to form complexes at specific sites on the surfaces (Dabrowski, 1999) (especially polar ones) that make them suitable for complexation onto the HAp surface and (iii) Pt-nanoparticles are very good for the electron trapping (Hiehata et al., 2007) that can be efficiently used for separation of the charge and increase of the efficacy of photocatalytic activity.

During optimization of the homogeneous precipitation method for the synthesis of HAp/Pt composites in the form of biophotocatalyst two different Pt-sources with abilities to bind the surface of HAp in different ways have been selected. In the case of H_2PtCl_6 used as Pt-precursor, chloroplatinic ions ($[PtCl_6]^{2-}$) were chemisorbed onto HAp surface that provided strong attachment. For the $C_{10}H_{14}O_4Pt$ as Pt-precursor, the complex was physisorbed onto HAp and in this case weaker attachment onto HAp was obtained. Functionalization of HAp took place during the sonication step (Figure 86a). In this step there were no conditions for reduction and formation of Pt-nanoparticles. Obtained results are in accordance with the literature since it was already shown that formation of Pt nanoparticles in water medium strongly depends on sonochemically formed radicals as reducing agent. During sonification of water, sonolysis results in formation of $H\cdot$ and $OH\cdot$ radicals which are inefficient to induce reduction process. However, if organic, surface active substances (like SDS) (Mizukoshi et al., 2001) or alcohols (such as isopropanol) (Caruso et al., 2000) are added, there is an increase of formed species and reducing ability of sonicated solutions is significantly increased. Sonochemical method with addition of a small quantity of alcohol was also used for formation of photocatalysts such as TiO_2/Pt (Sivakumar et al., 2010) and Pt/Ru/C (Angelucci et al., 2007) composites. Obtained results showed significantly improved photocatalytic activities of these metals which was assigned to contribution to morphological and structural properties developed by intensive mixing during the process of synthesis. Consequently, agglomeration was prevented and collisions among the support and formed particles provided strong contacts that are highly important for charge-transfer.

In the case of HAp/Pt synthesized in this work, sonochemical step was performed in water surroundings without addition of surfactants which resulted in formation of complexes. The next thermal treatment step, which was performed in reducing H_2-atmosphere at 400°C, induced partial reduction of formed complexes and formation of Pt nanoparticles (Figure 86b). Another part of the formed complexes remained onto the surface of HAp. It may be associated with possibility for the increased thermal stability after complexation since Pt-precursors that were used in this process had relatively low melting temperatures which were 60°C for H_2PtCl_6 and 250°C for H_2PtCl_6 (Vukomanović et al., 2012b).

Mechanism of formation of composite particles was very similar to the formation of HAp/Ag using nitrate-precursor, presented in Figure 85a, with the main difference in the type of complex formed before thermally-induced reduction and absence of Pt-ions incorporated within apatite structure. In this case HAp also had a role of templating agent since the fact that without its presence there were no conditions for formation of nanoparticles, their surface was unprotected and they tended to ingrowths into large micrometer-sized structures (Vukomanović et al., 2012b).

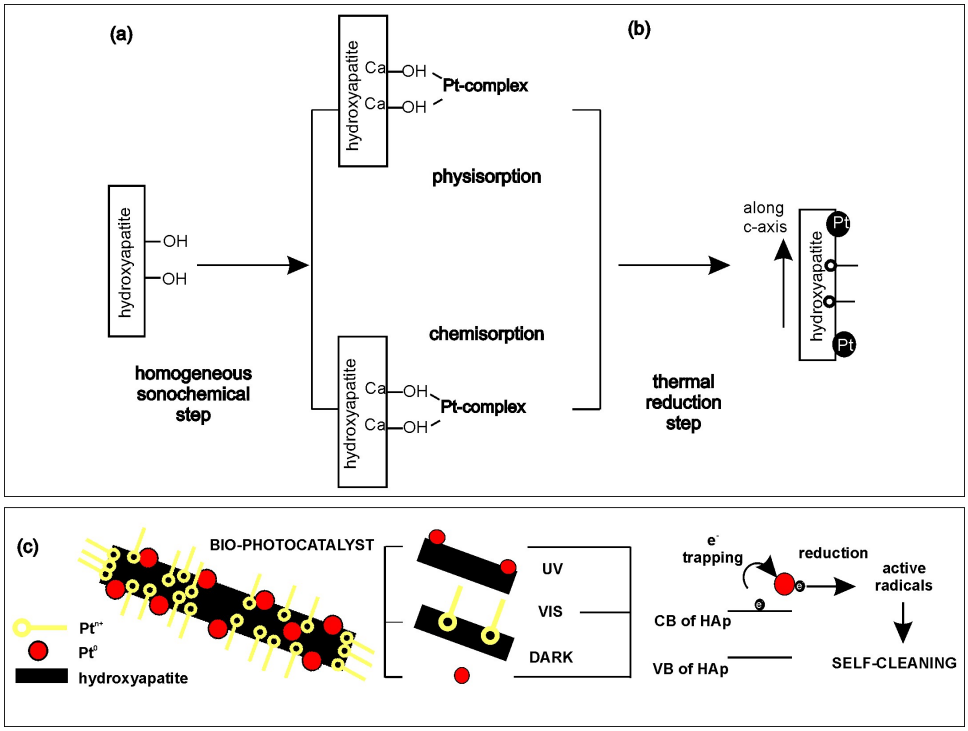

Figure 86: *Schematic illustration of the structure of HAp/Pt composite synthesized by sonochemical method with demonstration of the strategy used for activation of metallic part of the composite.*

Within HAp/Pt composite HAp has also the template role for Pt nanoparticles. These particles were formed upon complexes which were attached to the HAp surface by two different types of bonding – strong chemisorptions and weak physisorption of Pt-molecules. In the case of stronger attachment of $[PtCl_6]^{2-}$ions which were chemisorbed onto HAp after reduction small, non-agglomerated and well-crystallized Pt nanoparticles that were homogeneously distributed over the surface of micrometer-sized HAp plates were obtained. Consequently in this case strong, connections among HAp and Pt particles are obtained. According to the mechanism of nanoparticle formation, it may be expected that formed contacts between them and HAp surface are mechanical. Existence of these surface contacts between semiconductor and metallic component significantly contribute to the photocatalytic activity of formed material. The same contribution also belongs to the formation of well-crystallized metallic particles with ordered structure since the presence of the defects contributes to the recombination process, reduces concentration of formed active radicals and decrease efficacy of photocatalytic process (Carp et al., 2004; Chen, 2008). The contribution of the developed structural properties of components of HAp/Pt composite were proven during the investigation of ability of this material to induce photocatalytically-driven degradation of organic, azo dye.

In the case of the second Pt-precursor, when the type of an attachment of the complex to the HAp surface was physisorption formed Pt particles did not have sufficiently strong attachment. In this case they were prone to agglomerate and to ingrowths into larger

structures. These particles also had ordered and well-crystallized structure of Pt particles. Presence of agglomeration, however, affected the photocatalytic process of this material and decreased its efficacy compare to the HAp/Pt formed using $[PtCl_6]^{2-}$ ions.

In both cases, biophotocatalyst with Pt-complexes and Pt-nanoparticles attached onto the surface of HAp plates have been developed. Component of so-designed materials provide them ability for degradation of the dye under UV and VIS irradiation as well as in the dark (Figure 86c) (Vukomanović et al., 2012b).

5.1.3 Hydroxyapatite/gold composites

Similar to the platinum, gold is a bioinert metal without natural ability for antibacterial activity. Recently, different methods to the bioactivation of this metal has been developed which opened many branches for its application in biomedicine. Some of the most perspective once are use of the gold nanoparticles as carriers of the drugs (like antibiotics) (Ghosh et al., 2008), as diagnostics (as contrasting agents) (Ke et al., 2011) and as therapeutics (for photothermal therapy) (Patra et al. 2010). Such approach introduced gold as a novel biomaterial and opened a new chapter in biomaterial design.

The main strategy for activation of gold within HAp/Au composite in order to develop its activity against bacteria was to use different natural sourced amino acids and synthetic thiols/amines to functionalize their surface. In this case possibility of Au atoms to bind molecules with groups containing nitrogen of sulphur was used in order to enable their bioactivation and to provide interaction with cells. Illustration of the strategy and design of materials with activated gold is presented in Figure 87 (Vukomanović et al., 2012c).

During the process of optimization of sonochemical homogeneous precipitation for Au activation two different approaches to reduction of metallic part of the composite were developed. In the first case, when formed material was negative reference, gold has been reduced thermally. In this case HAp/Au was formed without any functionalization of the surface. In the second case, Au nanoparticles were formed during chemical reduction and in this case their surface has been functionalized. HAp has been synthesized by sonochemical method and ultrasonic processing was used for attachment of Au nanoparticles onto HAp surface. These two processes of formation of HAp/Au materials were investigated in detailed in order to reveal properties of developed materials.

In thermal reduction for formation of Au particles started along with precipitation of HAp. This process has been initiated sonochemically and induced by reactive radicals formed during water sonolysis. It should be mentioned that initial step reduced only small quantity of Au nanoparticles while majority of gold formed Au-urea complex. Sonochemically formed seeds of Au particles were further on grown during thermal reduction of Au-urea complex. This means that finally-formed Au particles were formed in two stages- first was fast sonochemical reduction and second was slow thermal reduction process. Mechanism of formation of these particles within HAp/Au composite was the same as for the HAp/Ag formed using lactates and acetates (Figure 85b, c).

Similar to the metallic nanoparticles within HAp/Ag and HAp/Pt composites, Au nanoparticles were templated by apatite within HAp/Au composite. Morphological properties of Au particles formed with and without presence of apatite phase could be explained by their early formation during reduction of gold precursor in sonochemical step. It is known from the literature that acoustic cavitations, caused by interactions of ultrasonic waves and liquids, result in water sonolysis and development of reactive radicals which initiate oxido-reduction process (Suslick et al., 1996; Bang and Suslick, 2010). It was the phase when Au seeds were formed. Propagation of ultrasonic wave causes variation of pressure resulting in intensive mixing, homogenation and dispersing of liquid. So obtained dynamic surroundings result in intensive collisions of formed

particles, there is a transfer of the heat at the place of collision resulting in local melting (Shchukin et al., 2011). Small Au particles formed during sonication have been intensively mixed which resulted in their high-energy collisions. Bulk gold has high melting temperature which is around 1060°C, but gold nanoparticles have significantly reduced melting temperature which is approximately between 300 and 400°C (Bieri et al., 2003; Yeshchenko et al., 2009). It means that collisions of Au nanoparticles during sonication are followed by the melting at the place of collision and their ingrowths into large structures forming micrometer-sized aggregates. However, when HAp was present, so formed Au seeds were attached onto its surface which prevented their aggregations and ingrowths into larger structures. These seed were grown into nanoparticles onto HAp surface during thermal reduction step as a consequence of decomposition of Au-urea complex.

So-far deposition-precipitation (Monkawa et al., 2006; Dominguez et al., 2009) and immobilization-precipitation (Gupta, 2006; Aryal et al., 2006; Sastry et al., 2008; You et al. 2009) were the only methods used for formation of HAp/Au composite, while sonochemical approach has been used for formation of SiO_2/Au (Chen et al., 2001) and SiO_2/Au/Pd (Nakagawa et al., 2005) composites. In all of these cases reduction of Au was performed either by addition of alcohol to increase the concentration of reducing species, by co-precipitation with other metal or by reducing ability of the specific groups of macromolecules. Here-developed sonochemical procedure for HAp/Au confirms ability for initiation of Au reduction only by sonolytically-formed radicals and shows improvement in efficiency since very large surface area of HAp plates was covered by Au nanoparticles.

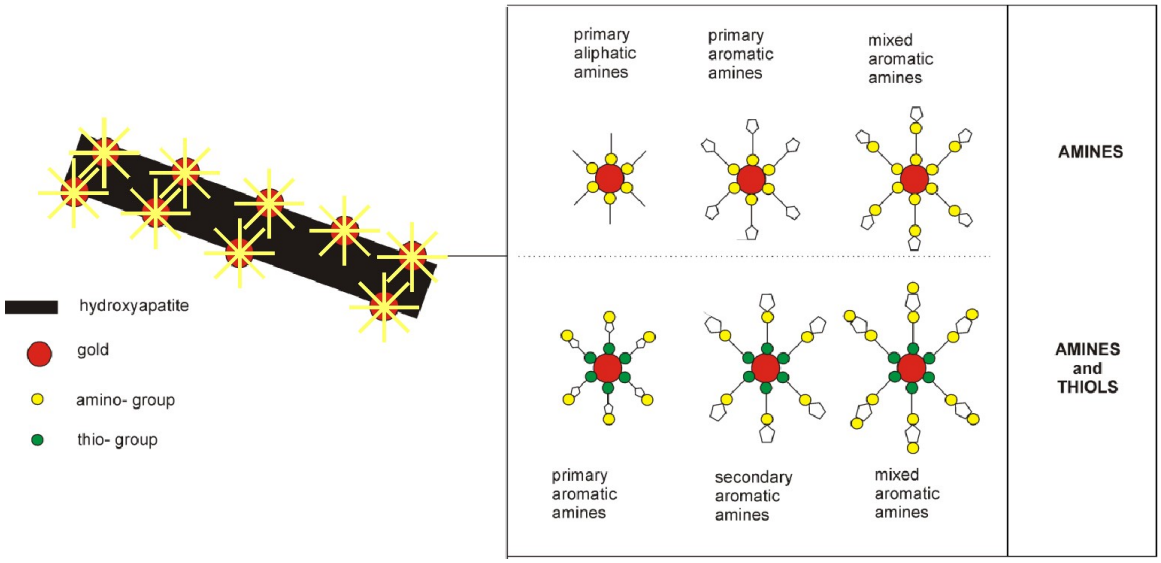

Figure 87: *Functionalization of the surface of HAp/Au particles during the process of chemical reduction.*

When the second approach was used for formation of HAp/Au composite in order to functionalize surface of Au nanoparticles, reduction was chemical and reaction of composite formation was significantly faster. Illustration of the functionalization process and formation of HAp/Au composites is presented in Figure 87. During this procedure HAp has been synthesized sonochemically and re-dispersed in water solution with addition of a low volume of isopropanol. Addition of isopropanol was a critical step because of two reasons: HAp activation as well as Au-reduction.

First reason of isopropanol addition was related to the significant increase of the concentration of cavitations per volume due to the presence of small quantity of easily-volatile, low-surface-tension organics. It is known that their presence in the system during

sonication make surroundings much aggressive which amplifies all effects able to affect morphological and surface properties of the sonicated solids (Shchukin et al., 2011). This type of the system allowed formation of very fine dispersion of HAp in water and activation of its surface for attachment of nanoparticles. It explains contribution of physical effects of ultrasound to formation of the composite.

The second reason for addition of isopropanol is related to reduction of Au when chemical effects of ultrasound were employed. According to the literature, addition of organic solvents (like isopropanol) to the sonicating system significantly contributes to formation of variety of active radicals. Mechanism of this process concerns water sonolysis when H· and OH· are formed (Eq. 3). They are able to react with the organics (R-OH) to form secondary radicals (R·) (Eq. 4). Additionally, due to the low surface tension, the organics are present at the interface between the liquid and gas phase of cavitation bubbles. These are places of high locally-developed temperature that are capable for thermal decomposition of organics. Decomposition additionally contributes to the number and variety of formed active radicals (Eq. 5) (Okitsu et al., 2007).

$$H_2O \xleftarrow{)))} H^{\bullet} + OH^{\bullet} \tag{3}$$

$$(CH_3)_2CHOH + H^{\bullet}(OH^{\bullet}) \longleftrightarrow (CH_3)_2C^{\bullet}OH + H_2(H_2O) \tag{4}$$

$$(CH_3)_2CHOH \xleftrightarrow{T} thermally-formed-radicals \tag{5}$$

So far this method was used for sonochemical formation of Au nanoparticles stabilized by different agents including citric acid, (Su et al. 2003) chitosan (Okitsu et al., 2007), polyvinylpyrrolidone (PVP) (Naveenraj et al., 2010), and sodium-duodecil-sulphate (SDS) (Park et al., 2006). In all these cases, except for the citric acid, the quantity of added isopropanol and related active radicals formed during the sonication process was high enough to provide complete reduction of gold and to form Au nanoparticles (according to Eq. 6 and 7). Stabilization was the next step and it was associated with surface adsorption or organics onto the surface of Au nanoparticles.

$$AuCl_4^- + 3(H^{\bullet}, OH^{\bullet}, (CH_3)C^{\bullet}OH) \longleftrightarrow Au^0 + 4Cl^- + 3R \tag{6}$$

$$nAu^0 \xleftrightarrow{T} (Au)_n \tag{7}$$

In the case of the method used in present work, the quantity of isopropanol was not able to initiate Au-reduction which was confirmed in a control experiment performed without addition of functionalizing substances. Some of the added functionalizing substances (amino acids, for example) were also unable to initiate reduction of Au without presence of pre-sonicated isopropanol. It means that combination of isopropanol and functionalizing substances had important role in reduction of gold and formation of HAp/Au composite. It can be speculated that active radicals formed during sonification of isopropanol are able to react with amino acids to turn them into radical form (Eq. 8). Activated forms of these molecules provide their interaction with Au-ions and reduce them into elemental state (Eq. 9) that provide formation of clusters which grow into Au nanoparticles (Eq. 7). Remained amino acids had role in stabilization of formed nanoparticles by chemisorptions on their surface (Eq. 10) and physisorption onto HAp template (Eq. 11).

Described approach provided significant improvement in morphological properties of formed Au nanoparticles in the sense of drastic reduction of particle size, complete prevention of agglomeration process and attachment of high content of Au particles onto HAp surface in comparison with to-date results regard usage of N-side of amino acids in stabilization of pre-formed Au nanoparticles (Koyama et al., 2008; Polavarapu et

al.,2008) and formation of these particles as a result of amino acid-induced reduction (Shao et al., 2004; Selvakannan et al., 2004; Bhargava et al., 2005).

$$NH_3{}^{+}CH(R)COO^{-} + (H^{\bullet}, OH^{\bullet}, (CH_3)C^{\bullet}OH) \longleftrightarrow NH_3{}^{\bullet+}CH(R)COO^{-} \quad (8)$$

$$AuCl_4^{-} + 3NH_3{}^{\bullet+}CH(R)COO^{-} \longleftrightarrow Au^0 + 4Cl^{-} + 3NH_3{}^{+}CH(R)COO^{-} \quad (9)$$

$$(Au^0)_n + NH_3^{+}CH(R)COO^{-} \longleftrightarrow (Au^0)_n - NH_2CH(R)COO^{-} \quad (10)$$

$$(Au^0)_n - NH_2CH(R)COO^{-} + HAp \longleftrightarrow (Au^0)_n - NH_2CH(R)COO^{-} \cdot\cdot HAp \quad (11)$$

In the case of the second group of reducing/stabilization agents which belongs to synthetic amines and/or thiols (5(bromo-pyridine)-2-thiol, and 4(methylthio)aniline) situation was different because of the presence of sulphur-containing groups. In this case proposed mechanism of Au nanoparticle formation starts with activation of thio group probably due to the lower activation energy compare to amine side of molecule (Eq.12). Formed radicals reduced Au-ions and turned them in elemental state (Eq. 13), which was followed by stabilization step when organic molecules used their S-sides to bond to the surface of Au nanoparticles (Eq. 14).

$$R - S(R') + (H^{\bullet}, OH^{\bullet}, (CH_3)C^{\bullet}OH) \longleftrightarrow R - S^{\bullet}(R') \quad (12)$$

$$AuCl_4^{-} + 3R - S^{\bullet}(R') \longleftrightarrow Au^0 + 4Cl^{-} + 3R - S^{-}(R') \quad (13)$$

$$(Au^0)_n + R - S^{-}(R') \longleftrightarrow (Au^0)_n - S - R(R') \quad (14)$$

Thiourea has possibility to form very strong complexes with gold (Yang et al., 2003b). Au-thiourea complex was reduced by additional strong reduction agent and after the process of formation of Au nanoparticles was finished remained thiourea bonded to the surface Au-layer by its S-side forming Au-S groups onto nanoparticle surface. Specifically case was also aniline which has ability to reduce gold without activation by sonochemical radicals. In this case reduction of Au was very fast process since it was a consequence of synergic activity of aniline and sonochemically formed radicals.

For the thermal reduction there was an electrostatic interaction between Au particles and HAp surface which resulted in high level of prevention of their growth. However, in the case of surface functionalization of Au nanoparticles their stability and stability of the whole composite depended on surface groups.

In the case of amine-functionalization, the best stability of both, Au nanoparticles and HAp/Au composite was achieved for amino acids. They functionalized surface of Au nanoparticles (by $–NH_2$ groups) and simultaneously allowed attachment of these particles onto the surface of HAp (by the interactions of –COOH with -OH groups) which allowed them very good prevention of growth and agglomeration. Completely opposite situation was detected for aniline. In this case, aniline molecules were bonded to the Au-surface using $–NH_2$ groups. However there were no polar groups on the opposite side of molecule to interact with HAp and surface charge of so obtained Au particles was almost completely stabilized by aniline rings. As a result stability of HAp/Au composite was low and a large quantity of Au particles existed separately.

The best stabilization achieved for thiol/amine containing molecules was obtained for 5(bromopyridine)-2-thiol. In the case of this molecule there is a presence of -SH group for bonding on the surface of Au nanoparticles and a presence of –Br group on opposite site of molecule for interaction with HAp surface. However, for thiourea and 4(methylthio)aniline, attachment to Au has been achieved through bonding of –SH with Au nanoparticles however there were no additional negative-charged polar groups for interaction with HAp and intensive agglomeration occurred.

5.2 Antibacterial action of hydroxyapatite/metal composites

Gold and platinum, as bioinert metals without natural ability for antibacterial activity, were included within specially developed strategies in order to investigate ability for their bioactivation. As a result newly developed materials composed of HAp as bioceramic and gold or platinum as metallic part were developed. They were used for investigation of the preferential direction of material design using material engineering in order to develop applicative properties like antibacterial activity. Materials were designed in two directions: (i) formation of HAp/metal composite with functionalized surface of HAp as a biophotocatalyst for light-induced self-cleaning and antibacterial activity and (ii) formation of HAp/metal composite with functionalized surface of metallic nanoparticles for antibacterial activity.

5.2.1 Self-cleaning vs. antibacterial action of hydroxyapatite/platinum composite

Self-cleaning action of HAp/Pt composite

Hybrid semiconductor/metallic composites made of apatite plates with Pt metallic nanoparticles attached on their surface and two different types of surface adsorbed complexes were tested for photocatalytic activity. Different kinetic parameters of photocatalytic activity of HAp/Pt composites obtained after their activation by UV and VIS light as well as their activity in dark are showing that different mechanisms run these processes (Vukomanović et al., 2012b).

UV activity. Composite activation by UV light is determined by excitation of HAp and proposed mechanism is illustrated in Figure 88a. As a wide band gap p-type semiconductor (Aronov et al., 2007a; Aronov et al., 2007b), HAp possesses a complex structure of electron/hole bulk and surface localized states. Such an electronic structure of HAp is very important for its interactions with cells and it was assumed that deep electron/hole charged states are the reason of its extremely good bioactivity (Aronov et al., 2007a). A value of the band gap energy of HAp was determined to be E_g=3.9 eV (Aronov et al., 2007b) which explains its ability to absorb light in UV region. A classical way of photocatalytic activation for this material is absorption of the UV light (Nishikawa and Omamiuda, 2002; Nishikawa, 2004; Nishikawa et al., 2005; Funakoshi and Nonami, 2006; Reddy et al., 2007; Ye et al., 2007) after which electrons are transferred from valence (VB) to conduction bend (CB) leaving positive holes. Separation of the charge is important for ability to form radicals. Electrons from CB are involved in reduction while positive holes enable oxidation process on particle surface. Formed radicals initiate degradation of the dye. Recombination of the separated charges is reduced due to the presence of the Pt particles at the surface of HAp because of the known ability of these metallic particles to trap electrons (Hiehata et al., 2007) and this is the way for enhancing of the efficacy of this process. Differences in photocatalytic abilities of HAp/Pt (H_2PtCl_6) and HAp/Pt ($C_{10}H_{14}O_4Pt$) composites indirectly depend on surface complexes since agglomeration of Pt particles present on HAp surface and involved in electron trapping depend on them. There is also a difference of HAp crystallinity within composite depend on the Pt-precursors which, in general, has potential to affect photocatalytic activity (Eufinger et al., 2007).

VIS activity. Without formation of composites like HAp/TiO_2/Ag, (Liu et al., 2010) HAp do not have ability for photocatalytic activity induced by visible light. Mechanism of here-obtained HAp/Pt activation by VIS light, illustrated in Figure 88b, is determined by the complexes adsorbed on the surface of HAp. In this mechanism the only role of HAp is in separation of the charge and transfer of the electrons formed by the complexes

adsorbed on its surface. The similar way was used for VIS activation of TiO_2 and it is known as "surface-complex-mediated path" which does not require band gap excitation (Kim and Choi, 2005b). In the case of HAp/Pt ($C_{10}H_{14}O_4Pt$), $C_{10}H_{14}O_4Pt$ is physically adsorbed on HAp surface, after absorption of the VIS light electrons are transferred directly to VB of HAp without excitation of the complex through the ligand-to-metal-charge transfer (LMCT) (Kim and Choi, 2005b). Due to the physical adsorption, in the case of HAp/Pt ($C_{10}H_{14}O_4Pt$) charge could be transferred through –Ca-OH·····O=C- pathway. The second type of surface activation is HAp/Pt (H_2PtCl_6), when $[PtCl_6]^{2-}$—ions are chemisorbed on HAp. After absorption of UV light, -O-Cl-Pt- adsorbed on HAp surface is transferred to excited state. Relaxation of the complex is followed by generation of electrons which are immediately transferred to CB of HAp. This activity was explained using analogy with the case when TiO_2 has been activated by adsorption of these ions and obtained platinum-chloride-modified TiO_2 showed the highest activity compare to doping by Pt ions and formation of composites with metallic Pt (Burgeth and Kisch, 2002). For both types of formation of electrons- with and without formation of excited state, they have been inserted into CB of HAp. These electrons are trapped by Pt nanoparticles and further on involved in formation of active radicals which increases efficiency of the photocatalytic process similar to the previously described case.

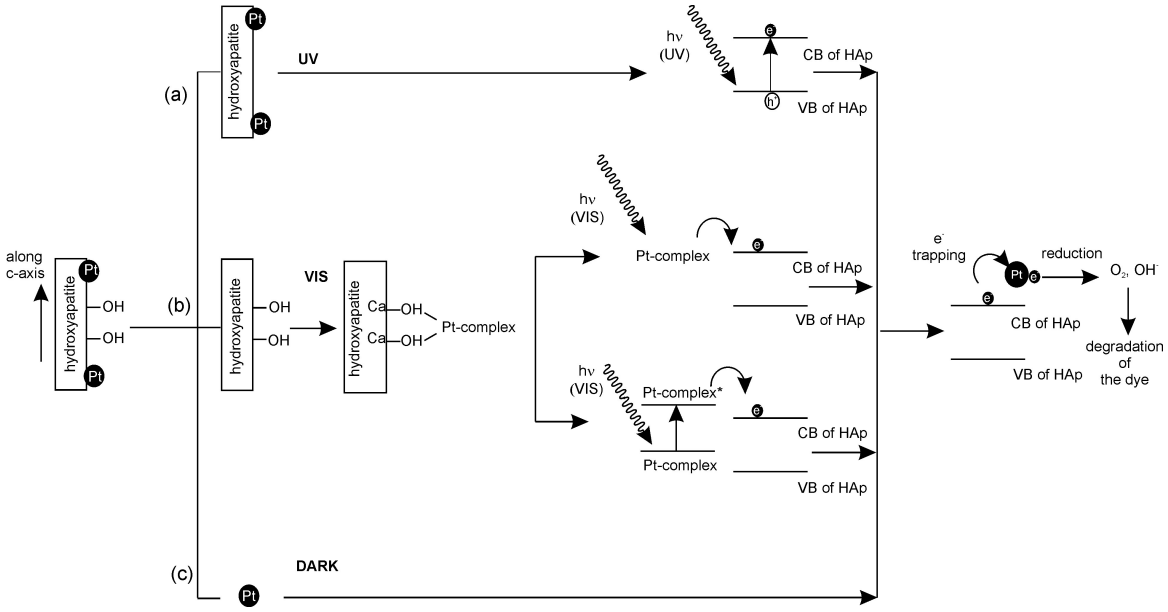

Figure 88: *Proposed mechanism for degradation of the dye induced by HAp/Pt composite after irradiation by UV (a) and VIS (b) light as well as in the dark (c).*

Dark activity. Activity of material in the dark can be assign only to the action of Pt nanoparticles. Proposed mechanism of their action has been illustrated in Figure 88c and as it was already described, photoelectrons which were formed by some of described mechanisms are collected or trapped within these particles. This is the way how they are kept safe from recombination and remain active for extension of material's action even when it has been kept in the dark.

In summary, HAp/Pt has been designed as a novel biophotocatalyst able to provide light-induced activity. Component used for formation of this material were carefully selected in order to exclude possibility for harm effect to human and environment. Apatite as a component of biomaterial significantly contributes to the properties important for its biomedical application (Vukomanović et al, 2011a, Vukomanović et al., 2011b,

Vukomanović et al., 2011c; Vukomanović et al., 2011d; Vukomanović et al., 2012a). Specific properties of the surface of this material are crucial for its biocompatibility (Vukomanović et al., 2012a). Hydrophilic nature of the HAp and high density of the surface polar groups, are very important because they provide potential for design of this material according to demands of different biomedical applications. One of the illustrative examples has been shown in this work when HAp has been designed for intensive UV/VIS photocatalytic activity. After activation of the material according to described mechanism it has ability to provide highly efficient process of photocatalytically induced degradation of non-degradable dyes.

Antibacterial action of HAp/Pt composite

Highly efficient photocatalytic activity of HAp/Pt showed ability of this material to induce production of active radicals. These radicals are involved in the process of degradation of the dye. Consequently, it was expected that these radicals could be used for induction of radical-induced oxidative stress- suggested as the main mechanism of antibacterial activity of silver (Wong and Liu, 2010).

The reactive oxygen species (ROS) are normally produced in cells- especially in complexes I and II which have been concerned as the primary sites of the production of these species in mitochondria. These species are involved in respiratory process, signal transduction and in general to the regulation of the redox state of the cell. Oxygen radicals could be beneficial because they are used in prevention of aging process (Gems and Partridge, 2008) and immune system used them in inactivation of the pathogens (Segal, 2005). However, overproduction of these species and inability of cells to inactivate them result in development of oxidative stress. Oxidative stress leads to the change of the redox state of the cell and may cause its dysfunction because formed radicals could damage cell compartments including proteins, lipids and nucleic acids (Schafer and Buettner, 2001). Complex I is present in mitochondrial inner membrane and this enzyme is involved in the oxidation of coenzyme nicotinamide adenine dinucleotide from NADH to NAD^+ form and reduction of ubiquinone (CoQ) to ubiquinol (CoQH) resulting in the transport of electrons from NADH to CoQ (Vogel et al., 2004). CoQH is an essential antioxidant in defence against oxidative stress (Åberg et al., 1992).

Recently, it has been determined that Pt nanoparticles can act very similarly to the mitochondrial electron transfer complexes (Hikosaka et al., 2008). These nanoparticles have potential for electron transfer which may be useful for design of photocatalyst because they are involved in the separation of the charge induced by absorption of the light. They are able to accept photoelectrons and to transfer them to the water to perform reduction and formation of reactive radicals. It was the principle applied for design of HAp/Pt composite. However, because of their ability to accept and release electrons, they can oxidize NADH to NAD^+ and reduce CoQ to CoQH. They do not have ability to connect these reactions into cycling transfer of electrons from NADH to CoQ, like it is achieved by mitochondrial electron transfer complexes; however they are still involved in production of CoQH antioxidant which has possibility for inactivation of photocatalytically formed radicals and to suppress oxidative stress.

HAp/Pt composite has strong photocatalytically-induced self-cleaning ability and exerts a tendency to affect bacterial growth. These properties may be related to the electron transfer in Pt which: (i) supports formation of active radicals for photocatalitycally induced degradation of dyes, but (ii) suppress formation of these radicals in living surroundings (when live bacteria cells are present) reducing oxidative stress that decrease antibacterial activity of photocatalyst. The observed performances of this material indicate that photocatalytic mechanism needs to be coupled with additional

non-oxidative-stress-induced process in order to gain self-cleaning activity coupled with significantly high antibacterial activity. This conclusion can be supported by comparison of results obtained for HAp/Pt to those obtained by HAp/Ag composite. In contrast to the low antibacterial activity of HAp/Pt, after irradiation by VIS light under the same conditions Ag-contained material showed much more intensive antibacterial activity. Different form the Pt nanoparticles, ability for trapping electrons was not observed for Ag nanoparticles. Ag nanoparticles are involved in intensive production of active radicals without possibility for their suppression (AshaRani et al., 2009). This property makes Ag material highly active in the process of photocatalitically-induced self-cleaning (Malagutti et al., 2009) as well as very strong antibacterial agent (Marambio-Jones et al., 2010). However, induction of oxidative stress is the point where intensive toxicity of Ag comes from (AshaRani et al., 2009). This topic is going to be discussed in later chapters.

Because of the limited antibacterial activity HAp/Pt composite material was not considered for further cytotoxic study. However its limited ability to destroy the bacterial membrane in order to cause bacterial death may be in some context correlated to its decreased toxicity and inability to destroy membrane of other living organisms such as human or at least human- and environmental- beneficial bacteria. It means that opposite toxicity to the one obtained for HAp/Ag could be expected. If so, formation of HAp/Pt succeeded in overcoming one of the issues of Ag nanoparticles related to their cytotoxicity. So far designed properties of HAp/Pt provide possibility for the use of this material for formation of self-cleaning coatings which are very important for the surfaces used in biomedicine (Vukomanović et al., 2012b).

5.2.2 Antibacterial action of hydroxyapatite/silver and hydroxyapatite/gold

HAp composites with Au nanoparticles were also tested for photocatalytic activity according to the same procedure used for the testing of HAp/Pt. Investigation was performed on HAp/Au without functionalization obtained during thermal reduction as well as on HAp/Au materials with different amino acid and thiol/amine functionalizations obtained by chemical reduction. None of these materials solely were able for this type of activity. In the case of HAp/Au without functionalization there was a close, mechanical attachment of Au particles onto HAp surface which is needed for a charge transfer between semiconductor and metallic nanoparticles. However, different from the HAp/Pt where HAp was functionalized by Pt-complexes, in the case of thermally obtained HAp/Au functionalization did not occurred and there were no conditions for light-induced photocatalytic activity following the same mechanism proposed for HAp/Pt (Figure 88). In the case of the second group of HAp/Au composites prepared by chemical procedure and with functionalized surface of Au nanoparticles (indirectly functionalized HAp surface) this activity was absent most probably due to the lack of mechanical contact between HAp and Au nanoparticles as well as due to the presence of large quantity of defects since these materials were not calcined. Nevertheless, absence of photocatalitically induced activity of these materials indicates their inability to produce active radicals that drives dye degradation process. Thermally formed HAp/Au was unable for antibacterial activity. However HAp/Au composites with functionalized surface were able for this type of activity with intensity which depended on the type of functionalizing molecule. The strongest antibacterial activity has been achieved in materials functionalized by amino acids and in some cases they were much efficient compare to HAp/Ag. Consequently, it means that antibacterial activity of this type of developed HAp/Au composites depended on functionalization and, in contrast to HAp/Ag, it was not induced by oxidative stress as the main mechanism.

Comparison between antibacterial activity of HAp/Ag and activity of newly developed HAp/Au materials was conducted by detailed investigation of activity of these materials against two types of bacteria- representatives of Gram positive and Gram negative bacteria, performed under the same conditions.

HAp/Ag antibacterial activity

According to numerous studies performed on Ag nanoparticles, Ag composites (polymer, glass of ceramic incorporated or deposited Ag particles), Ag-coatings (layers), Ag-compounds, ceramic- or glass- doped Ag-ions or polymer- incorporated Ag-ions or nanoparticles, different processes are included within mechanism of antibacterial activity of this metal (Sharma et al., 2009). Its activity against bacteria was classified into activity of: (i) Ag bulk, (ii) Ag-ions and (iii) Ag nanoparticles.

(i) Mechanism of antibacterial activity of Ag-bulk includes interaction between Ag surface and thiol groups that are present in membrane proteins of bacteria. These proteins are enzymes involved in the process of respiration. After interaction, respiration of bacteria is inhibited and bacteria die. However, this procedure is applicable only for aerobic bacteria. Alternatively, contact between bacteria and Ag-surface induce structural changes of proteins within bacterial wall.

(ii) Mechanism of antibacterial action of Ag-ions is associated with morphological and structural changes. It was observed experimentally that Ag-ions have potential to interact with proteins and nucleic acids and to inactivate their functions as well as the process of their synthesis. Besides loosening the function, these macromolecules change their structural and conformational characteristics. In addition, Ag-ions are associated with production of ROS species.

(iii) Mechanism of antibacterial activity of Ag nanoparticles is associated with increased ability for attachment of these particles onto bacterial membrane. Consequently, membrane-proteins are inactivated and they are able for crossing the membrane to the interior of bacteria. Inside bacteria these particles are dissolved and formed ions react with nucleic acids and proteins (Rai et al, 2009). Formed ions are able to induce production of ROS species. For nanoparticles, selectivity based on the shape, size and structure has been also included within mechanism of their action. For example, smaller particles (1-10 nm) are more active since they diffuse inside cells while larger are attached onto the surface of bacterial wall (Morones et al., 2005). In some cases ability of Ag-nanoparticles to induce bacterial cell damage directly and without dissolving is suggested. Mechanism was described as a contribution of electrostatic forces or by their ability to induce pit-shaped defects in membrane (Marambio-Jones, 2010). It is still unclear how negative Ag-particles cross the membrane (and they do cross it) and why these mechanical damages in bacterial wall are formed.

These mechanisms suggested for antibacterial activity of different forms of silver are overlapped. It suggests existence of one simple mechanism that could be amplified or reduced depend on the physicochemical properties of silver-form (bulk, ions or nanoparticles). So-far developed materials usually contained one or two forms of silver. Material which was synthesized in this work contained three different sources of silver: (i) silver nanoparticles attached onto HAp surface, (ii) Ag nanoparticles incorporated within HAp planes and (iii) Ag-ions doped into HAp structure. Ag has been present in two structures- cubic and hexagonal that corresponded to different particle shape- spherical and hexahedron. Besides, if size is concerned Ag particles within this material were grouped into two classes- small (a few nanometres in size) and larger (up to 20 nm in size) (Vukomanović et al., 2011d). According to the all previously proposed mechanisms here-presented HAp/Ag composite should have extraordinary antibacterial properties since every of this variations in size, shape, state and structure will contribute

to its total antibacterial activity by its specific antibacterial mechanism. However, it was not the case. Develop material was highly toxic; however according to its MIC and MBC concentrations, its antibacterial activity was not drastically amplified.

During investigations of antibacterial characteristics and solubility of HAp/Ag under different acidities of the medium starting from physiological (pH=7.4) to slightly (pH=5.4) and strongly acid (pH=3.4), material showed significant ability to release Ag-ions. Moreover, its activity against bacteria was increased after irradiation by VIS light. It was also observed that material was able to induce significant damages in bacterial wall which were manifested as mechanical ruptures.

Oxidative stress induced by overproduction of reactive radicals is mechanism used by host immune system to fight with pathogens. It has been shown that different metals, including iron (Fe), chromium (Cr), copper (Cu), cobalt (Co), cadmium (Cd) and vanadium (V), are able to induce oxidative stress. Many enzymes included within natural metabolite processes in the cell contain these metals in complexed form. However, if they are present in non-protected form, such as free ionic form, resulted oxidative stress is significantly increased (Valko et al., 2006). It is the case of Ag-containing materials. All bulk, nanoparticles or doped ions have a distinct possibility to release Ag-ions, free form of reactive silver able to induce production of reactive radicals and to induce oxidative stress.

Oxidative stress can have different levels depend on the type of produced reactive species. Production of reactive oxygen species is associated with production of free radicals, hydroxides, superoxides and peroxides. However, in the presence of unprotected forms of transition metals (such as Ag) these radicals are transferred into highly aggressive forms able to induce significant damages in bacterial cells, to affect proteins and nucleic acids as well as to induce damage of mitochondria resulting in inhibition of respiratory process (Valko et al., 2005; Valko et al., 2006). Very high levels of oxidative stress are able to induce damage of ATP depletion (Lelli et al., 1998). In that case controlled apoptotic death is disabled and cell is fallen apart which results in necrosis (Lee and Schacter, 1999). It means that significant mechanical damages of the bacterial cells induced by HAp/Ag composite are consequence of high level of oxidative stress present as the main mechanism of antibacterial action of this material.

HAp/Au antibacterial activity

In comparison to described antibacterial activity of HAp/Ag composite driven by initiation of non-selective oxidative stress, in the case of HAp/Au composites mechanism of action was different. Amino acid- functionalized HAp/Au had the strongest antibacterial activity among all functionalized materials (Vukomanović et al., 2012c). During investigation of the properties of these materials it was observed that: (i) HAp/Au/amino acid composites have very strong antibacterial activity that was stronger than activity of HAp/Ag in the case of Gram negative bacteria, (ii) materials were unable for production of reactive radicals and (iii) morphological changes induced on the bacterial wall did not concerned appearance of visually-detectable mechanical ruptures although nanoparticles were observed on the surface as well as inside bacterial cells. These were useful directions for suggestion of the mechanism of these types of materials in the action against bacteria.

Among numerous antibacterial agents and very different modes of their activity, (Simmons et al., 2010) developed HAp/Au materials have the most similar properties to the properties of antibacterial peptides (Hancock and Sahl, 2006). Antibacterial peptides are natural-sourced molecules usually isolated from insects, sea animals, algae or plants known as ingredients of host-developed immune system (Shi et al., 1994; Sagisaka et al., 2001; Liu et al. 2009). Some of the representative examples are honeybee antibacterial

peptide formed of 18 amino acid residues containing a few arginines (hydrophilic and charged) and the rest of proline (hydrophobic) (Taguchi et al., 1996); glycine-rich peptide form spider craba (Sperstad et al., 2009) and histidine-rich glycoprotein found in blood plasma of different vertebrates (including humans) (Jones et al., 2005). The main properties of these peptides/proteins are:

(i) Amphipathicity (hydrophobic and hydrophilic building blocks)

(ii) Charge (they are ions)

(iii) Amino acid- caused antibacterial activity (due to the charged amino acid residues)

These peptides are made of a specific sequence of amino acid residues containing a few charged hydrophilic amino acids and majority of the rest which are hydrophobic. They are building blocks of the hydrophilic and hydrophobic domains that form the structure of these peptides. Amphipathicity of these molecules provide them crossing the membrane and interaction with both, hydrophobic and hydrophilic components of membrane lipid bilayer. The main mechanism of their action is based on electrostatic interactions. Amino acid- residues with the charged groups make the whole peptide soluble ion (cation or anion). These charged molecules may attach the surface of the cellular wall and to disrupt its structure or/and to change permeability of the membrane, to cross it and enter the bacterial cell. Inside cell they affect intercellular compartments or they are involved in some essential functions as protein synthesis, membrane synthesis, nucleic acid structure etc. (Hancock and Sahl, 2006; Cinte et al., 2007).

Comparable properties possess HAp/Au composite particles. These particles also have amphipathic nature and their structure could be presented through hydrophilic and hydrophobic domains. Gold has hydrophobic, inert and non-reactive nature (Dreaden et al, 2012). Therefore hydrophobic building block of the composites is metallic part. Hydrophilic parts of the composites are HAp surface and amino acid functionalization. They are making hydrophiling building blocks of the composites. Hydrophobic Au nanoparticles functionalized by hydrophilic amino acids are attached onto the hydrophilic surface of HAp template. So formed structure may presents possible analogue to the natural-sourced antibacterial peptides.

The most important property of these particles, which is also the most important property of antibacterial peptides and the essence of their antibacterial activity (Hancock and Sahl, 2006), is their charge. It was determined that HAp/Au/amino acid particles are negatively charged. Arginine, glycine and histidine amino acids used for functionalization have charged, nonpolar and polar side chains, respectively. Arginine side chain contains three amino- groups and at pH=7.4 all of them are positively charged (Streitwieser and Heathcock, 1985). Consequently, addition of these positive groups decreases the magnitude of negative charge of HAp/Au composite from -14 mV for non-functionalized to -2.6 mV for arginine-functionalized composite particles. Histidine is amino acid with polar heterocyclic aromatic amines in the side chain which is charged only in acidic environment while glycine has nonpolar side chain (Streitwieser and Heathcock, 1985). In histidine and glycine charge comes from the main chain where NH_3^+ is used for attachment onto Au nanoparticles while COO^- groups are free and contribute to the negative charge which is increased from -14 mV for non-functionalized HAp/Au to -22 mV for glycine- and to -21 mV for histidine- functionalized HAp/Au.

Additional property of HAp/Au composite is ability for interaction with proteins. So far, these interactions have been intensively studied and there are numerous examples that confirm ability for Au-induced immobilization of protein on HAp/Au composite. It has been shown that HAp/Au has potential to be immobilized onto collagen. This sort of interaction is very important since collagen contains approximately 30% of the net weight of proteins in mammalian organism and it is responsible for the strength and stability of

different organs starting from the skin to the bones. Process of immobilization of collagen, as biomacromolecule, is assigned to the Au-collagen interactions (Aryal et al., 2006). Similar was observed for haemoglobin, redox protein responsible for the storage and transport of molecular oxygen in the blood of vertebrates. Au was able to interact with the haemoglobin and after immobilization HAp and Au had synergic contribution to the electron transfer in this protein (You et al., 2009). Fibrin, protein responsible for wound healing and blood clotting in the organism, with osteoconductive property is also capable to interact with Au and to be immobilized onto HAp/Au composite (Sastry et al., 2008). During investigation of the interactions between HAp, deposited onto Au base, with fibrinogen (structural protein of blood plasma) showed structural and conformational impact onto protein (Monkawa et al., 2006).

According to the following properties of HAp/Au composite with amino-acid-functionalized surface: (i) dual nature of HAp/Au/amino acid composites (hydrophilic and hydrophobic), (ii) presence of charged, amino-acid-sourced groups at the surface of material and (iii) general ability of HAp/Au to interact with different types of proteinsa mechanism very similar to the mechanism of antibacterial peptides could be proposed. Within this mechanism differences in the activity of materials functionalized by arginine (with positively charged surface groups) as well as glycine and histidine (with negatively charged surface groups) are highlighted.

Due to the strongly negative surface of bacteria membranes (Hancock and Sahl, 2006) and presence of negative groups at the surface of HAp/Au/arginine, electrostatic interactions among them are very intensive. These interactions are capable to affect the structure of bacterial cells (since all components of the cell in general are brought together by electrostatic forces) and/or to affect permeability of the membrane.

For HAp/Au/glycine and HAp/Au/histidine situation is slightly different since they have negatively charged groups at the surface that are been repulsed by negatively charged surface of bacteria. However, ability of HAp/Au to interact with proteins that result in their immobilization onto the surface may be involved in the way of their action against bacteria. HAp/Au has potential to interact with membrane proteins and to change their conformation. This type of interaction provides Au nanoparticles to cross the membrane and to get inside the bacterial cell.

Both types of proposed antibacterial actions of HAp/Au composites concern structural modifications in bacterial membrane as initial step. Possible reason for the differences in their activity against Gram positive and Gram negative bacteria may be associated with the difference in the structure of their wall. Gram negative bacteria have outer membrane (lipopolysaccharide layer and proteins) at the outer surface while Gram positive bacteria do not have outer membrane and they possess peptidoglycan at the surface (Seltmann and Holst, 2001).

Despite the similar mechanisms of action between antibacterial peptides and here-presented HAp/Au/amino acids, some of the benefits of the newly developed composites concerns higher mobility as well as higher chemical and structural stability of functionalized Au nanoparticles compare to the large peptides. Consequently, the same mode of antibacterial action could be improved by selection of more stable material and higher efficiency could be expected.

5.3 *In vitro* release of metal-ions and cytocompatibility of hydroxyapatite/metal composites

During investigations of toxicity, HAp/Ag and HAp/Au were firstly tested for metal-ion release and in the next step materials were tested for interaction with human osteosarcoma and human lung fibroblast cells.

Investigations of metal-ion-release were performed under three different pH values of release media: (i) physiological, (ii) slightly acidic and (iii) strongly acidic environments. This type of investigation was important since bacteria, which have exotoxins usually excrete acidic substances. It means that mechanism of the material interaction with them could be triggered by the change of pH since it can induce higher ion-release. The second reason why this type of investigation was important concerns ability for dissolution of nanoparticles in the regions with different acidities. It should be taken into consideration that nanoparticles are able of free diffusion into every compartment of the cell. Some of them are very acidic and my result in nanoparticles dissolution. Consequently local increase of the concentration of ions can induce toxicity.

Second step in investigation of the toxicity was analysis of the interaction of materials with human cells. In contrast to the literature where concentrations selected for testing of the toxicity are usually randomly selected, in this case toxicity was evaluated for MIC concentrations of materials. These are applicable concentrations of material able to induce inhibition of bacterial growth.

Cytotoxicity of HAp/Ag

During investigation of release of Ag-ions it was determined that HAp/Ag composite has possibility to release high concentration of these metallic ions and that this process depended on the acidity. It could be explained as increased solubility of Ag-nanoparticles due to the high contact to the surrounding liquid as well as release of Ag-ions incorporated within HAp structure. Decreased values of pH increase dissolution of HAp, which has potential for release of ions incorporation within its structure.

As it was already discussed, this material has oxidative stress as the main mechanism for antibacterial activity and it is associated with released metallic ions. The same activity possesses immune system and it is the central point of its interactions with pathogens. However, formed ROS species are non-selective and they are able to destroy host tissue together with the cell of pathogens. It was proposed that these ions are involved in ROS production. These radicals have their special role in the mechanism of antibacterial activity of this metal since they interact with membrane proteins and affect their conformation. Destroying the structure of intermembrane proteins affects integrity of the membrane and disintegrates it by formation of mechanical defects. The same is with the structure of host, mammalian cell (Lee and Schacter, 1999; Lelli et al., 1998).

Cytotoxicity of HAp/Au

During investigation of the interactions of HAp/Au composites functionalized by amino acids with human cells materials showed significantly increased cytocompatibility in comparison to highly toxic HAp/Ag. Moreover, among different amino acids used for functionalization, arginine showed the lowest cytotoxicity and the high concentration of this composite was required in order to initiate apoptosis and necrosis. Two reasons were responsible for this type of interaction of HAp/Au materials with human cells:

(i) Higher chemical stability – more than three times lower concentration of released Au-ions and inability for ROS production.

(ii) Higher selectivity of positively charged arginine in comparison to negatively charged glycine and histidine functionalizations.

First and the most important reason of significantly enhanced compatibility of

HAp/Au/amino acids in comparison to HAp/Ag is caused by more than three times lower concentrations of released Au-ions compare to the concentration of released Ag-ions and inability of these material to induce formation of reactive radicals. It means that induction of large-level oxidative stress was prevented (Valko et al., 2005; Valko et al., 2006).

Second reason for good compatibility was charge which was the main reason for better compatibility of arginine-functionalized compare to glycine and histidine- functionalized HAp/Au composites. As it was already mentioned, one of the very important properties of antibacterial peptides, which have the most similar antibacterial activity to the one obtained for HAp/Au composites with amino acids, concerns the fact, that these molecules have high level of selectivity. It provides them to make a difference between mammalian cells and cells of the bacteria. This property of antibacterial peptides is based on difference in the charge of the surface. Mammalian cells have less negative membranes compare to the bacterial cells which means that ionic molecule has different affinity to these host and pathogen surface which has special role in decreasing of the toxicity (Hancock and Sahl, 2006). Bacterial membrane contains strongly negatively charged phospholipids and antibacterial peptides interact with them mainly through electrostatic interactions. For mammalian and plant cells, outer side of the membrane contains mostly electroneutral zwitterionic form of phospholipids (phosphatidylcholine and sphingomyelin) and very low portion of negatively charged once (gangliosides). It means that interaction between mammalian cells and amphiphilic drug-molecule depends on interactions between zwiterionic electroneutral phospholipides of membrane and hydrophobic part of the molecule. HAp/Au/glycine and HAp/Au/histidine have highly negative surface which means that they are able to interact with both, bacterial and mammalian cell, which make them non-selective. However, this problem is completely overcomed by HAp/Au/arginine. Positively charged guanidine group with delocalized charged among all three amines allows very good selectivity. Due to the positive charge, material has much higher affinity for interaction with strongly negative surface of bacteria, compare to the less negative or positive surface of mammalian cells.

Unlike other metals, gold has very high resistance for corrosion and low ability to induce allergic reaction in live organism which are properties very important for *in vivo* conditions (Wiesenfeld, 1984; Brook, 2006). Accordingly, HAp/Au material functionalized by arginine binds two significant properties which are ability for high antibacterial activity and very high cytocompatibility with human cells. These properties make it highly perspective for biomedical applications as material with high potential to replace silver in all fields in which this toxic metal is currently applied.

6 Conclusions

In this work, homogeneous sonochemical precipitation was optimized as a new method for the synthesis of Ag, Au and Pt nanoparticles and their composites with hydroxyapatite. Three different strategies have been developed in order to optimize performance of each of the three noble metals selected to be centres of antibacterial activity. Hypothesized possibilities for their formulation using sonochemical approach, complexation before reduction and influence of the temperature factor have been confirmed.

The first strategy concerned design of HAp/Ag composite containing silver as metal with natural antibacterial activity in order to reach high performance of finally-formed material. It has been determined that composite particles obtained as the final outcome were composed of: (a) Ag ions incorporated into the apatite crystal structure, (b) smaller Ag particles embedded within the apatite plates and (c) larger Ag particles attached to the surface of these plates. The structure of the smaller and larger Ag particles in these systems is different (cubic and hexagonal). The optimization of the synthesis process revealed that the obtained properties of this material can be controlled by applying a particular type of the silver precursor, i.e., by making the selection with regard to its thermal properties that control the particle growth. A selection of precursors with a lower decomposition temperature enables the initiation of a rapid reduction process and the formation of the small Ag seeds during the sonication step. A second, thermal reduction, step is a slow process that uses sonochemically formed seeds for the formation of hexagonal Ag particles. The HAp surface has a special role in the formation of Ag particles within the HAp/Ag composite, preventing their aggregation and contributing to their growth. Used sonochemical approach makes it possible to control the phase composition in the system obtained before the reduction process and to influence the rate of silver reduction. Consequently, the structural and morphological properties of the metallic and metal/apatite composite nanoparticles are affected, which results in the formation of materials with an unusual design with the ability to provide very interesting activity against bacteria.

Based on obtained results it was concluded, that the main driving force of antibacterial activity of HAp/Ag was oxidative stress. Under physiological conditions material is able to release high concentrations of Ag-ions, which participate in formation of reactive radicals able to destroy structure and functionality of bacterial cells. Increasing of the acidity increases HAp/Ag solubility as well as the content of released Ag-ions. This conclusion also explains extremely high toxicity of silver. When the same concentration of HAp/Ag which was effective against bacterial growth was applied for cells, result was necrosis of almost 100% of human cells during 1h. High-level oxidative stress had the same effect to human cells as to the bacteria. It confirms toxicity of silver and explains its highly non-selective mechanism able to affect and destroy function of every living cell.

The second strategy concerned design of HAp/Pt composite with platinum as bioinert and non-reactive noble metal without natural ability for antibacterial activity. The idea for activation of this metal started from the fact, that a combination of photons and carefully designed nanostructures has potential for achievement of highly effective photocatalytic activity. Such systems have an enormous field of application, including basic hygiene and

health-care as well as water and earth purification and energy production. The special design of these materials depends on selection of building blocks and achievement of their arrangement into ordered structures. It has to be emphasized that the usage of plasmonic nanostructures belongs to perspective directions for the design of this type of materials. All demands needed for development of the described special design of photocatalyst could be achieved by directing the photocatalytic process to the field of biomaterials design. The main advantage of this approach is that the selection of natural building blocks is capable for estimation of: (i) high efficacy of photocatalytic process and (ii) increasing the compatibility of these systems with humans and the environment. Described approach has been used for formation of a novel bio-photocatalyst – a hybrid semiconductor/metallic composite made of hydroxyapatite submicrometre-sized plates with platinum metallic nanoparticles attached to their surface and two different types of surface-adsorbed Pt-complexes.

It was determined that newly developed HAp/Pt material provided highly effective photocatalytic activity after irradiation by visible or ultraviolet light. Its activity is extended during the period when it is kept in the dark. Accordingly, mechanism of photo-induced activity of HAp/Pt in the process of degradation of non-degradable dye has been proposed. The mechanism associates every component of so-designed material with a distinct role in its photon-induced activity. HAp is responsible for UV activity. Excitations induced by adsorption of the UV light result in transitions of electrons from valence to conductive band of HAp semiconductor and they are driving force for UV activity of the composite. So-formed electrons are transferred from HAp conduction bend to Pt nanoparticles which are mechanically attached onto HAp surface. Activity of material by VIS light is provided by Pt-complexes physically or chemically adsorbed onto HAp surface. Photons of VIS light are able to induce excitations of these complexes. Excited electrons are transferred to HAp conductive band. In the next step, complexes are relaxed while formed electrons are further on transferred to Pt nanoparticles. Electrons stored in Pt nanoparticles enable activity in the dark.

Low-efficacy antibacterial activity of HAp/Pt composites led to the conclusions that there is a need for coupling additional process to its photocatalytic activity in order to emphasize antibacterial activity of this material. Despite ability of developed HAp/Pt material to induce very intensive photo-induced degradation, which was the strongest after irradiation by VIS light, after irradiation by the same light, the material had low ability to suppress bacterial growth. It is speculated that the main reason for such response is in Pt nanoparticles. Under physiological conditions they are able to induce oxidoreduction of some macromolecules that have a role of antioxidant with possibility to inactivate formed reactive radicals. Consequently, there are no conditions for development of high-level oxidative stress required for intensive antibacterial activity as it was achieved for HAp/Ag composite.

Inability of HAp/Pt to induce oxidative stress highlights possibility for its non-toxicity for living cells. The concept of the formation of a bio-photocatalyst formed of building blocks selected from the nature introduces this type of materials as advanced self-cleaning systems. From that point of view, it could be expected that the obtained design of this bio-photocatalyst has the potential to provide very interesting outcome, important for its practical application since combination of photocatalitically-VIS-induced self-cleaning and non-toxicity are properties highly useful for formation of coatings applicable in biomedicine.

The third strategy concerned development of HAp/Au composite formed of HAp bioactive carrier and activated Au noble metal as centre of antibacterial activity. As for the platinum, gold also has bioinert and non-reactive nature. Its activation for activity against bacteria was induced by functionalization. Attachment of the specially-selected

molecules onto the surface of gold is one of the highly efficient approaches for its bioactivation for different functions such as therapeutic (attachment of drugs, such as antibiotics or anticancer agents, for target drug delivery), sensing (attachment of the recognition moieties such as antibodies or oligonucleotides for targeted detection of specific macromolecules responsible for some disease) and imaging (contrasting of the specific molecules, cells or tissues for the purpose of *in vivo* detection inside organism). Novel idea used in this work was to use molecules without antibacterial activity to functionalize Au surface in order to form structure, which will be able to use all its building blocks as well as their joints for creation of this type of activity.

It was determined that finally-formed HAp/Au composites contained HAp plate-like particles with Au nanoparticles with functionalized surface attached onto apatite plates. The most stable composites were obtained by functionalization using amino acids since the presence of dual groups. One part of these molecules was used for attachment onto Au surface by amine groups, while the opposite side of the molecule remained free or attached onto HAp. Sonification had important contribution to the process of functionalization since acoustic cavitation, which was enhanced by addition of small concentration of low surface tension alcohol, facilitated reduction process and provided activation of functionalizing molecules.

As it was hypothesized, modification of the surface activated antibacterial activity of noble metals. It was concluded that the basis of so-design material was the formation of an amphyphylic structure containing hydrophilic and hydrophobic components. While hydrophobic components were Au nanoparticles, surface attached molecules with the presence of reactive, polar groups were hydrophilic components. Dual groups in amino acids able to contribute to the charge of designed structures provided materials functionalized by them the most efficient. HAp/Au/amino acid composites were hydrophilic/hydrophobic structures and positively charged guanidine groups of arginine side chain or negatively charged carboxylic groups of glycine and histidine main chains. Amino acid-functionalized provided HAp/Au composites strong ability for antibacterial activity. Charge was used for destabilization of the structure and permeability of bacterial wall, while hydrophobic and hydrophilic domains allowed crossing the membrane and reaching the interior of the bacteria where these agents were involved in some of the metabolite processes or bacteria life cycle process essential for their life. Used approach for material design allowed formation of material with antibacterial activity stronger then HAp/Ag composite.

Mechanism of antibacterial activity of HAp/Au/amino acid composites based on electrostatic interactions was substantially different from the mechanism of HAp/Ag. Newly developed materials were unable for photocatalytic activity and they did not have possibility of excessive production of reactive radicals. However, HAp/Au functionalized by negatively charged molecules (glycine and histidine) were not selective and they had toxic influence to human cells. In opposite to them, HAp/Au functionalized by arginine had high level of selectivity. Positively charged protoned amines within guanidine group in side chain of this amino acid were able for intensive interaction with negatively charged bacteria walls and had significantly low affinity for interaction with positively charged human cells.

A novel approach of design of material by formation of metallic-bioceramic composite with the bioactivated surface of metallic component by functionalization showed high efficiency in development of antibacterial materials. It was the way for formation of human and environmental friendly material with strong activity against bacteria. Due to the developed selectivity and higher affinity for the action against bacteria then to the other cells and very strong activity against bacteria developed material has high potential to replace toxic and non-selective silver. All fields where silver is used as antibacterial

component are available to use more efficient HAp/Au/functionalization (arginine) replacement.

7 Acknowledgements

It is a great pleasure to thank the supervisor of this dissertation Assist. Prof. Dr. Srečo Davor Škapin for his essential contribution to all the stages of this PhD work and Prof. Dr. Danilo Suvorov, Head of the Advanced Materials Department at the Jožef Stefan Institute, for the advice, criticism and significant support that raised the quality of the presented work to a higher level. The author is grateful to Prof. Dr. Dragan Uskoković, co-supervisor of this dissertation, for providing her the knowledge which will always be the basis of her expertise.

The author would like to thank all the members of the Commission Board for their effort in evaluation of the presented dissertation.

The author is also grateful to the following colleagues for sharing the expertise and experience during their participation in different segments of this dissertation:

(i) Dr. Urška Repnik, Dr. Tina Zavašnik-Bergant and Prof. Dr. Boris Turk from Department of Biochemistry, Molecular and Structural Biology (B1) at the Jožef Stefan Institute for antibacterial and cytotoxicity investigations.

(ii) Prof. Dr. Rok Kostanjšek from Department of Biology at the Biotechnical Faculty for microscopic investigations of bacteria.

(iii) Dr. Janez Kovač from Department of Surface Engineering and Optoelectronics (F4) at the Jožef Stefan Institute for surface characterization of materials and evaluation of results.

(iv) Assist Prof. Dr. Ida Poljanšek (Faculty of Chemistry and Chemical Technology) and Dr. Polona Umek (Solid State Physics Department (F5) at the Jožef Stefan Institute) for spectroscopic measurements.

(v) Mrs. Vojka Žunič (Advanced Materials Department (K9) at the Jožef Stefan Institute) for photocatalytic measurements.

(vi) Dr. Manca Logar, Mrs. Ines Bračko and Mrs. Mojca Otoničar (Advanced Materials Department (K9) at the Jožef Stefan Institute) for TEM measurements.

The author is grateful to Mr. Saša Vukomanović for being an endless source of inspiration, support and understanding.

Marija Vukomanović

8 References

Åberg, F.; Appelkvist,E.-L.; Dallner, G.; Ernster,L. Distribution and redox state of ubiquinones in rat and human tissues. *Archives of Biochemistry and Biophysics* **295**, 230 (1992).

Abeylath, S. C.; Turos, E. Drug delivery approaches to overcome bacterial resistance to β-lactam antibiotics. *Expert Opinion on Drug Delivery* **5**, 931 (2008).

Andrews, J. M. Determination of minimum inhibitory concentrations, *Journal of Antimicrobial Chemotherapy* **48**, 5 (2001).

Angelucci, C. A.; Silva, M. D. V., Nartm, F. C., Preparation of platinum–ruthenium alloys supported on carbon by a sonochemical method. *Electrochimica Acta* **52**, 7293 (2007).

Apoptosis, http://www.flow-cytometry.us/index.php?page=apoptosis, (dostop: november, 2011).

Aronov, D.; Karlov, A.; Rosenman, G. Hydroxyapatite nanoceramics: Basic physical properties and biointerface modification. *Journal of the European Ceramic Society* **27**, 4181 (2007).a

Aronov, D.; Chaikina, M.; Haddad, J.; Karlov, A.; Mezinskis, G.; Oster, L.; Pavlovska, I.; Rosenman, G. Electronic states spectroscopy of Hydroxyapatite ceramics. *Journal of Materials Science: Materials in Medicine* **18**, 865 (2007).b

Arora, S.; Jain, J.; Rajwade, J. M.; Paknikar, K. M. Cellular responses induced by silver nanoparticles: In vitro studies. *Toxicology Letters* **179**, 93 (2008).

Arora, S.; Jain, J.; Rajwade, J. M.; Paknikar, K. M. Interactions of silver nanoparticles with primary mouse fibroblasts and liver cells. *Toxicology and Applied Pharmacology* **236**, 310 (2009).

Arumugam, S. K.; Sastry, T. P.; Sreedhar, B.; Mandal, A. B. One step synthesis of silver nanorods by autoreduction of aqueous silver ions with hydroxyapatite: an inorganic-inorganic hybrid nanocomposite. *Journal of Biomedical Materials Research* A **80**, 391 (2007).

Aryal, S.; Bahadur, R. K. C.; Bhattarai, S. R.; Prabu, P.; Kim, H. Y. Immobilization of collagen on gold nanoparticles: preparation, characterization, and hydroxyapatite growth. *Journal of Materials Chemistry* **16**, 4642 (2006).

AshaRani, P. V.; Mun, G. L. K.; Hande, M. P.; Valiyaveettil, S. Cytotoxicity and genotoxicity of silver nanoparticles in human cells. *ACS Nano* **3**, 279 (2009).

AshaRani, P. V.; Sethu, S.; Vadukumpully, S.; Zhong, S.; Lim, C. T.; Hande, P.; Valiyaveettil, S. Investigations on the structural damage in human erythrocytes exposed to silver, gold, and platinum nanoparticles. *Advanced Functional Materials* **20**, 1233 (2010).

Aslan, S.; Loebick, C. Z.; Kang, S.; Elimelech, M.; Pfefferle, L. D.; Van Tassel, P. R. Antimicrobial biomaterials based on carbon nanotubes dispersed in poly(lacticco-glycolic acid). *Nanoscale* **2**, 1789 (2010).

Australian Therapeutic Good Administration (TGA), Colloidal silver and related products, http://www.tga.gov.au/industry/cm-colloidal-silver.htm (dostop: december, 2011).

Aydin-Sevinc, B. A.; Hanley, L. Antibacterial activity of dental composites containing zinc oxide nanoparticles. *Journal of Biomedical Materials Research B Applied Biomaterials* **94**, 22 (2010).

Badrour, L.; Sadel, A.; Zahir, M.; Kimakh, L.; El Hajbi, A. Synthesis and physical and chemical characterization of $Ca_{10-x}Ag_x(PO_4)_6(OH)_{2-x}$ apatites. *Annales de Chimie: Science des Materiaux* **23**, 61 (1998).

Bai, X.; More, K.; Rouleau, C. M.; Rabiei, A. Functionally graded hydroxyapatite coatings doped with antibacterial components. *Acta Biomaterialia* **(6)**, 2264– 2273 (2010).

Baker, G. L.; Gupta, A.; Clark, M. L.; Valenzuela, B. R.; Staska, L. M.; Harbo, S. J.; Pierce, J. T.; Dill, J. A. *Toxicological Sciences* **101**, 122 (2008).

Bang, J. H.; Suslick, K. S. Applications of ultrasound to the synthesis of nanostructured materials. *Advanced Materials* **22**, 1 (2010).

Barefoot, R. R. Speciation of platinum compounds: a review of recent applications in studies of platinum anticancer drugs. *Journal of Chromatography B* **751**, 205 (2001).

Bellantone, M.; Coleman, J. N.; Hench, L. L. Silver-containing, sol-gel derived bioglass compositions. *WO00/76486A1* (2000).

Bhargava, S. K.; Booth, J. M.; Agrawal, S.; Coloe, P.; Kar, G. Gold nanoparticles formation during bromoaurate reduction by amino acids. *Langmuir* **21**, 5949 (2005).

Bhui, D. K.; Bar, H.; Sarkar, P.; Sahoo, G. P.; Prasad De, S.; Misra A. Synthesis and UV–vis spectroscopic study of silver nanoparticles in aqueous SDS solution. *Journal of Molecular Liquids* **145**, 33 (2009).

Bieri, N. R.; Chung, J.; Haferl, S. E.; Poulikakos, D.; Grigoropoulos, C. P. Microstructuring by printing and laser curing of nanoparticle solutions. *Applied Physics Letters* **82**, 3529 (2003).

Biris, A. S.; Mahmood, M.; Jensen, P. Advanced nanomaterials for regulating specific cell functions, *WO 2010/062561 A1* (2010).

Bokorny, S.; Stark, J. W.; Loher, F. S. Antimicrobial material. *WO2008/122131A1* (2008).

Bourg, M.-C.; Badia, A.; Lennox, R. B. Gold−Sulfur Bonding in 2D and 3D Self-Assembled Monolayers: XPS Characterization. *Journal of Physical Chemistry B* **104 (28)**, 6562 (2000).

Bozzola, J. J.; Russell, L. D. *Electron Microscopy* (Jones and Bartlett Publishers Inc., Boston, 1992).

Brady-Estévez, A. S.; Kang, S.; Elimelech, M. A single-walled-carbon-nanotube filter for removal of viral and bacterial pathogens. *Small* **4 (4)**, 481 (2008).

Bračko, I.; Jančar, B.; Logar, M.; Caglič, D.; Suvorov, D. Silver nanoparticles on titanate nanobelts via the self-assembly of weak polyelectrolytes: synthesis and photocatalytic properties. *Nanotechnology* **22**, 085705 (2011).

Brandl, D. W.; Oubre, C.; Nordlander, P. Plasmon hybridization in nanoshell dimers. *Journal of Chemical Physics* **123**, 024701 (2005).

Brook, M. A. Platinum in silicone breast implants. *Biomaterials* **27**, 3274 (2006).

Burgeth, G.; Kisch, H. Photocatalytic and photoelectrochemical properties of

titania/chloroplatinate(IV). *Coordination Chemistry Review* **230**, 41 (2002).

Carp, O.; Huisman, C. L.; Reller, A. Photoinduced reactivity of titanium dioxide. *Progress in Solid State Chemistry* **32**, 33 (2004).

Caruso, R. A.; Ashokkumar, M.; Grieser, F. Sonochemical formation of colloidal platinum. *Colloids and Surfaces A: Physicochemical and Engineering Aspects* **169**, 219 (2000).

Casaletto, M. P.; Longo, A.; Martorana, A.; Prestianni, A.; Venezia, A. M. XPS study of supported gold catalysts: the role of Au^0 and $Au^{+\delta}$ species as active sites. *Surface and Interface Analysis* **38**, 215 (2006).

Chamundeeswari, M.; Liji Sobhana, S. S.; Jacob, J. P.; Kumar, M. G.; Devi, M. P.; Sastry, T. P.; Mandal, A. B. Preparation, characterization and evaluation of a biopolymeric gold nanocomposite with antimicrobial activity. *Biotechnology and Applied Biochemistry* **55**, 29 (2010).

Chen, D. Design, synthesis and properties of highly functional nanostructured photocatalysts. *Recent Patents on Nanotechnology* **2**, 183 (2008).

Chen, W.; Cai, W.; Zhang, L.; Wang, G.; Zhang, L. Sonochemical processes and formation of gold nanoparticles within pores of mesoporous silica. *Journal of Colloid and Interface Science* **238**, 291 (2001).

Chen, W.; Liu, Y.; Courtney, H. S.; Bettenga, M.; Agrawal, C. M.; Bumgardner, J. D.; Ong, J. L. In vitro anti-bacterial and biological properties of magnetron co-sputtered silver-containing hydroxyapatite coating. *Biomaterials* **27**, 5512 (2006).

Chen, H. M.; Liu, R.-S. Architecture of metallic nanostructures: synthesis strategy and specific applications. *Journal of Physical Chemistry C* **115**, 3513 (2011).

Chen, Y. S.; Hung, Y. C.; Liau, I.; Huang, G. S. Assessment of the In Vivo Toxicity of Gold Nanoparticles. *Nanoscale Research Letters* **4**, 858 (2009).

Cheng, P.-T. Formation of octacalcium phosphate and subsequent transformation to hydroxyapatite at low supersaturation: model for cartilage calcification. *Calcified Tissue International* **40**, 339 (1987).

Cho, W. S.; Cho, M.; Jeong, J.; Choi, M.; Cho, H. Y.; Han, B. S.; Kim, S. H.; Kim, H. O.; Lim, Y. T.; Chung, B. H.; Jeong, J. Acute toxicity and pharmacokinetics of 13 nm-sized PEG-coated gold nanoparticles. *Toxicology and Applied Pharmacology* **236**, 16 (2009).

Choi, B.-h.; Lee, H.-H.; Jin, S.; Chun, S.; Kim, S.-H. Characterization of the optical properties of silver nanoparticle films. *Nanotechnology* **18**, 075706 (2007).

Choi, O.; Hu, Z. Size dependent and reactive oxygen species related nanosilver toxicity to nitrifying bacteria. *Environmental Science and Technology* **42**, 4583 (2008).

Choi, O.; Deng, K.; Kim, N.; Ross, L.; Surampalli, R.; Hu, Z. The inhibitory effects of silver nanoparticles, silver ions, and silver chloride colloids on microbial growth. *Water Research* **42**, 3066 (2008).

Choi, J. E.; Kim, S.; Ahn, J. H.; Youn, P.; Kang, J. S.; Park, K.; Yi, J.; Ryu, D. Y. Induction of oxidative stress and apoptosis by silver nanoparticles in the liver of adult zebrafish. *Aquatic Toxicology* **100**, 151 (2010).

Ciobanu, C. S.; Massuyeau, F.; Constantin, L. V.; Predoi, D. Structural and physical properties of antibacterial Ag-doped nanohydroxyapatite synthesized at 100 °C. *Nanoscale Research Letters* **6**, 613 (2011).

Cohen, M. L. Changing patterns of infectious disease. *Nature* **406**, 762 (2000).

Conte, M.; Aliberti, F.; Fucci, L.; Piscopo, M. Antimicrobial activity of various cationic molecules on foodborne pathogens. *World Journal of Microbiology and Biotechnology* **23**, 1679 (2007).

Costa, C. S.; Ronconi, J. V.; Daufenbach, J. F.; Gonçalves, C. L.; Rezin, G. T.; Streck, E. L.; Paula, M. M. In vitro effects of silver nanoparticles on the mitochondrial respiratory chain. *Molecular and Cellular Biochemistry* **342**, 51 (2010).

Dabrowski, A. *Adsorption and its application in industry and environmental protection*. (Elsevier, Amsterdam, 1999).

Daniel, M.-C.; Astruc, D. Gold nanoparticles: assembly, supramolecular chemistry, quantum-size-related properties, and applications toward biology, catalysis, and nanotechnology. *Chemical Reviews* **104**, 293 (2004).

Dastjerdi, R.; Montazer, M. A review on the application of inorganic nano-structured materials in the modification of textiles: Focus on anti-microbial properties. *Colloids and Surfaces B: Biointerfaces* **79**, 5 (2010).

De Araujo, T. S.; de Souza, S. O.; de Souza, E. M. B. Effect of Zn^{2+}, Fe^{3+} and Cr^{3+} addition to hydroxyapatite for its application as an active constituent of sunscreens. *Journal of Physics: Conference Series* **249**, 012012 (2010).

Dhar, S.; Daniel, W.L.; Giljohann, D. A.; Mirkin, C. A.; Lippard, S. J.; Polyvalent Oligonucleotide Gold Nanoparticle Conjugates as Delivery Vehicles for Platinum(IV) Warheads. *Journal of the American Chemal Society* **131**, 14652 (2009).

Di Nunzio, S.; Verne, E. Process for the production of silver-containing prosthetic devices. *EP1819372A1* (2007).

Diaz, M.; Barba, F.; Miranda, M.; Guitian, F.; Torrecillas, R.; Moya, J. S. Synthesis and antimicrobial activity of silver-hydroxyapatite nanocomposite. *Journal of Nanomaterials*, Art. Numb. 498505 (2009).

Diebold, U. Photocatalysts: Closing the gap. *Nature Chemistry* **3**, 271 (2011).

Dingeldein, E.; Gasqueres, C.; Witte, F.; Elizier, A. Osteosynthesis with nano-silver. *WO2010/139451A2* (2010).

Dominguez, M. I.; Romero-Sarria, F.; Centeno, M. A.; Odriozola, J. A. Gold/hydroxypatite cFatalysts synthesis, characterization and catalytic activity, *Applied Catalysis B-Environmental* **87**, 245 (2009).

Donlan, R. M.; Costerton, J. W. Biofilms: Survival Mechanisms of Clinically Relevant Microorganisms. *Clinical Microbiology Review* **15**, 167 (2002).

Dorozhkin, S. V. Calcium orthophosphates in nature, biology and medicine. *Materials* **9**, 399 (2009).

Dorozhkin, S. V. Bioceramics of calcium orthophosphates. *Biomaterials* **31**, 1465 (2010).

Dragnea, B. Bio-inspired materials: Unnatural life. *Nature Materials* **7**, 102 (2008).

Dreaden, E. C.; Mwakwari, S. C.; Sodji, Q. H.; Oyelere, A. K.; El-Sayed, M. A. Tamoxifen−Poly(ethylene glycol)−Thiol Gold Nanoparticle Conjugates: Enhanced Potency and Selective Delivery for Breast Cancer Treatment. *Bioconjugate Chemistry* **20**, 2247 (2009).

Dreaden, E. C.; Mackey, M. A.; Huang, X.; Kangy, B.; El-Sayed, M. A. Beating cancer in multiple ways using nanogold. *Chemical Society Reviews* **40**, 3391 (2011).

Dreaden, E. C.; Alkilany, A. M.; Huang, X.; Murphy, C. J.; El-Sayed, M. A. The golden age: gold nanoparticles for biomedicine. *Chemical Society Reviews* **41**, 2740 (2012).

Dykman, L.; Khlebtsov, N. Gold nanoparticles in biomedical applications: recent

advances and perspectives. *Chemical Society Reviews* **41**, 2256 (2012).

Ericsson, M.; Hanstorp, D.; Hagberg, P., Enger, J.; Nyström T. Sorting out bacterial viability with optical tweezers. *Journal of Bacteriology* **182**, 5551 (2000).

Estaban-Cubillo, A.; Pecharroman, C.; Aguilar, E.; Santaren, J.; Moya, J. S. Antibacterial activity of copper monodispersed nanoparticles into sepiolite. *Journal of Material Science* **41**, 5208 (2006).

Eufinger, K.; Poelman, D.; Poelman, H.; De Gryse, R.; Marin, G. B. Effect of microstructure and crystallinity on the photocatalytic activity of TiO_2 thin films deposited by dc magnetron sputtering. *Journal of Physics D- Applied Physics* **40**, 5232 (2007).

European Committee for Antimicrobial SusceptibilityTesting (EUCAST) of the European Society of Clinical Microbiology and Infectious Diseases (ESCMID). Determination of minimum inhibitory concentrations (MICs) of antibacterial agents by agar dilution. (EUCAST Definitive Document E.Def 3.1, 2000).

EU Food Standard Agency, Current EU approved additives and their E numbers. http://www.food.gov.uk/safereating/chemsafe/additivesbranch/enumberlist#h_2 (dostopp: december 2011).

Ewald, A.; Hösel, D.; Patel, S.; Grover, L. M.; Barralet, J. E.; Gbureck, U. Silver doped calcium phosphate cements with antimicrobial activity. *Acta Biomaterialia* **7**, 4064 (2011).

Federal Agency for Food and Drugs (FDA), Colloidal silver is not approved, http://www.fda.gov/AnimalVeterinary/NewsEvents/CVMUpdates/ucm127976.htm (dostop: december 2011).

Fricker, S. P. Medical uses of gold compounds: past, present and future. *Gold Bulletin* **29**, 53 (1996).

Funakoshi, K.; Nonami, T. Electrochemical properties of hydroxyapatite crystal surfaces on anatase photocatalysts. *Journal of the American Ceramic Society* **89**, 944 (2006).

Gao, Y.-H.; Zhang, N.-C.; Zhong, Y.-W.; Cai, H.-H.; Liu, Y.-L. Preparation and characterization of antibacterial Au/C core-shell composite, *Applied Surface Science* **256**, 6580 (2010).

Ge, X.; Leng, Y.; Bao, C.; Xu, S. L.; Wang, R.; Ren, F. Antibacterial coatings of fluorinated hydroxyapatite for percutaneous implants. *Journal of Biomedical Biomaterials Research A* **95**, 588 (2010).

Gems, D.; Partridge, L. Stress-response hormesis and aging: ‘‘That which does not kill us makes us stronger’’. *Cell Methabolism* **7**, 200 (2008).

Ghosh, P.; Han, G.; De, M.; Kim, C. K.; Rotello, V. M. Gold nanoparticles in delivery applications. *Advanced Drug Delivery Reviews* **60**, 1307 (2008).

Grace, A. N.; Pandian, K. Antibacterial efficacy of aminoglycosidic antibiotics protected gold nanoparticles—A brief study. *Colloids and Surface A: Physicochemical and Engineering Aspects* **297**, 63 (2007).

Gu, H.; Ho, P. L.; Tong, E.; Wang, L.; Xu, B. Presenting vancomycin on nanoparticles to enhance antimicrobial activities. *Nano Letters* **3**, 1261 (2003).

Gupta, Y.; Mathur, G. N.; Verma, S. Biomimetic synthesis and ultrastructural characterization of a zerovalent gold-hydroxyapatite composite. *Bioorganic and Medicinal Chemistry Letters* **16**, 363 (2006).

Hancock, R. E. W. and Sahl, H.-G. Antimicrobial and host-defense peptides as new anti-

infective therapeutic strategies. *Nature Biotechnology* **24**, 1551 (2006).

Harfenist, S. A.; Wang, Y. L.; Whetten, R. I.; Vezmar, I.; Alvarez, M. M. Three-dimensional hexagonal close-packed superlattice of passivated Ag nanocrystals. *Advanced Materials* **9**, 817 (1997).

Hashimoto, K.; Irie, H.; Fujishima, A. TiO_2 Photocatalysis: A Historical Overview and Future Prospects. *Japanese Journal of Applied Physics* **44**, 8269 (2005).

Hiehata, K.; Sasahara, A.; Onishi, H. Local work function analysis of Pt/TiO_2 photocatalyst by a Kelvin probe force microscope. *Nanotechnology* **18**, 084007 (2007).

Higby, G. J. Gold in medicine: a review of its use in the West before 1900. Gold Bulletin 15, 130 (1982).

Hikosaka, K; Kim, J.; Kajita, M.; Kanayama, A.; Miyamoto, Y. Platinum nanoparticles have an activity similar to mitochondrial NADH:ubiquinone oxidoreductase. *Colloids and Surfaces B: Biointerfaces* **66**, 195 (2008).

Hoffmann, M.; Edwards, J. O. Kinetics and mechanism of the oxidation of thiourea and N,N'-dialkylthioureas by hydrogen peroxide. *Inorganic Chemistry* **16(12)**, 3333 (1977).

Hou, Y.; Abrams, B. L.; Vesborg, P. C. K.; Bjorketun, M. E.; Herbst, K.; Bech, L.; Setti, A. M.; Damsgaard, C. D.; Pedersen, T.; Herbst, O.; Rossmeisl, J.; Dahl, S.; Norskov, J. K.; Chorkendorff, I. Bioinspired molecular co-catalysts bonded to a silicon photocathode for solar hydrogen evolution. *Nature Materials* **10**, 434 (2011).

Hribar, K. C.; Lee, M. H.; Lee, D.; Burdick, J. A. Enhanced release of small molecules from near-infrared light responsive polymer-nanorod composites. *ACS Nano* **5**, 2948 (2011).

Huang, X.; El-Sayed, I. H.; Yi, X.; El-Sayed, M. A. Gold nanoparticles: Catalyst for the oxidation of NADH to NAD^+. *Journal of Photochemistry and Photobiology B: Biology* **81**, 76 (2005).

Huang, W. C.; Tsai, P. J.; Chen, Y. C. Multifunctional Fe_3O_4@Au nanoeggs as photothermal agents for selective killing of nosocomial and antibiotic-resistant bacteria. *Small* **5**, 51 (2009).

Hsin, Y. H.; Chen, C. F.; Huang, S.; Shih, T. S.; Lai, P. S.; Chueh, P. J. The apoptotic effect of nanosilver is mediated by a ROS- and JNK-dependent mechanism involving the mitochondrial pathway in NIH3T3 cells. *Toxicology Letters* **179**, 130 (2008).

Huh, A. J.; Kwon, Y. J. "Nanoantibiotics": A new paradigm for treating infectious diseases using nanomaterials in the antibiotics resistant era. *Journal of Controlled Release* **156**, 128 (2011).

Hwang, K.-S.; Hwangbo, S.; Kim, J.-T. Silver-doped calcium phosphate nanopowders prepared by electrostatic spraying. *Journal of Nanoparticle Research* **10**, 1337 (2008).

Ignjatović, N.; Tomić, S.; Dakić, M.; Miljković, M.; Plavšić, M.; Uskoković, D. Synthesis and properties of hydroxyapatite/poly-L-lactide composite biomaterials. *Biomaterials* **20**, 809 (1999).

Ignjatović, N.; Ninkov, P.; Ajduković, Z.; Vasiljević-Radović, D.; Uskoković, D. Biphasic Calcium Phosphate/Poly-Dl-Lactide-Co-Glycolide Composite Biomaterial as Bone Substitute. *Journal of the European Ceramic Society* **27**, 1589 (2007).

Inoue, Y.; Hoshino, M.; Takahashi, H.; Noguchi, T.; Murata, T.; Kanzaki, Y.; Hamashima, H.; Sasatsu, M. Bactericidal activity of Ag-zeolite mediated by reactive oxygen species under aerated conditions. *Journal of Inorganic Biochemistry* **92**, 37 (2002).

Jain, P. K.; Huang, X.; El-Sayed, I. H.; El-Sayed, M. A. Review of Some Interesting Surface Plasmon Resonance-enhanced Properties of Noble Metal Nanoparticles and Their Applications to Biosystems. *Plasminics* **2**, 107 (2007).

Jena, B. K. and Raj, C. R. Electrochemical Biosensor Based on Integrated Assembly of Dehydrogenase Enzymes and Gold Nanoparticles. *Analytical Chemistry* **78**, 6332 (2006).

Jevtić, M.; Mitrić, M.; Škapin, S.; Jančar, B.; Ignjatović, N.; Uskoković, D. Crystal structure of hydroxyapatite nanorods synthesized by sonochemical homogeneous precipitation. *Crystal Growth and Design* **8**, 2217 (2008).

Jevtić, M.; Radulović, A.; Ignjatović, N.; Mitrić, M.; Uskoković, D. Controlled assembly of poly(D,L-lactide-co-glycolide)/hydroxyapatite core-shell nanospheres under ultrasonic irradiation. *Acta Biomaterialia* **5**, 208 (2009).

Ji, J. H.; Jung, J. H.; Kim, S. S.; Yoon, J. U.; Park, J. D.; Choi, B. S.; Chung, Y. H.; Kwon, I. H.; Jeong, J.; Han, B. S.; Shin, J. H.; Sung, J. H.; Song, K. S.; Yu, I. J. Twenty-eight-day inhalation toxicity study of silver nanoparticles in Sprague-Dawley rats. *Inhalation Toxicology* **19**, 857 (2007).

Jia, G.; Wang, H.; Yan, L.; Wang, X.; Pei, R.; Yan, T.; Zhao, T.; Guo, X. Cytotoxicity of carbon nanomaterials: single-wall nanotube, multi-wall nanotube, and fullerene. *Environmental Science and Technology* **39**, 1378 (2005).

Jiang, W.; Kim, B. Y. S.; Rutka, J. T.; Chan, W. C. W. C. Nanoparticle-mediated cellular response is size-dependent. *Nature Nanotechnology* **3**, 145 (2008).

Jin, S.; Oh, S. Articles comprising large-surface-area bio-compatible materials and methods for making and using them. *WO 2008/066965 A2* (2008).

Jones, A. L.; Hulett, M. D.; Parish, C. R. Histidine-rich glycoprotein: A novel adaptor protein in plasma that modulates the immune, vascular and coagulation systems. *Immunology and Cell Biology* **83**, 106 (2005).

Juhasz, J. A.; Best, S. M. Bioactive ceramics: processing, structures and properties. Journal of Materials Science **47**, 610 (2012).

Jung, W.; Koo, H.; Kim, K.; Shin, S.; Kim, S.; Park, Y. Antibacterial activity and mechanism of action of the silver ion in Staphylococcus aureus and Escherichia coli. *Applied and Environmental Microbiology* **74**, 2171 (2008).

Kamat, P. V. Photoinduced transformations in semiconductor-metal nanocomposite assemblies. *Pure and Applied Chemistry* **74**, 1693 (2002).

Kazachenko, A. S.; Legler, E. V.; Peryanova, O. V.; Vstavskaya, Y. A. Synthesis and antimicrobial activity of gold complexes with glycine, histidine, and tryptophan. *Pharmaceutical Chemistry Journal* **33**, 470 (1999).

Ke, H.; Wang,J.; Dai, Z.; Jin, Y.; Qu, E.; Xing, Z.; Guo, C.; Yue, X.; Liu, J. Gold-nanoshelled microcapsules: a theranostic agent for ultrasound contrast imaging and photothermal therapy. *Angewandte Chemie International Edition* **50**, 3017 (2011).

Khare, M. D.; Bukhari, S. S.; Swann, A.; Spiers, P.; McLaren, I.; Myers, J. Reduction of catheter-related colonisation by the use of a silver zeolite-impregnated central vascular catheter in adult critical care. *Journal of Infection* **54**, 146 (2007).

Kim, S; Hwang, S.- J.; Choi, W. Visible light active platinum-ion-doped TiO_2 photocatalyst. *Journal of Physical Chemistry B* **109**, 242620 (2005)a

Kim, S.; Choi, W. Visible-Light-Induced Photocatalytic Degradation of 4-Chlorophenol and Phenolic Compounds in Aqueous Suspension of Pure Titania: Demonstrating the Existence of a Surface-Complex-Mediated Path. *Journal of Physical Chemistry B* **109**,

5143 (2005).b

Kim, J.; Kuk, E.; Yu, K.; Kim, J.; Park, S.; Lee, H.; Kim, S.; Park, Y.; Park, Y.; Hwang, C.; Kim, Y.; Lee, Y.; Jeong, D.; Cho, M. Antimicrobial effects of silver nanoparticles. *Nanomedicine: Nanotechnology, Biology and Medicine* **3**, 95 (2007).

Kim, J.; Lee, J.; Kwon, S.; Jeong S. Preparation of biodegradable polymer/silver nanparticles composite and its antibacterial efficacy. *Journal of Nanoscience and Nanotechnology* **9**, 1098 (2009).

Kiyotomi, K.; Noritsugu, Y. Hydroxyapatite with the silver supported on the surface thereof. *US 2010/0331574A1* (2010).

Klasen, H. J. A historical review of the use of silver in the treatment of burns. II. Renewed interest for silver. *Burns* **26**, 131 (2000).

Kostonova, I. Platinum Complexes as Anticancer Agents. Recent *Patents on Anti-Cancer Drug Discovery* **1**, 1 (2006).

Koyama, M.; Shirashi, M.; Sasaki, K.; Kon-no, K. Preparation of L-alaninine crystals containing gold nanoparticles. *Journal of Dispersion Science and Technology* **29**, 1266 (2008).

Landi, E.; Tampieri, A.; Belmonte, M. M.; Celotti, G.; Sandri, M.; Gigante, A.; Fava, P.; Biagini, G. Biomimetic Mg- and Mg, CO_3- substituted hydroxyapatites: synthesis, characterization and in vitro behavior. *Journal of European Ceramic Society* **26**, 2593 (2005).

Lankveld, D. P.; Oomen, A. G.; Krystek, P.; Neigh, A.; Troost-de Jong, A.; Noorlander, C. W.; Van Eijkeren, J. C.; Geertsma, R. E.; De Jong, W. H. The kinetics of the tissue distribution of silver nanoparticles of different sizes. *Biomaterials* **31**, 8350 (2010).

Lee, Y. and Shacter, E. Oxidative Stress Inhibits Apoptosis in Human Lymphoma Cells. *The Journal of Biological Chemistry* **274**, 19792 (1999).

Lelli, J. L.; Becks, L. L.; Dabrowska, M. I.; Hinshaw, D. B. ATP converts necrosis to apoptosis in oxidant-injured endothelial cells. *Free Radical Biology & Medicine*. **25**, 694 (1998).

Lester, H. E. Hydroxyapatite material and methods of production. *WO2010/122354A1* (2010).

Li, Q.; Mahendra, S.; Lyon, D. Y.; Brunet, L.; Liga, M. V.; Li, D.; Alvarez, P. J. Antimicrobial nanomaterials for water disinfection and microbial control: potential applications and implications. *Water Research* **42**, 4591 (2008).

Li, L.; Sun, J.; Li, X.; Zhang, Y.; Wang, Z.; Wang, C.; Dai, J.; Wang, Q. Controllable synthesis of monodispersed silver nanoparticles as standards for quantitative assessment of their cytotoxicity. Biomaterials 33, 1714 (2012).

Liao, S.; Watari, F.; Xu, G.; Ngiam, M.; Ramakrishna, S.; Chan, C. K. Morphological effects of variant carbonates in biomimetic hydroxyapatite. *Materials Letters* **61**, 3624 (2007).

Liu, J.-K.; Yang, X.-H.; Tian, X.-G. Preparation of silver/hydroxyapatite nanocomposite spheres. *Powder Technology* **184**, 21 (2008).

Liu, H.-J.; Feng, Z.-G.; Lang, J.; Li, Y.-J.; He, G.-Y.; Chen, Z.-W. Fusion expression and high-level preparation of a glycine-rich antibacterial peptide (SK66) derived from *Drosophila* in *Escherichia coli*. *African Journal of Biotechnology* **8**, 4608 (2009).

Liu, Y.; Liu, C. Y.; Wei, J. H.; Xiong, R.; Pan, C. X.; Shi, J. Enhanced adsorption and visible-light-induced photocatalytic activity of hydroxyapatite modified Ag–TiO2

powders. *Applied Surface Science* **256**, 6390 (2010).

Lok, C.; Ho, C.; Chen, R.; He, Q.; Yu, W.; Sun, H.; Tam, P.; Chiu, J.; Che, C. Proteomic analysis of the mode of antibacterial action of silver nanoparticles. *Journal of Proteome Research* **5**, 916 (2006).

Lu, W.; Liu, G.; Gao, S.; Xing, S.; Wang, J. Tyrosine-assisted preparation of Ag/ZnO nanocomposites with enhanced photocatalytic performance and synergistic antibacterial activities. *Nanotechnology* **19**, 445711 (2008).

Lyon, D. Y.; Fortner, J. D.; Sayes, C. M.; Colvin, V. L.; Hughe, J. B. Bacterial cell association and antimicrobial activity of a C60 water suspension, *Environmental Toxicology and Chemistry* **24**, 2757 (2005).

Lyon, D. Y.; Brunet, L.; Hinkal, G. V.; Wiesner, M. R. Alvarez, P. J. Antibacterial activity of fullerene water suspensions (nC60) is not due to ROS-medicated damage. *Nano Letters* **8**, 1539 (2008).

Mahdihassan, S. Tan, cinnabar, as drug of longevity prior to alchemy. *American Journal of Chinese Medicine* **12**, 50 (1984).

Mahdihassan, S. Cinnabar-gold as the best alchemical drug of longevity, called makaradhwaja in India. *American Journal of Chinese Medicine* **13**, 93 (1985).

Mahdihassan, S. Alchemy, Chinese versus Greek, an etymological approach: a rejoinder. *American Journal of Chinese Medicine* **16**, 83 (1988).

Madhurambal, G.; Mariappan, M.; Mojumdar, S. C. TG-DTA, UV and FTIR spectroscopic studies of urea-thiourea mixed crystal. *Journal of the Thermal Analysis and Calorimetry* **100**, 853 (2010).

Malagutti, A. R.; Mourao, H. A. J. L.; Garbin, J. R.; Ribeiro, C. Deposition of TiO_2 and Ag:TiO_2 thin films by the polymeric precursor method and their application in the photodegradation of textile dyes. *Applied Catalysis B- Environmental* **90**, 205 (2009).

Malshe, P. A.; Jiang, W. Nanostructured hydroxyapatite coatings for dental and orthopedic implants. *WO2011/022642A1* (2011).

Mandel, S.; Tas, A. C. Brushite ($CaHPO_4 \cdot 2H_2O$) to octacalcium phosphate ($Ca_8(HPO_4)_2(PO_4)_4 \cdot 5H_2O$) transformation in DMEM solutions at 36.5 °C. *Materials Science and Engineering* **30**, 245 (2010).

Mandal, S.; Selvakannan, P. R.; Phadtare, S.; Pasricha, R.; Sastry, M. Synthesis of stable gold hydrosol by the reduction of chloroaurate ions by the amino acid, aspartic acid. *Proceedings of the Indian Academy of Science- Chemical Science* **114**, 513 (2002).

Marambio-Jones, C.; Hoek, E. M. V. A. A review of the antibacterial effects of silver nanomaterials and potential implications for human health. *Journal of Nanoparticle Research* **12**, 1531 (2010).

Martelli, L.; Tottolo, N.; Franco, M.; Martelli, M. Medical-surgical devices with antibacterial coating for human or animal implant and a method for their production. *EP2229962A1* (2010).

Marković, Z.; Todorović-Marković, B.; Kleut, D.; Nikolić, N.; Vranjes-Djurić, S.; Misirkić, M.; Vučičević, L.; Janjetović, K.; Isaković, A.; Harhaji, L.; Babić-Stojić, B.; Dramićanin, M.; Trajković, V. The mechanism of cell-damaging reactive oxygen generation by colloidal fullerenes. *Biomaterials* **28**, 5437 (2007).

Matsuura, T.; Abe, Y.; Sato, K.; Okamoto, K.; Ueshige, M.; Akagawa, Y. Prolonged antimicrobial effect of tissue conditioners containing silver zeolite. *Journal of Dentistry* **25**, 373 (1997).

Mayer, I.; Schlam, R.; Featherstone, F. D. B. Magnesium-containing carbonate apatites. *Journal of Inorganic Biochemistry* **66**, 1 (1997).

Mertens, H.; Polman, A. Depth-resolved nanostructure and refractive index of borosilicate glass doped with Ag nanocrystals. *Optical Materials* **29**, 326 (2006).

Mishra, A. K.; Mishra, S. B.; Manav, N.; Saluja, D.; Chandrac R.; Kaushika, N. K. Synthesis, characterization, antibacterial and cytotoxic study of platinum (IV) complexes. *Bioorganic & Medicinal Chemistry* **14**, 6333 (2006).

Mizukoshi, Y.; Takagi, E.; Okuno, H.; Oshima, R., Maeda, Y.; Nagata, Y. Preparation of platinum nanoparticles by sonochemical reduction of the Pt(IV) ions: role of surfactants. *Ultrasonics Sonochemistry* **8**, 1 (2001).

Mo, A.; Liao, J.; Xu, W.; Xian, S.; Li, Y.; Bai, S. Preparation and antibacterial effect of silver-hydroxyapatite/titania nanocomposite thin film on titanium. *Applied Surface Science* **255**, 435 (2008).

Monkawa, A.; Ikoma, T.; Yunoki, S.; Yoshioka, T.; Tanaka, J.; Chakarov, D.; Kasemo, B. Fabrication of hydroxypatite ultra-thin layer on gold surface and its application for quartz crystal microbalance technique. *Biomaterials* **27**, 5748 (2006).

Moreno-Alvarez, S. A.; Martinez-Castanon, G. A.; Nino-Martinez, N.; Reyes-Macias, J. F.; Patino-Marin, N.; Loyola-Rodriquez, J. P.; Ruiz, F. Preparation and bactericide activity of gallic acid stabilized gold nanoparticles. *Journal of Nanoparticle Research* **12**, 2741 (2010).

Morones, J. R.; Elechiguerra, J. L.; Camacho, A.; Holt, K.; Kouri, J. B.; Ramirez, J. T.; Yacaman, M. The antibacterial effect of silver nanoparticles. *Nanotechnology* **16**, 2346 (2005).

MubarakAli, D.; Thajuddin, N.; Jeganathan, K.; Gunasekaran, M. Plant extract mediated synthesis of silver and gold nanoparticles and its antibacterial activity against isolated pathogens. *Colloids and Surface B- Biointerface* **85**, 360 (2011).

Nair, L. S.; Laurencin, C. T. Silver nanoparticles: synthesis and therapeutic applications. *Journal of Biomedical Nanotechnology* **3**, 301 (2007).

Nakagawa, T.; Nitani, H.; Tanabe, S.; Okitsu, K.; Seino, S.; Mizukoshi, Y.; Yamamoto, T. A. Structural analysis of sonochemically prepared Au/Pd nanoparticles dispersed in porous silica matrix. *Ultrasonics Sonochemistry* **12**, 249 (2005).

Nam, Y. S.; Magyar, A. P.; Lee, D.; Kim, J.-W.; Yun, D. S.; Park, H.; Pollom Jr, T. S.; Weitz, A.; Belcher, A. M. Biologically templated photocatalytic nanostructures for sustained light-driven water oxidation. *Nature Nanotechnology* **5**, 340 (2010).

Narayan Bhat, M.; Dharmaprakash, S. M. Growth of nonlinear optical g-glycine crystals. *Journal of Crystal Growth* **236**, 376 (2002).

Naveenraj,S.; Anandan, S.; Kathiravan, A.; Renganathan, R.; Ashokkumar, M. The interaction of sonochemically synthesized gold nanoparticles with serum albumins. *Journal of Pharmaceutical and Biomedical Analysis* **53**, 804 (2010).

Nel, A.; Xia, T.; Madler, L.; Li, N. Toxic potential of materials at the nanolevel. *Science* **311**, 622 (2006).

Nishikawa, H.; Omamiuda, K. Photocatalytic activity of hydroxyapatite for methyl mercaptane. *Journal of Molecular Catalysis A- Chemical* **179**, 193 (2002).

Nishikawa, H. Surface changes and radical formation on hydroxyapatite by UV irradiation for inducing photocatalytic activation. *Journal of Molecular Catalysis A-Chemical* **206**, 331 (2003).a

Nishikawa, H. Radical generation on hydroxyapatite by UV irradiation. *Materials Letters* **58**, 14 (2003).b

Nishikawa, H. A high active type of hydroxyapatite for photocatalytic decomposition of dimethyl sulfide under UV irradiation. *Journal of Molecular Catalysis A- Chemical* **207**, 149 (2004).

Nishikawa, H.; Kato, S.; Ando, T. Rapid and complete oxidation of acetaldehyde on TiO_2 photocatalytic filter supported by photo-induced activated hydroxyapatite. *Journal of Molecular Catalysis A- Chemical* **236**, 145 (2005).

Nishikawa, H. Photo-induced Catalytic Activity of Hydroxyapatite Based on Photo-excitation. *Phosphorus Research Builletin* **21**, 97 (2007).

Nour, M.; Rady, A. H. *Synthesis and Reactivity in Inorganic Metal-Organic and Nano-Metal Chemistry* **21**, 1153 (1991).

Okitsu, K.; Mizukoshi,Y.; Yamamoto, T. A.; Maeda, Y.; Nagata, Y. Sonochemical synthesis of gold nanoparticles on chitosan. *Materials Letters* **61**, 3429 (2007).

Oyanedel-Craver, V. A.; Smith, J. A. Sustainable colloidal-silver-impregnated ceramic filter for point-of-use water treatment. *Environmental Science and Technology* **42**, 927 (2008).

Pal, S.; Tak, Y. K.; Song, J. M. Does the antibacterial activity of silver nanoparticles depend on the shape of the nanoparticle? A study of the Gram-negative bacterium Escherichia coli. *Applied and Environmental Microbiology* **73**, 1712 (2007).

Pan, Y.; Neuss, S.; Leifert, A.; Fischler, M.; Wen, F.; Simon, U.; Schmid, G.; Brandau, W.; Jahnen-Dechent, W. Size-dependent cytotoxicity of gold nanoparticles. *Small* **3**, 1941 (2007).

Paracchino, A.; Laporte, V.; Sivula, K.; Gratzel, M.; Thimsen, E. Highly active oxide photocathode for photoelectrochemical water reduction. *Nature Materials* **10**, 456 (2011).

Park, J.-E.; Atobe, M.; Fuchigami, T. Synthesis of multiple shapes of gold nanoparticles with controlled sizes in aqueous solution using ultrasound. *Ultrasonics Sonochemistry* **13**, 237 (2006).

Park, J. Photocatalytic activity of hydroxyapatite-precipitated potassium titanate whiskers. *Journal of Alloys and Compounds* **492**, L57 (2010).

Patra, C. R.; Bhattacharya, R.; Mukhopadhyay, D.; Mukherjee, P. Fabrication of gold nanoparticles for targeted therapy in pancreatic cancer. *Advanced Drug Delivery Review* **62**, 346 (2010).

Pavlikova, S.; Thomann, R.; Reichert, P.; Mulhaupt, R.; Marcincin, A.; Borsig, E. Fiber spinning from poly(propylene)-organoclay nanocomposite. *Journal of Applied Polymer Science* **89**, 604 (2003).

Peng, Z; Yang, H. Designer platinum nanoparticles: Control of shape, composition in alloy, nanostructure and electrocatalytic property. *Nano Today* **4**, 143 (2009).

Perkas, N.; Amirian, G.; Applerot, G.; Efenduev, E.; Kaganovskii, Y.; Ghule, A.; Chen, B.-J.; Ling, Y.-C.; Gedanken, A. Depositing silver nanoparticles on/in a glass slide by sonochemical method. *Nanotechnology* **19**, 1 (2008).

Pernodet, N.; Fang, X.; Sun, Y.; Bakhtina, A.; Ramakrishnan, A.; Sokolov, J.; Ulman, A.; Rafailovich, M. Adverse effects of citrate/gold nanoparticles on human dermal fibroblasts. *Small* **2**, 766 (2006).

Pleshko, N.; Boskey, A.; Mendelsohn, R. Novel infrared spectroscopic method for

determination of crystallinity of hydroxyapatite minerals. *Biophysical Journal* **60,** 786 (1991).

Polavarapu, L.; Xu, Q.-H. A single-step synthesis of gold nanochaines using an amino acid as a capping agent and characterization of their optical properties. *Nanotechnology* **19**, 075601 (2008).

Porcel, E.; Liehn, S.; Remita, H.; Usami, N.; Kobayashi, K.; Furusawa, Y.; Le Sech, C.; Lacombe, S. Platinum nanoparticles: a promising material for future cancer therapy? *Nanotechnology* **21**, 085103 (2010).

Quinet, M.; Lallemand, F.; Ricq, L.; Hihn, J.-Y., Delobelle, P. Adsorption of thiourea on polycrystalline platinum: Influence on electrodeposition of copper. *Surface & Coatings Technology* **204**, 3108 (2010).

Raad, I. Intravascular-catheter-related infections. *Lancet* **351**, 893 (1998).

Rademacher, W. T.; Bradman, G.; Penades-Ullate, S.; Ojeda Martinez De Castilla, R. Nanoparticles comprising antibacterial ligands. *WO2007/015105A2* (2007).

Raffi, M.; Hussain, F.; Bhatti, T.; Akhter, J.; Hameed, A.; Hasan, M. Antibacterial characterization of silver nanoparticles against E. coli ATCC-15224. *Journal of Materials Science and Technology* **24**, 192 (2008).

Rai, M.; Yadav, A.; Gade, A. Silver nanoparticles as a new generation of antimicrobials. *Biotechnology Advances* **27**, 76 (2009).

Rai, A.; Prabhune, A.; Perry, C. C. Antibiotic mediated synthesis of gold nanoparticles with potent antimicrobial activity and their application in antimicrobial coatings. *Journal of Materials Chemistry* **20**, 6789 (2010).

Raj, C. R.; Jena, B. K. Efficient electrocatalytic oxidation of NADH at gold nanoparticles self-assembled on three-dimensional sol-gel network. *Chemical Communications* **41**, 2005 (2005).

Rameshbabu, N.; Kumar, T. S. S.; Prabhakar, T. G.; Sastry, V. S.; Murty, K. V. G. K.; Rao, K. P. Antibacterial nanosized silver substituted hydroxyapatite: synthesis and characterization. *Journal of Biomedical Materials Research A* **80**, 581 (2007).

Rautaray, D.; Mandal, S.; Sastry, M. Synthesis of hydrxyapatite crystals using amino acid-capped gold nanoparticles as a scaffold. *Langmuir* **21**, 5185 (2005).

Reddy, M. P.; Venugopal, A.; Subrahmanyam, M. Hydroxyapatite photocatalytic degradation of calmagite (an azo dye) in aqueous suspension. *Applied Catalysis B-Environmental* **69**, 164 (2007).

Ren, G.; Hu, D.; Cheng, E. W. C.; Vargas-Reus, M. A.; Reip, P.; Allaker, R. P. Characterization of copper oxide nanoparticles for antimicrobial applications. *International Journal of Antimicrobial Agents* **33**, 587 (2009).

Rosemary, M. J.; MacLaren, I.; Pradeep, T. Investigations of the Antibacterial Properties of Ciprofloxacin@SiO_2. *Langmuir* **22**, 10125 (2006).

Rulis, P.; Ouyang, L.; Ching, W. Y. Electronic structure and bonding in calcium apatite crystals: Hydroxyapatite, fluorapatite, chlorapatite, and cromapatite. *Physical Review B* **70**, 155104 (2004).

Sagisaka, A.; Miyanoshita, A.; Ishibashi, J.; Yamakawa, M. Purification, characterization and gene expression of a glycine and proline-rich antibacterial protein family from larvae of a beetle, *Allomyrina dichotoma*. *Insect Molecular Biology* **10**, 293 (2001).

Saha, B.; Bhattacharya, J.; Mukherjee, A.; Ghosh, A. K.; Santra, C. R.; Dasgupta, A. K.; Karmakar, P. In vitro structural and functional evaluation of gold nanoparticles

conjugated antibiotics. *Nanoscale Research Letters* **2**, 614 (2007).

Saito, T.; Nakanaga, H. Antibacterial resin. *EP1329211A1* (2003).

Salkar, R. A.; Jeevanandam, P.; Aruna, S. T.; Koltypin, Y.; Gedanken, A. The sonochemical preparation of amorphous silver nanoparticles. *Journal of Materials Chemistry* **9**, 1333 (1999).

Samberg, M. E.; Oldenburg, S. J.; Monteiro-Riviere, N. A. Evaluation of silver nanoparticle toxicity in skin in vivo and keratinocytes in vitro. *Environmental Health Perspectives* **118**, 407 (2010).

Sastry, T. P.; Sundaraseelan, J.; Swarnalatha, K.; Liji Sobhana, S. S.; Uma Makheswari, M.; Sekar, S.; Mandal, A. B. Growth of hydroxyapatite on physiologically clotted capped gold nanoparticles. *Nanotechnology* **19**, 245604 (2008).

Sau, T. K.; Rogach, A. L. Nonspherical noble metal nanoparticles: colloid-chemical synthesis and morphology control. *Advanced Materials* **22**, 1781 (2010).

Schafer, F. Q.; Buettner, G. R. Redox environment of the cell as viewed through the redix state of the glutathione disulfide/glutathione couple. *Free Radical Biology & Medicine* **30**, 1191 (2001).

Schasfoort, R. B. M.; Tudos A. J. (Eds.) *Handbook of surface plasmon resonance* (Royal Chemical Society, Springer, New York, 2008).

Schmalz, G. Agar overlay method. *International Endodontic Journal* **21**, 59 (1988).

Schmidt, C. L.; Dinnebier, R. E.; Jansen, M. Phase transition and thermal decomposition of silver isocyanate (AgNCO). *Solid State Science* **11**, 1107 (2009).

Schreurs, W.; Rosenberg, H. Effect of silver ions on transport and retention of phosphate by Escherichia coli. *Journal of Bacteriology* **152**, 7 (1982).

Seckin, T.; Onal, Y.; Yesilada, O.; Gultek, A. Preparation and characterization of a clay–polyvinylpyridinium matrix for the removal of bacterial cells from water. *Journal of Materials Science* **32**, 5993 (1997).

Segal, A. W. How neutrophils kill microbes. *Annual Review of Immunology* **23**, 197 (2005).

Seltmann, G. and Holst, O. *Bacterial cell wall* (Springer, Berlin, 2001).

Selvakannan, P. R.; Mandal, S.; Phadtare, S.; Gole, A.; Pasricha, R.; Adyanthaya, S. D.; Sastry, M. Water-dispersible tryptophan-protected gold nanoparticles prepared by the spontaneous reduction of aqueous chloroaurate ions by the amino acid. *Journal of Colloid and Interface Science* **269**, 97 (2004).

Selvaraj, V.; Alagar, M. Analytical detection and biological assay of antileukemic drug 5-fluorouracil using gold nanoparticles as probe. *International Journal of Pharmaceutics* **337**, 275 (2007).

Shahidi, S.; Ghoranneviss, M. Investigation on dye ability and antibacterial activity of nanolayer platinum coated polyester fabric using DC magnetron sputtering. *Progress in Organic Coatings* **70**, 300 (2011).

Shannon, M. A.; Bohn, P. W.; Elimelech, M.; Georgiadis, J. G.; Marinas, B. J. Science and technology for water purification in the coming decades. *Nature* **452**, 301 (2008).

Shao, Y.; Jin, Y.; Dong, S. Synthesis of gold nanoplates by aspartate reduction of gold chloride. *Chemical Communications* **7**, 1104 (2004).

Sharifi, S.; Behzadi, S.; Laurent, S.; Forrest, M. L.; Stroevee, P.; Mahmoudi, M. Toxicity of nanomaterials. *Chemical Society Reviews*, (2012) doi: 10.1039/C1CS15188F.

Sharma, V. K.; Yngard, R. A.; Lin, Y. Silver nanoparticles: green synthesis and their antimicrobial activities. *Advances in Colloid and Interface Science* **145**, 83 (2009).

Shchukin, D. G.; Skorb, E.; Belova, V.; Möhwald, H. Ultrasonic Cavitation at Solid Surfaces. *Advanced Materials* **23**, 1922 (2011).

Shi, J.; Ross, C. R.; Chengappa, M. M.; Blecha, F. Identification of proline-arginine-rich antibacterial peptide from neutrophils that is analogous to PR-39, an antibacterial peptide from the small intestine. *Journal of Leukocyte Biology* **56**, 807 (1994).

Shirkhanzadeh, M.; Azadegan, M.; Liu, G. Q. Bioactive delivery for the slow release of antibiotics: incorporation of Ag^{+} ions into micro-porous hydroxyaptite coatings. *Materials Letters* **24**, 7 (1995).

Shukla, R.; Bansal, V.; Chaudhary, M.; Basu, A.; Bhonde, R. R.; Sastry, M. Biocompatibility of gold nanoparticles and their endocytotic fate inside the cellular compartment: a microscopic overview. *Langmuir* **21**, 10644 (2005).

Silvestry-Rodriguez, N.; Sicairos-Ruelas, E. E.; Gerba, C. P.; Bright, K. R. Silver as a Disinfectant. *Revew of Environmental Contamination and Toxicology* **191**, 23 (2007).

Simmons, K. J.; Chopra, I.; Fishwick, C. W. G. Structure-based discovery of antibacterial drugs. *Nature Reviews* **8**, 501 (2010).

Sivakumar, M.; Towata, A.; Yasui, K.; Tuziuti, T.; Kozuka, T.; Tsujimoto, M.; Zhong, Z.; Iida, Y. Fabrication of nanosized Pt on rutile TiO_2 using a standing wave sonochemical reactor (SWSR) – observation of an enhanced catalytic oxidation of CO. *Ultrasonics Sonochemistry* **17**, 213 (2010).

Smetana, A. B.; Klabunde, K. J.; Marchin, G. R.; Sorensen, C. M. Biocidal Activity of Nanocrystalline Silver Powders and Particles. *Langmuir* **24**, 7457 (2008).

Smith, B. *Infrared spectral interpretation: A systematic approach* (CRC Press, 1999).

Sondi, I.; Goia, D. V.; Matijević, E. Preparation of highly concentrated stable dispersions of uniform silver nanoparticles. *Journal of Colloid and Interface Science* **260**, 75 (2003).

Sondi, I.; Salopek-Sondi, B. Silver nanoparticles as antimicrobial agent: a case study on E. coli as a model of Gram-negative bacteria. *Journal of Colloid and Interface Science* **275**, 177 (2004).

Sonavane, G.; Tomoda, K.; Sano, A.; Ohshima, H.; Terada, H.; Makino, K. In vitro permeation of gold nanoparticles through rat skin and rat intestine: effect of particle size. *Colloids and Surface B Biointerfaces* **65**, 1 (2008).

Sperstad, S. V.; Haug, T.; Vasskog, T.; Stensvåg, K. Hyastatin, a glycine-rich multi-domain antimicrobial peptide isolated from the spider crab (Hyas araneus) hemocytes. *Molecular Immunology* **46**, 2604 (2009).

Srivastava, A.; Srivastava, O. N.; Talapatra, S.; Vajtai, R.; Ajayan, P. M. Carbon nanotube filters. *Nature Materials* **3**, 610 (2004).

Stadtländer, C. T. K.-H. Scanning Electron Microscopy and Transmission Electron Microscopy of Mollicutes: Challenges and Opportunities. In: Méndez-Vilas, A.; Díaz, J. (Eds.) *Modern Research and Educational Topics in Microscopy*. 122–131 (Formatex, 2007)

Stewart, J. E. Infrared absorption of spectra of urea, thiourea, and some thiourea-alkali halide complexes. *Journal of Chemical Physics* **26**, 248 (1957).

Streitwieser, A.; Heathcock, C. H. *Introduction to organic chemistry* (Macmillan Publishing Group, New York, 1985).

Stroyuk, A. L.; Kryukov, A. I.; Kuchmii, S. Y.; Pokhodenko, V. D. Semiconductor photocatalytic systems for the production of hydrogen by the action of visible light *Theoretical and Experimental Chemistry* **45**, 209 (2009).

Su, C.-H.; Wu, P.-L.; Yeh, C.-S. Sonochemical synthesis of well-dispersed gold nanoparticles at the ice temperature. *Journal of Physical Chemistry B* **107**, 14240 (2003).

Sun, L.; Li, J.; Wang, C.; Li, S.; Lai, Y.; Chen, H.; Lin, C. Ultrasound aided photochemical synthesis of Ag loaded TiO_2 nanotube arrays to enhance photocatalytic activity. *Journal of Hazards Materials* **171**, 1045 (2009).

Sung, J. H.; Ji, J. H.; Yoon, J. U.; Kim, D. S.; Song, M. Y.; Jeong, J.; Han, B. S.; Han, J. H.; Chung, Y. H.; Kim, J.; Kim, T. S.; Chang, H. K.: Lee, E. J.; Lee, J. H.; Yu, I. J. Lung function changes in Sprague-Dawley rats after prolonged inhalation exposure to silver nanoparticles. *Inhalation Toxicology* **20**, 567 (2008).

Sung, J. H.; Ji, J. H.; Song, K. S.; Lee, J. H.; Choi, K. H.; Lee, S. H.; Yu, I. J. Acute inhalation toxicity of silver nanoparticles. *Toxicology and Industrial Health* **27**, 149 (2011).

Suresh, A. K.; Pelletiera, D. A.; Wang, W.; Morrell-Falveya, J. L.; Gu, B.; Doktycza, M. J. Cytotoxicity induced by engineered silver nanocrystallites is dependent on surface coatings and cell types. *Langmuir*, (2012) doi: 10.1021/la2042058.

Suslick, K. S.; Hyeon, T.; Fang, M. Nanostructured materials generated by high-intensity ultrasound: sonochemical synthesis and catalytic studies. *Chemistry of Materials* **8**, 2172 (1996).

Sygnatowicz, M.; Keyshar, K.; Tiwari, A. Antimicrobial properties of silver-doped hydroxyapatite nano-powders and thin films. *Journal of the Minerals, Metals and Materials Society* **62**, 65 (2010).

Taguchi, S.; Ozaki, A.; Nakagawa, K.; Momose, H. Functional mapping of amino acid residues responsible for the antibacterial action of apidaecin. *Applied and Environmental Microbiology* **62(12)**, 4652 (1996).

Tan, Y.; Li, Y.; Zhu, D. Preparation of silver nanocrystals in the presence of aniline. *Journal of Colloid and Interface Science* **258**, 244 (2003).

Taubes, G. The bacteria fight back. *Science* **321**, 356 (2008).

Ternane, R.; Ferid, M.; Kbir-Ariguib, N.; Trabelsi-Ayedi, M. The silver lead apatite $Pb_8Ag_2(PO_4)_6$: hydrothermal preparation. *Journal of Alloys and Compounds* **308**, 83 (2000).

Trickler, W. J.; Lantz, S. M.; Murdock, R. C.; Schrand, A. M.; Robinson, B. L.; Newport, G. D.; Schlager, J. J.; Oldenburg, S. J.; Paule, M. G.; Slikker, W. Jr.; Hussain, S. M.; Ali, S. F. Silver nanoparticle induced blood-brain barrier inflammation and increased permeability in primary rat brain microvessel endothelial cells. *Toxicological Science* **118**, 160 (2010).

Trickler, W. J.; Lantz, S. M.; Murdock, R. C.; Schrand, A. M.; Robinson, B. L.; Newport, G. D.; Schlager, J. J.; Oldenburg, S. J.; Paule, M. G.; Slikker, W. Jr.; Hussain, S. M.; Ali, S. F. Brain microvessel endothelial cells responses to gold nanoparticles: In vitro pro-inflammatory mediators and permeability. *Nanotoxicology* **5**, 479 (2011).

Trop, M.; Novak, M.; Rodl, S.; Hellbom, B.; Kroell, W.; Goessler, W. Silver-coated dressing acticoat caused raised liver enzymes and argyria-like symptoms in burn patient. *Journal of Trauma* **60**, 648 (2006).

Tsukada, M.; Wakamura, M.; Yoshida, N.; Watanabe, T. Band gap and photocatalytic

properties of Ti-substituted hydroxyapatite: Comparison with anatase-TiO_2. *Journal of Molecular Catalysis A- Chemical* **338**, 18 (2011).

Valappil, S. P.; Ready, D.; Neel, E. A. A.; Pickup, D. M.; Chrzanowski, W.; O'Dell, A.; Newport, L. R. J.; Smith, M. E.; Wilson, M.; Knowles, J. C. Antimicrobial gallium doped phosphate-based glasses. *Advanced Functional Material* **18**, 732 (2008).

Valko, M.; Morris, H.; Cronin, M. T. D. Metals, toxicity and oxidative stress. *Current Medicinal Chemistry* **12**, 1161 (2005).

Valko, M.; Rhodes, C. J.; Moncola, J.; Izakovic, M.; Mazura, M. Free radicals, metals and antioxidants in oxidative stress-induced cancer. *Chemico-Biological Interactions* **160**, 1 (2006).

Vogel, R.; Nijtmans, L.; Ugalde, C.; van den Heuvel, L.; Smeitink, J. Complex I assembly: a puzzling problem. *Current Opinion in Neurology* **17**, 179 (2004).

Vukomanović, M.; Škapin, S. D.; Maksin, T.; Ignjatović, N.; Uskoković, V.; Uskoković, D. Poly(d,l-lactide-co-glycolide)/hydroxyapatite Core-shell Nanospheres: Part 1: A Multifunctional System for Controlled Drug Delivery. *Colloids and Surface B: Biointerface* **82**, 404 (2011).a

Vukomanović, M.; Škapin, S. D.; Poljanšek, I.; Žagar, E.; Kralj, B.; Ignjatović, N.; Uskoković, D. Poly(D,L-lactide-co-glycolide)/hydroxyapatite core-shell nanospheres: Part 2: Simultaneous release of a drug and prodrug. *Colloids and Surfaces B: Biointerface* **82**, 414 (2011).b

Vukomanović, M; Zavašnik–Bergant, T; Bračko, I.; Radmilović, V.; Škapin, S. D.; Ignjatović, N.; Uskoković, D. Poly(D,L-lactide-co-glycolide)/hydroxyapatite Core-shell Nanospheres. Part 3: Properties of hydroxyapatite nano-rods and investigation of a distribution of the drug within the composite. *Colloids and Surfaces B: Biointerfaces* **87**, 226 (2011).c

Vukomanović, M.; Bračko, I.; Poljanšek, I.; Uskoković, D. P.; Škapin, S. D.; Suvorov, D. The Growth of Silver Nanoparticles and their Combination with Hydroxyapatite to Form Composites via a Sonochemical Approach, *Crystal Growth and Design*, **11**, 3802 (2011).d

Vukomanović, M.; Šarčev, I.; Petronijević, B.; Škapin, S. D.; Ignjatović, N.; Uskoković, D. Poly(D,L-lactide-co-glycolide)/hydroxyapatite core-shell nanospheres. Part 4: A change of the surface properties during degradation process and the corresponding in vitro cellular response. *Colloids and Surfaces B: Biointerfaces* **91**, 144 (2012).a

Vukomanović, M; Žunič, V.; Otoničar, M.; Repnik, U.; Turk, B.; Škapin, S.D.; Suvorov, D. Hydroxyapatite/Platinum Bio-Photocatalyst: A Biomaterial Approach to Self-cleaning. *Journal of Materials Chemistry* **22***,* 10571 (2012).b

Vukomanović, Škapin, S.D.; Suvorov, D. Functionalized ceramic/metallic composites as "green" materials with antibacterial activity, method of production the same and use thereof, Patent Application, *submitted* (2012).c

Wakamura, M.; Hashimoto, K.; Watanabe, T. Photocatalysis by Calcium Hydroxyapatite Modified with Ti(IV): Albumin Decomposition and Bactericidal Effect. *Langmuir* **19**, 3428 (2003).

Wakamura, M.; Masato, K. Antibacterial paint for materials and materials coated therewith. *EP1985675A1* (2008).

Wang, X.; Maeda, K.; Thomas, A.; Takanabe, K.; Xin, G.; Carlsson, J. M.; Domen, K.; Antonietti, M. A metal-free polymeric photocatalyst for hydrogen production from water under visible light. *Nature Materials* **8**, 76 (2009).a

Wang, X.-K.; Shao, L.; Guo, W.-L.; Wang, J.-G.; Yhu, Y.-P.; Wang, C. Synthesis of dendritic silver nanostructures by means of ultrasonic irradiation. *Ultrasonic Sonochemistry* **16**, 747 (2009).b

Weaver, J. F.; Hoflund, G. B. Surface characterization study of the thermal decomposition of AgO. *Journal of Physical Chemistry* **98**, 8519 (1994).

Wel, Q.; Yu, L.; Wu, N.; Hong, S. Preparation and characterization of copper nanocomposite textiles. *Journal of Industrial Textiles* **37 (3)**, 275 (2008).

Weller, R. B. Nitric oxide-containing nanoparticles as an antimicrobial agents and enhancer of wound healing. *Journal of Investigative Dermatology* **129**, 2335 (2009).

Wetli, E.; Hochstrasser, M.; Erbudak, M. Epitaxial growth of Ag in the hexagonal structure. *Surface Science* **377–379**, 876 (1997).

Wiesenfeld, D.; Ferguson, M. M.; Forsyth, A.; MacDonald, D. G.; Path, M. R. C. Allergy to dental gold., *Oral Surgery, Oral Medicine, Oral Pathology* **57**, 158 (1984).

Wilson, M. J. Clay mineralogy and related characteristics of geophagic materials. *Journal of Chemical Ecology* **29**, 1525 (2003).

Willoughby, A. J. Dental uses of silver hydrosol. *WO 2010/143075 A2* (2010).

Wong, K. K. Y.; Liu, X. Silver nanoparticles- the real silver bullet in clinical medicine?. *MedChemCommun* **1**, 125 (2010).

Wright, J. B.; Lam, K.; Burrell, R. E. Wound management in an era of increasing bacterial antibiotic resistance: A role for topical silver treatment. *American Journal of Infection Control* **26**, 572 (1998).

Yamagishi, K.; Onuma, K.; Suyuki, T.; Okada, F.; Tagami, J.; Otsuki, M.; Senawangse, P. Materials chemistry: A synthetic enamel for rapid tooth repair. *Nature* **433**, 819 (2005).

Yang, Y.; Nogami, M.; Shi, J.; Chen, H.; Liuc, Y.; Qian, S. Self-assembled semiconductor capped metal composite nanoparticles embedded in $BaTiO_3$ thin films for nonlinear optical applications. *Journal of Materials Chemistry* **13**, 3026 (2003).a

Yang, Y.; Shi, J.; Huang, W.; Dai, S.; Wang, L. Preparation and optical properties of gold nanoparticles embedded in barium titanate thin films. *Journal of Materials Science* **38**, 1243 (2003).b

Yang, M.; Yang, Y.; Liu, Y.; Shen, G.; Yu, R. Platinum nanoparticles-doped sol–gel/carbon nanotubes composite electrochemical sensors and biosensors. *Biosensors and Bioelectronics* **21**, 1125 (2006).

Yang, W.; Shen, C.; Ji, Q.; An, H.; Wang, J.; Liu, Q.; Zhang, Z. Food storage material silver nanoparticles interfere with DNA replication fidelity and bind with DNA. *Nanotechnology* **20**, 085102 (2009).

Ye, F.-X.; Ohmori, A.; Tsumura, T.; Nakata, K.; Li, C.-J. Microstructural analysis and photocatalytic activity of plasma-sprayed titania-hydroxyapatite coatings. *Journal of Thermal Spray Technology* **16**, 776 (2007).

Yeshchenko, O. A.; Dmitruk, I. M.; Grytsenko, K. P.; Prokopets, V. M; Kotko, A. V.; Schrader, S. Influence of interparticle interaction on melting of gold nanoparticles in Au/polytetrafluoroethylene nanocomposites. *Journal of Applied Physics* **105**, 094326 (2009).

Yi, Z.; Ye, J.; Kikugawa, N.; Kako, T.; Ouyang, S.; Stuart-Williams, H.; Yang, H.; Cao, J.; Luo, W.; Li, Z.; Liu, Y.; Withers, R. L. An orthophosphate semiconductor with photooxidation properties under visible-light irradiation. *Nature Materials* **9**, 559

(2010).

Yildirimer, L.; Thanh, N. T. K.; Loizidou, M.; Seifalian, A. M. Toxicological considerations of clinically applicable nanoparticles. *Nano Today* **6**, 585 (2011).

Yoon, K.; Byeon, J.; Park, C.; Hwang, J. Antimicrobial effect of silver particles on bacterial contamination of activated carbon fibers. *Environmental Science and Technology* **42**, 1251 (2008).

Yoon, T. P.; Ischay, M. A.; Du, J. Visible light photocatalysis as a greener approach to photochemical synthesis. *Nature Chemistry* **2**, 527 (2010).

You, J.; Ding, W.; Ding, S.; Ju, H. Direct electrochemistry of hemoglobin immobilized on colloidal gold-hydroxyapatite nanociomposite for electrocatalytic detection of hydrogen peroxide. *Electroanalysis* **21**, 190 (2009).

Zamborini, F. P.: Bao, L.; Dasari, R. Nanoparticles in Measurement Science. *Analytic Chemistry* **84**, 541 (2012).

Zhang, Y.; Peng, H.; Huanga, W.; Zhou, Y.; Yana, D. Facile preparation and characterization of highly antimicrobial colloid Ag or Au nanoparticles. *Journal of Colloid and Interface Science* **325**, 371 (2008).

Zhang, Y.; Xu, J.; Xu, P.; Zhu, Y.; Chen, X.; Yu., W. Decoration of ZnO nanowires with Pt nanoparticles and their improved gas sensing photocatalytic performance., *Nanotechnology* **21**, 285501 (2010).a

Zhang, X. D.; Wu, H. Y.; Wu, D.; Wang, Y. Y.; Chang, J. H.; Zhai, Z. B.; Meng, A. M.; Liu, P. X.; Zhang, L. A.; Fan, F. Y. Toxicologic effects of gold nanoparticles in vivo by different administration routes. *International Journal of Nanomedicine* **5**, 771 (2010).b

Zhao, Y.; Tian, Y.; Cui, Y.; Liu, W.; Ma, W.; Jiang, X. Small molecule-capped gold nanoparticles as potent antibacterial agents that target gram-negative bacteria. *Journal of the American Chemical Society* **132**, 12349 (2010).

Zhu, Y.; Wang, X.; Guo, W.; Wang, J.; Wang, C. Sonochemical synthesis of silver nanorods by reduction of silver nitrate in aqueous solution. *Ultrasonic Sonochemistry* **17**, 675–679 (2010)

Žunič, V.; Škapin, S. D.; Maček–Kržmanc, M.; Bračko, I.; Sever–Škapin, A.; Suvorov, D. Influence of the triblock copolymer P123 and phosphorous on the physico-chemical properties of TiO_2. *Applied Catalysis A- General* **397**, 241 (2011).

Index of Figures

Index of Tables

Appendix (Bibliography)

Publications as a part of this doctoral dissertation

Full length articles

Vukomanović, M.; Bračko, I.; Poljanšek, I.; Uskoković, D. P.; Skapin, S. D.; Suvorov, D. The Growth of Silver Nanoparticles and their Combination with Hydroxyapatite to Form Composites via a Sonochemical Approach, *Crystal Growth and Design*, **11 (9)**, 3802 (2011).

Vukomanović, M; Žunič, V.; Otoničar, M.; Repnik, U.; Turk, B.; Škapin, S.D.; Suvorov, D. Hydroxyapatite/Platinum Bio-Photocatalyst: A Biomaterial Approach to Self-cleaning. *Journal of Materials Chemistry,* **22***,* 10571 (2012).

Patent application

Vukomanović, M.; Škapin, S.D.; Suvorov, D. Functionalized ceramic/metallic composites as "green" materials with antibacterial activity, method of production the same and use thereof, *submitted* (2012).

Conference abstracts

Vukomanović, M.; Repnik, U.; Škapin, S. D.; Uskoković, D.; Suvorov, D. Antibacterial activity of hydroxyapatite/silver nanocomposites synthesized by a sonochemical approach. 13th Conference YUCOMAT 2011, Herceg Novi, Montenegro, September 5-9, 2011, Book of Abstracts, p. 69.

Vukomanović, M.; Uskoković, D.; Škapin, S. D.; Suvorov, D. Sonochemical synthesis of platinum nanoparticles and their composite with hydroxyapatite, 5. Dan Mladih Raziskovalcev KMBO, Institut Jožef Stefan, Ljubljana, Slovenia, 17. February, 2011, Book of Abstracts, p. 70.

Vukomanović, M.; Škapin, S. D. Application of sonochemistry for formation of nanosized silver and silver/hydroxyapatite composite particles, Proceedings of the 2nd Jožef Stefan International Postgraduate School Students' Conference-IPSSC, May 27, 2010, Ljubljana, Slovenia, Book of Abstracts, p. 72-73.

Vukomanović, M.; Bračko, I.; Škapin, S. D.; Suvorov, D.; Uskoković, D. Sonochemical synthesis of silver nanoparticles and silver/hydroxyapatite nanocomposites, 12th Conference YUCOMAT 2010, Herceg Novi, Montenegro, September 6-10, 2010, Book of Abstracts, p. 63.

Vukomanović, M.; Repnik, U.; Zavašnik, T.; Škapin, S. D.; Uskoković, D.; Suvorov, D. Antibacterial activity of hydroxyapatite/silver nanocomposite, 9th Conference for Young Researchers, Science and Engineering of New Materials 2010, December 20-22, Belgrade, 2010, Book of Abstracts, p. 15.

Vukomanović, M.; Otoničar, M.; Uskoković, D.; Srečo, S. D.; Suvorov, D. Sonochemical synthesis of gold nanoparticles and their composites with hydroxyapatite, 18th Conference on Materials and Technology, 15-17 November 2009, Portorož, Slovenia, Book of Abstracts, p. 48.

Other publications

Full length articles

Vukomanović, M.; Šarčev, I.; Petronijević, B.; Škapin, S. D.; Ignjatović, N.; Uskoković, D. Poly(d,l-lactide-co-glycolide)/hydroxyapatite core–shell nanospheres. Part 4: A change of the surface properties during degradation process and the corresponding in vitro cellular response. *Colloids and Surfaces B: Biointerfaces* **91**, 144 (2012).

Vukomanović, M.; Zavašnik-Bergant, T.; Bračko, I.; Radmilović, V.; Škapin, S. D.; Ignjatović, N.; Uskoković, D. Poly(D,L-lactide-co-glycolide)/hydroxyapatite Core-shell Nanospheres. Part 3: Properties of hydroxyapatite nano-rods and investigation of a distribution of the drug within the composite. *Colloids and Surfaces B: Biointerfaces* **87**, 226 (2011).

Vukomanović, M.; Škapin, S. D.; Poljanšek, I.; Žagar, E.; Kralj, B.; Ignjatović, N.; Uskoković, D. Poly(D,L-lactide-co-glycolide)/hydroxyapatite core-shell nanosphere. Part 2: Simultaneous release of of a drug and a prodrug (clindmycin and clindamycin phosphate). *Colloids and Surfaces B: Biointerfaces* **82**, 414 (2011).

Vukomanović, M.; Škapin, S. D.; Maksin, T.; Ignjatović, N.; Uskoković, V.; Uskoković, D. Poly(D,L-lactide-co-glycolide)/hydroxyapatite core-shell nanosphere. Part 1: Multifunctional system for controlled drug delivery, *Colloids and Surfaces B: Biointerfaces* **82**, 404 (2011).

Vukomanović, M.; Mitrić, M.; Škapin, S. D.; Žagar, E.; Plavec, J.; Ignjatović, N.; Uskoković, D. Influence of ultrasonic processing on the macromolecular properties of poly(D,L-lactide-co-glycolide) alone and in its biocomposite with hydroxyapatite. *Ultrasonics Sonochemistry* **17**, 902 (2010).

Jevtić, M.; Radulović, A.; Ignjatović, N.; Mitrić, M.; Uskoković, D. Controlled Assembly of Poly(D,L-lactide-co-glycolide)/Hydroxyapatite Core-Shell Nanospheres under Ultrasonic Irradiation. *Acta Biomaterialia* **5**, 208 (2009).

Jevtić, M.; Mitrić, M.; Škapin, S. D.; Jančar, B.; Ignjatović, N.; Uskoković, D. Crystal structure of hydroxyapatite nano-rods synthesized by sonochemical homogeneous precipitation. *Crystal Growth and Design* **8(7)**, 2217 (2008).

Jevtić, M.; Uskoković, D. Influence of Urea as Homogeneous Precipitation Agent on Sonochemical Hydroxyapatite Synthesis. *Materials Science Forum* **555**, 285 (2007).